

**SCANNING THE ASTHMATIC AIRWAY:  
DEFINING RELATIONSHIP BETWEEN PHYSIOLOGY,  
INFLAMMATION AND AIRWAY STRUCTURE IN SEVERE  
ASTHMA USING COMPUTED TOMOGRAPHY**

**Thesis submitted for the degree of**

**Doctor of Philosophy**

**at the University of Leicester**

by

**Sumit Gupta MBBS, MRCP(UK)**

Department of Infection, Immunity and Inflammation,

University of Leicester

2012

**Supervisors: Professor Christopher E. Brightling and Dr James Entwisle**

# MAIN TABLE OF CONTENTS

ABSTRACT.....	II
ACKNOWLEDGEMENTS .....	III
STATEMENT DETAILING WORK PERSONALLY PERFORMED .....	V
PUBLICATIONS AND PRIZES.....	VIII
CONTENTS .....	XII
TABLE OF FIGURES .....	XIX
LIST OF TABLES.....	XXII
ABBREVIATIONS.....	XXIV
MAIN BODY OF THESIS.....	1
REFERENCES .....	285

# ABSTRACT

---

## **Scanning the Asthmatic Airway: Defining Relationship between Physiology, Inflammation and Airway Structure in Severe Asthma using Computed Tomography.**

**Sumit Gupta**

Severe asthma is a complex and heterogeneous disease characterised by chronic airway inflammation, disordered airway physiology and airway remodelling. Computed tomography (CT) has emerged as a non-invasive tool for assessment of airway structural changes. A critical gap in our understanding of severe asthma is the ability to relate structural changes to important clinical outcomes. This thesis examines the relationship between CT assessed airway structure, airway inflammation and airway physiology in severe asthma patients. I first present the largest qualitative study of CT findings in severe asthma patients. I have shown that airway structural changes such as bronchiectasis and bronchial wall thickening are common and demonstrate association with disease duration and airflow obstruction. I then present a study describing airway and densitometry phantom models that were developed to study errors associated with quantitative airway morphometry and lung densitometry and device validation and standardisation methods for quantitative CT indices. In the next quantitative cross-sectional study, I report for the first time that right upper lobe apical bronchus (RB1) percent wall area (%WA) was associated with the preceding burden of neutrophilic inflammation over time measured by repeated sputum analysis. RB1 dimensions were not significantly different in four severe asthma phenotypes determined based on clinical and physiological indices. I also present a study demonstrating a decrease in RB1 wall dimensions after 1 year of treatment with mepolizumab (anti-IL-5) compared to placebo providing strong evidence in favour of the eosinophils playing a key role in airway remodelling determined by CT. Finally, I report for the first time three distinct asthma phenotypes identified based on CT assessed proximal and distal airway remodelling. Temporal assessment in severe asthma subjects demonstrates increase in RB1 wall dimensions over time but no change in RB1 lumen dimensions. These findings underpin the role of CT in multi-dimensional phenotyping of severe asthma.

# ACKNOWLEDGEMENTS

---

This thesis is the result of my initial meeting with Chris Brightling about four years ago to discuss a ‘small’ imaging project I was keen to get involved in. That project has grown to something much bigger over the years. During these years, I have worked with a great number of people whose contribution in assorted ways to the research work and shaping of this thesis deserves special mention. It is a pleasure to convey my gratitude to all those people in my humble acknowledgement.

First and foremost, I am grateful to all the patients and healthy subjects whose altruistic demeanor has made any of this possible.

It is difficult to overstate my gratitude to my supervisors Chris Brightling and James Entwisle. I have been very fortunate to have supervisors who gave me freedom to explore on my own and at the same time provide guidance to recover when my steps faltered. Chris reviewed my research data and writings with unbridled enthusiasm and offered painstakingly comprehensive comments. I read his comments on my work with a queer mix of gratitude (for his attention to smallest of details), exhilaration (as he always finds ways to dramatically improve it!) and jealousy (‘why did I not think of that?’). James, has been always there, to listen and give advice particularly on the radiological aspects of my work. He always encouraged me to think about the ‘clinical relevance’ in any research work that I chose to pursue. I am indebted to my supervisors for guiding me through this research project, immensely contributing to my professional development and most importantly teaching me invaluable life lessons.

I thank the members of my thesis committee and postgraduate tutors for keeping tab on my progress and providing me with insightful comments at various stages of my research. I also wish to acknowledge my colleagues and supervisors from the radiology department in Leicester and Boston who have encouraged me constantly and went out of their way to help me complete this thesis while training in radiology.

It has been a pleasure to work with senior members in the department. I sincerely thank Ian Pavord, Ruth Green, Peter Bradding and Andy Wardlaw who with their sound advice and constructive criticisms (during data presentation meetings) have helped me tremendously in improving my work.

I am grateful to David Parr and Deepak Subramanian for their help with densitometry phantom and standardisation on quantitative CT indices. I thank Sarah Hainsworth for her help with the development of airway phantom. Catalin Fetita provided us with MedView software and his collaboration has been very rewarding. I am thankful to VIDA Diagnostics team for providing their software and technical assistance. My thanks to Vimal Raj for being a mentor and a friend and academically stimulating me with new challenges from time to time.

I also wish to acknowledge Glaxo Smith Kline, The Wellcome trust and EvA study EU FP7 for funding this work.



I would like to acknowledge all my colleagues and fellow researchers. I thank Salman Siddiqui and Pranab Halder helping me with various aspects of my research project. Thanks to Dhananjay Desai, Mona Bafedhel, Manoj Menon, and Chandra Ohri who provided thought provoking and engaging research discussions and were great companions to go to conferences with. Thanks to Josh Agbetile for all his help with installing analysis software on my computer and troubleshooting any problems I encountered during electronic database setup. Thanks to Glenn Cruse, Mark Duffy, Camille Doe, Amanda Sutcliffe and Aarti Shikotra for making me feel welcome when I started working in the department and shared their office. Will Monteiro, Vijay Mistry and Mitesh Pancholi have been instrumental in processing sputum samples and deserve a special thank you.

I am grateful to research nurses Bev Hargadon, Maria Shelly, Sue McKenna and Michelle Bourne as well as research assistants Amisha Singapuri and Sarah Terry for their tremendous efforts with patient recruitment, clinical characterisation and electronic database completion. They were my colleagues when I started but over the years have become great friends. I also thank Dean Mawby, Anne Oldershaw and all the radiographers at Glenfield Hospital for their help with CT scanning and answering my innumerable technical questions about CT protocols and reconstruction algorithms.

Many thanks to Jean MacDonald and Gail Fretter for their assistance in many ways and much needed encouragement and humour.

I thank my friends outside work, who helped me remain sane by providing much needed distraction during the initial years and not criticising me for being unsocial when I got completely engrossed in work as the deadline approached.

I could not have done any of this without the love and support my family for which I am eternally grateful. I dedicate this thesis to the memory of my grandfather, Mohan Lal Gupta, who instilled in me the belief that no hard work goes unrewarded. My grandmother, Hari Priya Gupta, always had words of encouragement for me and assured me that there is light at the end of the tunnel. My parents, Pradeep Kumar Gupta and Shashi Gupta, had faith in me, and allowed me to be as ambitious as I wanted. My sister, Neha, whose support I have always treasured. Most importantly, special thanks to my wife, Renu who helped me in more ways than I could ever expect or imagine. She stood by me during every hindrance that I encountered and celebrated with me every small achievement. She stayed up late and worked weekends with me to troubleshoot Linux, fractal analysis and word processing problems. Her love, patience and persistent confidence in me kept me going. She is everything to me, suffice to say, I am searching for ways to make it up to her.

# STATEMENT DETAILING WORK PERSONALLY PERFORMED

---

All work was performed under supervision of Prof. Christopher E Brightling and Dr James Entwisle.

## **Study 1: Qualitative Analysis of High Resolution Computed Tomography Scans in Severe Asthma**

I collected the data for performing this study from the clinical database for patients attending the ‘Difficult Asthma Clinic’ at the Glenfield Hospital in Leicester. Thoracic radiologists at Glenfield Hospital evaluated HRCT scans. Dr Vimal Raj performed HRCT assessment for inter-observer reliability analysis. I planned the methodology for this study and performed all the analyses related to this study. I wrote the manuscript for the published study.

## **Study 2: Use of Airway and Densitometry Phantoms for Standardisation and Validation of Quantitative Computed Tomography Indices**

I was part of the research team involved in design of this study including the CT scanning protocols for the airway and densitometry phantoms. I performed all quantitative analysis using EmphyxlJ, MedView and PW2 software programs. Dr Deepak Subramanin performed the quantitative analysis using Pulmo software. Dr Salman Siddiqui and Prof. Sarah Hainsworth were involved in designing the airway phantom. Dr Deepak Subramanian, Dr David Parr and Dr Greg Gibbons were involved in designing the densitometry phantom.

### **Study 3: Quantitative Analysis of Airway Remodeling Using High Resolution Computed Tomography Scans in Severe Asthma**

I collected the data for performing this study from the clinical database for patients attending the 'Difficult Asthma Clinic' at the Glenfield Hospital in Leicester. I performed all the quantitative CT analysis for this study. Dr Salman Siddiqui performed quantitative CT assessment for inter-observer repeatability analysis. I planned the methodology for this study and performed all the analyses related to this study. I wrote the manuscript for the published study.

### **Study 4: Mepolizumab (Anti-IL 5) and Exacerbations of Refractory Eosinophilic Asthma**

I was part of the clinical team involved in recruitment and characterization of patients for this study. I performed all the quantitative CT analysis for this study. I was part of the research team involved in data analysis, data interpretation and writing the manuscript for this study.

### **Study 5: Asthma Phenotypes based on Quantitative Computed Tomography Analysis of Proximal and Distal Airway Remodelling**

I was involved in design of this study and writing the study protocol in conjunction with Prof. Chris Brightling and Dr James Entwisle. I have prepared all study related paperwork and obtained ethical approval for this study. I have developed standardised low-dose CT acquisition protocols for this study. I have also designed a password-protected electronic database using *Microsoft Access* for the purpose of this study. I was directly responsible for recruitment, review of inclusion / exclusion criteria and consent of all asthma and healthy subjects in this study. I personally supervised all CT scans for this study including explanation of breathing instructions to study subjects and practice

of breath-hold prior to inspiratory and expiratory CT scans. I performed approximately 15% of the clinical assessments. Experienced laboratory technician, Mr William Monteiro, performed sputum processing and cell count analysis. Full lung function analysis was performed in the respiratory physiology department by trained technicians. I have performed all quantitative CT analysis including airway morphometry, lung densitometry and fractal analysis for this study. I have also performed all statistical analysis and interpretation of data related to this study.

# PUBLICATIONS AND PRIZES

---

## Original Articles:

**Gupta S**, Siddiqui S, Haldar P, Raj JV, Entwisle JJ, Wardlaw AJ et al. Qualitative analysis of high-resolution CT scans in severe asthma. *Chest* 2009; 136(6):1521-1528.

**Gupta S**, Siddiqui S, Haldar P, Entwisle JJ, Mawby D, Wardlaw AJ et al. Quantitative analysis of high-resolution computed tomography scans in severe asthma subphenotypes. *Thorax* 2010; 65(9):775-781.

Haldar P, Brightling CE, Hargadon B, **Gupta S**, Monteiro W, Sousa A et al. Mepolizumab and exacerbations of refractory eosinophilic asthma. *N Engl J Med* 2009; 360(10):973-984.

Siddiqui S, **Gupta S**, Cruse G, Haldar P, Entwisle J, McDonald S, Whithers PJ, Hainsworth SV, Coxson HO, Brightling C. Airway wall geometry in asthma and nonasthmatic eosinophilic bronchitis. *Allergy*. 2009 Jun;64(6):951-8. Epub 2009 Feb 11.

Bafadhel M, Umar I, **Gupta S**, Raj JV, Vara DD, Entwisle JJ, Pavord ID, Brightling CE, Siddiqui S. The Role of CT Scanning in Multidimensional Phenotyping of COPD. *Chest*. 2011 Sep;140(3):634-42. Epub 2011 Mar 31.

Kulkarni NS, Hollins F, Sutcliffe A, Saunders R, Shah S, Siddiqui S, **Gupta S**, Haldar P, Green R, Pavord I, Wardlaw A, Brightling CE. Eosinophil protein in airway macrophages: a novel biomarker of eosinophilic inflammation in patients with asthma. *J Allergy Clin Immunol*. 2010 Jul;126(1):61-9.e3.

Zigler-Heitbrock L, Frankenberger M,...Brightling C, **Gupta S**. et al. The EvA Study: Aims and Strategy. *European Respiratory Journal* 2012 (accepted for publication).

## Review Articles and Book chapters:

**Gupta S**, Raj V, Castro M, Brightling CE. Imaging in severe asthma. *European Respiratory Monograph* 2011; 51:160-181.

**Gupta S\***, Walker C\*, Hartley R, Brightling CE. Computed tomography scans in severe asthma: utility and clinical implications. *Curr Opin Pulm Med*. 2012 Jan;18(1):42-7 (\* equal contribution).

Brightling CE, **Gupta S**, Gonem S, Siddiqui S. Lung Damage and Airway Remodelling in Severe Asthma Clinical and Experimental Allergy 2011(Epub ahead of print).

Brightling CE, **Gupta S**, Hollins F, Sutcliffe A, Amrani Y. Immunopathogenesis of severe asthma. Curr Pharm Des. 2011;17(7):667-73.

## **Prizes:**

1) The Royal College of Radiologists Ansell Poster Prize and RAD magazine first prize for best poster, UK Radiology Congress, June 2010.

2) Selected to present poster at SET for BRITAIN event 2010 in House of Commons, March 2010.

3) Travel bursary for European Congress of Radiology 2009, The Royal College of Radiologists, UK.

4) Nick Messios bursary for Radiological Society of North America 2010, Department of Radiology, University Hospital of Leicester NHS Trust.

## **Abstracts:**

**Gupta S**, Raj V, Pavord ID, Brightling CE, Entwisle JJ. **Radiological Bronchiectasis: Time to Re-think?** 96<sup>th</sup> Scientific Assembly and Annual Meeting, Radiological Society of North America (RSNA) 2010. Educational Exhibit, Poster presentation.

**Gupta S**, Raj V, Entwisle JJ, Brightling CE. **Quantitative Computed Tomography Assessment of Severe Asthma.** 96<sup>th</sup> Scientific Assembly and Annual Meeting, Radiological Society of North America (RSNA) 2010. Educational Exhibit, Poster presentation.

**Gupta S\***, Subramanian D\*, Brightling CE, Parr D. Comparison of computed tomography lung densitometry (CTLD) analysis software platforms for emphysema measurements. \*Equal contribution. 20<sup>th</sup> European Respiratory Society Annual Congress 2010. Thematic Poster Session.

**Gupta S. Scanning The Asthmatic Airway...With A Little Help From (Our) Friends.** Festival of Postgraduate Research, University of Leiceser. June 2010. Poster presentation.

**Gupta S, Raj JV, Fetita C, Mawby D, Entwisle JJ, Brightling CE. Standardisation of quantitative measures of airway remodelling in severe asthma using different software platforms.** UK Radiology Congress. June 2010. Poster presentation.

**Gupta S, Siddiqui S, Haldar P, Entwisle JJ, Mawby D, Wardlaw AJ, Bradding P, Pavord ID, Green RH, Brightling CE. Quantitative Analysis of High Resolution Computed Tomography Scans in Severe Asthma Sub-phenotypes.** UK Radiology Congress. June 2010. Poster presentation.

**Gupta S, Brightling CE. Scanning the Asthmatic Airway: Defining Relationship Between Physiology, Inflammation and Airway Structure in Severe Asthma using Computed Tomography.** SET for BRITAIN. March 2010. Poster presentation.

**Gupta S, Haldar P, Hargadon B et al. CT assessment of changes in airway dimensions with Mepolizumab treatment in refractory eosinophilic asthma.** American Thoracic Society International Conference 2009. Oral presentation.

**Gupta S, Clark R, Siddiqui S, Haldar P, Entwisle J, Green R, Pavord I, Wardlaw A, Brightling C.E. Quantitative assessment of airway remodeling in difficult asthma.** European Radiology supplements, ECR 2009 book of abstracts, volume 19, supplement 1, March 2009, B-439. Oral presentation.

**Gupta S, Siddiqui S, Haldar P et al. A qualitative radiological evaluation of difficult asthma cohort.** 94<sup>th</sup> Scientific Assembly and Annual Meeting, Radiological Society of North America (RSNA) 2008. Oral presentation.

**Gupta S, Siddiqui S, Mawby D, Entwisle J, Brightling C. Computational error in intrathoracic airway dimensions due to oblique orientation on computed tomography is correctable.** British Journal of Radiology Congress Series, Proceedings of UK Radiological Congress 2008:33. Oral presentation.

**Gupta S, Siddiqui S, Hainsworth S.V., Mawby D, Entwisle J, McDonald S, Withers P.J., Brightling C.E. Validation of airway wall volume using micro-CT.** European Radiology supplements, ECR 2008 book of abstracts, volume 18, supplement 1, February 2008, C-245. Poster presentation.

**Gupta S, Siddiqui S, Haldar P, Berry M, Entwisle J, Green R, Pavord I.D., Wardlaw A.J., Brightling C.E. A qualitative analysis of HRCT scans in difficult asthma.** Thorax, December 2007, vol. 62, supplement III, S11. Oral presentation.

**Gupta S, Siddiqui S, Mawby D et al. Oblique orientation of airways does not influence the measurement of computed tomography percentage wall area.** 17<sup>th</sup> European Respiratory Society Annual Congress 2007. Poster presentation.

**Gupta S, Siddiqui S, Haldar P et al. Bronchiectasis and bronchial wall thickening are common features of severe asthma.** 17<sup>th</sup> European Respiratory Society Annual Congress 2007. Poster presentation.



# CONTENTS

---

<b>1</b>	<b>INTRODUCTION .....</b>	<b>1</b>
<b>1.1</b>	<b>Asthma .....</b>	<b>2</b>
1.1.1	Asthma definition and epidemiology.....	3
1.1.2	Severe asthma: A global burden .....	4
1.1.3	Pathogenesis of severe asthma.....	5
1.1.3.1	Severe asthma: A complex heterogeneous disease .....	5
1.1.3.2	Airway Inflammation in severe asthma.....	6
1.1.3.3	Airway remodelling in severe asthma .....	9
1.1.3.4	Functional impairment in severe asthma.....	19
1.1.4	Phenotyping severe asthma.....	22
1.1.5	Figures and Tables .....	25
<b>1.2</b>	<b>Imaging in Severe Asthma .....</b>	<b>30</b>
1.2.1	Computed Tomography in Severe Asthma.....	30
1.2.1.1	Historical overview .....	30
1.2.1.2	Qualitative assessment of CT scans in severe asthma.....	31
1.2.1.3	Quantitative assessment of proximal airways in severe asthma.....	32
1.2.1.4	Quantitative assessment of distal airways in severe asthma .....	37
1.2.1.5	Fractals and asthma .....	40
1.2.1.6	CT associated radiation exposure and risks .....	41
1.2.1.7	New developments in CT technology .....	44
1.2.2	Other imaging techniques in asthma.....	47
1.2.2.1	Chest radiographs .....	47
1.2.2.2	Endobronchial ultrasound.....	48

1.2.2.3	Positron emission tomography .....	49
1.2.2.4	Magnetic resonance imaging .....	50
1.2.2.5	Optical coherence tomography .....	53
1.2.2.6	Confocal florescence endomicroscopy .....	54
1.2.2.7	Molecular imaging .....	54
1.2.3	Figures and Tables .....	56
<b>1.3</b>	<b>Hypotheses.....</b>	<b>57</b>
<b>1.4</b>	<b>Aims .....</b>	<b>58</b>
<b>2</b>	<b>METHODS .....</b>	<b>60</b>
<b>2.1</b>	<b>Clinical Methods .....</b>	<b>61</b>
2.1.1	Baseline demographics and history .....	61
2.1.2	Peripheral blood .....	61
2.1.3	Allergen skin testing .....	61
2.1.4	Spirometry and lung function tests .....	62
2.1.5	Fractional exhaled nitric oxide .....	62
2.1.6	Methacholine challenge test .....	62
2.1.7	Sputum Induction.....	63
2.1.8	Asthma symptom and quality of life scores .....	64
2.1.8.1	Juniper Asthma Control Questionnaire (JACQ) score .....	64
2.1.8.2	Visual Analogue Scale .....	65
2.1.8.3	Juniper Asthma Quality of Life Questionnaire (AQLQ).....	65
<b>2.2</b>	<b>Laboratory Methods.....</b>	<b>66</b>
2.2.1	Sputum processing protocol .....	66
<b>2.3</b>	<b>Radiological Methods .....</b>	<b>67</b>
2.3.1	Computed Tomography scanning protocols .....	67

2.3.1.1	Standard high-resolution computed tomography (HRCT).....	67
2.3.1.2	Limited CT imaging protocol for right upper lobe apical bronchus .....	67
2.3.1.3	Full thoracic inspiratory and expiratory CT protocol.....	68
2.3.2	Analysis of Computed Tomography scans .....	69
2.3.2.1	Qualitative analysis .....	69
2.3.2.2	Quantitative Analysis .....	70
2.3.3	Computed Tomography radiation safety .....	77
2.4	<b>Figures and Tables.....</b>	<b>78</b>
3	<b>STUDIES .....</b>	<b>89</b>
3.1	<b>STUDY 1: Qualitative Analysis of High Resolution Computed Tomography Scans in Severe Asthma. ....</b>	<b>90</b>
3.1.1	Abstract.....	90
3.1.2	Introduction.....	92
3.1.3	Methods .....	93
3.1.3.1	Subjects .....	93
3.1.3.2	Clinical Characterisation .....	94
3.1.3.3	HRCT scanning protocol and qualitative analysis .....	94
3.1.3.4	Statistical analysis .....	94
3.1.4	Results.....	96
3.1.5	Discussion.....	98
3.1.6	Figures and Tables.....	103
3.2	<b>STUDY 2: Use of Airway and Densitometry Phantoms for Standardisation and Validation of Quantitative Computed Tomography Indices .....</b>	<b>109</b>
3.2.1	Abstract.....	109
3.2.2	Introduction.....	111
3.2.3	Materials and Methods .....	114

3.2.3.1	Phantom models for validation of quantitative CT airway morphometry.....	114
3.2.3.2	Steromicroscopy and micro-CT .....	115
3.2.3.3	CT scanning of airway phantoms .....	116
3.2.3.4	Two-dimensional quantitative analysis of airway phantom tubes using EmphylxJ software.....	116
3.2.3.5	Three-dimensional quantitative analysis of airway phantom tubes using Pulmonary Workstation 2 software.....	120
3.2.3.6	Phantom models for validation of quantitative CT densitometry analysis .....	121
3.2.3.7	CT lung densitometry .....	122
3.2.3.8	Statistical Analysis .....	124
3.2.4	Results.....	125
3.2.4.1	Comparison of cross sectional geometry using micro CT and stereomicroscopy.....	125
3.2.4.2	Accuracy of airway morphometry assessed using EmphylxJ .....	125
3.2.4.3	Influence of oblique orientation on CT airway morphometry assessed using EmphylxJ .....	126
3.2.4.4	Correction methodology for size and oblique orientation associated errors in CT airway morphometry assessed using EmphylxJ .....	126
3.2.4.5	Effect of varying tube current-time product (mAs) on CT airway morphometry assessed using EmphylxJ.....	127
3.2.4.6	Inter-scanner variability in CT airway morphometry assessed using EmphylxJ and validation of proposed standardisation methodology .....	127
3.2.4.7	Inter-software variability in CT airway morphometry .....	128
3.2.4.8	Accuracy of airway morphometry assessed using PW2.....	128
3.2.4.9	Inter-scanner variability in CT airway morphometry assessed using PW2 .....	129
3.2.4.10	Inter-scanner variability in CT lung densitometry and validation of proposed standardisation methodology .....	129
3.2.4.11	Inter-software variability in CT lung densitometry.....	130
3.2.4.12	Inter-observer and intra-observer variability in CT lung densitometry.....	130
3.2.5	Discussion.....	131

3.2.6	Figures and Tables .....	136
<b>3.3</b>	<b>STUDY 3: Quantitative Analysis of Airway Remodelling Using High Resolution Computed Tomography Scans in Severe Asthma. ....</b>	<b>164</b>
3.3.1	Abstract.....	164
3.3.2	Introduction.....	166
3.3.3	Methods .....	167
3.3.3.1	Subjects .....	167
3.3.3.2	HRCT scanning protocol and quantitative airway morphometry.....	168
3.3.3.3	Data analysis.....	170
3.3.3.4	Statistical analysis .....	171
3.3.4	Results.....	172
3.3.4.1	Assessment of inter-observer variability of RB1 dimensions .....	172
3.3.4.2	Variability of RB1 dimensions across its length .....	172
3.3.4.3	Severe asthma patients dichotomised into clinically relevant groups .....	173
3.3.4.4	Unbiased phenotyping of severe asthma subjects using cluster analysis. ....	173
3.3.4.5	Univariate and multiple regression analysis to explore structure and function relationship in severe asthma.....	175
3.3.5	Discussion.....	176
3.3.6	Figures and Tables.....	182
<b>3.4</b>	<b>STUDY 4: Mepolizumab (Anti-IL-5) and Exacerbations of Refractory Eosinophilic Asthma .....</b>	<b>197</b>
3.4.1	Abstract.....	197
3.4.2	Introduction.....	199
3.4.3	Methods .....	200
3.4.3.1	Subjects .....	200
3.4.3.2	Design of the study.....	201
3.4.3.3	Safety Assessment.....	204

3.4.3.4	Statistical analysis .....	204
3.4.4	Results.....	205
3.4.4.1	Enrolment and baseline characteristics .....	205
3.4.4.2	Efficacy .....	206
3.4.5	Discussion.....	210
3.4.6	Figures and Tables.....	213
<b>3.5</b>	<b>Study 5: Asthma Phenotypes based on Quantitative Computed Tomography Analysis of Proximal and Distal Airway Remodelling .....</b>	<b>222</b>
3.5.1	Abstract.....	222
3.5.2	Introduction.....	224
3.5.3	Methods .....	226
3.5.3.1	Study Design .....	226
3.5.3.2	Subjects .....	227
3.5.3.3	Computed tomography imaging.....	228
3.5.3.4	Quantitative airway and air trapping analysis using automated software .....	228
3.5.3.5	Statistical Analysis .....	229
3.5.4	Results.....	231
3.5.4.1	Adequacy of breath-hold on inspiratory and expiratory CT scans.....	232
3.5.4.2	Proximal airway remodelling .....	232
3.5.4.3	Air-trapping as indirect measure of distal airway remodelling.....	233
3.5.4.4	Fractal dimension .....	233
3.5.4.5	Univariate analysis to explore structure-function relationship and proximal–distal airway remodelling relationship in asthma.....	233
3.5.4.6	Unbiased CT phenotyping of asthma subjects using factor and cluster analysis.....	234
3.5.4.7	Temporal assessment of subset of eosinophilic severe asthma subjects .....	236
3.5.4.8	Effective radiation dose for research CT scans .....	237

3.5.5	Discussion.....	238
3.5.6	Figures and Tables.....	248
<b>4</b>	<b>CONCLUSIONS.....</b>	<b>273</b>
<b>4.1</b>	<b>Final discussions and critique.....</b>	<b>274</b>
4.1.1	CT assessed structural changes in severe asthma .....	274
4.1.2	Relationship between structure (assessed by CT), function and inflammation in severe asthma .....	276
4.1.3	Standardisation of quantitative CT indices.....	277
4.1.4	Role of CT in phenotyping asthma.....	277
4.1.5	Criticisms.....	278
<b>4.2</b>	<b>Key questions arising from this thesis and future directions .....</b>	<b>280</b>

# TABLE OF FIGURES

---

FIGURE 1.1: AMERICAN THORACIC SOCIETY CLINICAL CRITERIA FOR DIAGNOSIS OF REFRACTORY ASTHMA .....	25
FIGURE 1.2: IMMUNOPATHOGENESIS OF ASTHMA .....	26
FIGURE 1.3: STRUCTURE-FUNCTION RELATIONSHIP IN ASTHMATIC AIRWAYS .....	27
FIGURE 1.4: MULTI-DIMENSIONAL HETEROGENEITY IN SEVERE ASTHMA.....	28
FIGURE 1.5: AIR-TRAPPING QUANTIFICATION INDICES .....	56
FIGURE 2.1: STANDARD HRCT SEQUENTIAL SCANNING .....	78
FIGURE 2.2: LIMITED THORACIC CT SCAN OF RB1 BRONCHUS .....	79
FIGURE 2.3: ELECTRON DENSITY RODS.....	80
FIGURE 2.4: BRONCHIECTASIS: CT DIAGNOSTIC CRITERIA.....	81
FIGURE 2.5: FULL-WITH AT HALF MAXIMUM METHOD OF 2-D QUANTITATIVE AIRWAY MORPHOMETRY .....	83
FIGURE 2.6: SEGMENTATION AND 3-D AIRWAY MORPHOMETRY USING VIDA PW2 SOFTWARE .....	84
FIGURE 2.7: PULMONARY DENSITOMETRY USING VIDA PW2 SOFTWARE.....	85
FIGURE 2.8: STANDARDISATION OF DENSITOMETRY INDICES.....	86
FIGURE 2.9: FRACTAL ANALYSIS OF SEGMENTED AIRWAY TREE USING FRACLAC (IMAGEJ) SOFTWARE .....	87
FIGURE 2.10: FRACTAL DIMENSION OF LOW ATTENUATION AREAS IN LUNGS.....	88
FIGURE 3.1: QUALITATIVE CT CHARACTERISATION OF SEVERE ASTHMA.....	103
FIGURE 3.2: ROC CURVE .....	104
FIGURE 3.3: LEICESTER AIRWAY PHANTOM .....	136
FIGURE 3.4: CTP674 PHANTOM, THE PHANTOM LABORATORY .....	137



FIGURE 3.5: STEREOMICROSCOPE IMAGE OF LAP TUBE.....	138
FIGURE 3.6: OBLIQUE ORIENTATION OF LAP TUBE.....	139
FIGURE 3.7: PHANTOM TUBE MORPHOMETRY USING PW2 SOFTWARE .....	140
FIGURE 3.8: WARWICK DENSITOMETRY PHANTOM .....	141
FIGURE 3.9: BLAND-ALTMAN PLOTS, INTER-OBSERVER REPEATABILITY USING EMPHYLXJ .....	142
FIGURE 3.10: COMPARISON OF LAP TUBE MORPHOMETRY USING FWHM METHOD AND STEROMICROSCOPE .....	143
FIGURE 3.11: INFLUENCE OF OBLIQUE ORIENTATION ON LUMEN AREA .....	144
FIGURE 3.12: INFLUENCE OF OBLIQUE ORIENTATION ON WALL AREA .....	145
FIGURE 3.13: INFLUENCE OF OBLIQUE ORIENTATION ON PERCENT WALL AREA.....	146
FIGURE 3.14: CORRECTION OF SIZE AND OBLIQUE ORIENTATION ASSOCIATED ERRORS IN CT AIRWAY MORPHOMETRY .....	147
FIGURE 3.15: INFLUENCE OF STANDARDISATION ON INTER-SCANNER VARIABILITY IN %WA .....	148
FIGURE 3.16: BLAND-ALTMAN PLOTS, INTRA-OBSERVER REPEATABILITY USING PW2. ....	149
FIGURE 3.17: ACCURACY OF AIRWAY MORPHOMETRY ASSESSED USING PW2.....	150
FIGURE 3.18: INTER-SCANNER VARIABILITY IN AIRWAY MORPHOMETRY ASSESSED USING PW2 .....	151
FIGURE 3.19: INFLUENCE OF STANDARDISATION ON INTER-SCANNER VARIABILITY IN PERC15 .....	152
FIGURE 3.20: COMPARISON OF LUNG DENSITOMETRY USING PW2 AND PULMO .....	153
FIGURE 3.21: INTER-OBSERVER VARIABILITY IN CT LUNG DENSITOMETRY .....	154
FIGURE 3.22: INTRA-OBSERVER VARIABILITY IN CT LUNG DENSITOMETRY.....	155
FIGURE 3.23: INTER-OBSERVER VARIABILITY OF RB1 %WA .....	182
FIGURE 3.24: RB1 LA/BSA .....	183

FIGURE 3.25: RB1 %WA.....	184
FIGURE 3.26: RB1 %WA AND RB10 %WA .....	185
FIGURE 3.27: RB1 %WA AND POST BRONCHODILATOR FEV1 %PREDICTED .....	186
FIGURE 3.28: RB1 %WA AND SPUTUM NEUTROPHILS AUC (%).....	187
FIGURE 3.29: DESIGN OF THE STUDY .....	213
FIGURE 3.30: SCREENING, ENROLMENT AND RANDOMISATION OF STUDY SUBJECTS.....	214
FIGURE 3.31: SEVERE EXACERBATIONS DURING THE COURSE OF THE STUDY .....	215
FIGURE 3.32: COMPARISON OF STUDY OUTCOMES BETWEEN STUDY GROUPS.....	216
FIGURE 3.33: COMPARISON CT ASSESSED STUDY OUTCOMES BETWEEN STUDY GROUPS	217
FIGURE 3.34: QUANTITATIVE CT IN HEALTHY AND SEVERE ASTHMA SUBJECTS .....	249
FIGURE 3.35: FRACTAL DIMENSION OF SEGMENTED AIRWAY TREE .....	250
FIGURE 3.36: COMPONENT NUMBER BASED ON KAISER CRITERION .....	251
FIGURE 3.37: PROXIMAL AIRWAY REMODELLING IN ASTHMA PHENOTYPES .....	252
FIGURE 3.38: TEMPORAL CHANGE IN RB1 WA/BSA.....	253
FIGURE 3.39: TEMPORAL CHANGE IN RB1 LA/BSA .....	254
FIGURE 3.40: TEMPORAL ASSESSMENT OF AIRWAY REMODELLING IN ASTHMA CLUSTERS .....	255

# LIST OF TABLES

---

TABLE 1.1: INNOVATIVE MEDICINES INITIATIVE (IMI) SEVERE REFRACTORY ASTHMA DEFINITION (2011) .....	29
TABLE 3.1: BASELINE CLINICAL CHARACTERISTICS OF DIFFICULT ASTHMA COHORT .....	105
TABLE 3.2: CLINICAL CHARACTERISTICS OF INDIVIDUAL GROUPS .....	106
TABLE 3.3: LOGISTIC REGRESSION .....	107
TABLE 3.4: CTP674 PHANTOM TUBE MEASUREMENTS .....	156
TABLE 3.5: LEICESTER AIRWAY PHANTOM TUBE MEASUREMENTS .....	157
TABLE 3.6: SCANNER-SPECIFIC IMAGING PROTOCOLS .....	158
TABLE 3.7: EFFECT OF VARYING TUBE CURRENT-TIME PRODUCT (MAS) ON AIRWAY DIMENSIONS .....	159
TABLE 3.8: MEAN AIRWAY MEASUREMENTS OF THE CTP674 PHANTOM IMAGED AT EACH EVA CENTRE. ....	160
TABLE 3.9: IMAGING PROTOCOLS USED FOR VALIDATION OF INTER-SCANNER DENSITOMETRY STANDARDISATION .....	161
TABLE 3.10: INTER-SOFTWARE VARIABILITY IN CT AIRWAY MORPHOMETRY .....	162
TABLE 3.11: INTER-SOFTWARE VARIABILITY IN CT LUNG DENSITOMETRY .....	163
TABLE 3.12: SEVERE ASTHMA WITH OR WITHOUT CHRONIC PERSISTENT AIRFLOW OBSTRUCTION .....	188
TABLE 3.13: SEVERE ASTHMA SUBJECTS DICHOTOMISED BASED ON SMOKING HISTORY .....	189
TABLE 3.14: SEVERE ASTHMA SUBJECTS DICHOTOMISED BASED ON GENDER .....	190
TABLE 3.15: EOSINOPHILIC AND NON-EOSINOPHILIC SEVERE ASTHMA .....	191
TABLE 3.16: CLINICAL CHARACTERISTICS OF SEVERE ASTHMA CLINICAL PHENOTYPES AND HEALTHY CONTROLS .....	192
TABLE 3.17: RB1 DIMENSIONS .....	194

TABLE 3.18: UNIVARIATE ANALYSIS OF RELATIONSHIP BETWEEN RB1 DIMENSIONS AND CLINICAL INDICES. ....	195
TABLE 3.19: STANDARD MULTIPLE REGRESSION.....	196
TABLE 3.20: BASELINE CHARACTERISTICS OF SUBJECTS IN THE INTENTION-TO-TREAT POPULATION .....	218
TABLE 3.21: OVERVIEW AND COMPARISON OF CHANGES IN SECONDARY OUTCOMES AFTER TREATMENT WITH MEPOLIZUMAB OR PLACEBO .....	220
TABLE 3.22: REPORTED ADVERSE EVENTS DURING THE 50-WEEK TREATMENT PHASE OF THE STUDY.....	221
TABLE 3.23: CLINICAL CHARACTERISTICS OF ASTHMATIC AND HEALTHY SUBJECTS.....	256
TABLE 3.24: RB1 DIMENSIONS OF ASTHMATIC AND HEALTHY SUBJECTS.....	258
TABLE 3.25: OTHER PROXIMAL AIRWAY DIMENSIONS.....	259
TABLE 3.26: DIMENSIONS OF HYPOTHETIC AIRWAYS (Pi10, Po20) .....	260
TABLE 3.27: DENSITOMETRY INDICES IN ASTHMATIC AND HEALTHY SUBJECTS .....	261
TABLE 3.28: FRACTAL DIMENSIONS .....	262
TABLE 3.29: UNIVARIATE ANALYSIS OF RELATIONSHIP BETWEEN PROXIMAL AIRWAY DIMENSIONS ON INSPIRATORY SCAN AND CT AIR-TRAPPING INDICES. ....	263
TABLE 3.30: UNIVARIATE ANALYSIS OF RELATIONSHIP BETWEEN PROXIMAL AIRWAY DIMENSIONS ON INSPIRATORY SCAN AND CLINICAL INDICES. ....	264
TABLE 3.31: UNIVARIATE ANALYSIS OF RELATIONSHIP BETWEEN CT AIR-TRAPPING INDICES AND CLINICAL INDICES. ....	265
TABLE 3.32: COMPONENT LOADING OF SELECTED VARIABLES .....	266
TABLE 3.33: CLINICAL CHARACTERISTICS OF ASTHMA PHENOTYPES.....	267
TABLE 3.34: QUANTITATIVE CT INDICES OF ASTHMA PHENOTYPES .....	269
TABLE 3.35: BETWEEN-GROUP AND WITHIN-GROUP CHANGES IN RB1 DIMENSIONS AT THREE TIME POINTS.....	271
TABLE 3.36: RADIATION RISK ASSOCIATED WITH COMMON RADIOLOGICAL EXAMINATIONS IN UK COMPARED TO RESEARCH CT EXAMINATIONS .....	272

# ABBREVIATIONS

%WA	Percent Wall Area
%WT	Percent Wall Thickness
%WV	Percent Wall Volume
129-Xenon	$^{129}\text{Xe}$
3-Helium	$^3\text{He}$
3D	Three-dimensional
ABPA	Allergic Bronchopulmonary Aspergillosis
AC	Asthma Clusters
AHR	Airway Hyperresponsiveness
aOCT	Anatomical Optical Coherence Tomography
AQLQ	Juniper Asthma Quality of Life Questionnaire
ASM	Airway Smooth Muscle
ATS	American Thoracic Society
AUC	Area under the curve
BAL	Bronchoalveolar Lavage
BDP	Beclometasone Dipropionate
BE	Bronchiectasis
BMI	Body Mass Index
BronInt	Bronchus Intermedius
BSA	Body Surface Area
BTS	British Thoracic Society
BWT	Bronchial Wall Thickening
CFD	Computational Fluid Dynamics
cGy	Centigray
CI	Confidence Interval
COPD	Chronic Obstructive Pulmonary Disease
CS	Corticosteroids
CT	Computed Tomography
CTDI <sub>vol</sub>	Volume CT Dose Index
DAC	Difficult Asthma Clinic
DALYs	Disability Adjusted Life Years
D <sub>av</sub>	Averaged Fractal Dimension
D <sub>e</sub>	Most-efficient cover Fractal Dimension

DLP	Dose-length Product
Dmax	Maximum Airway Lumen Diameter
Dmin	Minimum Airway Lumen Diameter
D <sub>sc</sub>	Slope-corrected Fractal Dimension
D <sub>sce</sub>	Slope-corrected most-efficient covering Fractal Dimension
EA	Eosinophilic Asthma
EB	Eosinophilic Bronchitis
EBB	Endobronchial Biopsy
EBUS	Endobronchial Ultrasound
ECM	Extracellular Matrix
ECP	Eosinophilic Cationic Protein
ED	Effective Dose
EDCE	Energy Driven Contour Estimation
EDR	Electron Density Rods
ERR	Excess Relative Risk
ERS	European Respiratory Society
EvA	Emphysema versus Airway Disease
FAO	Fixed Airflow Obstruction
FD	Fractal Dimension
FE <sub>NO</sub>	Fraction of Exhaled Nitric Oxide
FEV <sub>1</sub>	Forced Expiratory Volume in 1 Second
FMT	Fluorescence Molecular Tomography
FRC	Functional Residual Capacity
FVC	Forced Vital Capacity
FWHM	Full Width at Half Maximum
GINA	Global Initiative for Asthma
HC	Healthy Control
HP	Hyperpolarised
HRCT	High Resolution Computed Tomography
HU	Hounsfield Unit
IA	Incident Angle
ICC	Intraclass Correlation
ICRP	International Commission on Radiological Protection
IFM	Image Functional Modelling
IL	Interleukin
IMI	Innovative Medicine Initiative
IQR	Interquartile Range

JACQ	Juniper Asthma Control Questionnaire
JPEG	Joint Photographic Experts Group
kVp	Peak Kilovoltage
LA	Lumen Area
LABA	Long Acting $\beta_2$ Agonist
LAC	Low Attenuation Clusters
LAP	Leicester Airway Phantom
LB	Left Bronchus
LNT	Linear No-threshold Hypothesis
LTB4	Leukotriene B4
LTRA	Leukotriene receptor antagonist
LV	Lumen Volume
MA	Mild / Moderate Asthma
mAs	Milliampere-seconds
MC (TC)	Mast Cell Tryptase <sup>+</sup> Chymase <sup>+</sup>
MDCT	Multi-detector Computed Tomography
MIP	Macrophage Inflammatory Protein
MLD	Mean Lung Density
MLD E/I	Mean Lung Density Expiratory to Inspiratory Ratio
MMP-9	Matrix Metalloproteinase-9
MRI	Magnetic Resonance Imaging
mSv	Milli-sievert
NC	Normalised Effective Dose Coefficients
NEA	Non-eosinophilic Asthma
NIRF	Near-infrared Fluorescent
NPV	Negative Predictive Value
OCT	Optical Coherence Tomography
OX40L	OX40ligand
PBS	Phosphate Buffered Saline
PC <sub>20</sub> MCh	Provocative concentration of methacholine causing a 20% fall in FEV <sub>1</sub>
PEF	Peak Expiratory Flow
Perc15	15 <sup>th</sup> Percentile Point
PET	Positron Emission Tomography
PG	Prostaglandin
Pi	Internal Airway Perimeter
Pi10	Hypothetic Airway with Pi of 10 mm

Po	Outer Airway Perimeter
Po20	Hypothetic Airway with Po of 20 mm
PPV	Positive Predictive Value
PU	Polyurethane
Pulmo	Pulmo-CMS Software
PW2	VIDA Pulmonary Workstation version 2.0
RB	Right Bronchus
RB1	Right Upper Lobe Apical Segmental Bronchus
RB10	Right B10 Bronchus
RBM	Reticular Basement Membrane
RMB	Right Main Bronchus
ROC	Receiver Operating Characteristic
ROI	Region of Interest
RUL	Right Upper Lobe Bronchus
SA	Severe Asthma
SEM	Standard Error of Mean
SPECT	Single Photon Emission Tomography
Sv	Sievert
TA	Total Area
TBB	Transbronchial Biopsy
Tc1	CD8+ T cells type 1
TGF- $\beta$	Transforming Growth Factor-beta
Th1	T helper cell type 1
Th2	T helper cell type 2
TIMP-1	Tissue Inhibitor of Metalloproteinases-1
TLC	Total Lung Capacity
TNF	Tumour Necrosis Factor
TSLP	Thymic Stromal Lymphopoietin
TV	Total Volume
VAO	Variable Airflow Obstruction
VEGF	Vascular Endothelial Growth Factor
VI	Voilex Index
VL <sub>850</sub> E-I	VI-850 change on paired inspiratory and expiratory CT scans
VL <sub>850-950</sub> E-I	Voxel index change of percent voxels between -950 HU and -850 HU on paired inspiratory and expiratory CT scan
WA	Wall Area
WDP	Warwick Densitometry Phantom



WHO	World Health Organisation
WT	Wall Thickness
WV	Wall Volume

# 1 INTRODUCTION

---

## 1.1 Asthma

From its first account to present day, meaning of asthma and its description has changed several times. Asthma is a Greek word that is derived from the verb *aazein*, meaning to exhale with open mouth, to pant. 'Asthma,' as a descriptive term for shortness of breath, first appeared in The Iliad of Homer, but the earliest text where the word is found as a medical term is the *Corpus Hippocraticum*.<sup>1</sup> More advanced clinical description of asthma was provided by a Greek physician, Aretaeus of Cappadocia (100 A.D.). Lucius Annaeus Seneca, Roman orator, author and statesman likened his asthma attacks to a “last gasp” and wrote ‘*nothing seems to me more troublesome*’. Bernardino Ramazzini, an Italian physician in the early 18<sup>th</sup> century, studied bakers, mill workers, and farmers and described a link between certain patients’ asthma and their specific occupations. It was only in mid-nineteenth century that asthma was recognised as disease of variable airflow obstruction and was defined as ‘*Paroxysmal dyspnea of a peculiar character with intervals of healthy respiration between attacks*’ by Dr Henry Hyde Salter following observations made on 50 patients in London and published in his treatise *On Asthma and its Treatment*.<sup>2</sup> Detailed descriptions of asthma including clinical observation, physiology and pathology was provided for the first time by William Osler in his 1860 publication *Principles and Practice of Medicine*.<sup>3</sup> Airway inflammation was included in asthma definition after airway sampling was made possible by bronchoscopy.<sup>4</sup>

### 1.1.1 Asthma definition and epidemiology

Asthma is complex disease characterized by typical symptoms of breathlessness, wheeze and cough together with episodes of marked worsening of symptoms known as exacerbations.<sup>5</sup> These symptoms occur on a background of disordered airway physiology characterised by variable airflow limitation, airway hyperresponsiveness and in more severe disease persistent airflow obstruction. The symptoms and airway dysfunction are a consequence of complex interactions between infiltrating inflammatory cells and the structural elements in the airway wall. These interactions lead onto persistent airway inflammation and remodelling which underpin the immunopathogenesis of asthma. The Global Initiative For Asthma (GINA) report (2010 update)<sup>5</sup> defines asthma as *'a chronic inflammatory disorder of the airways in which many cells and cellular elements play a role. The chronic inflammation is associated with airway hyperresponsiveness that leads to recurrent episodes of wheezing, breathlessness, chest tightness, and coughing, particularly at night or in the early morning. These episodes are usually associated with widespread, but variable, airflow obstruction within the lung that is often reversible either spontaneously or with treatment.'*<sup>5</sup>

Asthma affects an estimated population of 300 million worldwide with prevalence in UK being one of the highest in the developed world.<sup>6</sup> The global prevalence of asthma continues to rise, though there is evidence suggesting that international differences in asthma prevalence have been reduced.<sup>7</sup> Asthma is responsible for loss of 15 million disability-adjusted life years (DALYs) annually representing 1% of the total global disease burden as estimated by the World Health Organisation (WHO).<sup>6</sup> Although asthma deaths

have been falling since the 1980s, approximately 250,000 patients worldwide die from asthma annually.<sup>6</sup>

### **1.1.2 Severe asthma: A global burden**

Majority of patients who suffer from asthma have mild to moderate disease, which is well controlled by a combination anti-inflammatory drugs, particularly corticosteroids and  $\beta$ 2-adrenoreceptor agonists. Previous GINA reports classified asthma severity based on the level of patient symptoms, airflow limitation and lung function variability into four categories: (i) intermittent, (ii) mild persistent, (iii) moderate persistent, and (iv) severe persistent.<sup>5</sup> This classification was only valid for patients not on inhaled corticosteroid treatment. Erroneous use of this classification for patients on treatment as well as its limited value in predicting patient's requirement of treatment and response, has led to change in emphasis to treatment-based classification. Current GINA<sup>5</sup> and BTS<sup>8</sup> guidelines describe a five-step treatment approach driven by patients' asthma control status. Asthma that requires high intensity treatment (treatment level equivalent to at least GINA step 4) to maintain good control or where good control is not achieved despite high intensity treatment is classed as severe asthma.<sup>5,9</sup>

Approximately 5-10% of asthma patients suffer from severe and/or difficult-to-treat asthma.<sup>10</sup> This severe asthma group is important as these patients suffer severe morbidity, are at a particularly high risk of death<sup>11</sup> and consume a disproportionately high amount of healthcare resources attributed to asthma through unscheduled visits and use of emergency services.<sup>12</sup> One asthma related death occurs every hour in Western Europe according to the

WHO,<sup>13</sup> majority of which are preventable. It is therefore not surprising that the economic burden of asthma in Europe is estimated at 17.7 billion euros a year, in addition to lost productivity estimated at 9.8 billion euros.<sup>14</sup>

### **1.1.3 Pathogenesis of severe asthma**

#### **1.1.3.1 Severe asthma: A complex heterogeneous disease**

Various severe / difficult-to-treat asthma definitions have been proposed through national and international guidelines including those proposed by the European Respiratory Society (ERS) and American Thoracic Society (ATS) [Figure 1.1].<sup>5,8,9,15-17</sup> These definitions include an assessment of asthma control, exacerbating factors / comorbidities and response to treatment. More recently the WHO<sup>18</sup> and Innovative Medicine Initiative (IMI)<sup>19</sup> have proposed severe / difficult-to-treat asthma definitions that include asthma groups with sub-optimal treatment which may be secondary to various factors. WHO defines severe asthma as *‘Uncontrolled asthma which can result in risk of frequent severe exacerbations (or death) and / or adverse reactions to medications and / or chronic morbidity (including impaired lung function or reduced lung growth in children).’* Three severe asthma subgroups are identified: (1) untreated severe asthma, an enormous problem in areas of the world where current therapies for asthma are not widely available; (2) difficult-to-treat (but potentially responsive) asthma; and (3) treatment-resistant severe asthma, which is further differentiated into two sub-groups: (a) control can be maintained only with the highest level of recommended treatment; and (b) control not achieved despite highest level of recommended treatment (refractory asthma and corticosteroid-resistant asthma). IMI have

proposed an umbrella term ‘problematic severe asthma’, which includes all asthma and asthma-like symptoms that remain uncontrolled despite the prescription of high-intensity asthma treatment. The consensus statement then divided problematic severe asthma into two groups: (1) difficult asthma, a group in whom the disease itself may not be severe but poor compliance, persistence of triggers, and untreated comorbidities make it difficult to control; and (2) severe refractory asthma, a term reserved for patients with persistent poor control, frequent exacerbations despite compliance to high-intensity treatment and treatment comorbidities (Table 1.1). Recent definitions of severe asthma, although resolving confusion between overlapping nomenclature such as severe, difficult or treatment-resistant asthma, still rely primarily on non-specific clinical characteristics. Variations in definition of severe asthma accentuate the fact that it is a heterogeneous disorder with different clinical and pathophysiological characteristics.<sup>10</sup> A recent report presenting cross-sectional data on 382 patients with severe refractory asthma from four UK centres as part of British Thoracic Society (BTS) Difficult Asthma Network, found that despite having standard ATS definition and assessment protocols differences in multiple characteristics, including disease severity were demonstrated, further supporting the heterogeneous nature of this disease.<sup>20</sup> Severe asthma heterogeneity is also highlighted by different phenotypes identified using cluster analysis.<sup>21,22</sup> I have discussed various aspects of severe asthma phenotyping [section 1.1.4].

### **1.1.3.2 Airway Inflammation in severe asthma**

Atopic asthma has classically been associated with an increased expression of T helper cell type 2 (Th2) cytokines, which are increased in sputum,<sup>23</sup> bronchoalveolar T-cells<sup>24</sup> and

bronchial biopsies.<sup>25</sup> A major effector axis resulting in induction of Th2 polarization is the recognition of allergen presented by dendritic cells in local lymph nodes to CD4+ T cell. The differentiation of naive T cells or reactivation of memory T cells depends on various co-stimulatory molecules primarily expressed on the surface of T cell, and their cognate ligands such as OX40 and OX40ligand (OX40L). OX40L is directly mediated by thymic stromal lymphopoietin (TSLP), which is produced by epithelial cells,<sup>26</sup> mast cells,<sup>27</sup> airway smooth muscle (ASM),<sup>28</sup> and dendritic cells,<sup>29</sup> which are all involved in Th2 responses. In severe asthma TSLP but not OX40/OX40L is up-regulated.<sup>30-32</sup> Interestingly there is emerging evidence that T helper cells type 1 (Th1) / CD8+ T cells type 1 (Tc1) pathways with activation of neutrophils may play a role in asthma.<sup>33-36</sup> The Th1/Th2 mediated cellular interactions that drive airway remodelling are summarised in [Figure 1.2]. Importantly, these inflammatory profiles do not necessarily occur independently but may co-exist to varying degrees within an individual.

As a consequence of this inflammation there is epithelial damage and ciliary dysfunction.<sup>37</sup> Mucus gland and goblet cell hyperplasia together with impaired ciliary function lead to increased mucus production coupled with reduced lung clearance which is likely to perpetuate the risk for exacerbations.<sup>38,39</sup> The activated epithelium release several growth factors e.g. transforming growth factor-beta (TGF- $\beta$ )<sup>40</sup> and pro-angiogenic factors e.g. vascular endothelial growth factor.<sup>41</sup> In concert with pro-inflammatory cells TGF- $\beta$  activates sub-epithelial mesenchymal cells to release matrix and proliferate.<sup>42</sup> Mesenchymal progenitors known as fibrocytes are recruited to the airway in response to the 'chronic wound'.<sup>43,44</sup> ASM mass is increased as a consequence of fibrocyte and myofibroblast recruitment, differentiation and local proliferation. The activated ASM releases chemotactic



factors to recruit mast cells in asthma, which interact with the ASM to promote airway hyperresponsiveness<sup>45,46</sup> and further recruitment of myofibroblasts.<sup>47</sup> ASM also releases matrix proteins, which further alter the airway geometry and biomechanical properties.<sup>48</sup> In addition to the epithelium, angiogenic factors released by the ASM promote neovascularisation to further increase the sub-epithelial vascularity.<sup>49,50</sup>

Critically, there is no clear pathological definition that distinguishes severe asthma from asthma in general. However, a number of studies have suggested some features that are more prominent in severe disease. Induced sputum is a simple, well-tolerated, validated, non-invasive technique to assess airway inflammation.<sup>51,52</sup> The analysis of the type and magnitude of airway inflammation in severe asthma has proven to be helpful in distinguishing clinical phenotypes, especially the analysis of sputum inflammatory cells.<sup>21,53</sup> Studies addressing cytokines and chemokines in severe asthma have also shown that severe asthma is not a classical Th2 inflammatory disease and that both Th1 and Th2 cytokines can be expressed and the Th17 axis is up-regulated.<sup>54,55</sup> In biopsies, the quantification of neutrophils and eosinophils in the airway mucosa and structural changes of the airways such as the thickening of the reticular basement membrane (RBM) and lamina reticularis has suggested different clinical phenotypes.<sup>33</sup> Some patients with severe refractory asthma have persistent eosinophilia of the airways, whereas others are neutrophil predominant.<sup>33,36</sup> Eosinophilic asthma (EA) is associated with thickening of the RBM and corticosteroid responsiveness.<sup>33,56</sup> The eosinophil number, related to the severity of asthma, is associated with increased risk of exacerbations,<sup>57</sup> is related to persistent airflow limitation<sup>58</sup> and increased airway reactivity to methacholine.<sup>59</sup> Non-eosinophilic asthma (NEA), in contrast to EA, is characterised by absence of RBM thickening<sup>56</sup> and

corticosteroid resistance,<sup>60</sup> though mast cell infiltration of ASM is a feature of both NEA and EA.<sup>56</sup> NEA may be subdivided into neutrophilic and paucigranulocytic types based on presence or absence of sputum neutrophil count >61%.<sup>61,62</sup> Although the presence of neutrophils in severe asthma may be attributed to the use of corticosteroids, which cause increased neutrophil survival, they may also be central in the pathogenesis, as neutrophilic inflammation is associated with chronic airway narrowing in asthma.<sup>59,63</sup> Leukotriene B4 (LTB4), interleukin (IL)-8, macrophage inflammatory protein (MIP)-1 $\alpha$  and tumour necrosis factor (TNF)  $\alpha$  are increased in severe asthma,<sup>64</sup> and can induce neutrophil chemotaxis. Mast cells are in an activated state in asthma particularly in severe disease.<sup>65,66</sup> In the healthy lung the predominant mast cell phenotype is tryptase<sup>+</sup> chymase<sup>-</sup>, but in severe disease there is a tryptase<sup>+</sup> chymase<sup>+</sup> [MC(TC)] predominance in the lamina propria and within airway structures such as the epithelium. These MC(TC) are also an important source of prostaglandin (PG)D<sub>2</sub>, which is increased in bronchoalveolar lavage in severe asthma.<sup>66</sup> In severe asthma MC(TC) are increased in the smaller airways and intriguingly are positively correlated with lung function suggesting that they may be protective for lung function at this site.<sup>67</sup>

### **1.1.3.3 Airway remodelling in severe asthma**

Airway wall remodelling on its own accord has consequences with regard to symptoms, exacerbations, loss of lung function, decline in lung function and response to treatment. The complex interplay between different structural components of the airway wall and the heterogeneity of various disease processes contribute to incomplete understanding of the contribution of specific elements of remodelling to the symptoms, progression and response

to treatment of the airway diseases. Though bulk of evidence suggests that structural remodelling is detrimental, there are some theoretical benefits that may have protective effect on the airways.<sup>68</sup> Airway remodelling is considered fundamental to the chronicity of the asthma disease complex.<sup>69</sup> Remodelling in asthma usually affects the larger, more proximal airways though in severe asthma changes in small airway wall with infiltration of neutrophils, mast cells<sup>70</sup> and increased in number of CD8+ cells<sup>71</sup> has been reported. Remodelling of airway structure in asthma has been associated with airflow limitation,<sup>72-75</sup> airway hyper-responsiveness,<sup>76,77</sup> and eosinophilic inflammation.<sup>33,56,78</sup>

#### **1.1.3.3.1 Definition, features and mechanisms of airway remodeling**

Tissue remodelling is defined as modification in size, quantity, composition, or organisation of its structural components that occurred during growth or in response to physiological and mechanical stress. Various organs and tissues such as heart,<sup>79</sup> skin,<sup>80</sup> blood vessels,<sup>81</sup> lung<sup>82</sup> and airways<sup>83-85</sup> undergo remodelling when exposed to chronic inflammation and /or injury. Airway remodelling is a complex process that involves all component tissues of the airway from epithelium to the adventitia. In asthmatic patients, airway remodelling is characterized by changes such as epithelial alteration,<sup>73,86-90</sup> increased smooth muscle mass,<sup>73,91-93</sup> thickening of the subepithelial basement membrane,<sup>33,73,94,95</sup> glandular hyperplasia,<sup>73,96</sup> dysregulated extracellular matrix deposition<sup>73,97</sup> and increased vasculature.<sup>49,98</sup>

Structural cells of the airways, such as epithelial cells and ASM cells, contribute to the inflammatory response and are capable of producing a number of inflammatory mediators such as chemokines, cytokines and growth factors. Epidermal growth factor receptor, as a

marker of epithelial stress/damage, is increased in severe asthma, suggestive of ongoing epithelial cell activation.<sup>99</sup> The activated epithelium releases several pro-angiogenic growth factors such as TGF- $\beta$ <sup>40</sup> and vascular endothelial growth factor (VEGF).<sup>41</sup> In concert with pro-inflammatory cells, TGF- $\beta$  activates sub-epithelial mesenchymal cells to release matrix and proliferate.<sup>42</sup> The epithelium in severe asthma has distinct features and has been reported to be thicker compared to that of patients with mild asthma.<sup>100</sup> Epithelial cells from severe asthmatics secrete a number of chemokines, in particular IL-8, which is an important neutrophil chemoattractant.<sup>101</sup> ASM mass is increased in severe asthma compared to mild-moderate asthma or chronic bronchitis.<sup>73,85,102,103</sup> The strongest predictors of airflow obstruction are ASM mass, smooth muscle hypertrophy and sub-epithelial fibroblasts;<sup>73</sup> whether this increase in ASM mass is due to hyperplasia,<sup>104</sup> hypertrophy or both remains uncertain.

Interactions between structural and infiltrating cells are likely to play an important role in the development and persistence of airway dysfunction. The activated ASM releases chemotactic factors to recruit mast cells in asthma, which interact with the ASM to promote further recruitment of myofibroblasts.<sup>47</sup> Microlocalisation of mast cells to the ASM bundle is related to the degree of airway hyper-responsiveness across the severity of disease<sup>45,105</sup> and to the loss of the bronchodilator response to deep breath.<sup>106</sup> These mast cells are predominantly MC(TC) and express Th2 cytokines such as IL-4 and IL-13.<sup>46,104</sup> Mesenchymal progenitors, fibrocytes, also infiltrate the ASM bundle in severe disease,<sup>43</sup> are increased in peripheral blood<sup>45,105</sup> and are related to airflow obstruction.<sup>44</sup> ASM also releases matrix proteins, which further alter the airway geometry and biomechanical properties.<sup>48</sup> In addition to the epithelium, angiogenic factors released by the ASM promote

neovascularisation to further increase the sub-epithelial vascularity and MC(TC) are associated with areas of increased vascularity.<sup>49</sup> Importantly, neutrophils and mast cells localise to glands and are associated with increased mucus plugging in fatal asthma.<sup>48,49</sup>

Increased production and deposition of the extracellular matrix (ECM) is a characteristic of severe asthma. Thickening of the RBM due to ECM deposition has been extensively studied in asthma as a marker of remodelling. The results are not always consistent, but the majority of studies showed that severe asthmatics have thicker sub-epithelial layers<sup>45,96,100,105,107</sup> compared to those with mild disease together with evidence of epithelial proliferation in some.<sup>100</sup> Indeed, in one study thickening of the RBM was the most discriminate feature of severe asthma.<sup>107</sup> Fibrosis in the airways is generally irreversible, and treatment has little effect on this feature. It could also contribute to fixed airway obstruction in severe asthmatic individuals.<sup>108</sup> Involvement of the small airways in asthma has been related to disease severity, as suggested by functional and radiological studies.<sup>109-111</sup> However, it is not clear whether severe asthmatics have more small airways involvement compared to mild or moderate asthma. It is difficult to conduct invasive bronchoscopy in these patients, and thus most of the information to date on the involvement of small airways in severe asthma is based upon autopsy studies.<sup>112,113</sup> Studies of fatal asthma found decreased elastic fibre content in the periphery and abnormal alveolar attachments. These features would promote the abnormalities in airway elastance, loss of compliance and promote airway closure.<sup>114,115</sup> In contrast, changes in the more proximal airways may contribute to airway wall stiffness and oppose airway narrowing in response to ASM contraction. For example, subepithelial fibrosis might also prevent airway narrowing, increase airway wall stiffness and resistance to compression and tension. In

severe and fatal asthma, the proteoglycans versican, biglycan and lumican are increased in the lamina propria and around the ASM,<sup>114,116,117</sup> although they are not increased within the ASM-bundle.<sup>117</sup> The increased elastic fibres in the ASM-bundle and the distribution of proteoglycans may increase resistance to airway wall deformation and provide a preload to the ASM that opposes its shortening and therefore airway narrowing. The potential physiological consequences of these changes are summarized in [Figure 1.3]. In stable disease, inhaled corticosteroid therapy for 6 weeks did not affect collagen III expression<sup>118</sup> and following allergen challenge extracellular matrix increased and was augmented by corticosteroids<sup>116</sup> suggesting that corticosteroids may promote rather than attenuate the deposition of certain matrix proteins.

Taken together, structural and cellular changes within the airway wall in asthma, notably increased ASM mass,<sup>91</sup> vascular remodelling, thickening of the RBM and increased fibroblast numbers in the lamina propria, have been shown to correlate with airflow limitation. Furthermore, cellular infiltration of the airway wall in asthma is related to decline in lung function.<sup>119</sup> The association of structural change in the airway wall in asthma with airway hyper-responsiveness is much more tenuous. A number of reports have drawn conflicting conclusions about the association of airway hyper-responsiveness with epithelial desquamation/loss of tight junctions,<sup>73,108,110,120</sup> RBM thickening,<sup>121,122</sup> vascular remodelling<sup>41,49,123</sup> and ASM mass.<sup>113</sup>

#### **1.1.3.3.2 Measurement of airway remodeling**

Targeting airway remodelling in severe asthma with pharmacological and non-pharmacological therapies may potentially decrease severity, improve asthma control and

prevent disease expression. However, accurate and standard methods to measure airway remodelling in severe asthma are essential to understand natural history and monitor response to treatment.

First descriptions of airway remodelling come from *post mortem* studies in fatal and non-fatal asthma.<sup>92,96,120,124-131</sup> *Post mortem* tissue specimens provide a global view of the pathological features of asthma with detailed assessment of the entire airway tree from the proximal airways to small airways and alveoli as well as pulmonary circulation. Increase in airway wall thickening and smooth muscle area was found in distal airways of fatal asthmatics compared to asthmatics who died of other causes.<sup>132</sup> However, there are limitations of *post mortem* tissues such as inability to perform physiological tests, influence of mechanical ventilation or other forms of treatment on airway pathology.

Endobronchial biopsies (EBB) performed using flexible bronchoscopy are the major source of proximal airway tissue for direct remodelling studies.<sup>91,133</sup> Flexible bronchoscopy is relatively simple to perform and a minimally invasive technique but requires specialist expertise. Analysis of airway tissue obtained by EBB allows analysis of pathological changes as well as effect of pharmacological therapies. Limitations of EBB include ability to study only the proximal airway and sampling of partial thickness of the airway wall.

Few studies have used transbronchial biopsies (TBB) performed under flexible bronchoscopy to study remodelling.<sup>67,134,135</sup> An obvious advantage of TBB is the ability to sample and study distal lung including small airways and alveolar tissue. However, this method of obtaining tissue samples is limited by major complications, such as haemorrhage and pneumothorax, and poor success rate (~ 30 – 50 %) per biopsy.<sup>136</sup>

Airway tissue obtained by above detailed procedures requires processing, visualisation and quantification to study remodelling.<sup>136</sup> Airway tissue embedded in paraffin preserves the airway wall morphology and is preferred over other methods for remodelling studies. Methods to assess remodelling include electron microscopy,<sup>137</sup> histochemical or immunohistochemical staining, specific antibodies directed against cytokines and *in situ* hybridization to detect mRNA expression of cytokines.

Tools for indirect assessment of remodelling include analysis of cellular composition and fluid phase mediators in induced sputum and bronchoalveolar lavage (BAL). Induced sputum is relatively non-invasive technique, which is well tolerated and is relatively simple to perform. Induced sputum helps to evaluate eosinophilic and non-eosinophilic airway inflammation.<sup>51,138</sup> Variety of soluble remodelling-associated proteins have been measured in sputum supernatant and BAL. VEGF, an angiogenic factor, was found to be elevated in asthmatic sputum<sup>139</sup> and correlates with vascular permeability of the airways in asthma.<sup>140</sup> The ratio of matrix metalloproteinase-9 to tissue inhibitor of metalloproteinase-1 (MMP-9/TIMP-1),<sup>141,142</sup> representing matrix turnover have been shown to relate to airway wall thickening assessed by computed tomography (CT) in asthma.<sup>143</sup> One of the major limitation of both BAL and induced sputum is inconsistency of yield and dilution factor.

Multi-detector CT (MDCT) has emerged as a non-invasive, repeatable and reliable tool for quantitative assessment of airway remodelling in asthmatic adult<sup>72,75,144,145</sup> and paediatric<sup>146-148</sup> patients. Quantitative CT techniques in asthma now enable three-dimensional (3D) objective morphometric assessment of the proximal airways<sup>72</sup> as well as indirect assessment of small airways by densitometric assessment of paired inspiratory and expiratory scans.<sup>149</sup> CT assessed proximal airway remodelling in asthma has been shown to



correlate with airway epithelial thickness<sup>72</sup> and smooth muscle layer area<sup>150</sup> measured on biopsy specimens. However, CT is limited by its inability to differentiate structural components in the proximal airway wall and is limited by its resolution in assessment of small airway remodelling. Other imaging tools such as endobronchial ultrasound (EBUS) and optical coherence tomography (OCT) have also been developed and can be utilized to assess airway remodeling. Researchers were able to identify five different layers of the bronchial wall using EBUS.<sup>151</sup> OCT uses low-coherence near-infrared light for airway imaging and has been assessed using various validation studies.<sup>152-154</sup> OCT unlike CT can be used for small airway imaging in vivo with near microscopic resolution and no associated risks to patients from weak near-infrared light. Measures of airway dimensions using both OCT<sup>155</sup> and EBUS<sup>151</sup> correlated well with CT measures and lung function.

Recently, tissue engineering has enabled development of physiological 3D tissue model of the airway wall and mucosa.<sup>156</sup> *In vitro* organ culture models in asthma<sup>157</sup> will prove instrumental in studying airway remodelling in response to tissue injury and experimental therapies.

#### **1.1.3.3.3 Natural history and reversibility of remodelling**

The natural history of remodelling and the degree to which it is reversible is unclear. It has been shown that asthma patients experience an accelerated decline in lung functions, which is significantly more than healthy subjects and is proportional to the disease duration and severity.<sup>158-160</sup> In contrast, there are reports that children with asthma have poor lung function, suggesting that airway remodelling may be established early in the course of the disease.<sup>161-163</sup> Young children with reversible airflow obstruction and wheezing did not

demonstrate any structural changes in airway tissue specimens obtained by EBB,<sup>133,164</sup> despite clear evidence of airway inflammation in wheezing infants.<sup>165-169</sup> On the contrary, Saglani *et al.*<sup>170</sup> have shown that pre-school children with wheeze had evidence of airway structural changes such as thickened RBM, epithelial damage and eosinophilic inflammation; also reported in children with moderate / severe asthma.<sup>94,166,169,171</sup>

Research on influence of treatment on airway remodelling has primarily been focused on inhaled and oral corticosteroids due to their ability to modulate airway inflammation. However new pharmacological and non-pharmacological therapies and their influence on remodelling will profoundly enhance our understanding of asthma pathogenesis. Some studies have reported that inhaled corticosteroids may decrease basement membrane thickness in asthmatic subjects<sup>172,173</sup> thereby altering sub-epithelial fibrosis, a major feature of remodelling, while others have demonstrated none or only modest impact on RBM.<sup>77,172,174-176</sup> Variation in dose and duration of treatment may explain the conflicting results from different studies, with use of lower dose and / or shorter duration of treatment showing little effect. Effects of inhaled corticosteroids on ASM of asthmatic patients includes *in vitro* anti-proliferative effects,<sup>177-179</sup> modulation of chemokines and cytokines involved in ASM function and proliferation,<sup>180</sup> and reduction of contractile protein expression.<sup>181</sup> Moreover corticosteroids have apoptotic effects on airway epithelial cells<sup>182</sup> and decrease the proliferation and inflammatory mediator release of lung fibroblasts.<sup>183,184</sup> Inhaled corticosteroids may also influence subepithelial matrix deposition as shown by De Kluijver<sup>116</sup> and colleagues in their study where submucosal density of the proteoglycans biglycan and versican was increased after two weeks treatment following low dose allergen challenge. On the contrary, Bergeron *et al.*<sup>118</sup> did not find any effect on large or small

airway total collagen or collagen III deposition after 6 weeks of treatment with HFA-Flunisolide. In addition, three different studies have demonstrated a significant decrease in CT assessed airway wall thickness / wall area after use of inhaled corticosteroids.<sup>185-187</sup>

Remodelling modulation effects of Montelukast, a cysteinyl leukotriene receptor antagonist, have also been studied in asthma. Kelly *et al.* have shown that eight weeks of montelukast therapy reduces the lymphocyte and myofibroblast counts after allergen challenge.<sup>188</sup> CT assessed regional air-trapping was shown to be less in asthma patients on 4 weeks montelukast treatment in a placebo controlled double-blind crossover study.<sup>189</sup>

Significant reduction in the glycoproteins tenascin, lumican and procollagen III in the reticular basement membrane in asthma as well as greater than 50% reduction in tissue and bone marrow eosinophilia was demonstrated on treatment with Mepolizumab, a humanized monoclonal antibody to IL-5.<sup>190,191</sup>

Novel non-pharmacological treatment by radiofrequency ablation of the ASM in patients with severe asthma, in the form of bronchial thermoplasty has demonstrated an improvement in quality of life as well as reduction in rate of severe exacerbations, emergency department visits and days lost from school or work.<sup>192,193</sup> Bronchial thermoplasty results in reduction of the bulk of ASM, which is replaced by fibrous connective tissue although no significant change in airway hyperresponsiveness (AHR) or forced expiratory volume in 1 second (FEV<sub>1</sub>) has been demonstrated.

#### 1.1.3.4 Functional impairment in severe asthma

Pulmonary dysfunction in asthma is characterized by variable airflow obstruction with reversibility in response to bronchodilators or spontaneously, and airway hyperresponsiveness. Airflow limitation is a characteristic feature of asthma<sup>194-196</sup> and is thought to occur due to ASM contraction, mucosal oedema and mucus accumulation in the airways. In asthma, airflow limitation is usually reversible, although in large proportions of patients with severe asthma it becomes irreversible<sup>160,162,197,198</sup> at least partly secondary to airway remodeling. Asthma patients with fixed airflow obstruction (FAO) are likely to have a poor prognosis compared to patients with completely reversible airflow obstruction. Several studies have demonstrated that persistently impaired post-bronchodilator FEV<sub>1</sub> is an important predictor of morbidity and mortality in severe asthma patients, irrespective of smoking habits.<sup>199-201</sup> Increased rate of decline in lung function has been demonstrated by longitudinal studies in asthma patients with shorter disease duration<sup>202</sup> and more severe<sup>203</sup> disease. Patients who develop FAO following childhood asthma; the majority of lung function impairment is already established by early adulthood.<sup>160,162</sup> In adult-onset non-atopic asthma that manifests after age of 50 years, the rate of lung function decline is even greater than childhood-onset asthma.<sup>58,204-206</sup> Lung function decline is intricately related to worsening airway inflammation associated with asthma exacerbation as demonstrated by longitudinal studies involving both adult<sup>207,208</sup> and paediatric<sup>208</sup> asthma patients. A variety of factors may contribute to the development of irreversible airflow obstruction in asthma including childhood respiratory disease,<sup>209,210</sup> smoking,<sup>158,211</sup> female sex,<sup>212</sup> sensitisation to *Aspergillus fumigatus*,<sup>213-215</sup> occupational exposures,<sup>216,217</sup> increased bronchodilator reversibility,<sup>162,203</sup> AHR<sup>58,162,218,219</sup> and airway inflammation.<sup>58,63,220</sup>

AHR is the hallmark feature of asthma, defined by excessive airway narrowing, usually reversed with bronchodilators that relax airway smooth muscle. It remains contentious whether AHR is secondary to abnormal ASM or normal ASM functioning in an abnormal airway tissue environment.<sup>221</sup> The relationship between AHR and airway inflammation is not completely understood. Several studies have demonstrated modest association between AHR to methacholine and eosinophilic airway inflammation in sputum and BAL fluid<sup>222,223</sup> with indirect AHR showing stronger correlations with airway inflammation.<sup>224,225</sup> On the contrary there is evidence suggesting that AHR is dissociated with eosinophilic airway inflammation,<sup>226</sup> also supported by absence of AHR in non-asthmatic eosinophilic bronchitis (EB) despite eosinophilic airway inflammation<sup>227,228</sup> and presence of marked AHR in NEA with minimal airway eosinophilic inflammation.<sup>33,138</sup> The relationship between airway remodeling and AHR is complex with some studies showing correlations between features of remodelling and AHR<sup>73</sup> supported by mathematical modeling suggesting that increased ASM mass is the most important factor responsible for the increased resistance observed in response to bronchoconstricting stimuli in asthma,<sup>229</sup> and other studies have demonstrated dissociation between AHR and airway wall structural remodelling.<sup>46</sup>

Another hallmark feature of severe asthma is frequent and severe exacerbations that are associated with significant morbidity, mortality and healthcare costs.<sup>12,230</sup> Several studies have confirmed that history of a previous asthma exacerbation is the best predictor for subsequent asthma exacerbation in both children and adults.<sup>231-233</sup> Other risk factors for frequent asthma exacerbation include ethnicity, lower socio-economic status, cigarette smoking, increased body mass index, allergic or non-allergic asthma triggers and

psychological factors.<sup>234-237</sup> Recurrent exacerbations often associated with pathogens, suggesting abnormalities in innate/adaptive immunity. Respiratory virus infections are strongly associated with the inception of asthma.<sup>238</sup> But viruses may also be involved in the persistence of inflammation and injury in chronic asthma. An *in situ* RT-PCR study of bronchial biopsy specimens demonstrated the presence of rhinovirus infection in the bronchial mucosa in clinically stable asthma.<sup>239</sup> In asthma there is impaired secretion of beta and lambda interferons from the airway epithelium in response to human rhinovirus.<sup>239,240</sup> This leads to decreased viral clearance and is associated with worsening symptoms at exacerbation. However, it is unknown whether respiratory pathogens are linked to asthma severity. Data in severe asthma indicate that there is a strong association between the presence of fixed airflow limitation and positive serology for intracellular pathogens: *Chlamydia Pneumonia*.<sup>241</sup> These data suggest that a single pathogen infectious episode or latent/persistent infection may play a role in specific childhood or adult asthma phenotypes. Thus, the role of viral or bacterial pathogens in persistent asthma needs to be further assessed in different severe asthma phenotypes by microbiome analysis using multiplex and metagenomic techniques.<sup>39</sup> It is possible that relative corticosteroid insensitivity in severe asthma<sup>242</sup> is, in part, driven by persistent or latent infection within the airways.<sup>243</sup> Exacerbations respond poorly to usual inhaled therapy and are closely linked to eosinophilic inflammation, both through increases in sputum eosinophils<sup>244</sup> and also in tissue obtained from patients who have died of acute severe asthma exacerbation.<sup>245,246</sup> Asthma exacerbations are shown to correlate to pulmonary hyperinflation,<sup>247</sup> loss of elastic recoil<sup>248</sup> and mucous plugging.<sup>249</sup> Moreover therapeutic strategies to control eosinophilic airway inflammation are associated with reduction in exacerbation frequency.<sup>57,250</sup>

### 1.1.4 Phenotyping severe asthma

A phenotype is any observable characteristic that results from the genetic background as well as the influence of environmental factors and possible interactions between the two. In context of asthma, different strategies have been used to identify phenotypes, including those related to aetiology (allergic, aspirin sensitive, occupational and exercise induced); clinical characteristics (age of disease onset, severity, obesity linked and fixed airflow obstruction); and pathophysiological characteristics (EA / NEA and fixed airflow obstruction / variable airflow obstruction). This traditional system of asthma phenotyping is limited by its uni / pauci-dimensional approach that fails to capture the true heterogeneity of disease.

Severe asthma is complex and heterogeneous disease.<sup>251</sup> Moreover, the heterogeneity in severe asthma is multi-dimensional spanning all aspects of disease pathogenesis and disease expression [Figure 1.4], and is further complicated by natural history of the disease (progression over time) and response to treatment. It is well recognized that a ‘one size fits all’ approach for severe asthma is insufficient and ineffective, but phenotyping this heterogeneity remains a major challenge. Early observational studies of refractory asthma have identified clinical and pathological features associated with persistent airflow obstruction and exacerbation frequency using multiple regression.<sup>58,252</sup> These disease outcomes are closely associated with the morbidity and mortality of asthma and modification of these parameters remains the goal of clinical management. The integration of data derived from non-invasive markers of airway inflammation has provided new inflammatory phenotypes of EA and NEA.<sup>33,36,138</sup> As we move our classification from

clinical descriptions to include cellular biology, another dimension is added increasing the phenotypic granularity of severe asthma. Recently, these descriptions have begun to embrace expression profiling and have moved the complexity to include molecular phenotyping.<sup>253</sup> Moreover, statistical modeling using factor and cluster analysis has provided further insight into the complexity of severe asthma phenotypes.<sup>21,22</sup>

The goal of multi-dimensional approach to severe asthma phenotyping is not simply to provide an alternative to traditional classification. It is hoped that these phenotypes will generate new insights into disease pathogenesis, predict disease progression and identify responders to current and novel therapies. To achieve this goal several aspects of severe asthma at genetic, molecular, cellular, tissue, organ and patient level should be examined in an unbiased manner to identify novel phenotypes. Severe asthma ‘endotypes’ or ‘endophenotypes’ could then be recognised which represent stable phenotypes defined functionally and pathologically by a distinct molecular mechanism or treatment response.<sup>251,254</sup> Severe asthma endotypes may prove instrumental in identifying novel biomarkers and disease mechanisms that will unravel the complexity of severe asthma and help in development of new therapies. Biomarkers discovery that are non-invasive and can accurately identify severe asthma ‘phenotype’ or ‘endotype’ will be more clinically relevant and will make personalised healthcare a reality. Several studies have begun to take an unbiased approach towards examining biomarker expression in severe asthma including hierarchical clustering of BAL<sup>255</sup> and sputum inflammatory mediators, the analysis of volatile organic components of exhaled breath using an electronic nose<sup>256</sup> and the transcriptomic analysis of bronchial biopsies<sup>257,258</sup> have supported the possibility of several distinct phenotypes of severe asthma. There is paucity of studies that have identified severe



asthma phenotypes based on airway remodelling. In [section 3.5] I have described three distinct severe asthma phenotypes identified based on CT assessed proximal and distal airway remodelling.

As we begin to include increasingly complex information from clinical descriptions, airway structure and function, cellular and molecular biology, genome-wide expression as well as detailed environmental analysis, it is likely that we will begin to accurately characterise the multi-dimensional heterogeneity of severe asthma, gaining insight into risk factors and at risk phenotypes for disease progression and phenotypes with favorable response to specific therapies.

### 1.1.5 Figures and Tables

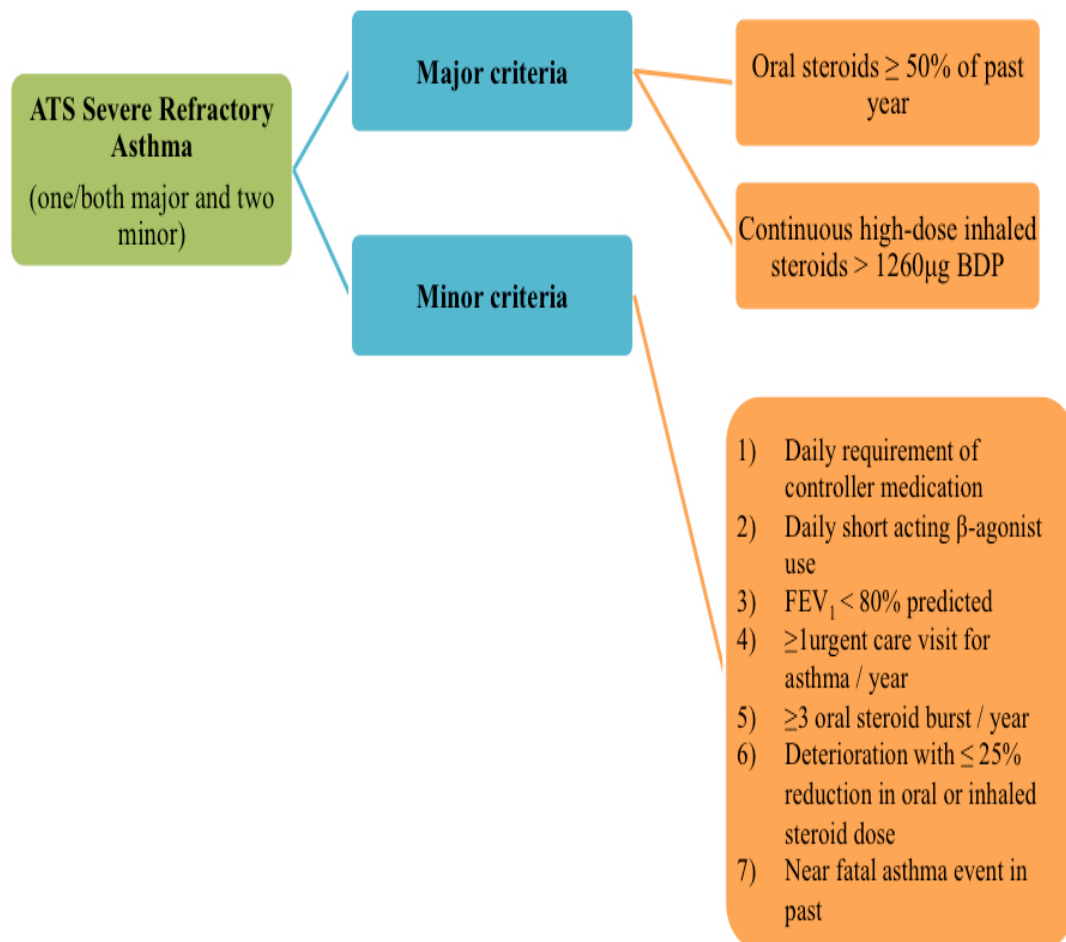


**Figure 1.1: American Thoracic Society clinical criteria for diagnosis of refractory asthma**

The definition requires that other conditions have been excluded, exacerbating factors treated, and patients adherence with therapy is deemed satisfactory.

*Definitions of abbreviations:* BDP = Beclomethasone dipropionate

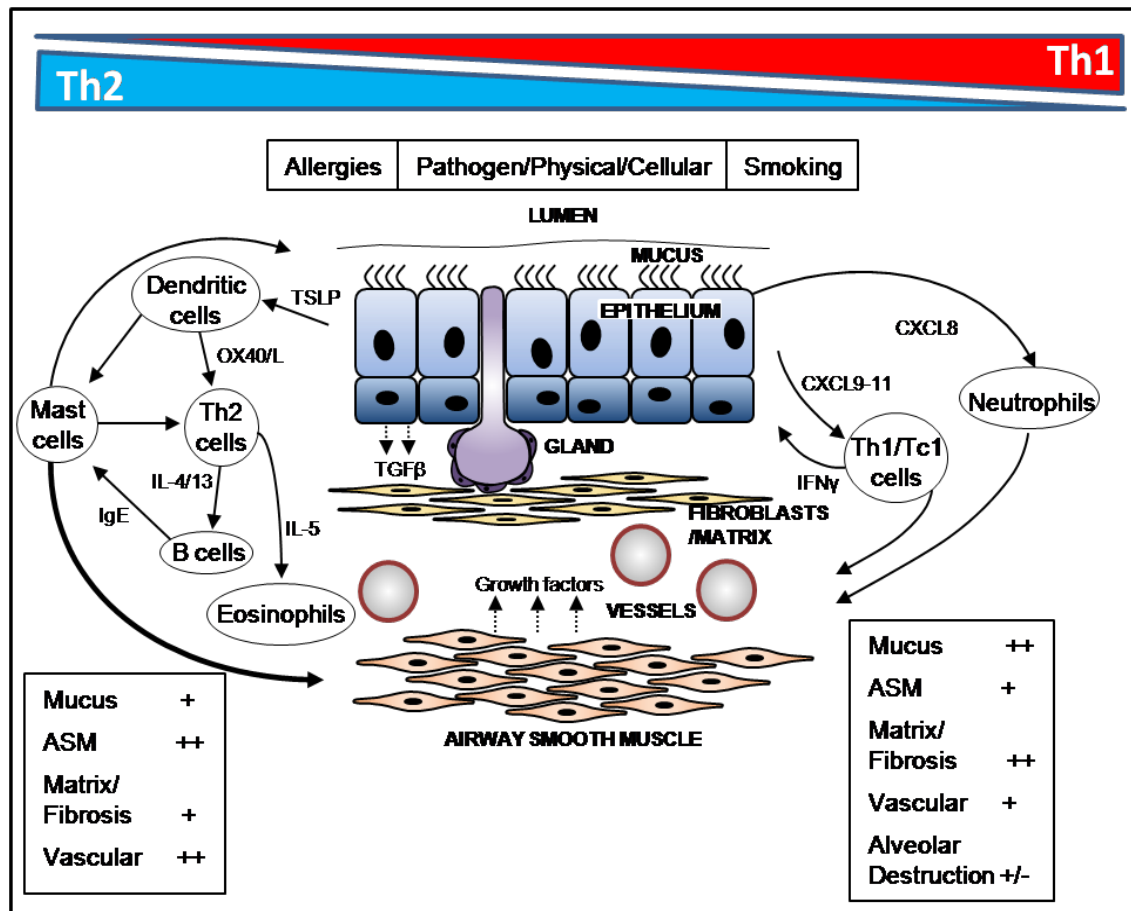


**Figure 1.2: Immunopathogenesis of asthma**

Schematic diagram of the immunopathogenesis of asthma illustrating the interaction between the Th1/Th2 inflammatory cells and the structural components of the airway and the consequent development of airway remodelling.

*Definitions of abbreviations:* ASM = Airway smooth muscle

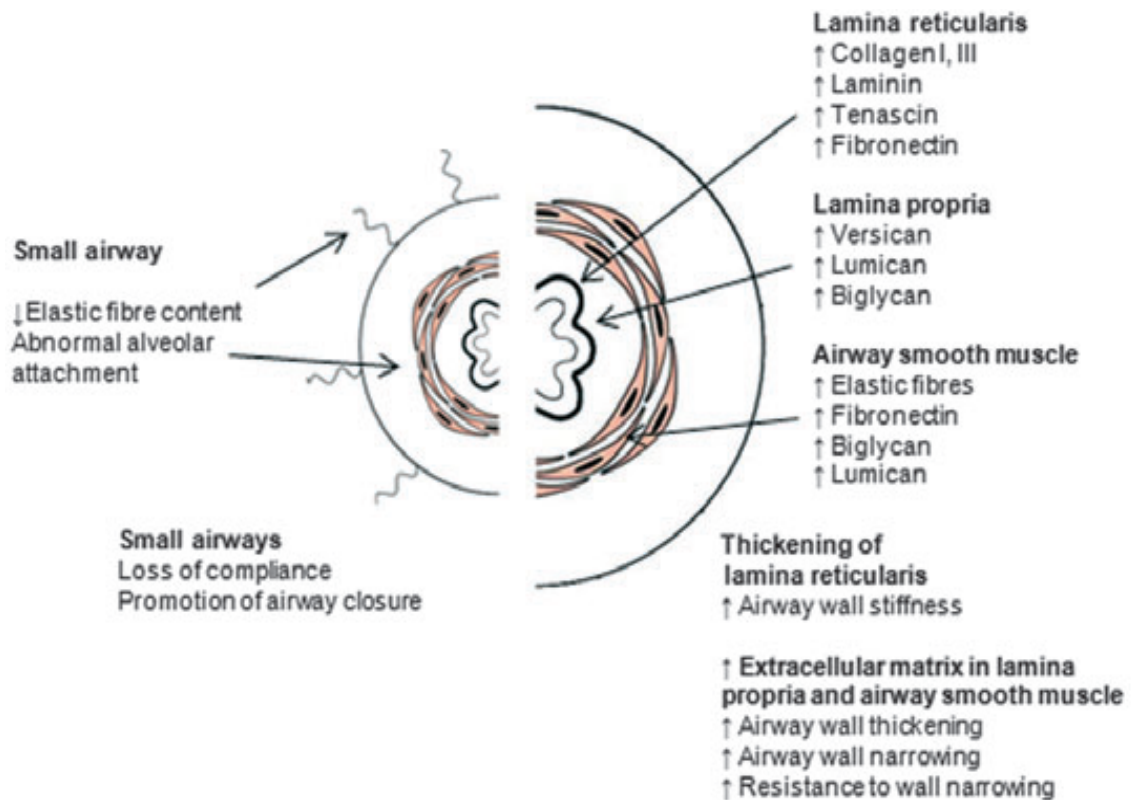


**Figure 1.3: Structure-function relationship in asthmatic airways**

Illustration of the changes in matrix and alveolar attachments in the large and small airway and their potential functional consequences.

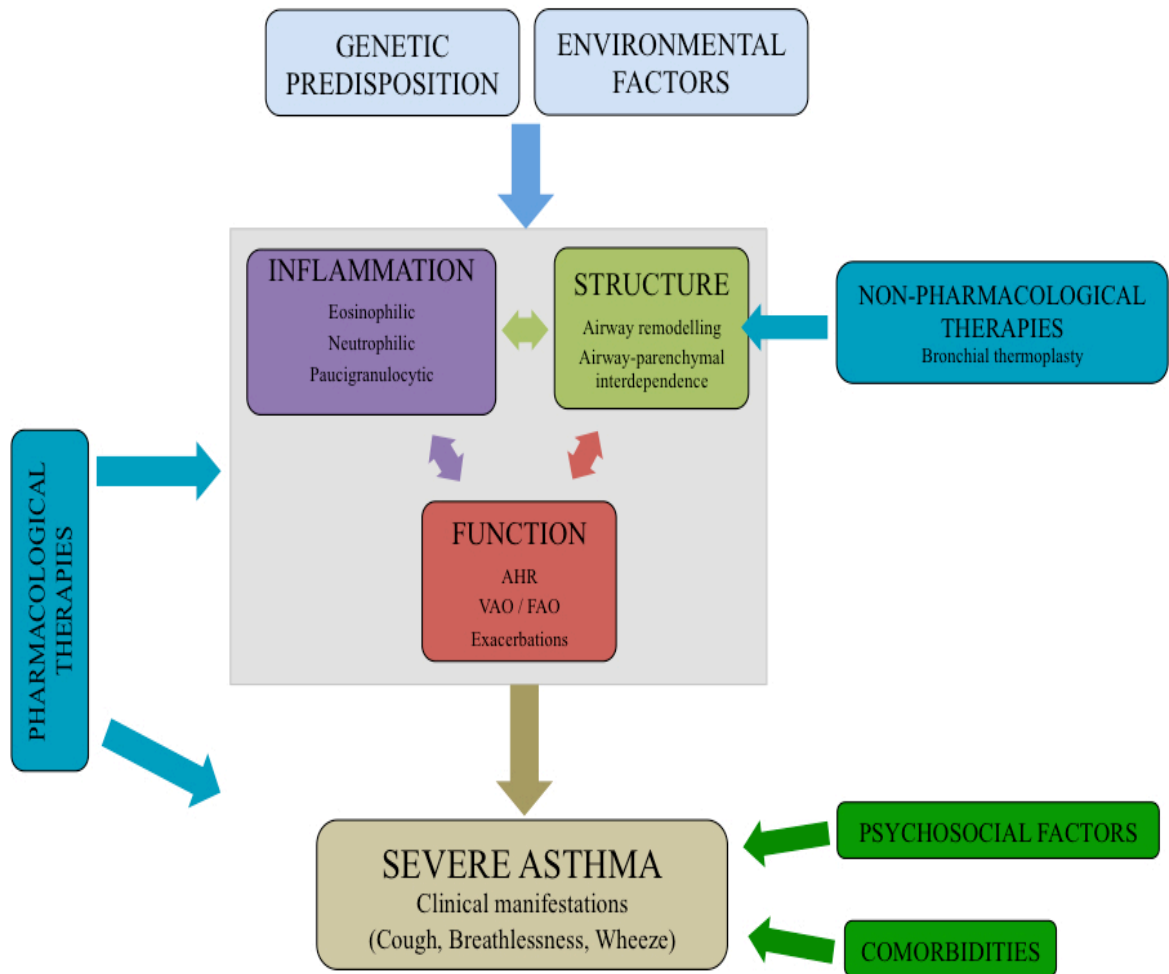


**Figure 1.4: Multi-dimensional heterogeneity in severe asthma**

*Definitions of abbreviations:* AHR = Airway hyperresponsiveness, VAO = Variable airflow obstruction, FAO = Fixed airflow obstruction.

**Table 1.1: Innovative Medicines Initiative (IMI) severe refractory asthma definition (2011)**

**Severe Refractory Asthma**

**Patients with confirmed diagnosis with alternate diagnosis excluded, comorbidities treated, trigger factors removed (if possible) and compliance with treatment checked**

**Requires poor asthma control or frequent ( $\geq 2$ ) severe exacerbations per year despite treatment with high-intensity treatment; or adequate control maintained only when taking systemic corticosteroids and thereby at risk of serious adverse effects.**

**For Adults:**

- (a) Poor control defined as 7-item JACQ score  $\geq 1.5$  (or any other standardized asthma control questionnaire)**
- (b) High-intensity treatment: high-dose ICS and / or systemic CS combined with LABA (or any other controller medication). High-dose ICS is fluticasone equivalent  $\geq 1000 \mu\text{g} / \text{day}$**

*Definitions of abbreviations:* ICS = inhaled corticosteroids, LABA = long acting  $\beta_2$ -agonists, CS = corticosteroids, JACQ = Juniper Asthma Control Questionnaire

## **1.2 Imaging in Severe Asthma**

Imaging plays an important role in assessment of severe asthma.<sup>9,10</sup> A gamut of new imaging technologies that have emerged in recent years allow non-invasive, comprehensive anatomical and functional assessment of the lungs. This has contributed to a better understanding of pathophysiology in severe asthma, as well as effective assessment of appropriate treatment options.

### **1.2.1 Computed Tomography in Severe Asthma**

#### **1.2.1.1 Historical overview**

The first commercially viable CT scanner was invented by Sir Godfrey Hounsfield in Hays, United Kingdom at EMI Central Research Laboratories. He shared the 1979 Nobel Prize in Medicine with Allan Cormack of Tufts University in Massachusetts for this invention. Initially CT was not considered suitable for the thorax and the scepticism is evident in an article by Kollins,<sup>259</sup> who had concluded that, though useful for head, abdominal and pelvic imaging, “*the ultimate role of computed tomography in the study of diseases of the chest is not as certain.*” Spectacular advances in technology have placed CT as a forerunner for thoracic imaging. Improvement in axial resolution meant that 1 mm thick CT images could be obtained, which lead to development of high-resolution computed tomography (HRCT). HRCT has allowed detailed macroscopic anatomical examination of the lung parenchyma, previously only possible from pathological specimens.<sup>260,261</sup> The advent of MDCT scanners

enabled isotropic acquisition of the whole chest with sub-millimetre resolution within a single breath hold.

In addition, exponential advances in post-processing software for CT images has opened up innumerable avenues and allows multi-planar reconstruction, three-dimensional surface and volume rendering of the airway tree and lung parenchyma, detailed quantitative analysis and virtual bronchoscopy. Quantitative imaging techniques have enabled us to obtain direct measurements by three-dimensional objective assessment of the large airways as well as indirect assessment of small airways by densitometric measures of paired inspiratory and expiratory scans.<sup>149</sup> In addition to detailed anatomic data, CT can provide functional assessment of perfusion and ventilation.

#### **1.2.1.2 Qualitative assessment of CT scans in severe asthma**

Several authors have performed qualitative assessment of CT findings in asthma subjects<sup>159,262-270</sup> with different proportions of the asthmatic population studied having severe disease. The prevalence of bronchiectasis (BE) reported in asthmatic subjects was high (range, 9-77%; median, 31%)<sup>159,262-271</sup> when compared to healthy asymptomatic subjects (range, 0-20%; median, 12.5%).<sup>262,266,267,272,273</sup> Presence of bronchiectasis among asthmatics was found to be associated with longer disease duration<sup>264,268,270</sup> and poorer lung function.<sup>159</sup> The association of bronchiectasis with disease severity was supported by some reports,<sup>264,274</sup> but not others.<sup>262,267</sup> There are some suggestions that the bronchial dilatation observed in asthmatic patients may be partly explained by reduction in pulmonary artery diameter which may be physiologic or due to change in blood volume and local hypoxia.<sup>265,275</sup> It remains unclear whether bronchiectasis in severe asthma is co-morbidity,



making the asthma “difficult” to manage or whether it represents structural change or remodelling with natural progression of the disease.<sup>214,267</sup> Bronchial wall thickening (BWT) prevalence was reported to be increased in asthmatic subjects (range, 16-92%; median, 65%)<sup>159,262-266,268-270</sup> when compared to healthy controls (range, 4-30%; median, 19%).<sup>262,265,266,269</sup> Both asthma severity and longer disease duration are shown to be associated with bronchial wall thickening.<sup>159,262,264,266,268,270</sup> Other abnormal radiological findings, such as mosaic lung attenuation; mucus plugging; prominent centrilobular opacities; and atelectasis,<sup>263-265,276,277</sup> are not uncommon in asthmatic subjects. Emphysema though reported in severe asthma is an uncommon finding.<sup>268</sup>

### **1.2.1.3 Quantitative assessment of proximal airways in severe asthma**

Quantitative assessments of both airway tree and lung parenchyma have now been made possible by tremendous improvement in CT technology and post-processing software. Initial methods of quantification of proximal airways involved manually or digital tracing of the airway wall inner and outer boundaries on CT images.<sup>278-282</sup> Such techniques were phased out rapidly as they were very labour intensive and prone to large between and within observer errors.<sup>282</sup> Researchers explored alternate techniques through which semi-automated / automated computer-aided quantitative assessment of the proximal airways was possible. Initial methods were focused on quantitative assessment of just the airway lumen by using a Hounsfield unit (HU) threshold cut-off value. McNitt-Gray and colleagues<sup>283</sup> were among the first to use such technique and using a phantom model demonstrated that a threshold cut-off of -500 HU most accurately quantified the airway lumen area. King *et al.* used excised formalin-fixed porcine lungs to establish that a

threshold of -577 HU quantified airway lumen area with least errors.<sup>284</sup> Accurate measurement of airway wall dimensions, which involve identification of lumen-wall and wall-parenchyma boundaries on CT images, continues to be a difficult task with various different algorithms being proposed by researchers. One of the earliest and most widely used techniques is based on 'Full-Width at Half Maximum (FWHM)' principle.<sup>285</sup> This technique is explained in [section 2.3.2.2]. FWHM technique, is known to cause systematic errors in airway wall and lumen estimation<sup>286</sup> due to various factors including CT scanner point spread function causing blurring of edges, oblique orientation of the airways, algorithm used for image reconstruction and size of the airway analysed. To overcome such problems various techniques have been developed. These include (i) laplacian of Gaussian algorithm<sup>150</sup> which utilises smoothening and edge detection filters to segment airways; (ii) maximum-likelihood method,<sup>287</sup> whereby the attenuation threshold along each ray is matched to an ideal calculated ray; (iii) energy driven contour estimation method,<sup>288,289</sup> which incorporates shape independent quantification; (iv) integral based method,<sup>290,291</sup> which minimises the CT's blurring effect and; (v) phase congruency method,<sup>292,293</sup> which uses multiple reconstruction algorithms to localise airway wall. Most of the newer software platforms are designed to work on volumetric CT scans and not the standard sequential HRCT scans limiting their application to retrospective analysis of archived scans. Methods have been devised to correct for errors associated with airway dimension quantification using FWHM technique.<sup>284,294</sup> Such techniques allow for correction of potential oblique orientation related errors in quantification of airway dimensions. More recent software platforms utilise volumetric CT scans for three-dimensional analysis of the airway tree which allows lumen extraction, generation of the airway centreline, segmentation of airway tree up to 5<sup>th</sup>- 6<sup>th</sup> airway generation and

measurement of airway dimensions on reformatted images orthogonal to the long axis to minimise errors due to oblique orientation.<sup>150,155,287,289,293</sup>

Several studies have used CT for non-invasive quantitative assessment of proximal airway structural changes in asthmatic adults<sup>72,75,144,295,296</sup> and children.<sup>146-148</sup> Right upper lobe apical segmental (RB1) bronchus has been preferred by researchers for quantitative CT analysis, particularly prior to three dimensional analysis capabilities, because of relatively perpendicular orientation of the bronchus to the scanning plane and paucity of surrounding structures.<sup>75</sup> Moreover, despite heterogeneity<sup>72,297</sup> remodelling in a RB1 bronchus has been shown to correlate well with non-RB1 proximal airways in severe asthma.<sup>72</sup> Pathological correlation of CT assessed airway remodelling has been reported by some authors.<sup>72,296</sup> Kasahara *et al.* demonstrated that the indices of airway wall thickness on HRCT using the manual tracing method in mild-to-moderate asthmatics correlated with epithelial RBM thickness on biopsy.<sup>296</sup> In children with severe / difficult-to-treat asthma similar correlation between bronchial wall thickening and RBM thickness were demonstrated by De Blic *et al.*<sup>146</sup> but not by Saglani and colleagues.<sup>148</sup> MDCT scans analysed using one of the newer software platforms by Aysola *et al.*<sup>72</sup> show similar results with correlation between percent wall area (%WA) [WA expressed as percent of total area (TA)] or percent wall thickness (%WT) [WT expressed as percentage of total diameter] and epithelial or lamina reticularis thickness on biopsy specimens.

While some studies show that asthma patients have increased airway WT regardless of the disease severity,<sup>76,282,295,296</sup> others have demonstrated a correlation between CT assessed airway remodelling and asthma severity.<sup>72,75,144</sup> There is less agreement between researchers regarding the airway lumen area (LA) in asthma. Niimi *et al.* reported that there

was no significant difference in LA of asthma subjects of varying severity and healthy controls.<sup>75</sup> However, Beigelman-Aubry and colleagues have shown reduced LA in mild asthmatics compared to controls.<sup>298</sup> This difference in LA disappeared after inhalation of short-acting beta-agonist suggesting that it was secondary to reversible bronchoconstriction as a consequence of ASM shortening. It has been shown that bronchoconstriction may cause airway luminal narrowing without change in WA.<sup>299</sup> Airway wall thickening in asthma has been shown to correlate with airflow limitation,<sup>72,74,75</sup> AHR,<sup>72,300,301</sup> and air trapping on expiratory CT,<sup>74,302</sup> in asthma. Relation of AHR with CT assessed proximal airway wall remodelling is not completely clear. While there is evidence that AHR is related to the thickness of the proximal airway wall in asthma / severe asthma,<sup>72</sup> Niimi *et al.* demonstrated that airway reactivity is inversely associated with RB1 thickness<sup>300</sup> and in contrast the sensitivity (the point of initial rise in airway resistance during methacholine challenge) of airways in asthma is directly associated with eosinophilic airway inflammation. It has also been shown that in non-asthmatic EB, which is characterised by eosinophilic airway inflammation without any evidence of variable airflow obstruction (VAO) or AHR,<sup>23,45,227,303</sup> there is lack of RB1 airway wall thickening and lumen narrowing<sup>76</sup> suggesting that AHR may be linked to structural alteration in proximal airways. This view is also supported by studies involving mathematical models of asthma.<sup>304</sup> It has been shown that although non-asthmatic EB and asthma are immunopathologically similar, there are some important differences, such as mast cell localization to ASM bundle and increased IL-13 expression in asthma.<sup>23,45</sup> These differences limit direct comparison of non-asthmatic EB with asthma, although clues about variable manifestations due to eosinophilic airway inflammation may be obtained.

Only a few studies have explored the associations between remodelling assessed by CT and airway inflammation in asthma. Little *et al.* and Niimi *et al.* did not find any association between airway wall geometry and airway inflammation.<sup>75,144,300</sup> De Blic *et al.* demonstrated in a childhood severe asthma cohort that BAL eosinophil cationic protein (ECP) levels were related to airway wall thickening in severe asthma.<sup>146</sup> Association of other markers of airway inflammation in sputum such as TGF- $\beta$ <sup>305</sup> and the MMP-9 / TIMP-1 ratio<sup>143</sup> and airway wall thickening has also been demonstrated.

CT assessment of airway remodelling has proven to be a sensitive measure to detect and quantify change after current and novel therapies. A significant decrease in airway wall thickness / area was demonstrated after use of inhaled corticosteroids in three different studies,<sup>185-187</sup> one of which included a small number of severe asthma subjects.<sup>186</sup> On the contrary, further follow up of asthma subjects on inhaled corticosteroids from a previous study<sup>185</sup> for a mean duration of 4.2 years did not show any change in airway dimensions.<sup>306</sup> Similarly, no change in CT assessed airway dimensions were demonstrated by Brillet *et al.* in 12 patients with poor asthma control treated for 12 weeks with inhaled long acting  $\beta$ 2 agonist and inhaled corticosteroids despite improvement in physiological measures of airway obstruction and air-trapping.<sup>307</sup> It is contentious whether this altered geometry in severe asthma patients as compared to healthy controls may be important in determination of physiological characteristics such as airway hyperresponsiveness and airflow obstruction.<sup>72,75,76,85,300</sup> Methodological variations or difficulties in measurement of proximal airway dimensions, inability of CT to dissect out various individual components of airway remodeling, and complexity of interactions between structural and functional

aspects of severe asthma may explain the discrepancy between CT studies. This highlights the need for further prospective interventional and longitudinal studies.

#### **1.2.1.4 Quantitative assessment of distal airways in severe asthma**

The small airways (peripheral membranous bronchioles < 2mm in diameter) are also significantly affected in asthma<sup>308</sup> with strong evidence that small airways make a significant contribution to total airway resistance.<sup>309</sup> More than seven-fold increase in small airway resistance in asymptomatic asthma subjects with normal spirometry and normal plethysmographic airway resistance has been demonstrated by Wagner *et al.*<sup>310</sup> Presence of significant inflammation<sup>70,126,311,312</sup> and airway remodelling<sup>92,132</sup> has also been demonstrated in small airways of asthma subjects. Dimensions of small airways are beyond the resolution of currently available CT scanners for direct evaluation. CT scans still can be used for ‘small airways imaging’ as the changes in these airways are indirectly reflected in the changes of the lung parenchyma. Although the pathophysiological mechanisms underlying these parenchymal changes are not completely understood, it is known that small airways dysfunction results in reduced ventilation of part of the lung which causes a reflex reduction in perfusion highlighted as areas of decreased attenuation on CT images.<sup>313</sup>

In asthmatic subjects heterogeneity of lung attenuation though evident on inspiratory scans, can be markedly accentuated in expiratory scans due to regional differences in small airway closure or emptying rate. Such low attenuation areas can be quantified using ‘density mask’ technique.<sup>314</sup> Using CT to assess emphysema, researchers have suggested that attenuation threshold of -970 to -910 HU with images obtained at full inspiration [lungs held at near total lung capacity (TLC)] delineate emphysematous regions of the lungs.<sup>315-318</sup> Various

indices to quantify air trapping using CT in asthma have been used [Figure 1.5] including - 850 HU attenuation threshold at functional residual capacity (FRC),<sup>302</sup> percentage of pixels below -900 HU in expiratory scans,<sup>319</sup> mean lung density expiratory to inspiratory ratio,<sup>74</sup> difference between inspiratory and expiratory lung attenuation,<sup>320</sup> and median lung attenuation or lowest 10<sup>th</sup> percentile lung attenuation frequency distribution.<sup>321</sup> Although asymptomatic subjects with no abnormality of lung functions also show low attenuation areas on CT scans,<sup>322</sup> such areas of air-trapping are markedly increased in asthmatic subjects and correlate well with lung function abnormalities.<sup>74,298,302,319,323</sup>

Relationship between asthma severity and extent of air trapping seems to be complex. Air trapping has been shown to correlate with asthma severity<sup>109,324</sup> and significantly higher in uncontrolled asthma during an exacerbation as compared to controlled asthma and in healthy control subjects.<sup>325</sup> In a recent study, Busacker and colleagues<sup>302</sup> did not find a significant relationship between air trapping and asthma severity defined by ATS criteria.<sup>9</sup> However, they reported that subjects with air trapping were significantly more likely to have history of asthma-related hospitalisations, intensive care unit visits, and / or mechanical ventilation compared to subjects without air trapping suggesting that CT assessed air trapping may identify ‘at-risk’ asthma phenotype. CT assessed air trapping in asthmatic patients has also been associated with AHR,<sup>109,283,321</sup> suggesting that small airways make a significant contribution towards this hallmark feature of asthma; disease duration,<sup>302</sup> and airflow limitation.<sup>74,302,319,324</sup> In a cohort of paediatric mild-to-moderate asthmatics, CT assessed air trapping showed significant correlation with lung functions and serum ECP.<sup>326</sup> Air trapping on CT has also been used for evaluation of response to therapy. The effect of extra-fine inhaled corticosteroids and conventional inhaled corticosteroids on

asthmatic patients was studied.<sup>320,327</sup> Air trapping was found to be more sensitive than proximal airway dimensions in detecting the difference in response.<sup>327</sup> Goldin *et al.* demonstrated that extra-fine inhaled corticosteroids had a greater effect on functional parameters reflecting small airway obstruction and a more favourable effect on regional hyper-reactivity than conventional inhaled corticosteroids.<sup>327</sup> On the contrary, Tunon-de-Lara and colleagues found that inhaled corticosteroids decreased air trapping in uncontrolled asthma regardless of their aerosol particle size,<sup>320</sup> suggesting a predominant systemic effect of inhaled corticosteroids which leads to improvement in air trapping indices. Beneficial effect on air trapping was also noted by Zeidler *et al.*<sup>189</sup> on use of montelukast, a systemic anti-leukotriene and by Mitsunobu and colleagues<sup>325</sup> on use of systemic corticosteroids in asthmatic individuals.

Different methods of air trapping analysis which incorporates heterogeneity perception have been utilised. Mitsunobu *et al.* have described fractal analysis to describe the complexity of terminal airspace geometry in addition to low attenuation areas, both of which may be critical for assessment of small airway involvement in asthma.<sup>328</sup> Novel methods of assessing regional air trapping using optical flow method<sup>329</sup> to align inspiratory and expiratory MDCT datasets have also been described. As with the proximal airway assessment, there are large variations in the scanning protocols and the indices of air trapping employed by researchers. Nevertheless, quantitative CT assessment of distal airway involvement in severe asthma shows great promise and will undoubtedly further our understanding of disease pathogenesis and unravel novel imaging ‘biomarkers’.



### 1.2.1.5 Fractals and asthma

The concept of fractal geometry was formulated by the mathematician Benoit Mandelbrot.<sup>330</sup> He used biological specimens such as mammalian brain folds and alveolar cell membranes to illustrate the relationships of length-area-volume. The word ‘fractal’ is derived from the Latin *fractus*, meaning irregular or fragmented, which reflects one of the fundamental properties of a fractal structure: self-scaling similarity or scale-invariance.<sup>331</sup> Fractal objects are composed of subunits (and further subunits and so on) that resemble the structure of the entire object itself. Fractal structures therefore look essentially the same irrespective of the scale they are examined on and do not have any natural scale for measurement. Many complex anatomic structures also exhibit fractal geometry,<sup>332</sup> including areas of low attenuation on CT scans of asthmatic<sup>328</sup> and chronic obstructive pulmonary disease (COPD)<sup>333</sup> patients, branching networks such as retinal vasculature,<sup>334</sup> His-Purkinje conducting system,<sup>335</sup> and the tracheobronchial tree.<sup>332,336,337</sup> Euclidean geometry, which is traditionally used to describe the airway tree, is sufficient for assessment of basic dimensions but incapable of generating a precise measure of complex structures such as the tracheobronchial tree. Fractal geometry allows there to be measures, which change in a non-integer or fractional way when the unit of measurement changes. Fractal dimension (FD) is used to quantify the degree of self-similarity exhibited by fractal structures and is closely related to a power law distribution.<sup>338,339</sup> FD can be used to quantitate global description of shapes of objects and is associated with its complexity.<sup>340</sup> FD for a branching structure like vascular tree<sup>341</sup> or tracheobronchial tree,<sup>342</sup> describes the complexity of the structure by estimating the degree of branching. In a two-dimensional image of the tracheobronchial tree the FD can take on any decimalised value between 0 and

2. Decreased FD in asthmatic patients compared to healthy subjects has been shown with analyses of bronchial tree,<sup>342</sup> peak expiratory flow (PEF) time series<sup>343</sup> and, fluctuation in daily fraction of exhaled nitric oxide.<sup>344</sup> In addition, Mitsunobu *et al.* have demonstrated that FD of low attenuation clusters (LAC) at -950 HU was significantly lower in severe asthma in comparison to mild and moderate asthma.<sup>328</sup>

#### **1.2.1.6 CT associated radiation exposure and risks**

CT examinations are now extensively used for clinical diagnostic and research purposes. Explosive increase in utilisation of CT scanning has been reported in various countries<sup>345,346</sup> including UK.<sup>347,348</sup> X-ray radiation dose due to CT, although considered low-level radiation exposure, is greater than most conventional radiological examinations. For instance, a standard clinical thoracic CT scan [3-6 milli-sievert (mSv)] imparts 90 to 180 times more radiation dose compared to postero-anterior chest radiograph acquired using digital radiography [ $\sim 0.03$  mSv].

Ionising radiation are associated with essentially two types of effects: (1) deterministic effects seen immediately after large radiation exposure, and (2) stochastic effect which is associated with low exposures and has a considerable latent period (6 – 25 years). Stochastic risks are believed to be cumulative with successive exposures resulting in increased risk and are dependent of type of ionizing radiation administered, nature of receptive tissue and subjects' age. The detrimental effect due to low-level radiation, as imparted by CT examination, is a contentious matter. Biological effects of low-level ionising radiations have been evaluated on populations exposed to high doses of radiation i.e. nuclear explosion survivors<sup>349</sup> by the International Commission on Radiological

Protection (ICRP) based on linear no-threshold (LNT) hypothesis under which cancer risk increases linearly as the radiation dose increases.<sup>350</sup> It was estimated by ICRP that 50 additional fatal cancers were induced per million people exposed to 1 mSv of radiation due to medical reasons.<sup>349</sup> However, conflicting evidence from the French Academy of Science suggests that no significant risk of increased cancer exists with radiation exposures less than 20 mSv.<sup>351</sup> Berrington *et al.* in a long-term follow up study of British radiologists showed lower cancer associated mortality than predicted by atomic bomb data and no evidence of increase in cancer associated mortality among radiologists who first registered after 1954.<sup>352</sup> In addition, tissue culture experiments have demonstrated that low level radiation exposure induces mechanisms leading to free radical detoxification, suggesting that low-level radiation may be beneficial.<sup>353</sup> There are reports supporting the radiation hormesis model which, unlike the LNT model, assumes that adaptive / protective mechanisms can be stimulated by low-dose radiation.<sup>354</sup> Recently, a study of 407,000 radiation workers followed for 20 years in 15 different countries providing 5.2 million person-years follow-up, showed that an excess relative risk (ERR) for all cause mortality was 0.42 per Sievert (0.00042 per mSv).<sup>355</sup> Moreover, risk estimates were not driven by just the higher dose category when assessment was made after dividing the subjects in four categories based on radiation dose received (less than – 400, 200, 150 and 100 mSv) suggesting that small but statistically significant cancer risk exists even with low-dose radiation. Children are more sensitive to radiation than adults and it has been shown that risk in women is approximately twice that of males for the same level of radiation exposure.<sup>356,357</sup> In addition, radiation field for thoracic CT includes radiosensitive breast tissue in females, increasing the risk of breast cancer in younger females exposed to radiation.<sup>358,359</sup> Calculated<sup>358</sup> and measured<sup>359,360</sup> radiation dose to breast tissue during

thoracic CT examination show variable results. Hurwitz *et al.* have demonstrated that radiation dose to breast tissue from CT scans performed on 16 slice MDCT for pulmonary embolism protocol ranged from 4-6 centigray (cGy)<sup>359</sup> which is substantially greater than the average glandular dose of 0.3 cGy<sup>358</sup> for standard two-view screening mammography.

Radiation dose measurement can be performed using numerous methods. Effective dose (ED) estimates the whole body dose required to produce the same stochastic risk as the partial body dose delivered due to localized CT scan. Unit of measurement of ED is sievert (Sv) or mSv. ED can be calculated by summing the product of absorbed dose of each organ and their tissue weighting factors (based on organ radio-sensitivity).<sup>349</sup> Another simpler method of estimating the ED is multiplication of dose-length product (DLP) by normalized effective dose coefficients for the scanned part of the body.<sup>361</sup> In addition ED can also be calculated using the ImPACT CT dosimetry calculator that is based on Monte Carlo simulations<sup>362</sup> of calculated x-ray spectra in an adult, hermaphrodite, mathematical phantom.<sup>363</sup> CT radiation dose reduction can be achieved by controlling various acquisition factors such as tube-current time product, tube voltage, pitch and scan length.<sup>361</sup> On the other hand, certain dose reduction techniques such as tube-current modulation<sup>364</sup> may introduce significant errors in quantitative densitometry for emphysema and air-trapping analysis.<sup>316</sup> Adequate balance is required between dose reduction and obtaining CT images of clinically diagnostic quality. CT images obtained for research purposes should also fulfill the need of qualitative or quantitative assessment.

Mean ED for common radiological examinations in UK is presented in [Section 3.5.4.8, Table 3.36]. The mean ED due to thoracic (cancer staging) CT is 6.8 mSv. Compared to this, the average natural background radiation in the UK is 2.2 mSv; range [1.5 - 7.5

mSv].<sup>365</sup> ED of 8 mSv (equivalent to 3.6 years of natural background radiation) leads to approximately 1 additional cancer per 2500 exposed.<sup>365</sup> This increase in the possibility of a fatal cancer from radiation can be compared to the natural incidence of fatal cancer in the UK population, about 1 chance in 4.<sup>366</sup> The long-term fatal cancer risk is estimated to be 5% per Sv of whole body ED. This suggests that an additional radiation dose of 5 mSv would add an additional 0.025% to a person's 25% risk of dying from cancer.<sup>366</sup>

### **1.2.1.7 New developments in CT technology**

Comprehensive assessment of asthma by a 'single' imaging test is perhaps no longer an enigma. Evaluation of asthma includes both morphological assessment of airways and functional analysis of regional ventilation. As described previously, due to its superior spatial resolution MDCT is preferred for morphological assessment whereas, analysis of regional ventilation is currently performed by magnetic resonance imaging (MRI) using hyperpolarised gases. An ideal technique would combine the utility of MDCT and MRI to provide both morphological and functional data in one test.

This can be achieved by using synchrotron radiation CT / dual-energy CT. Ventilation imaging can be accomplished by performing non-radioactive Xenon enhanced CT. Due to its radiodense nature, using CT, it is possible to track the density changes occurring regionally at the bronchoalveolar levels after inhalation of Xenon. Two Xenon CT techniques have been developed to assess regional ventilation: single breath and multi breath. In the former, imaging is performed after the subject takes a single deep breath of high Xenon concentration mixture. In multi breath technique, multiple sets of scans are performed at end expiration with help of respiratory gating in a series of standardised tidal

breaths during wash-in and/or wash-out of Xenon.<sup>367-369</sup> As the dynamic multi breath technique requires respiratory gating, to ensure acquisition of images at the same point of a standardised tidal breath, its use has been most effective in research animals by use of respirators. As a result of this complexity and higher radiation burden there is more interest in single breath technique.<sup>367</sup>

Synchrotron radiation CT and dual energy CT can both be used for single breath technique. In these, subjects are simultaneously scanned by two x-ray beams of different energies after inhalation of Xenon. By using different energy beams, it is possible to differentiate materials such as bone, air, soft tissue and Xenon from one another based on their specific attenuation differences at low and high x-ray energies.<sup>370</sup>

In synchrotron radiation CT two monochromatic x-ray beams produced from the continuous synchrotron radiation spectrum are tuned to energy levels above and below the K-edge of Xenon. Images obtained at higher energy are then subtracted (on a logarithmic scale) from the lower energy image, thereby removing the contribution of bone and soft tissue, yielding the distribution of Xenon in the lungs.<sup>371,372</sup> This technique, called K-edge subtraction technique, has several advantages over conventional CT such as improved contrast resolution by avoidance of non-selective contrast and beam hardening; simultaneous acquisition of morphological as well as functional data and; ability to assess both spatial distribution and absolute density of Xenon regionally.<sup>373</sup> Monfraix *et al.* performed quantitative measurement of regional lung gas volume and regional lung compliance in rabbit lung using synchrotron radiation CT.<sup>374</sup> Bayat and colleagues using synchrotron radiation CT demonstrated that the airway reaction to inhaled histamine and subsequent recovery are significantly slower in proximal than in distal bronchi of healthy

rabbit.<sup>375</sup> Using the same technique on healthy and ovalbumin sensitised rabbits, Bayat and colleagues observed strong correlations of forced oscillation technique measured airway conductance and tissue elastance with central airway cross-sectional area and ventilated alveolar area respectively.<sup>376</sup> K-edge subtraction imaging can also provide measures of regional perfusion and permeability.<sup>377</sup>

Dual energy MDCT scanner has two x ray sources which can work at two different energy levels simultaneously. One source is operated at an energy level of 140 peak kilovoltage (kVp) while the other is operated at 80 kVp. The entire thorax is usually scanned in one single breath-hold of approximately 10-15 seconds. From each scan, 3 sets of images of 80 kVp, 140 kVp and weighted average images are automatically generated. The weighted average image is formed by a combination of 80 and 140 kVp data and can be used for morphological assessment of airways. The separate 80 and 140 kVp images are then post processed using multi-modality software to obtain a 'Xenon map' depicting the regional ventilation of the airways by Xenon.<sup>378</sup> The radiation burden from dual energy MDCT of thorax is not substantially different from traditional MDCT.<sup>378,379</sup> Due to the limited availability of synchrotron x-ray sources dual energy MDCT is likely to be used more often in future for both clinical and research purposes.

Chae *et al.* in their study showed that ventilation defects can be demonstrated in stable asthmatics by Xenon ventilation dual energy CT.<sup>378</sup> They also showed that the ventilation defect score correlated with FEV<sub>1</sub> / forced vital capacity (FVC) ratio, diffusion capacity and residual lung volumes. The configuration and location of regional ventilation defects on dual energy CT were similar to those on Helium MRI.<sup>378</sup> Lung perfusion imaging can also be performed using dual energy CT scanning as it can provide an iodine map of the

lung microcirculation.<sup>380</sup> Although true perfusion imaging is not performed using dual energy CT as it visualises only blood volume and not blood flow, it may help in assessment of perfusion alterations due to vascular remodelling, an important feature of asthma.<sup>49</sup> Apart from demonstrating morphology and regional perfusion or ventilation defects, dual energy CT can potentially be helpful in understanding the pathogenesis of the disease especially helping in phenotyping patients with severe asthma and evaluating response to treatment.

## **1.2.2 Other imaging techniques in asthma**

### **1.2.2.1 Chest radiographs**

Plain chest radiography is relatively non-specific in diagnosis and characterisation of asthma. The use of chest radiographs is largely to exclude other conditions, like cardiogenic pulmonary oedema; tumours; pneumothorax or pneumonia, which may imitate or complicate asthma. Increased lung volume, increased lung lucency, bronchial wall thickening and mild prominence of hilar vasculature resulting from transient pulmonary hypertension are the features that could be seen on radiographs of patients with asthma.<sup>381-</sup>  
<sup>385</sup> Yield for unselected routine chest radiographs has been shown to be very low.<sup>385,386</sup> Zieverink *et al.* assessed 528 chest radiographs among 122 patients with asthma presenting to emergency department, of which only 2.2% were abnormal.<sup>385</sup> There is poor correlation between the severity of radiographic findings and the severity and reversibility of an asthma attack.<sup>381,384,385</sup> Routine use of chest radiographs in clinical assessment of known asthmatics is discouraged unless there are atypical features or there is suspicion of a



complication. Tsai *et al.*, have proposed guidelines for restricted use of chest radiographs in patients who fulfil one or more of the following criteria: clinical diagnosis of chronic obstructive pulmonary disease (as defined by ATS); fever or temperature more than 37.8 °C; clinical or electrocardiograph evidence of right heart disease; intravenous drug abuse; seizures; immunosuppression; other lung disease or prior thoracic surgery.<sup>382,387</sup> Using these guidelines, it is not only possible to reduce the performance of unnecessary chest radiographs but also improve its clinical utility.<sup>387,388</sup>

### **1.2.2.2 Endobronchial ultrasound**

Endobronchial ultrasound (EBUS) has emerged as a promising new technique to assess airway remodelling in asthmatic patients. Shaw *et al.* used EBUS to measure the ratio of wall thickness to diameter as well as wall area percentage in sheep and healthy human subjects and found no significant difference between measurements made using EBUS or HRCT.<sup>389</sup> Soja and colleagues in a study of 35 asthmatic and 23 control subjects have confirmed that measures of total bronchial wall thickness and wall area were comparable when performed using EBUS or HRCT.<sup>151</sup> In addition, using EBUS they could identify five different layers of the bronchial wall. They demonstrated that the thickness and wall area of the bronchial wall and its layers were significantly greater in asthmatic subjects when compared to healthy controls. Airway remodelling assessed with EBUS correlated well with histologically assessed RBM thickness and pre-bronchodilator FEV<sub>1</sub> in asthma patients. EBUS has also been used to assess the effect of therapy on airway wall changes by Yamasaki *et al.* They demonstrated a decrease in subepithelial oedema in an asthmatic patient after montelukast therapy.<sup>390</sup>

### 1.2.2.3 Positron emission tomography

Positron emission tomography (PET) imaging, which enables quantitative non-invasive *in vivo* assessment of pulmonary perfusion and ventilation, provides valuable insights into the pathophysiology of asthma.<sup>391-395</sup> Vidal Melo and colleagues have demonstrated that ventilation-perfusion distributions during experimental bronchoconstriction results from both, (i) ventilation-perfusion heterogeneity between large lung regions of segmental level as well as (ii) intraregional heterogeneity within lung structures with volume lower than 2.2 cm<sup>3</sup>.<sup>392,393</sup> Anafi *et al.*, with help of single terminal airway model have concluded that heterogeneity of whole lung constriction is a consequence of bi-stable terminal bronchiolar constriction.<sup>395</sup> Venegas *et al.*,<sup>394</sup> on basis of experimental data and network airway model, demonstrated that (i) as the smooth muscle tone is increased an initially uniform distribution of ventilation gives rise to a catastrophic, stepwise development of clusters of hypoventilated units; (ii) there is coexistence of ventilated and poorly ventilated terminal units within the clusters of hypoventilated units; (iii) with decreasing tidal volume the hypoventilated cluster size and number of severely constricted terminal bronchioles increase suggesting that in severe asthma as tidal volume is reduced due to increasing respiratory effort and fatigue, the remaining open part of the lung is exposed to catastrophic airway closures which can lead to respiratory failure without prompt treatment. PET has also been used for assessment of lung inflammation through evaluation of metabolic activity of neutrophils as well as by using it for reporter gene imaging.<sup>396,397</sup>

#### **1.2.2.4 Magnetic resonance imaging**

The delayed evolution of MRI of the lungs has been attributed to factors that make lungs inhospitable for generating MR images, like low proton density and field inhomogeneity. Conventional proton MRI has limited spatial resolution at field strengths employed in routine clinical imaging. Recent developments in pulse sequences with very short echo times have considerably improved lung parenchymal imaging using proton MRI.<sup>398</sup> In addition, functional imaging using proton MRI, with use of arterial spin-tagging method of perfusion imaging<sup>399</sup> and oxygen-enhanced MRI for ventilation imaging,<sup>400</sup> have been reported. Hyperpolarised (HP) MRI has revolutionised the field of pulmonary imaging and continues to develop rapidly since the first images acquired in the early 1990s.<sup>401</sup> This technique utilises hyperpolarised noble gases, such as 3-Helium ( $^3\text{He}$ ) and 129-xenon ( $^{129}\text{Xe}$ ), which act as contrast agents that can diffuse rapidly to occupy the airspaces in the lung and allow visualisation and measurement of the ventilated airways and alveolar spaces. Functional imaging is therefore possible with HP MRI techniques, providing 3D regional information; quantitative static and dynamic measures of ventilation and perfusion; small airway size and configuration using diffusion imaging; and regional intrapulmonary oxygen partial pressure measures. Ability of HP MRI to provide these novel physiological measures within the lung and its potential use in longitudinal studies due to lack of ionising radiation makes this one of the most attractive modalities in pulmonary imaging.

Apparent diffusion coefficient is the measured value of average travelled distance of gas atoms during a given duration of time. Apparent diffusion coefficient therefore can reveal

changes in lung microstructure (alveolar size and small airways)<sup>402-404</sup> and be utilised for early detection<sup>405</sup> and progression<sup>406</sup> of parenchymal disease. Since Chen and colleagues<sup>407</sup> first demonstrated use of HP  $^3\text{He}$  MRI for in vivo measurement of parenchymal structure, many advances have been made in this field. In addition to the short-range apparent diffusion coefficient measurements made over few milliseconds which are sensitive to alveolar morphology,<sup>403,404,408</sup> long-range apparent diffusion coefficient measurements have been described which are made over a period of about 1 second and may be sensitive to factors that affect connectivity of the small airways.<sup>409-412</sup> Apparent diffusion coefficient measurements have been shown to correlate with CT assessed air trapping / emphysema indices<sup>413</sup> as well as with histology.<sup>414,415</sup> Wang and colleagues,<sup>410</sup> who developed a novel hybrid MR pulse sequence to obtain co-registered apparent diffusion coefficient maps of Helium at both short and long time-scales during a single breath-hold, demonstrate that apparent diffusion coefficient values in asthmatic patients are significantly elevated as compared to healthy subjects and were heterogeneous. These findings suggest that changes in lung microstructure in asthma can be detected using HP  $^3\text{He}$  MRI and such changes may reflect tissue remodelling including permanent changes in airway structure.

In addition to quantification of the microstructural changes, HP MRI allows assessment of functional aspects of asthma such as oxygenation, ventilation and perfusion.<sup>416,417</sup> Measurement of regional alveolar oxygen tension in lungs with HP gas MRI using both  $^3\text{He}$ <sup>418-421</sup> and  $^{129}\text{Xe}$ <sup>422</sup> has been described and validated using phantom models.<sup>423</sup> In addition novel technique of simultaneous measurement of alveolar partial pressure of oxygen and apparent diffusion coefficient during single breath-hold has been developed.<sup>424</sup> Ventilation defects assessed with HP  $^3\text{He}$  MRI are present in asthmatic subjects in contrast

to healthy controls.<sup>425</sup> Techniques to quantify steady state assessment of the ventilation defects<sup>426,427</sup> and image dynamic gas flow in lungs have been described.<sup>428,429</sup> Further improvements in HP gas MRI techniques have enabled investigators to perform dynamic 3D imaging of the lungs<sup>430,431</sup> and compare HP gas MRI assessed regional ventilation defects in asthmatics with spirometry, body plethysmography and MDCT.<sup>432 433</sup> Extent of HP <sup>3</sup>He MRI determined ventilation defects in asthma was related to neutrophilic inflammation,<sup>433</sup> disease severity<sup>434</sup> and airway hyperresponsiveness.<sup>435</sup> Using HP gas MRI it also became evident that ventilation defects are already present in asthma subjects with normal lung functions. These ventilation defects tend to disappear after bronchodilator treatment but predominantly reappear in regions where they existed before.<sup>425,435</sup> Furthermore, concurrent assessment of apparent diffusion coefficient and ventilation data in a single breath-hold not only helps conserve HP gas and reduce patient inconvenience but allows quantitative cross-correlation between the two indices.<sup>436</sup> Regional pulmonary perfusion can be measured by HP MRI using indirect or direct method. Regional ventilation perfusion ratios derived from measurements of partial pressure of oxygen and separate assessment of regional ventilation allows calculation of pulmonary perfusion on a regional basis.<sup>437</sup> Direct evaluation of pulmonary perfusion using contrast-enhanced MRI<sup>438,439</sup> as well as by using HP 13-Carbon<sup>440</sup> has been demonstrated. Development of open-access, low-field MR system for both horizontal and upright imaging by Tsai and co-workers<sup>441</sup> exemplify the continuing advances in HP gas MRI technology. HP MRI though currently a research tool has potential to soon become an essential clinical tool.

### 1.2.2.5 Optical coherence tomography

Optical coherence tomography (OCT) is a new imaging technique, which uses low-coherence near-infrared light to image cellular and extracellular structures by detecting light reflected from tissue structures and forming a cross-sectional image through optical interferometry. OCT produces high spatial resolution images of 3 – 16  $\mu\text{m}$  with tissue penetration to 1-3 mm.<sup>442-444</sup> OCT use for airway imaging has been assessed using various validation studies.<sup>152-154</sup> OCT unlike CT can be used for small airway imaging *in vivo* with near microscopic resolution and no associated risks to patients from weak near-infrared light. OCT is performed during bronchoscopic examination and therefore does involve local anaesthesia and sedation. Coxson *et al.* performed the first proof-of-principle study to assess use of OCT in COPD patients.<sup>155</sup> OCT measures of airway dimensions correlated well with CT measures and lung function. Compared to CT, OCT estimation of LA and WA was lower by 31 and 66 % respectively. Recently Williamson and coworkers<sup>445</sup> have also shown a reduced LA in asthma subjects compared to controls using OCT. Novel techniques such as anatomical OCT (aOCT)<sup>446-448</sup> have been developed which allow real-time 3D imaging<sup>449</sup> of changes at the luminal surface including the mucosal folds of the airway and its temporal relation with corresponding dynamic changes within the entire inner airway wall with mucosa and ASM, and partial cartilaginous outer wall.<sup>450</sup> This technique therefore enables real-time assessment of patho-physiological phenomena fundamental to asthma such as relationship between ASM shortening and luminal narrowing.

### **1.2.2.6 Confocal florescence endomicroscopy**

Confocal florescence endomicroscopy is an emerging technique that utilises 488 nm or 660 nm excitation laser light and thin flexible miniprobes that are introduced into the working channel of the bronchoscope for real-time, microscopic, *in vivo* imaging of the pulmonary tissue with lateral resolution of 3  $\mu\text{m}$  and a field of view of 600  $\mu\text{m}$ .<sup>451,452</sup> Potential applications include qualitative and quantitative assessment of the basement membrane, terminal airways and alveoli in obstructive lung diseases including asthma. Despite limitations such as small field of view and limited depth of tissue penetration, this technique coupled with molecular imaging<sup>453</sup> may assist in early diagnosis, disease phenotyping based on molecular markers and assessment of response to current and novel therapies in the near future.

### **1.2.2.7 Molecular imaging**

Molecular imaging is a relatively new addition to the ever increasing imaging armamentarium. This has provided a new direction where, using remote imaging detectors, non-invasive measurements of molecular pathway and biochemistry in animal models and humans is possible at cellular and molecular level. A variety of processes such as signal transduction, host response to pathogen, receptor density and function and gene transfer can be studied using PET, single photon emission tomography (SPECT), optical imaging and MRI. Optical imaging will be discussed further in this section as other modalities if relevant to asthma have been discussed in their respective sections. Optical fluorescence imaging is one such technique where near-infrared fluorescent (NIRF) probes are used to

image molecular events in living tissue. There have been reports on fluorescent probes that allow visualisation of key processes of asthma *in vivo* including probes targeting proteases of the cathepsin family.<sup>454,455</sup> Many other molecules and processes can be targeted such as matrix metalloproteinases,<sup>456</sup> mast cell tryptase, integrins or physiological responses associated with vascularisation, blood flow, and blood oxygenation.<sup>455</sup> Optical fluorescence imaging does not pose an ionising radiation risk and is relatively inexpensive. Three-dimensional fluorescence molecular tomography (FMT) is a technology developed to quantitatively image the up-regulation and function of tumoral proteases, cellular receptors and other proteins.<sup>457</sup> Assessment of eosinophil activity in response to dexamethasone treatment in mouse models of allergic airway inflammation using FMT in conjunction with activatable fluorescent probes has been reported.<sup>454,455</sup> FMT, with ability for 3D imaging; potential for concurrent resolution of multiple targets by imaging at different wavelengths; and use of safe non-ionising radiation, may be well suited to study disease progression and characterisation of drug efficacy longitudinally.



### 1.2.3 Figures and Tables

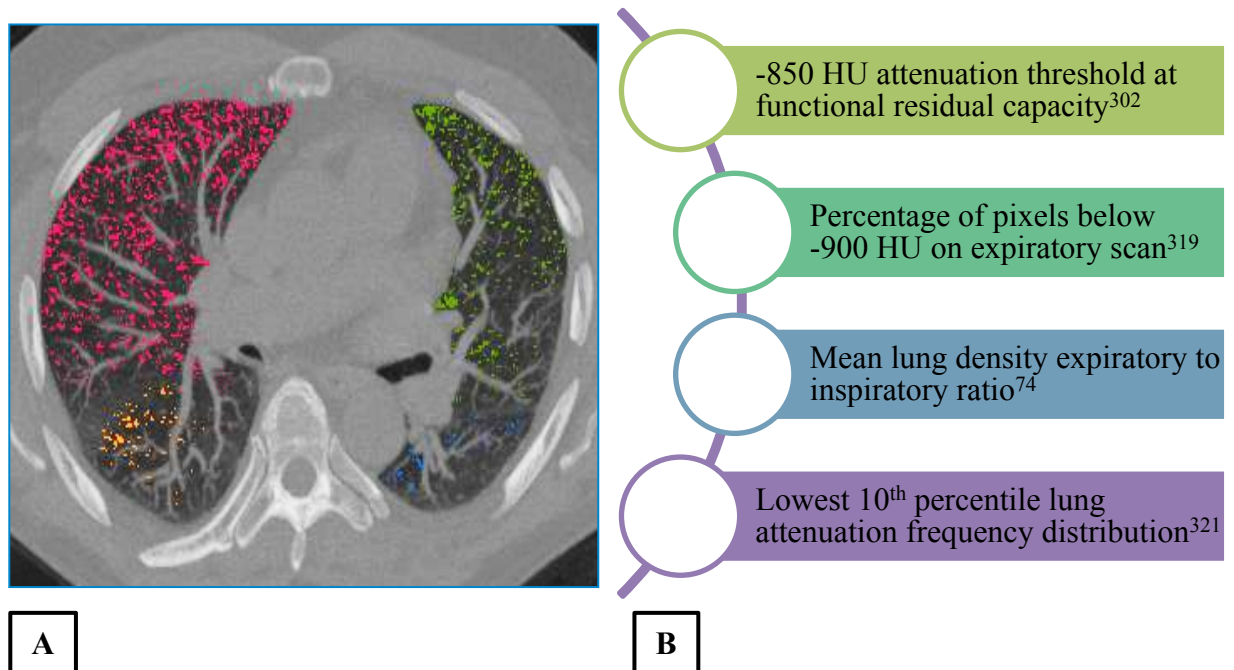


**Figure 1.5: Air-trapping quantification indices**

(A) Air-trapping, defined as voxels in the lung field below -850 HU on expiratory CT, depicted and colour coded by lobe in severe asthma patient; (B) Various indices for air trapping quantification

## 1.3 Hypotheses

1. I hypothesise that airway structural changes on computed tomography are not common in severe asthma patients and show no correlation with lung function.
2. I hypothesise that airway and densitometry phantom models cannot be used to validate and standardise quantitative computed tomography indices.
3. I hypothesise that airway remodelling assessed by computed tomography does not differ between severe asthma phenotypes.
4. I hypothesise that specific inhibition of eosinophilic inflammation will not reduce asthma exacerbations in refractory eosinophilic asthma patients and will not modulate the airway remodelling as assessed by computed tomography.
5. I hypothesise that asthma phenotypes, determined by quantitative CT measures of proximal and distal airway remodelling, do not have distinct clinical and physiological features.

## **1.4 Aims**

### **Qualitative Analysis of High Resolution Computed Tomography Scans in Severe Asthma.**

1. To assess the prevalence of airway structural changes i.e. bronchial wall thickening and bronchiectasis, as assessed by HRCT in severe asthma patients.
2. To define the clinical characteristics of those subjects with and without bronchiectasis and/or bronchial wall thickening and assess the validity of these clinical parameters to guide the application of HRCT in severe asthma.

### **Use of Airway and Densitometry Phantoms for Standardisation and Validation of Quantitative Computed Tomography Indices**

3. To assess different sources of errors in airway morphometry and lung densitometry.
4. To assess the variability in airway morphometry and lung densitometry measures arising from scanner non-conformity.
5. To develop novel airway and densitometry phantoms and assess their validity for standardisation of quantitative CT measures in multicentre studies as well as correction of different errors associated with airway morphometry and lung densitometry.

### **Quantitative Analysis of Airway Remodeling Using High Resolution Computed Tomography Scans in Severe Asthma.**

6. To compare CT derived dimensions of RB1 bronchus between severe asthma phenotypes.
7. To assess whether clinical features relating to patients' demographic profiles, symptoms, pulmonary functions or airway inflammation are associated with geometry of RB1 bronchus.

#### **Mepolizumab (Anti-IL 5) and Exacerbations of Refractory Eosinophilic Asthma.**

8. To assess the effect of 12 month therapy with mepolizumab, an anti-interleukin-5 antibody, in patients with refractory eosinophilic asthma on asthma exacerbations and CT assessed RB1 dimensions.

#### **Asthma Phenotypes based on Quantitative Computed Tomography Analysis of Proximal and Distal Airway Remodelling**

9. To assess the use of factor and cluster analysis with quantitative proximal and distal airway CT indices in identification of novel asthma phenotypes and compare their clinical and physiological features.
10. To compare quantitative CT measures of proximal and distal airway remodelling from volumetric paired inspiratory and expiratory CT scans between severe asthma, mild / moderate asthma and healthy controls.
11. To compare fractal dimension of segmented airway tree and terminal air space between severe asthma, mild / moderate asthma and healthy controls.
12. To assess temporal pattern of proximal airway remodelling in quantitative CT asthma clusters from a subset of severe eosinophilic asthma patients.

## 2 METHODS

---

## **2.1 Clinical Methods**

### **2.1.1 Baseline demographics and history**

Baseline demographic details and clinical history was recorded which included disease duration, age of onset, triggers, co-morbidities, smoking history, occupational history, exacerbations and treatment.

### **2.1.2 Peripheral blood**

Peripheral venous blood was obtained for analysis including full blood count, eosinophil count, neutrophil count, aspergillus IgG, total and specific IgE.

### **2.1.3 Allergen skin testing**

Allergen skin sensitivity will be measured by skin prick for a panel of common aeroallergens (cat fur, dog dander, grass pollen, *Dermatophagoides pteronyssinus* and *Aspergillus fumigatus*), with controls consisting of normal saline and histamine. Wheal response were measured at 15 minutes and a positive response to an allergen on the skin prick tests was recorded in the presence of a wheal diameter  $\geq 2$  mm that of the negative control. A positive response to one or more allergen constituted atopy. All subjects were instructed to withhold therapy with anti-histamines for at least 3 days prior to testing.

### **2.1.4 Spirometry and lung function tests**

Spirometry was performed using rolling seal spirometer (Vitalograph, Buckinghamshire, UK) as the best of three successive readings within 100 mls in a seated position. Bronchodilator reversibility was assessed 20 minutes after inhalation of 200 µg salbutamol via a large volumatic spacer or administration of 2.5 mg of nebulised salbutamol. Full lung function analysis was performed in the respiratory physiology department by trained technicians using body plethysmography (Pulmolink constant pressure body box) or helium dilution technique (Spiro Air, Medisoft, Belgium).

### **2.1.5 Fractional exhaled nitric oxide**

Fractional exhaled nitric oxide (FE<sub>NO</sub>) was measured at a flow rate of 50 mL/s using an online chemiluminescence analyser (NIOX; Aerocrine, Stockholm, Sweden) as the best of two readings.<sup>458</sup> The test was performed prior to any other measurements and before administration of any other inhaled medications on the day, in accordance with ERS recommendations. Patients were instructed to refrain from taking long acting beta agonist or antihistamine medications for 48 hours prior to the test.

### **2.1.6 Methacholine challenge test**

Bronchial responsiveness is expressed as provocative concentration of methacholine causing a 20% fall in FEV<sub>1</sub> (PC<sub>20</sub>MCh). Bronchial provocation testing to methacholine was performed using the standard tidal breathing method as described previously.<sup>459</sup> Long

acting beta-2 agonist and ipratropium bromide was withheld for 24 hours and short acting beta-2 agonist for six hours before testing. A baseline FEV<sub>1</sub> measurement was made initially and the provocation test could only proceed if the baseline FEV<sub>1</sub> > 60% predicted or baseline FEV<sub>1</sub> > 1 litre and subjects had no other contraindication such as poorly controlled hypertension.<sup>460</sup> The subjects initially inhaled saline and a fall in FEV<sub>1</sub> of >10% after saline inhalation precluded continuation of the methacholine challenge and PC<sub>20</sub>MCh was assigned a value of 0.015. Doubling concentrations of methacholine were inhaled from 0.03 mg/ml to the maximum concentration of 16 mg/ml via a Wright's nebuliser at an output of 0.13 ml/min. Subjects were instructed to continue breathing with a tidal pattern during inhalation of the solution for 2 minutes. A nose clip was applied to ensure that the respiration was entirely via patient's mouth. FEV<sub>1</sub> measurements were made 30 and 90 s after each methacholine nebulisation. Spirometry was repeated at 3 minutes if the FEV<sub>1</sub> at 90 seconds was lower than the reading at 30 seconds. The lowest FEV<sub>1</sub> after each dose of methacholine was used to calculate the % drop from baseline. If there was a fall in FEV<sub>1</sub> of more than 20% from baseline or the highest concentration of methacholine was reached no further inhalations were given. PC<sub>20</sub>MCh was calculated by linear interpolation of the log-concentration response plot.

### **2.1.7 Sputum Induction**

Sputum was collected and processed as previously described.<sup>51</sup> Subjects were pretreated with 200 µg of inhaled salbutamol via a volumatic chamber 15 minutes before starting sputum induction in order to minimise bronchoconstriction. Sputum was induced using 3, 4 and 5% saline inhaled in sequence for five minutes via an ultrasonic nebuliser (Medix,



Harlow, UK; output 0.9 ml/min; mass median diameter 5.5  $\mu\text{m}$ ). Subjects were instructed to breathe normally (tidal breathing) and to take a slightly deep breath every minute. After each saline inhalation patients blew their noses and rinsed their mouths to minimise nasal contamination. Following this, expectorated sputum was collected into a sterile pot. FEV<sub>1</sub> was monitored closely and measurements were made after each inhalation. If the fall in FEV<sub>1</sub> was more than 10% but less than 20% of the best post-bronchodilator value the same concentration of saline is administered during the next inhalation. If the fall in FEV<sub>1</sub> was more than 20% of the best post-bronchodilator value, or if the patient experienced significant symptoms, the saline nebulisation was stopped and the patient was treated with short-acting beta-agonist.

## **2.1.8 Asthma symptom and quality of life scores**

### **2.1.8.1 Juniper Asthma Control Questionnaire (JACQ) score**

Juniper Asthma Control Questionnaire has 7 elements, 5 questions about different aspects of symptom control, rescue bronchodilator use and measurement of airflow obstruction, expressed as pre-bronchodilator % predicted FEV<sub>1</sub>.<sup>461</sup> For each of the five questions, subjects describe their control for the preceding two weeks on a severity scale of 0-6. Rescue bronchodilator use and pre-bronchodilator FEV<sub>1</sub> (% predicted) are also scored on a scale of 0-6. Scores of all the 7 attributes are added together and the total is divided by seven to give the overall score. JACQ score  $\geq 1.57$  indicates suboptimal control of asthma symptoms and a change in the JACQ score of 0.5 between visits is considered clinically significant.<sup>461</sup> Three shortened versions of the JACQ (symptoms alone, symptoms plus

FEV1 and symptoms plus short-acting  $\beta$ 2-agonist) have also been validated for use in clinical trials with excellent agreement between the modified shortened JACQ scores and the original 7-point JACQ score.<sup>462</sup> The minimum clinically significant difference between visits for the modified JACQ score was also 0.5.

### **2.1.8.2 Visual Analogue Scale**

This is a validated scoring method that examines the perception of dyspnoea by patients with airways disease on a linear scale of 100 mm.<sup>463</sup> Subjects are presented with a horizontal scale of 100 mm for each of the symptoms of cough, breathlessness or wheeze<sup>57</sup> and were asked to mark their perceived control over the preceding 2 weeks for each symptom on the linear scale (0 mm = no symptoms; 100 mm = worst ever symptoms). Analyses of composite score as arithmetic mean of each score as well as each independent symptom score were performed.

### **2.1.8.3 Juniper Asthma Quality of Life Questionnaire (AQLQ)**

This scoring system is used for quantifying asthma related quality of life.<sup>464</sup> AQLQ consists of 32 items representing four domains: symptoms (12 items), activities (11 items), emotion (5 items), and environment (4 items). Standardised version of AQLQ pre-specifies five activities upon which subjects responds.<sup>465</sup> Each item is scored from 1 – 7 with higher scores indicative of better quality of life. A score is calculated for each domain as the arithmetic mean of item scores or that domain and a composite score is calculated from arithmetic mean of the domain scores.

## **2.2 Laboratory Methods**

### **2.2.1 Sputum processing protocol**

Sputum free from salivary contamination was selected and weighed. To the selected sputum was added 4x volume/weight of 0.1% dithiothrietol (DTT) (Sigma, Poole Dorset). The sputum was dispersed by gentle aspiration into a Pasteur pipette, vortexing for 15 s and rocking on a bench spiromix for 15 mins. After the addition of an equal volume of Dulbecco's phosphate buffered saline (D-PBS) (Sigma, Poole, Dorset) the sputum suspension was filtered through 48µm nylon gauze and centrifuged 2000rpm (790g) for 10 mins. The sputum supernatants was removed and stored at -80°C for future mediator assay. The cell pellet was resuspended in a small volume of PBS. An aliquot was removed and a total cell count, squamous cell contamination and viability were assessed using a Neubauer haemocytometer by the trypan blue exclusion method. The cell suspension was adjusted with PBS to  $0.5-0.75 \times 10^6$  cells/ml and cytopins were prepared from 75µl aliquots at 450rpm (18.1g) for 6 mins using a Shandon III cytocentrifuge (Shandon, UK). The cytopins were stained in neat Romanowski stain for 5 mins and fixed in dilute stain for 25 mins. A differential cell count was obtained by counting >400 non-squamous cells on a Romanowski stained cytospin.

## **2.3 Radiological Methods**

### **2.3.1 Computed Tomography scanning protocols**

#### **2.3.1.1 Standard high-resolution computed tomography (HRCT)**

HRCT was performed using a Picker PQS (February 2000–March 2003) or Siemens Sensation 16 (March 2003–April 2008) scanner. Sequential scanning was performed at 10mm increments with 1mm collimation, from the apex of the lung to the diaphragm [Figure 2.1]. The number of CT slices obtained varied between patients based on their body habitus. Patients were scanned in the supine position at maximal inspiration (adequate breath holding rehearsed prior to scan), with their arms held over their head. Images were reconstructed using a high spatial frequency algorithm, through a 512 X 512 matrix, with a small field of view targeted to image only pulmonary areas. Scanning time ranged between 30-45s with a peak voltage of 120kVp and effective tube current of 140 milliamperereconds (mAs). Long acting bronchodilator therapy was not withheld prior to HRCT scan. Images were saved and reported at a window width of 1600 Hounsfield units (HU) and a window level of -500HU.<sup>279</sup>

#### **2.3.1.2 Limited CT imaging protocol for right upper lobe apical bronchus**

A limited thoracic CT imaging protocol was devised to image the RB1 bronchus [Figure 2.2]. This approach was chosen because: (a) It will minimise radiation exposure by scanning at a single site.<sup>466</sup>, (b) Reference measures of RB1 geometry in asthma<sup>75</sup> and

COPD<sup>466</sup> have been published, (c) RB1 is relatively perpendicular to the CT scanning plane and therefore the errors associated with oblique orientation on two-dimensional quantitative analysis are minimised, (d) RB1 geometry serves as a good surrogate for airway remodelling throughout the airway tree as measurements of RB1 are closely associated with the measurement of multiple airways in asthma<sup>72</sup> and COPD<sup>467</sup>. All subjects were administered a dose of long acting  $\beta$ 2-agonist within 3 hours of the CT being undertaken. Limited thoracic CT scan was performed in supine position at full inspiration with shoulders fully abducted. Adequate breath holding was practiced by the patients prior to the scan. CT scanning was performed with a Siemens Sensation 16 MDCT scanner, at Glenfield Hospital, Leicester. Scans were obtained, with dose modulation switched off, at 16x0.75mm collimation, 120 kVp, 50 mAs, pitch 1.1, scan length 53 mm and scan time of 2.85 s. Images were reconstructed with slice thickness 0.75 mm and slice interval 0.5 mm, using both high (B70f) and low (B35f) spatial frequency algorithm, through a 512 X 512 matrix, with a field of view targeted to include pulmonary areas.

### **2.3.1.3 Full thoracic inspiratory and expiratory CT protocol**

CT scans were acquired using MDCT scanner, Siemens Sensation 16, at Glenfield Hospital, Leicester. All subjects were scanned, within 30 minutes of inhalation of nebulised salbutamol 2.5 milligrams, in the supine position and with shoulders fully abducted, to avoid streak artefacts from arm bones. A foam box (LD15, Styrotech Ltd, West Bromwich, UK) housing three electron density rods (EDR) [LN300, LN450, 'solid water'] from an RMI467 electron density CT phantom (Gammex – RMI Ltd, Nottingham, UK) was secured over the mid-point on the sternum using a *Velcro* belt [Figure 2.3]. Electron density rods

LN300, LN450 and 'solid water' have electron density relative to water of 0.28, 0.40 and 0.99 respectively. Volumetric whole-lung scans were acquired at full inspiration (near TLC) and at the end of normal expiration (near FRC), in a caudo-cranial direction, to minimise motion artefacts secondary to diaphragmatic motion. All subjects rehearsed inspiratory and expiratory breath-hold, at least twice, prior to the CT scan. CT scans were acquired with dose modulation switched off at 16 x 0.75 mm collimation, 1.5 mm pitch, 120 kVp, 40 mAs, 0.5 seconds rotation time and scanning field of view of 500 mm. Images were reconstructed with slice thickness 0.75 mm and slice interval 0.5 mm, using a low spatial frequency algorithm (B35f), through a 512 X 512 matrix, with a field of view targeted to include pulmonary areas and foam box containing three electron density rods.

## **2.3.2 Analysis of Computed Tomography scans**

### **2.3.2.1 Qualitative analysis**

All HRCT scans were qualitatively evaluated by one of the thoracic radiologists. The radiologists were unaware of the patient's inclusion in the study. BE was considered to be present when HRCT scan showed presence of one or more of the following: (a) internal diameter of the bronchus greater than that of the adjacent pulmonary artery, (b) lack of tapering of the bronchial lumen towards the periphery, or (c) visualisation of bronchus within 1 cm of the pleural surface [Figure 2.4].<sup>468</sup> Determination of presence of BWT was based on subjective assessment. The presence of BE or BWT was recorded but the total number of airways assessed could not be determined as with standard HRCT scans an airway cannot always be tracked all the way from its origin to its division and hence the

same airway may be assessed on multiple CT slices. A randomly selected subset of 50 CT scans was reported by another blinded thoracic radiologist, and an inter-observer reliability analysis using the Kappa statistic was performed. Patients were categorised into those with: A) neither BWT or BE (BWT- / BE-), B) BE only (BWT- / BE+), C) presence of both BWT and BE (BWT+ / BE+) or D) BWT only (BWT+ / BE-).

### **2.3.2.2 Quantitative Analysis**

#### **2.3.2.2.1 Two-dimensional quantitative analysis of proximal airway geometry using semi-automated software**

##### ***2.3.2.2.1.1 Assessment using EmphylyxJ software***

A semi-automated program EmphylyxJ V 1.00.01<sup>469</sup> using the FWHM technique<sup>470</sup> was used to determine the airway cross-sectional geometry. CT images reconstructed with high (B70f) spatial frequency algorithm were used. Image data were transferred from the CT workstation to a personal computer in DICOM 3.0 format. After identifying the RB1 bronchus the operator placed a seed point in the airway lumen. Rays are cast out radially from this seed point towards the airway wall. X-ray attenuation values are measured along the rays as they pass from airway lumen to wall and then to the lung parenchyma. As the ray enters the airway wall from the lumen x-ray attenuation increases and then as it passes from the wall to the lung parenchyma x-ray attenuation decreases. The inner and outer boundary points of the airway wall are detected based on the attenuation profiles along the rays.<sup>286,466,471</sup> The point at which the attenuation is half way to the maximum on the lumen side marks the inner boundary and the point at which the attenuation is halfway to the local

minimum on the parenchymal side marks the outer boundary. These points are then connected using an interpolation method to form the inner and outer airway edge<sup>472</sup> from which the airway dimensions are derived [Figure 2.5]. The airway measurements, LA and WA were corrected for size dependent and oblique orientation associated errors as described in [Section 3.2.3.4.3]. LA and WA were also corrected for body surface area (BSA). The total area (TA) and %WA were derived from WA and LA ( $TA = LA + WA$ ;  $\%WA = WA/TA \times 100$ ).

#### ***2.3.2.2.1.2 Assessment using MedView software***

A semi-automated program, MedView beta release version 1.0 (Department ARTEMIS, Institut TELECOM, Evry, France), was used for quantification of the bronchial parameters on CT cross-section images.<sup>289</sup> CT images reconstructed with high (B70f) spatial frequency algorithm were used. The software relies on mathematical morphology and energy-based contour matching for quantification of two-dimensional airway measurements. The image is first normalised with the FWHM method and then segmented in order to extract the inner and outer contours of the bronchus. The outer wall (due to the presence of adjacent vessels) is regularised using reliable wall-based smoothening method. The areas enclosed by the inner and outer walls are then computed pseudo-continuously by a parameterisation of the contour and a triangulation of the surface method.



#### **2.3.2.2.2 Quantitative proximal airway and air-trapping analysis using fully automated software**

Fully automated software, VIDA Pulmonary Workstation, version 2.0 (PW2) [VIDA Diagnostics, Coralville, Iowa, <http://www.vidadiagnostics.com/>] was used for quantitative airway and densitometry analysis. CT images reconstructed with low (B35f) spatial frequency algorithm were used.

##### ***2.3.2.2.2.1 Three-dimensional Quantitative airway analysis***

First five to six generations of the airway tree can be segmented, labeled and reliably measured using PW2, as described and validated before [Figure 2.6].<sup>473-476</sup> Morphological airway measurements were obtained along each centreline voxel of the lumen perpendicular to the long axis on each airway, and averaged over the middle third of the airway segment. LA, TA and length of the right RB1 bronchus and other segmented airways were measured. WA was derived from LA and TA ( $WA = TA - LA$ ). Wall volume (WV), lumen volume (LV) and total volume (TV) were calculated by multiplying respective cross-sectional area measurement with airway length. Percentage wall volume (%WV) was derived from WV and TV ( $\%WV = WV/TV \times 100$ ). The airway measurements, LA, WA and TA were corrected for BSA.

Airway dimensions of two hypothetical airways with internal (lumen) perimeter of 10 mm ( $Pi10$ )<sup>85</sup> and outer airway (external wall) perimeter of 20 mm ( $Po20$ ) were calculated using regression equations based on airway dimension data for each subject. Internal airway perimeter ( $Pi$ ) was plotted against the square root of wall area for all the measured airways.

The wall area (Pi10 WA) for a hypothetical airway with a Pi of 10 mm was then determined. Outer airway wall perimeter (Po) was plotted against the square root of wall area and the square root of lumen area for all the measured airways. The wall area (Po20 WA) and lumen area (Po20 LA) for hypothetical airway with a Po of 20 mm was then determined. Po20 %WA was determined from Po20 WA and Po20 LA ( $\text{Po20 \%WA} = \text{Po 20 WA} / [\text{Po20 WA} + \text{Po20 LA}] \times 100$ ).

#### **2.3.2.2.2.2 *Quantitative air-trapping analysis***

Air-trapping quantification was performed by whole lung densitometry of inspiratory (TLC) and expiratory (FRC) CT scans using PW2 software. Threshold-based technique is used to segment the lungs from rest of the thoracic structures and derives densitometric indices from voxel frequency distribution histogram. Air-trapping indices derived were:

- a) Voxel index (VI) at a threshold of -850 HU at FRC.<sup>302</sup> This is defined as proportion of lung voxels of low density, expressed as percentage, below a threshold of -850 HU at functional residual capacity. CT density of -850 HU represents the density of a fully distended alveolus. Therefore any voxels below -850 HU on an expiratory CT scan must represent areas of air-trapping.
- b) Mean lung density expiratory to inspiratory (MLD E/I) ratio.<sup>74</sup>
- c) VI-850 change on paired inspiratory and expiratory CT scan ( $\text{VI}_{-850} \text{ E-I}$ ).<sup>477</sup> The percentage of lung voxels with attenuation values lower than -850 HU was calculated on both inspiratory and expiratory scans. To evaluate the change in VI-850, the difference between VI-850 on expiratory CT and inspiratory CT was calculated ( $\text{VI}_{-850} \text{ E-I} = \text{VI-850 expiratory CT} - \text{VI-850 inspiratory CT}$ ).

d) Voxel index change of percent voxels between -950 HU and -850 HU on paired inspiratory and expiratory CT scan ( $VI_{-850/-950}$  E-I).<sup>477</sup> The percentage of lung voxels with attenuation values higher than -950 HU and lower than -850 HU were calculated on both inspiratory and expiratory scans. On CT scans the attenuation threshold of -950 HU has been shown macroscopically<sup>478</sup> and microscopically<sup>479</sup> to delineate emphysematous areas of the lungs. Voxel index change of percent voxels between -950 HU and -850 HU ( $VI_{-850/-950}$ ) was calculated for both inspiratory and expiratory scans by subtracting  $VI_{-950}$  from  $VI_{-850}$ . This ensures that any voxels with low attenuation value due to emphysema are eliminated and not included in air-trapping quantification. To evaluate the change in  $VI_{-850/-950}$ , the difference between  $VI_{-850/-950}$  on expiratory CT and inspiratory CT was calculated ( $VI_{-850/-950} \text{ E-I} = VI_{-850/-950} \text{ expiratory CT} - VI_{-850/-950} \text{ inspiratory CT}$ ).

$VI$  at a threshold of -950 HU and 15<sup>th</sup> Percentile point (Perc15) in HU on inspiratory scans at TLC was also calculated to assess degree of emphysema (if any).<sup>478,479</sup> The Perc15 is defined as cut-off value in Hounsfield Units below which 15% of all lung voxels are distributed. Basic densitometry indices are demonstrated in the line diagram [Figure 2.7 (B)].

All densitometry indices were standardised for extra-thoracic air, blood and three electron density rods as described in [Section 3.2.3.7, Figure 2.8].

### **2.3.2.2.3 Fractal dimension of the airway tree and low attenuation area in lungs**

#### ***2.3.2.2.3.1 Fractal dimension of the airway tree***

In order to perform the fractal analysis first the image of the tracheobronchial tree segmented using PW2 was saved as a joint photographic experts group (JPEG) file [Figure 2.9 (A)]. Standard setting were used for each image, with a size of 513 x 518 pixels, resolution of 72 pixels / inch and subject in normal anatomical orientation. Images were first binarised by using an automated thresholding procedure [Figure 2.9 (B)], where the pixel colour (black or white) for foreground (segmented tracheobronchial tree) and background was automatically assigned by ImageJ software. Fractal analysis was performed by using the morphological image analysis software ImageJ plug-in FracLac (ver. 2.5 Rel. 1e).<sup>480,481</sup> Box-counting algorithm was used to determine the FD of the binarised image of the segmented tracheobronchial tree for each subject. This algorithm places several grids of decreasing box size over the region of interest (ROI) i.e. binarised image of the tracheobronchial tree [Figure 2.9 (C) and (D)]. The number of boxes containing pixels with ROI detail is then counted for each grid and data gathered for each box of every grid. The FD is then expressed as the slope of the regression line for the log-log plot of box size and count.<sup>481</sup>

Standard FracLac analyses protocol was selected in accordance with the recommendations of the FracLac user manual.<sup>481</sup> The size of the series of grids was set to decrease linearly from a maximum box size of 45% of the horizontal ROI size to a minimum size of 1 pixel. Ten global scans were performed for each ROI, with randomly selected starting grid locations to improve the accuracy of the box-counting result. The following measures were

derived by FracLac to describe the tracheobronchial branching in asthmatic and healthy subjects:

- a) Averaged FD ( $D_{av}$ ): fractal dimension averaged over ten global scans that were done at different grid positions.
- b) Slope-corrected FD ( $D_{sc}$ ): As box size increases relative to image size, the number of boxes required to cover an image stays the same over a long interval of change in size and causes a plateau in the log-log plot of box size and count. Slope corrected FD is fractal dimension corrected for periods of no change in the regression data.
- c) Most-efficient cover FD ( $D_e$ ): fractal dimension generated from box-counting data where for each grid size the box-count that required the lowest number of boxes (most-efficient cover) was used.
- d) Slope-corrected most-efficient covering FD ( $D_{sce}$ ): combination of  $D_{sc}$  and  $D_e$ .

#### ***2.3.2.2.3.2 Fractal dimension of low attenuation areas in lungs***

PW2 software was used to calculate the fractal dimension of the low attenuation areas in lungs on inspiratory and expiratory scans. The low attenuation cluster (LAC) regions on CT scan are contiguous areas of voxels with CT attenuation values below a given threshold. Summing the number of voxels in a LAC provides the cluster size. The fractal dimension (LAC-D) is then expressed as the slope of the regression line for the log-log histogram plot created with LAC size and LAC number.<sup>328,482</sup> PW2 calculates the fractal dimension (LAC-D) for each lung (right and left) separately. Fractal dimension of low attenuation areas for each subject was expressed as an average of right and left lung fractal dimensions. Threshold CT attenuation value of -950 HU on inspiratory scan, and -850 HU on expiratory

scan was used to define LAC to assess size and distribution of emphysematous lesions and air-trapping areas respectively [Figure 2.10].

### 2.3.3 Computed Tomography radiation safety

Assessment of radiation exposure due to research CT scans was performed. ED for both full thoracic CT scan and limited thoracic CT scan was calculated based on Monte Carlo simulations<sup>362</sup> of calculated x-ray spectra in an adult, hermaphrodite, mathematical phantom, using the ImPACT CT dosimetry calculator.<sup>363</sup> Absorbed dose to breast tissue was also estimated using the ImPACT CT dosimetry calculator.<sup>363</sup> In addition, estimation of the effective dose was made using a simpler method, which involves calculation using the following equations:

$$1) \text{ DLP (mGy.cm) = CTDI}_{\text{vol}} \text{ (mGy) x scan length (cm)}^{361,483}$$

$$2) \text{ ED (mSv) = DLP (mGy.cm) x NC (mSv.mGy}^{-1}\text{.cm}^{-1}\text{)}^{361,483}$$

Where volume CT dose index ( $\text{CTDI}_{\text{vol}}$ ) is an index that quantifies the relative intensity of radiation that is incident on the patient,<sup>484</sup> DLP is the dose length product on the scanner console ( $\text{mGy}\cdot\text{cm}$ ), NC is normalised effective dose coefficients ( $\text{mSv.mGy}^{-1}\cdot\text{cm}^{-1}$ ) that varies according to body region scanned (NC: chest =  $0.017 \text{ mSv}\cdot\text{mGy}^{-1}\cdot\text{cm}^{-1}$ )<sup>485</sup> and scan length is the length of the area scanned. The scan length for limited thoracic CT was 5.3 cm and for full thoracic CT was taken as 30 cm for calculation purposes, though it varied slightly from patient to patient. The estimation of ED by this method generally varies by <15% of calculations based upon the Monte Carlo approximation.<sup>486</sup>

## 2.4 Figures and Tables

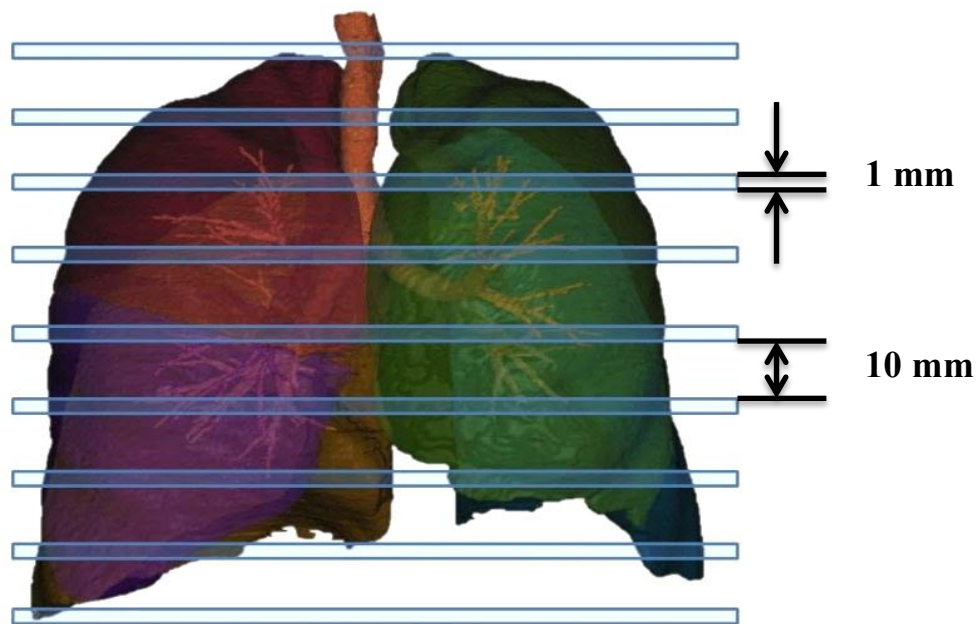


**Figure 2.1: Standard HRCT sequential scanning**





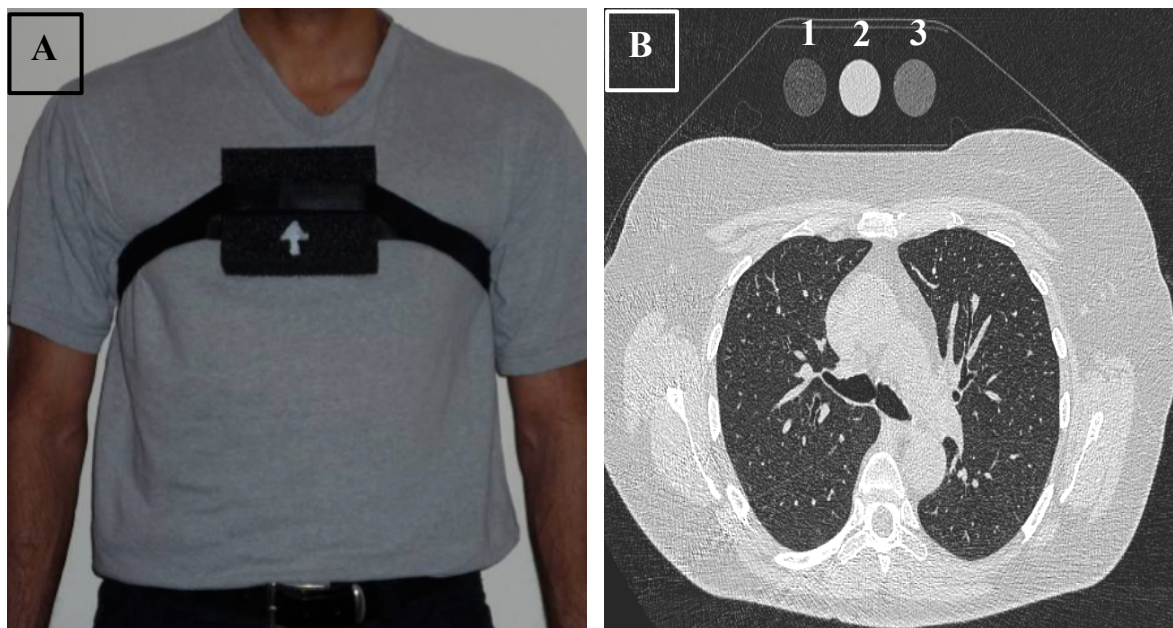


**Figure 2.3: Electron Density rods**

(A) Picture depicting placement of the foam box (housing electron density rods) on the patient prior to CT scan; (B) Axial CT scan image showing the positioning of three electron density rods over the sternal region (EDR 1 = LN300; EDR 2 = 'solid water'; EDR 3 = LN450)

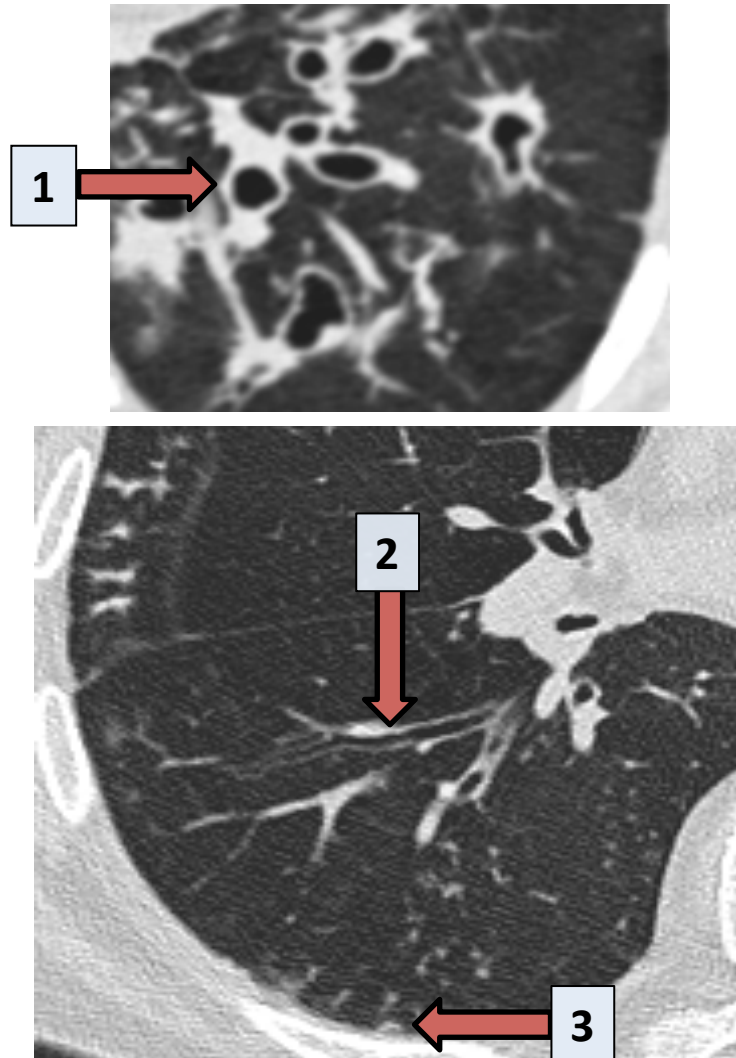


**Figure 2.4: Bronchiectasis: CT diagnostic criteria**

(1) internal diameter of the bronchus greater than that of the adjacent pulmonary artery, (2) lack of tapering of the bronchial lumen towards the periphery, or (3) visualisation of bronchus within 1 cm of the pleural surface

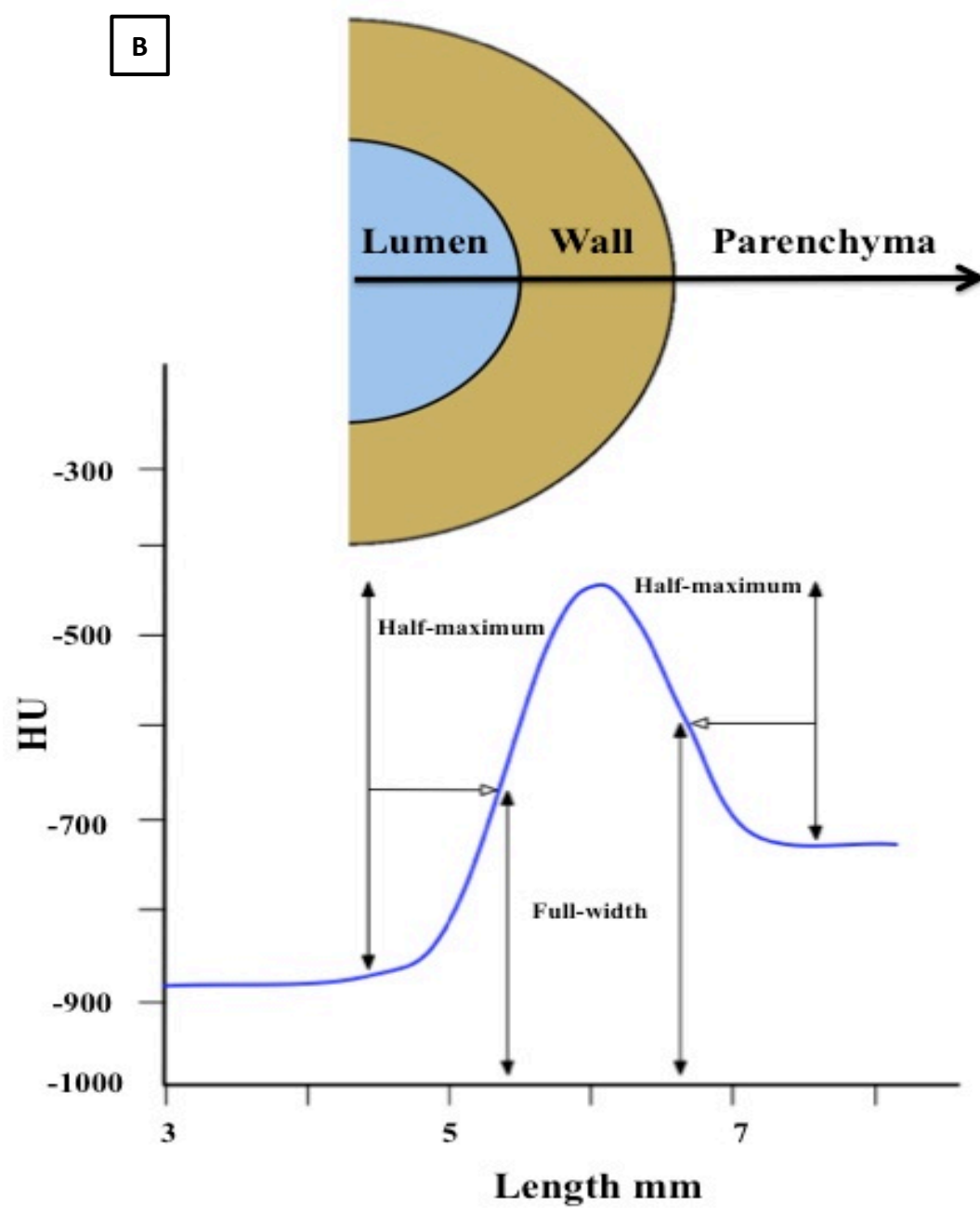
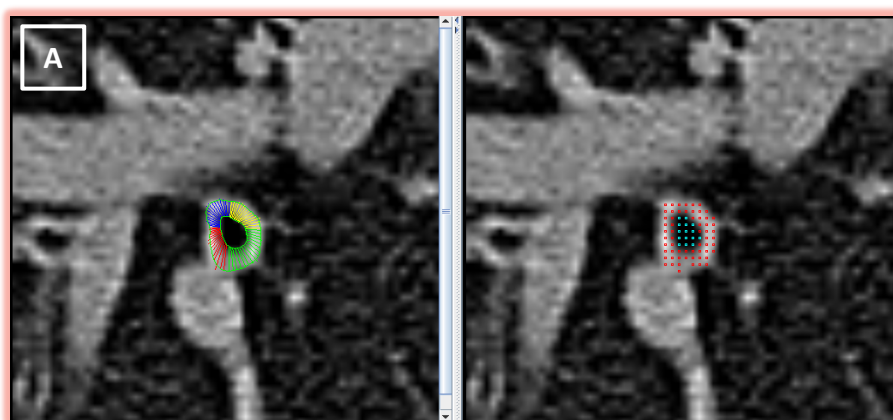


**Figure 2.5: Full-width at half maximum method of 2-D quantitative airway morphometry**

To measure the airway dimensions using full-width at half maximum method a seed point is placed in the lumen and rays are cast out radially from this seed point towards the airway wall (A). X-ray attenuation values are measured along the rays as they pass from airway lumen to wall and then to the lung parenchyma. The inner and outer boundary points of the airway wall are detected based on the attenuation profiles along the rays. The point at which the attenuation is half way to the maximum on the lumen side marks the inner boundary and the point at which the attenuation is halfway to the local minimum on the parenchymal side marks the outer boundary (B)

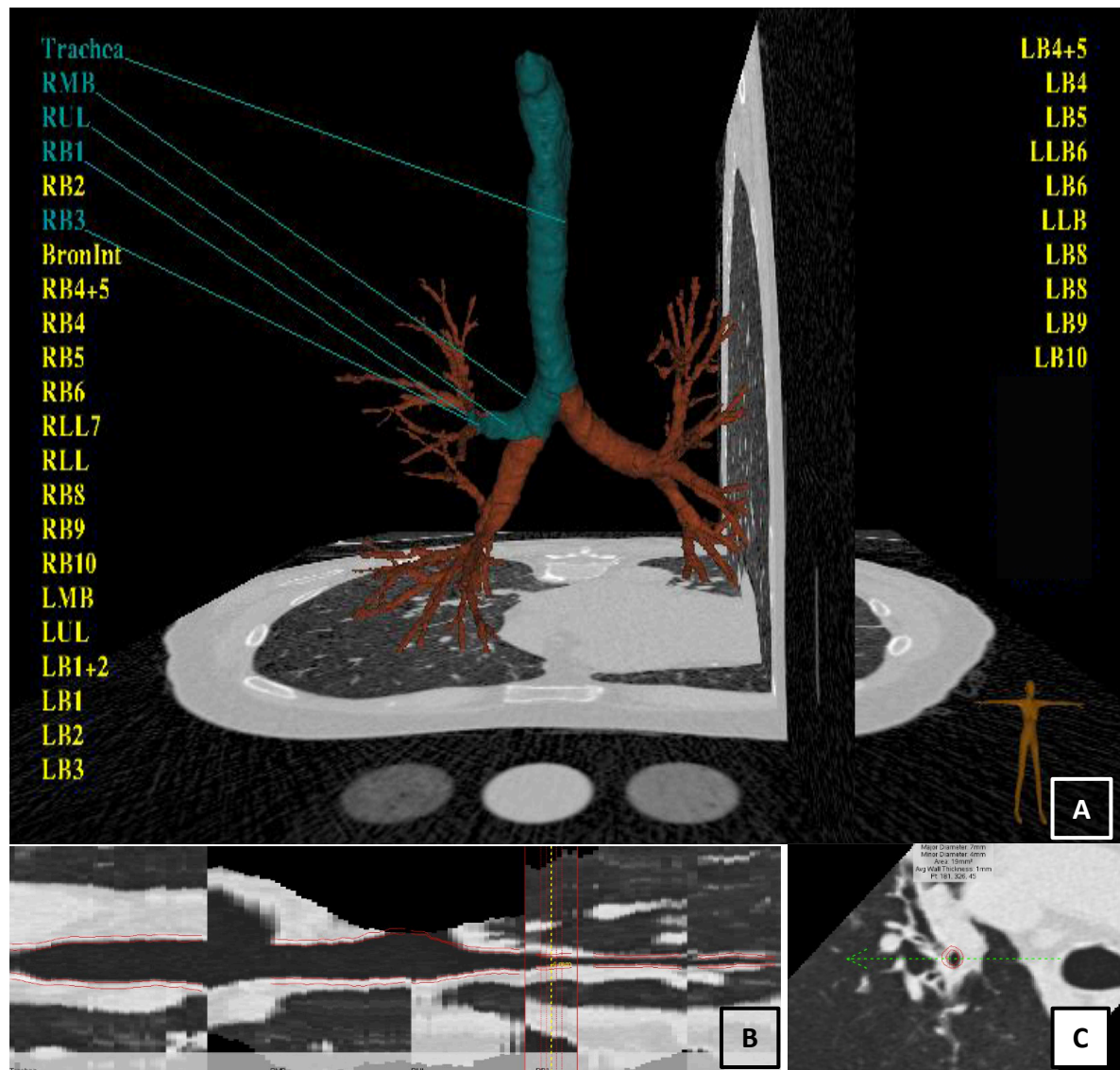


**Figure 2.6: Segmentation and 3-D airway morphometry using VIDA PW2 software**

(A) Quantitative rendering of airway tree in three dimensions, (B) The highlighted (colour green) pathway in [A] is selected for measurement, (C) Cross-section of RB1 at right angle to the centre line.

*Definitions of Abbreviations:* RMB = right main bronchus, RUL = right upper lobe bronchus, RB = right bronchus (number after RB identifies various segmental bronchi), LB = left bronchus (number after LB identifies various segmental bronchi), BronInt = Bronchus intermedius

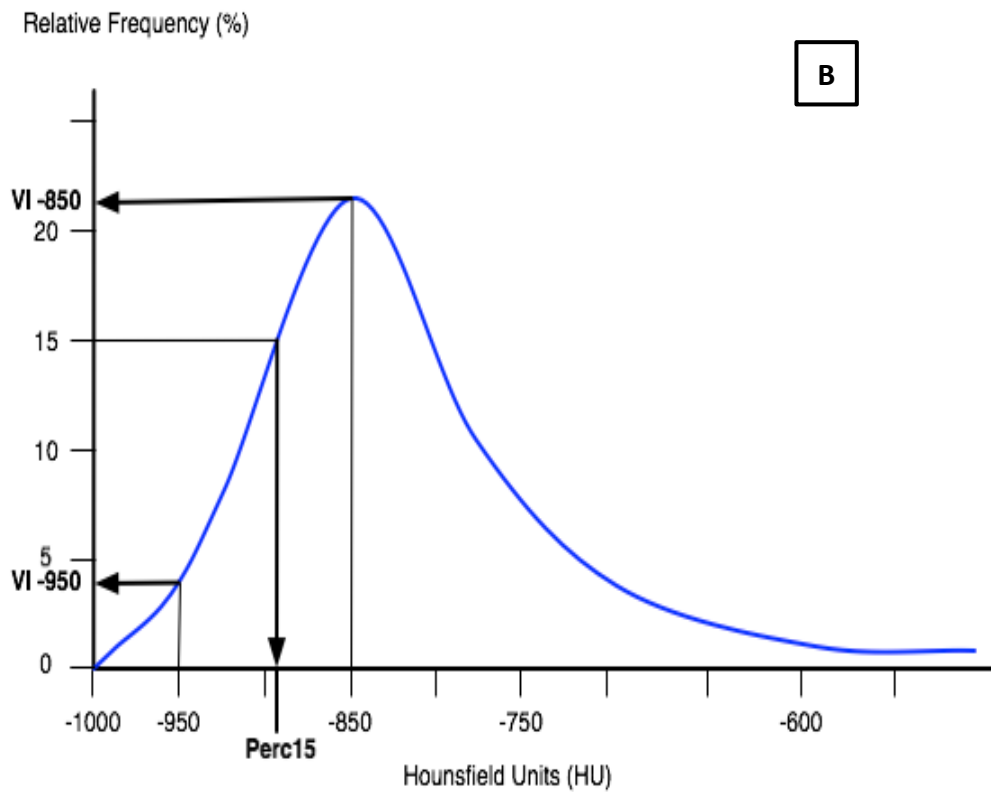
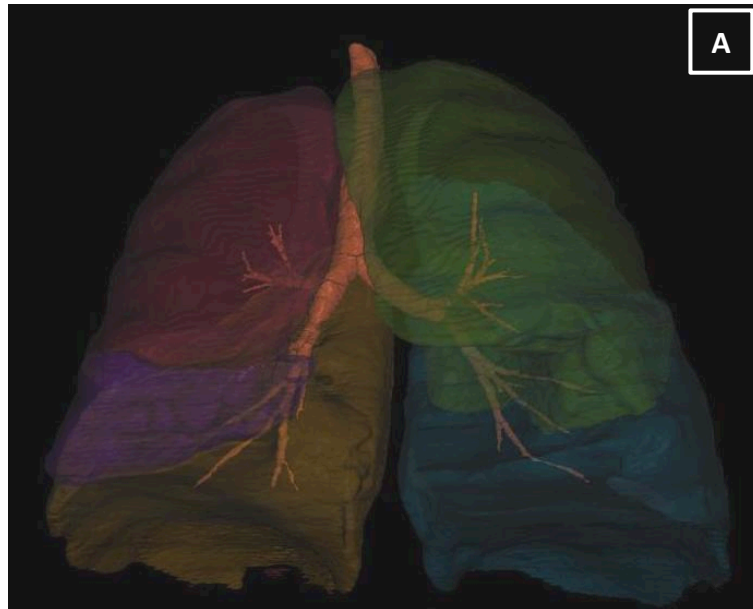


**Figure 2.7: Pulmonary densitometry using VIDA PW2 software**

(A) Automated segmentation of lungs with different lobes highlighted in different colours,  
 (B) Cumulative voxel distribution histogram showing derivation of various densitometry indices

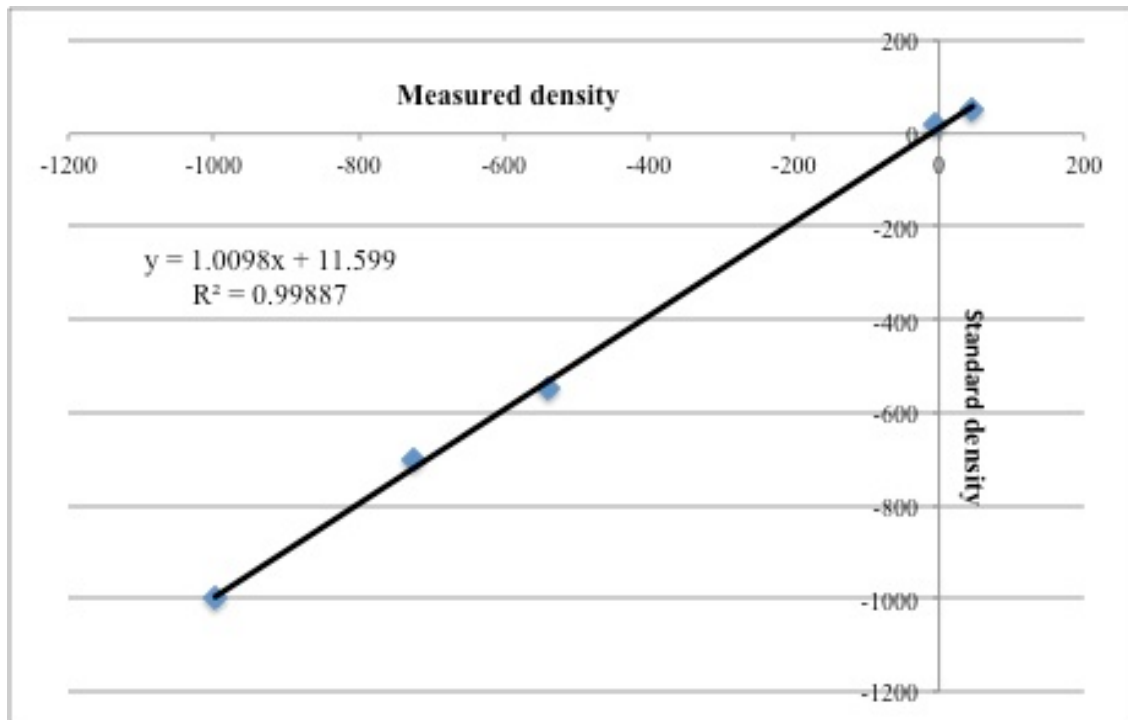


**Figure 2.8: Standardisation of densitometry indices**

Regression equations were calculated from measurements of the densitometry standards (extra-thoracic air, blood and 3 EDR) for each CT scan of every subject in relation to the standard density measures of the densitometry standards. The regression equations derived were used to adjust all the densitometry indices for each CT scan of every subject. The figure illustrates derivation of regression equation for standardisation of densitometry indices for one of the subjects.



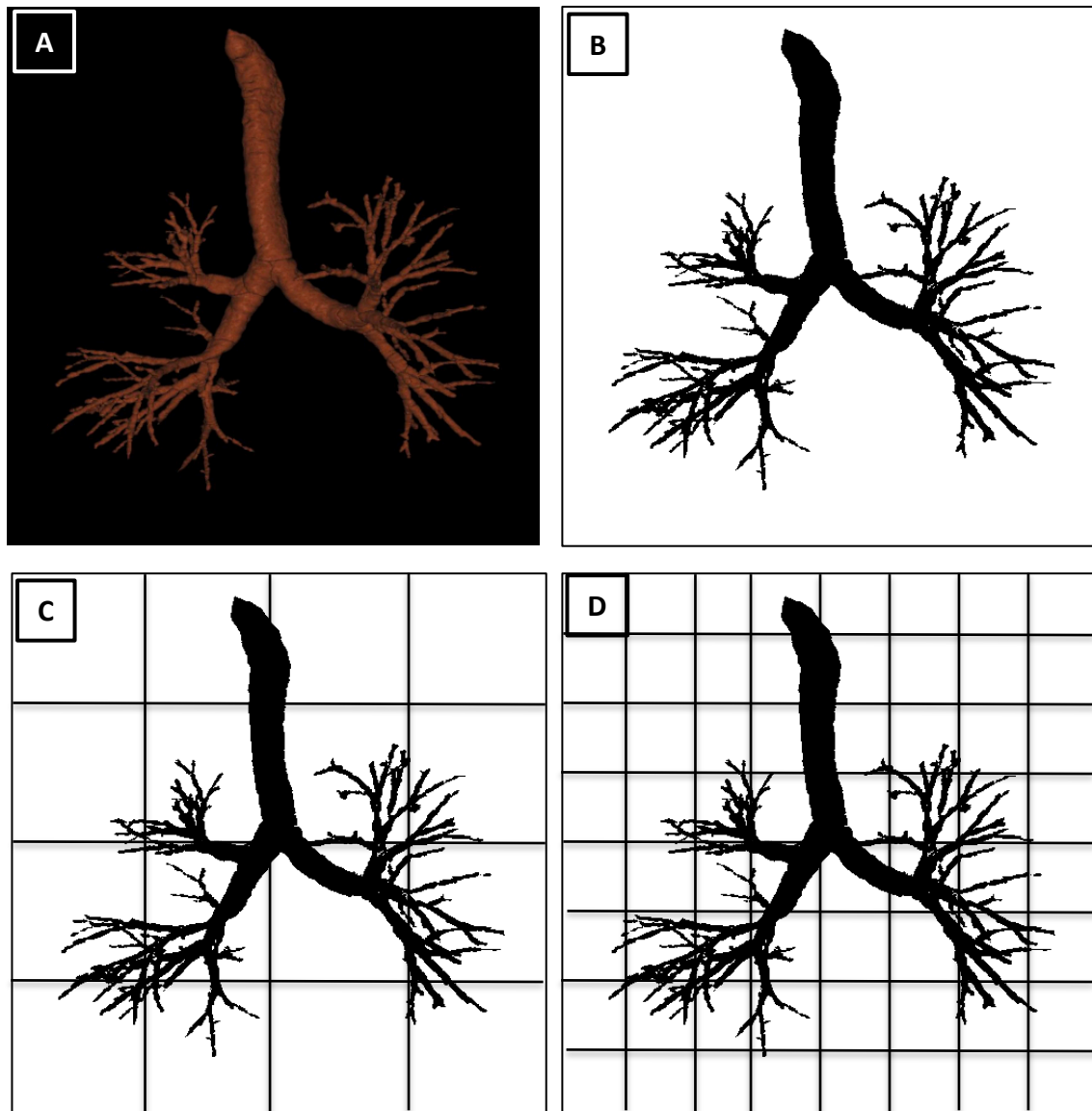


**Figure 2.9: Fractal analysis of segmented airway tree using FracLac (ImageJ) software**

JPEG image (A) of segmented airway tree, is binarised (B) by ImageJ software by assigning black pixel colour for airway tree and white pixel colour for background. Box-counting algorithm places several grids of decreasing box size (C and D) over the region of interest (ROI) i.e. binarised image of the tracheobronchial tree to determine the fractal dimension



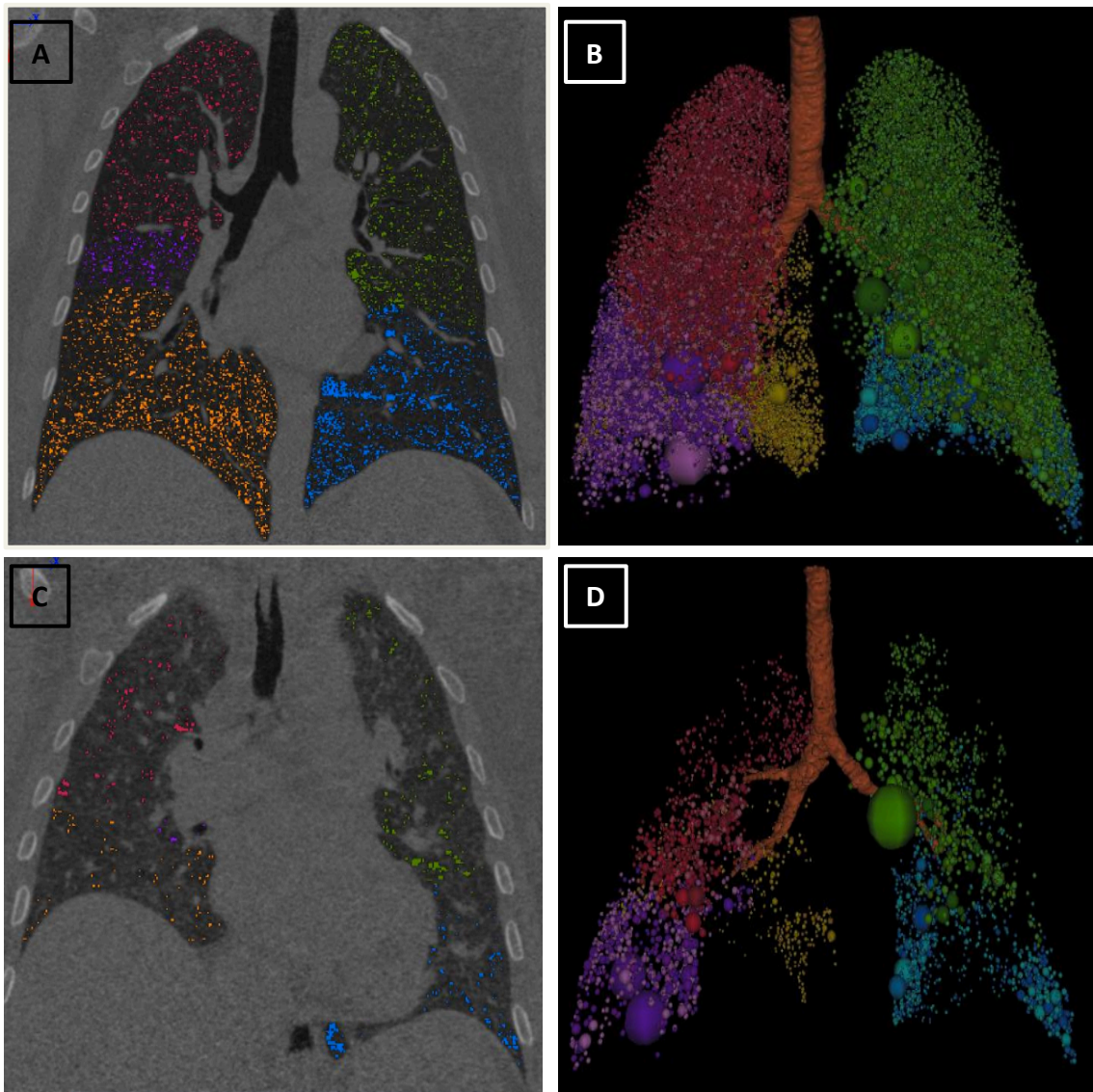


**Figure 2.10: Fractal dimension of low attenuation areas in lungs**

Coronal CT image showing areas of low attenuation below threshold CT attenuation value of -950 HU on inspiratory scan (A), and -850 HU on expiratory scan (C), each lobe coded with different colour. Respective LAC are shown in (B) and (D) which are used to assess size and distribution of emphysematous lesions and air-trapping areas respectively

## 3 STUDIES

---

## **3.1 STUDY 1: Qualitative Analysis of High Resolution Computed Tomography Scans in Severe Asthma.**

### **3.1.1 Abstract**

#### **Background**

High resolution computed tomography is part of the management of severe asthma, but its application varies between centres. We sought to describe the HRCT abnormalities of a large severe asthma cohort and to determine the utility of clinical features to direct the use of HRCT in this group of patients.

#### **Methods**

Subjects attending our Difficult Asthma Clinic (DAC) between 02/2000-11/2006 (n=463) were extensively re-characterised and 185 underwent HRCT scan. The HRCT scans were analysed qualitatively and the inter-observer variability assessed. Using logistic regression we defined clinical parameters that were associated with bronchiectasis and bronchial wall thickening alone or in combination.

#### **Results**

HRCT abnormalities were present in 80% of subjects and often co-existed including bronchial wall thickening (62%), bronchiectasis (40%) and emphysema (8%). The inter-observer agreement for bronchiectasis (Kappa=0.76) and bronchial wall thickening

(Kappa=0.63) was substantial. DAC patients that underwent HRCT compared to those that did not were older, had longer disease duration, poorer lung function, were on higher corticosteroid treatment and had increased neutrophilic airway inflammation. The sensitivity and specificity of detecting bronchiectasis clinically was 74% and 45% respectively. FEV<sub>1</sub>/FVC emerged as an important predictor for both bronchiectasis and bronchial wall thickening, but had poor discriminatory utility for subjects without airway structural changes (FEV<sub>1</sub>/FVC  $\geq$  75%; sensitivity 67%, specificity 65%).

## **Conclusion**

HRCT abnormalities are common in severe asthma. Non-radiological assessments fail to reliably predict important bronchial wall changes and therefore CT acquisition may be required in all severe asthmatics.

### 3.1.2 Introduction

Asthma is increasing in prevalence worldwide with an estimated 300 million affected individuals.<sup>487</sup> Asthma affects ~5% of adults in general population, of which approximately 5-10% suffer from severe and/or difficult-to-treat asthma.<sup>10</sup> These patients with inadequately controlled severe asthma are at particular high risk of exacerbations, hospitalisation and death, and often have severely impaired quality of life. Although this group represents a relatively small proportion of the asthma population, they consume disproportionately high amount of healthcare resources attributed to asthma.<sup>12</sup>

HRCT plays a role in diagnostic work-up of severe asthma.<sup>10</sup> It has emerged as a useful tool to non-invasively assess airway wall changes in patients with asthma.<sup>144,268,270,488</sup>

HRCT studies in asthmatic subjects may reveal abnormal radiological findings, such as bronchial wall thickening, bronchial wall dilatation, bronchiectasis, mosaic lung attenuation, mucus plugging, prominent centrilobular opacities, emphysema and atelectasis.<sup>263-265,276,277</sup> However, in which asthmatic patients HRCT should be undertaken is uncertain and varies between specialist centres.

In the current, qualitative, cross-sectional study we describe the HRCT findings in a large severe asthma cohort, define the clinical characteristics of those subjects with and without BE and/or BWT and assess the validity of these clinical parameters to guide the application of HRCT in severe asthma.

### **3.1.3 Methods**

#### **3.1.3.1 Subjects**

We performed a cross sectional single centre retrospective study based upon the DAC at Glenfield Hospital, Leicester, UK. The diagnosis of asthma is confirmed by a physician based on history and one or more of the following objective criteria (maximum diurnal PEF variability >20% over a 2 week period, significant bronchodilator reversibility defined as an increase in FEV<sub>1</sub> of >200mls post bronchodilator or a PC<sub>20</sub>MCh of <8mg/ml). FAO was defined as post-bronchodilator FEV<sub>1</sub><80% and FEV<sub>1</sub>/FVC<70%. Out of 463 patients attending DAC between February 2000 and November 2006, 185 had HRCT scans. The clinical indications for the HRCT were determined by the attending physician. The commonest indication was a clinical suspicion of BE in 116 (63%) cases. Other indications for HRCT request were interstitial lung disease (15%), emphysema (12%) and miscellaneous (10%) including unresolved infection and cryptogenic organising pneumonia. Consent for analysis of previously collected, clinical and CT data was obtained from all patients. The consent was obtained by, either one of the respiratory physicians in difficult asthma clinic or myself. None of the patients declined to consent for retrospective analysis of their clinical and CT data as part of this study. The Leicestershire, Northamptonshire and Rutland research ethics committee approved the study.

### **3.1.3.2 Clinical Characterisation**

Patients attending DAC undergo extensive re-characterisation and investigations including history, health status, spirometry before and after bronchodilator (400 µg inhaled salbutamol), allergen skin prick tests for common aeroallergens, blood for peripheral eosinophil count, total and specific IgE and aspergillus IgG and sputum induction.<sup>51</sup> Clinical methods are described in [Section 2.1].

### **3.1.3.3 HRCT scanning protocol and qualitative analysis**

HRCT scanning protocol is described in [Section 2.3.1.1] and the qualitative analysis of HRCT images is elucidated in [Section 2.3.2.1]. On the basis of qualitative analysis, severe asthma patients were categorised into those with: A) neither BWT or BE (BWT- / BE-), B) BE only (BWT- / BE+), C) presence of both BWT and BE (BWT+ / BE+) or D) BWT only (BWT+ / BE-) [Figure 3.1].

### **3.1.3.4 Statistical analysis**

Statistical analysis was performed using GraphPad Prism version 5.00 for Windows, GraphPad Software, San Diego California USA, [www.graphpad.com](http://www.graphpad.com) and SPSS for Windows, Rel. 16.0.1.2008. Chicago: SPSS Inc.

Parametric data was expressed as mean [standard error of mean (SEM)] and non-parametric data was described as median [interquartile range (IQR)]. One-way analysis of variance with Tukey's post test was used for across group comparison of parametric data. Kruskal-

Wallis one-way analysis of variance with Dunn's post test was used for across group comparison of non-parametric data. Chi squared tests were used to compare categorical data. Kappa statistic was used for an inter-observer reliability analysis. Kappa statistics were interpreted as indicating poor ( $\kappa < 0.2$ ), fair ( $0.21 < \kappa < 0.4$ ), moderate ( $0.41 < \kappa < 0.6$ ), substantial ( $0.61 < \kappa < 0.8$ ) and almost perfect ( $0.81 < \kappa < 1.0$ ) observer agreement.<sup>489,490</sup>

Logistic regression analysis and reporting were performed as described previously.<sup>491,492</sup> The variables were considered for multivariate logistic regression based on: a) association in prior univariate analysis ( $p < 0.2$ ); b) biological plausibility. This analysis was performed for: (1) Whole DAC cohort ( $n=185$ ) and (2) DAC patients with smoking history of less than 20 pack years ( $n=123$ ). Variables entered into the regression model were, disease duration; post-bronchodilator FEV<sub>1</sub>% predicted; post-bronchodilator FEV<sub>1</sub>/FVC; % sputum neutrophil count and % sputum eosinophil count. The final multivariate logistic regression model was determined, using block entry of variables, to assess factors which best predicted BE and/or BWT. Hosmer and Lemeshow chi-square test of goodness of fit was used to test the overall fit of the logistic regression model (non-significant p value implying that the model adequately fits the data). Wald statistic was used to test the significance of individual logistic regression coefficients for each independent variable. Nagelkerke's R<sup>2</sup> (pseudo R<sup>2</sup>) was used to estimate the percent of variance explained by the model. The measure of discriminative power of the logistic equation was reported in the form of c-statistic. No multi-collinearity or significant interactions were found between independent variables. Conformity to a linear gradient for continuous independent variables was



assessed using Box-Tidwell transformation. A p value of  $<0.05$  was taken as the threshold for statistical significance.

### **3.1.4 Results**

Baseline demographics and clinical characteristics of those difficult asthma patients that did (DAC 1) and did not (DAC 2) undergo thoracic HRCT are as shown [Table 3.1]. In both groups subjects had severe disease requiring high dose inhaled corticosteroids, long acting bronchodilators and often maintenance oral corticosteroids. Patients that underwent HRCT were older, had longer disease duration, poorer lung function, were treated with higher dose of inhaled corticosteroids and oral corticosteroids, and had increased neutrophilic airway inflammation [Table 3.1].

BWT and BE was present in 62% and 40% respectively in those subjects that underwent HRCT scans. Inter-observer reliability for the reporting radiologists was substantial for BE (Kappa=0.76) and BWT (Kappa=0.63). Allergic bronchopulmonary aspergillosis (ABPA) according to Greenberger criteria<sup>493</sup> was present in 5% (ABPA-central bronchiectasis in 0.5% and ABPA-seropositive in 4.5%) of DAC 1 patients and 2.2% of DAC 2 patients. Other radiological findings were: ground glass shadowing 4.3%; air trapping 7.6% and emphysema 8.1%. HRCT scan was reported as normal in 20% of the cohort. Radiological findings on HRCT in DAC patients who were current or ex-smokers compared to never smokers were BWT 59 Vs 63% ( $p=0.6$ ), BE 48 Vs 26% ( $p=0.004$ ), and emphysema 17 Vs 3% ( $p=0.002$ ); and in those with and without FAO were BWT 63 Vs 60% ( $p=0.8$ ); BE 50 Vs 34% ( $p=0.04$ ) and emphysema 12 Vs 6% ( $p=0.2$ ). The sensitivity and specificity of

detecting BE clinically, when radiological detection was considered as gold standard, was 74% and 45% respectively.

Clinical characteristics for individual groups (A) BWT- / BE-, (B) BWT- / BE+, (C) BWT+ / BE+ and (D) BWT+ / BE- are shown in [Table 3.2]. Patients in group B were older than patients in other groups. Disease duration was increased and post bronchodilator FEV<sub>1</sub>/FVC was decreased in subjects in group B and C compared to those in A and D [Table 3.2].

The presence of BE or BWT alone were best predicted by post-bronchodilator FEV<sub>1</sub>/FVC ratio [Table 3.3 (a), (b); equation (1), (2)]

$$\text{Predicted logit of (BE)} = 26.411 + (-0.387) * \text{FEV}_1/\text{FVC ratio (1)}$$

$$\text{Predicted logit of (BWT)} = 7.259 + (-0.084) * \text{FEV}_1/\text{FVC ratio (2)}$$

In those patients with a smoking history of less than 20 pack years BE + BWT combined was best predicted by disease duration [Table 3.3 (c); equation (3)] and BWT was best predicted by post-bronchodilator FEV<sub>1</sub>/FVC ratio [Table 3.3 (d); equation (4)]

$$\text{Predicted logit of (BE+BWT)} = -9.144 + (0.503) * \text{disease duration (3)}$$

$$\text{Predicted logit of (BWT)} = 36.286 + (-0.511) * \text{FEV}_1/\text{FVC ratio (4)}$$

We evaluated the utility of FEV<sub>1</sub>/FVC ratio, in identifying DAC patients with normal airways, by calculating the area under the receiver operating characteristic (ROC) curve (positive state=absence of both BWT and BE) [Figure 3.2]. The area under the ROC curve was 0.67 (95% CI 0.58–0.76; p=0.001). FEV<sub>1</sub>/FVC ratio ( $\geq 75\%$ ) identified DAC patients with normal airways with a sensitivity 67% and specificity 65% [positive likelihood ratio

1.9; negative likelihood ratio 0.5; positive predictive value (PPV) 39%; negative predictive value (NPV) 85%].

### **3.1.5 Discussion**

We report here the largest qualitative study of HRCT findings in severe asthma. We found that BE and BWT were common; present in 40 and 62% of cases respectively, whereas scans were reported as normal in only 20% of cases. Importantly our findings may be an over estimate of CT abnormalities as HRCT was only undertaken in those subjects in which it was considered clinically indicated. The commonest indication was a clinical suspicion of BE, but this only had 74% sensitivity and 45% specificity to identify subjects with BE on HRCT. Using logistic regression we determined which clinical parameters were associated with CT abnormalities. FEV<sub>1</sub>/FVC ratio was the strongest predictor for airway wall changes but was inadequate to effectively discriminate between patients with normal airways and those with BE and/or BWT. Our findings therefore do support the view that CT is an important investigation in the management of severe asthma, but to define fully the prevalence of CT abnormalities, CT will need to be undertaken in all patients.

This is one of the largest qualitative CT study of severe asthma subjects.<sup>262-270</sup> Using qualitative HRCT analysis we have demonstrated that there is a high prevalence of BE and BWT in severe asthma population. Several other authors have investigated the prevalence of BE and BWT on HRCT analysis of asthmatic populations.<sup>92,262,263,265-267,269</sup> The prevalence of BE reported in asthmatic patients varies from 9-77%<sup>262-271</sup> with a median of 31%, which was similar to the 40% in our study. The prevalence of bronchiectasis reported in COPD<sup>268,494-496</sup> was similar to asthmatics (range, 20-50%; median, 38%). The wide

variation in the reported prevalence of BE is likely to be due to differences in patient population, scanning technique and definition of bronchiectasis. Bronchiectasis is defined as irreversible localised or diffuse bronchial dilatation.<sup>468</sup> Current MDCT diagnostic criteria for bronchiectasis<sup>468,497</sup> are based on those originally established by Naidich *et al.*<sup>498</sup> for conventional CT with 10 mm sections, which include presence of any of the following features: (i) bronchial dilatation with respect to accompanying pulmonary artery (i.e. bronchoarterial ratio >1) , (ii) lack of tapering of bronchi, and (iii) identification of bronchi within 1 cm of the pleural surface. The accuracy of bronchial dilatation alone, as diagnostic criteria for bronchiectasis, may be limited by multiple factors, including physiological variation<sup>272</sup> and orientation of bronchovascular bundle with respect to the imaging plane.<sup>265</sup> Lack of bronchial tapering on CT has been shown to be more sensitive than bronchial dilatation in detection of bronchiectasis using pathology as the reference standard.<sup>499</sup> There was much lower prevalence of BE in healthy asymptomatic subjects, with a range from 0-20%<sup>262,266,267,272,273</sup> and a median of 12.5%. We found that BE, irrespective of the presence or absence of BWT, is associated with longer disease duration and poorer lung function. However, the view that BE is related to disease severity is contentious and is supported by some previous reports,<sup>264,274</sup> but not others.<sup>262,267</sup> It remains unclear whether BE in severe asthma is a co-morbidity, making the asthma “difficult” to manage or it represents structural change or remodelling with natural progression of the disease.<sup>214,267</sup> Longitudinal studies are required to determine whether BE is a consequence or a cause of severe asthma.

BWT was present in 62% of our severe asthma cohort which is consistent with previous findings.<sup>264,268,269</sup> Reported prevalence of BWT has varied between 16-92%<sup>262-266,268-270</sup> and this can be attributed to differences in patient population, HRCT window settings, and

perhaps most importantly the lack of an objective definition of BWT. We did not find any significant difference in prevalence of BWT between smoking and non-smoking patients or between patients with or without FAO. Similarly Laurent et al<sup>269</sup> found that BWT was more frequent in asthmatics irrespective of the smoking status when compared to smoking and non-smoking healthy controls. The association of BE but not BWT with significant smoking history and FAO may represent alteration in remodelling process in more severe and progressive disease. Emphysema was present in 8% of severe asthmatics, consistent with earlier reports<sup>262,263,265,268</sup> and as expected its prevalence was higher in smokers and ex-smokers compared to non-smokers. Interestingly the prevalence of emphysema in smokers was 27% in a group of Italian smokers that underwent HRCT scans as part of a lung cancer screening programme<sup>500</sup> and was over 50% in a study of Japanese smokers.<sup>501</sup> The prevalence of emphysema amongst severe asthmatics in our study, with significant smoking histories is therefore perhaps lower than predicted. Whether severe asthmatics have an altered risk of developing emphysema in response to smoking warrants further study.

Current difficult/refractory asthma guidelines<sup>5,8,9,16</sup> highlight HRCT as a tool for disease evaluation, but there are no well defined criteria for HRCT scan evaluation for this disease group. Detection of bronchial wall changes, in particular BE, is important in severe asthma as this may impact on the management strategy. Therefore identification of clinical features related to HRCT abnormalities may provide an opportunity to appropriately target the application of HRCT scanning in severe asthma. We found that the subjects that underwent HRCT scanning were older, more severe in terms of treatment requirements and had more neutrophilic inflammation. These features are likely to have influenced our clinical

suspicion of BE and therefore precipitated a HRCT scan request. However, clinical suspicion of BE had a relatively poor specificity and sensitivity to identify BE defined by HRCT scanning. In keeping with earlier reports,<sup>502,503</sup> logistic regression analysis in our study revealed disease duration and in particular FEV<sub>1</sub>/FVC ratio as important predictors of BWT and BE. We therefore analysed the performance of airflow obstruction to predict these HRCT changes. However, FEV<sub>1</sub>/FVC ratio could not effectively discriminate between severe asthmatics with or without airway wall changes. This suggests that without a CT scan it would be impossible to predict presence or absence of airway wall changes in this group of patients indicating that CT scan evaluation of all severe asthma patients is probably required.

One limitation with our study is its cross-sectional design. We therefore do not have any longitudinal data to establish whether BE observed on HRCT scans in severe asthma group is progressive with disease state or responsive to treatment. However serial HRCT scans among asthmatics in longitudinal study involving small number of patients do suggest that these changes are persistent<sup>267</sup> and do not respond to oral steroids.<sup>263</sup> Future studies need to further assess the relationship between airway structural changes identified by CT and clinical features of disease such as frequency of exacerbations over time. Another limitation of our study is the use of qualitative method to describe changes of BE and BWT. We used well recognised criteria for the identification of BE. However, there is a lack of standardisation for the assessment of BWT and this was determined subjectively by an experienced radiologist. Standard HRCT scans obtained for this study are limited due to their acquisition protocol (sequential scanning with 1 mm collimation at 10 mm increments) in tracking the airways from its origin to its division. Therefore the number of

airways assessed and the ratio of abnormal to normal airways could not be determined. In spite of these potential shortcomings we are confident that our findings are robust as all the scans were reported by blinded thoracic radiologists unaware of patient involvement in the study and inter-observer agreement was substantial. Quantitative assessment of airway wall geometry is widely used as a research tool,<sup>75,466</sup> but its application using HRCT scans, with images at 10 mm increments, is limited due to incompatibility with most current software analysis platforms. To date, quantitative thoracic CT is not validated for clinical use and further studies are required to determine the role of quantitative CT analysis in airways disease.

In conclusion, we have demonstrated that bronchial structural changes, particularly BE are prevalent in severe asthma population. Non-radiological assessments fail to reliably predict these airway structural changes. CT scan acquisition in all severe asthmatics, to detect BE may therefore help alter management strategies and improve treatment outcomes.

### 3.1.6 Figures and Tables

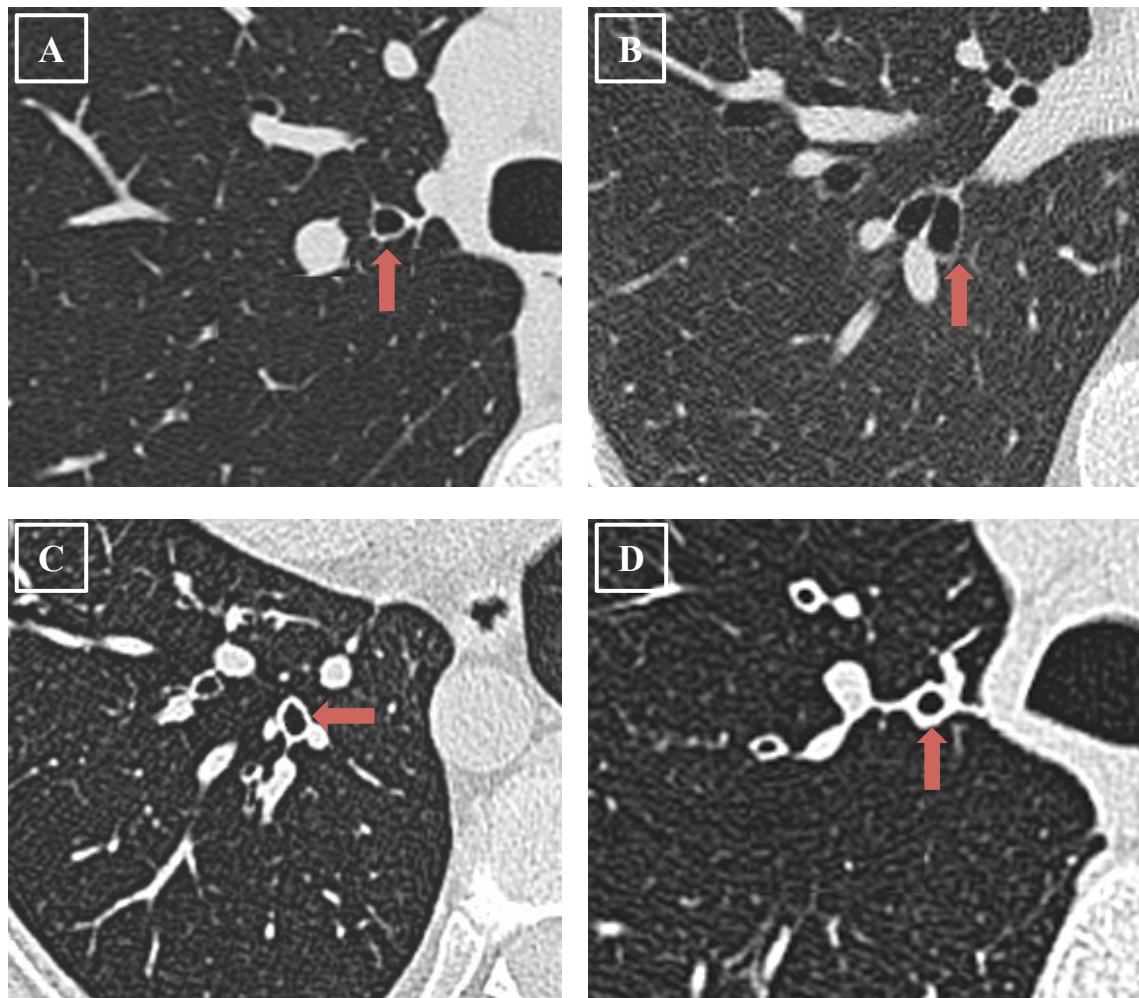


**Figure 3.1: Qualitative CT characterisation of severe asthma**

Representative images of patient categories based on presence or absence of bronchial wall thickening (BWT) and bronchiectasis (BE) on HRCT: (A) BWT- / BE-, (B) BWT- / BE+, (C) BWT+ / BE+ and (D) BWT+ / BE-



### ROC CURVE

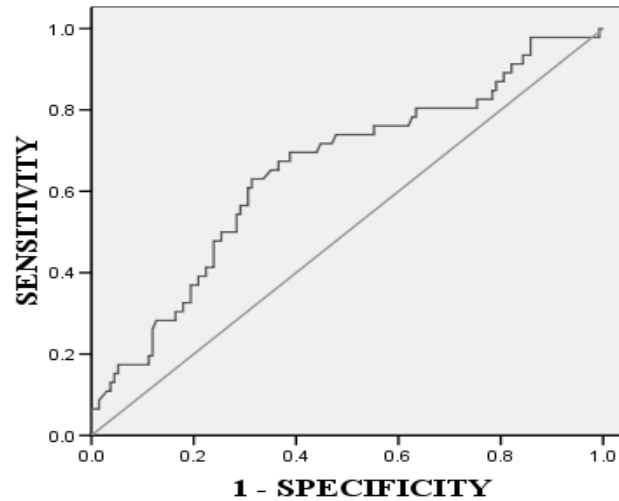


**Figure 3.2: ROC curve**

ROC curve assessing the ability of FEV<sub>1</sub>/FVC ratio in discriminating severe asthma patients without airway wall changes from those with airway wall changes. The AUC was 0.67 (95% CI 0.58–0.76; p=0.001)

**Table 3.1: Baseline clinical characteristics of difficult asthma cohort**

<b>n=463</b>		<b>DAC 1 (n=185)</b>	<b>DAC 2 (n=278)</b>
<b>Clinical Characteristics</b>			
<b>Age (yrs)#</b>		50.2(1.1)	40.4(0.9)
<b>Gender M:F</b>		73:112	97:181
<b>Disease duration (yrs)#</b>		25.7(1.4)	21.9(0.9)
<b>Smoking status (%)</b>	<b>Never</b>	59.7	61.9
	<b>Ex</b>	30.1	24.9
	<b>Current</b>	10.2	13.2
<b>Smoking history (PY)</b>	<b>Ex #</b>	16.8(2.1)	10.7(1.4)
	<b>Current</b>	19.3(3.0)	13.7(2.5)
<b>Atopy (%)</b>		64.7	67.8
<b>Severe exacerbations/year</b>		2.5(0.2)	2.4(0.2)
<b>Pre Bronchodilator FEV<sub>1</sub> % predicted #</b>		66.80(1.8)	74.6(1.3)
<b>Pre Bronchodilator FEV<sub>1</sub>/FVC (%) #</b>		69.3(1.0)	72.3(0.7)
<b>Post Bronchodilator FEV<sub>1</sub> % predicted #</b>		71.9(1.8)	80.0(1.3)
<b>Post Bronchodilator FEV<sub>1</sub>/FVC (%) #</b>		70.7(1.0)	74.4(0.7)
<b>Bronchodilator response (BDR) %</b>		9.1(1.0)	8.4(0.8)
<b>Inhaled CS dose BDP (µg/24hrs) #</b>		2042(72.4)	1623(51.2)
<b>LABA (%)</b>		97.1	92.6
<b>Oral CS (%) ##</b>		41.6	23
<b>LTRA (%) ###</b>		37%	27%
<b>Sputum Characteristics</b>			
<b>Eosinophils (%) ^</b>		1.7 [0.3-8.4]	2.7 [0.5-9.8]
<b>Neutrophils (%) ^*</b>		73.5 [44.7-88.4]	64.2[35.4-83.5]
<b>Total cells (x10<sup>6</sup>/g) ^*</b>		3.2 [1.3-8.0]	1.2 [0.5-2.9]
<b>Total Neutrophils (x10<sup>6</sup>/g) ^*</b>		1.5 [0.8-4.9]	0.7 [0.2-1.8]

Data expressed as mean (SEM); ^Median [IQR]. #p<0.05, Unpaired t test; \*p<0.05, Mann-Whitney U test; ##p<0.0001, Fisher's exact test; ###p<0.05, Fisher's exact test.  
BDP equivalents; Fluticasone 2:1, Budesonide 1.25:1, Mometasone 1.25:1, QVAR 2:1, Ciclesonide 2.5:1.

**Table 3.2: Clinical characteristics of individual groups**

n=185		Group A BWT-/BE- (n=47)	Group B BWT-/BE+ (n=24)	Group C BWT+/BE+ (n=50)	Group D BWT+/BE- (n=64)
<b>Clinical Characteristics</b>					
Age (yrs)		48.7(1.8)	61(2.8)*	49.4(2.1)	47.1(1.7)
Gender M:F		16:31	9:15	25:25	23:41
Disease duration(yrs)		20.9(2.3)	33.0(4.7)*	29.5(2.6)*	24.0(1.9)
Smoking status (%)	Never	58	58	50	71
	Ex	25	33	42	23
	Current	18	8	8	7
Smoking history (PY)	Ex	14.7(6.1)	11.3(1.9)	17.4(3.5)	20.3(4.3)
	Current	20.2(6.6)	25.3(0.3)	28.5(9.4)	13.6(3.9)
Atopy (%)		57	46	71	62
Severe exacerbations/year		2.5(0.4)	1.9(0.5)	2.6(0.6)	2.3(0.3)
Pre Bronchodilator FEV <sub>1</sub> % predicted		72.0(3.6)	62.0(6.0)	61.5(3.0)	68.9(2.8)
Pre Bronchodilator FEV <sub>1</sub> /FVC (%)		75.0(1.8)	69.1(3.4)	65.5(2.1)*	68.2(1.5)
Post Bronchodilator FEV <sub>1</sub> % predicted		77.2(3.6)	65.3(6.4)	68.8(3.3)	73.0(2.9)
Post Bronchodilator FEV <sub>1</sub> /FVC (%)		76.3(1.7)	63.0(3.5)*	68.5(2.2)*	71.2(1.3)
Bronchodilator response (BDR) %		7.2(2.1)	12.8(3.7)	10.1(2.0)	8.3(1.5)
Inhaled CS dose BDP (µg/24hrs)		1942(138.2)	2480(234.7)	1972(140.9)	2011(115.1)
LABA (%)		98	88	96	95
Oral CS (%)		29	58	46	40
LTRA (%)		33	46	39	37
<b>Sputum Characteristics</b>					
Eosinophils (%) ^		0.8[0-12.3]	0.8[0-6.8]	2.6[0.1-10.7]	1.5[0.3-6.3]
Neutrophils (%) ^		72.6[33.8-90.5]	75.4[46.0-84.0]	71.9[38.9-89.5]	71.8[45.0-87.5]
Total cells (x10 <sup>6</sup> /g) ^		3.3[1.2-7.7]	3.6[1.4-5.1]	2.8[1.3-9.4]	3.9[1.4-10.9]
Total Neutrophils (x10 <sup>6</sup> /g)^		1.2[0.5-4.9]	2.1[0.9-3.4]	1.4[0.8-6.0]	3.2[0.7-6.1]

Data expressed as mean (SEM); ^Median [IQR]. Intergroup comparison: parametric data, one-way ANOVA with Tukey test to compare all pairs of columns, \*p<0.05; non-parametric data, Kruskal-Wallis test with Dunn's multiple comparison test to compare all pairs of columns.

**Table 3.3: Logistic Regression**

(a)

<b>DAC cohort: Group A and B patients (n=71)</b> <b>Dichotomous dependent variable: BE only</b>				
<b>Predictor variables</b>	<b>B (SE)</b>	<b>Wald's <math>\chi^2</math></b>	<b>p</b>	<b>Odds Ratio (95% CI)</b>
<b>Disease duration</b>	0.02 (0.04)	0.15	0.70	1.02 (0.94 - 1.10)
<b>Post Bronchodilator FEV<sub>1</sub> % predicted</b>	0.09 (0.05)	3.68	0.06	1.10 (0.99 - 1.21)
<b>Post Bronchodilator FEV<sub>1</sub>/FVC (%)</b>	<b>-0.39 (0.16)</b>	<b>5.59</b>	<b>0.02</b>	<b>0.68 (0.49 - 0.94)</b>
<b>Sputum Eosinophils (%)</b>	-0.14 (0.08)	3.11	0.08	0.87 (0.75 - 1.02)
<b>Sputum Neutrophils (%)</b>	-0.05 (0.03)	2.45	0.12	0.95 (0.89 - 1.01)
Goodness-of-fit test: Hosmer & Lemeshow; $\chi^2 = 4.77$ , p = 0.78 Nagelkerke R <sup>2</sup> = 0.7, c-statistic = 86.3% Model accuracy in classification = 90%, Improvement in classification from baseline = 24% Sensitivity = 87.5%, Specificity = 91.2%, PPV = 82.3%, NPV = 93.9%				

(b)

<b>DAC cohort: Group A and D patients (n=111)</b> <b>Dichotomous dependent variable: BWT only</b>				
<b>Predictor variables</b>	<b>B (SE)</b>	<b>Wald's <math>\chi^2</math></b>	<b>p</b>	<b>Odds Ratio (95% CI)</b>
<b>Disease duration</b>	-0.03 (0.03)	1.46	0.23	0.97 (0.92 - 1.02)
<b>Post Bronchodilator FEV<sub>1</sub> % predicted</b>	0.002 (0.01)	0.02	0.89	1.00 (0.97 - 1.03)
<b>Post Bronchodilator FEV<sub>1</sub>/FVC (%)</b>	<b>-0.08 (0.03)</b>	<b>6.19</b>	<b>0.01</b>	<b>0.92 (0.86 - 0.98)</b>
<b>Sputum Eosinophils (%)</b>	-0.01 (0.02)	0.07	0.79	0.99 (0.96 - 1.03)
<b>Sputum Neutrophils (%)</b>	0.01 (0.01)	1.20	0.27	1.01 (0.99 - 1.04)
Goodness-of-fit test: Hosmer & Lemeshow; $\chi^2 = 4.63$ , p = 0.79 Nagelkerke R <sup>2</sup> = 0.21, c-statistic = 70.6% Model accuracy in classification = 71.1%, Improvement in classification from baseline = 9.7% Sensitivity = 86.3%, Specificity = 46.9%, PPV = 72.1%, NPV = 68.2%				

(c)

<b>DAC cohort, smoking &lt;20 pack-yr: Group A and C patients (n=84)</b>				
<b>Dichotomous dependent variable: BE+BWT</b>				
<b>Predictor variables</b>	<b>B (SE)</b>	<b>Wald's <math>\chi^2</math></b>	<b>p</b>	<b>Odds Ratio (95% CI)</b>
<b>Disease duration</b>	<b>0.50 (0.23)</b>	<b>4.85</b>	<b>0.03</b>	<b>1.65 (1.06 - 2.59)</b>
<b>Post Bronchodilator FEV<sub>1</sub> % predicted</b>	-0.06 (0.07)	0.85	0.36	0.94 (0.82 - 1.08)
<b>Post Bronchodilator FEV<sub>1</sub>/FVC (%)</b>	-0.17 (0.09)	3.44	0.06	0.84 (0.70 - 1.01)
<b>Sputum Eosinophils (%)</b>	0.003 (0.05)	0.004	0.95	1.00 (0.91 - 1.10)
<b>Sputum Neutrophils (%)</b>	0.09 (0.06)	2.41	0.12	1.09 (0.98 - 1.21)
Goodness-of-fit test: Hosmer & Lemeshow; $\chi^2 = 1.72$ , p= 0.97 Nagelkerke R <sup>2</sup> = 0.85, c-statistic = 75.1% Model accuracy in classification = 91.3%, Improvement in classification from baseline = 34.8% Sensitivity = 90%, Specificity = 92.3%, PPV = 90%, NPV = 92.3%				

(d)

<b>DAC cohort, smoking &lt; 20 pack-yr: Group A and D patients (n=100)</b>				
<b>Dichotomous dependent variable: BWT only</b>				
<b>Predictor variables</b>	<b>B (SE)</b>	<b>Wald's <math>\chi^2</math></b>	<b>p</b>	<b>Odds Ratio (95% CI)</b>
<b>Disease duration</b>	-0.10(0.05)	3.58	0.06	0.91 (0.82 - 1.00)
<b>Post Bronchodilator FEV<sub>1</sub> % predicted</b>	0.07(0.05)	2.33	0.13	1.07 (0.98 - 1.17)
<b>Post Bronchodilator FEV<sub>1</sub>/FVC (%)</b>	<b>-0.51(0.21)</b>	<b>5.98</b>	<b>0.01</b>	<b>0.60 (0.40 - 0.90)</b>
<b>Sputum Eosinophils (%)</b>	-0.02(0.02)	0.58	0.45	0.98 (0.94 - 1.03)
<b>Sputum Neutrophils (%)</b>	0.06(0.28)	3.70	0.05	1.06 (0.99 - 1.12)
Goodness-of-fit test: Hosmer & Lemeshow; $\chi^2 = 4.61$ , p= 0.80 Nagelkerke R <sup>2</sup> = 0.73, c-statistic = 72.7% Model accuracy in classification = 85.9%, Improvement in classification from baseline = 21.8% Sensitivity = 90.2%, Specificity = 78.3%, PPV = 88.1%, NPV = 81.8%				

## **3.2 STUDY 2: Use of Airway and Densitometry Phantoms for Standardisation and Validation of Quantitative Computed Tomography Indices**

### **3.2.1 Abstract**

#### **Background**

Quantitative CT analysis of airway morphometry and lung densitometry in asthma and COPD provide novel methods for disease phenotyping and monitoring disease progression. We sought to assess different sources of errors associated with quantitative CT analysis and attempt to standardise and correct such errors using phantom models.

#### **Methods**

Airway and densitometry phantom models were developed to study errors associated with quantitative airway morphometry and lung densitometry. Airway phantom morphometry was performed using semi-automated two-dimensional (EmphyxJ and MedView) software, as well as fully automated three-dimensional (VIDA PW2) software. Densitometry phantom analysis was performed using Pulmo-CMS and VIDA PW2 software. Multi-centre CT scanning of phantom was undertaken to assess inter-scanner variability.

## **Results**

Three-dimensional software is more accurate in airway morphometry compared to 2D software with reduced errors due to oblique orientation of airways and inter-scanner variability in LA ( $p=0.2$ ) and WA ( $p=0.6$ ) measurement. Both quantitative airway and densitometry indices have excellent inter-observer and intra-observer repeatability. Between scanner variability in quantitative CT analysis can be reduced significantly for airway morphometry ( $p=0.002$ ) and lung densitometry ( $p<0.001$ ) using standardisation phantom models.

## **Conclusions**

Quantitative airway morphometry and lung densitometry can be assessed accurately using MDCT with excellent repeatability. Airway and densitometry phantoms are critically important to standardise and reduce errors encountered in quantitative CT assessment of asthma and COPD.

### 3.2.2 Introduction

Multi-detector technology has enabled volumetric high-resolution computed tomography images to be acquired in routine clinical practice, providing detailed images of the airway tree and pulmonary parenchyma with visualisation of the pulmonary structures with theoretical *in vivo* resolution of approximately 0.5 mm. Such high-resolution CT images along with tremendous improvement in post-processing software permits quantitative assessment of airway tree and lung parenchyma with accurate segmentation of lungs, lobes and airway tree to the fifth through seventh generation bronchi. Researchers have utilised quantitative morphometry of the airways and lungs to study variety of respiratory diseases including asthma,<sup>72,75</sup> COPD,<sup>466,504</sup> bronchiectasis<sup>505,506</sup> and eosinophilic bronchitis.<sup>76</sup> Quantitative morphometry therefore has a potential to accurately monitor disease progression,<sup>306,507</sup> patient selection for novel therapies and assessment of treatment efficacy [Section 3.4].

A variety of techniques have been used to assess airway morphometry, including manual or semi-automated border tracing methods<sup>280,508,509</sup> and more objective computer-aided semi-automated / automated methods including ‘FWHM method’ which assumes that the image CT attenuation value at the true airway wall will be halfway between the minimum and maximum CT attenuation values along a ray crossing the airway wall [see Section 2.3.2.2]. Multiple factors influence the CT x-ray attenuation curve including image reconstruction algorithms, partial volume averaging due to field of view and orientation of the airway within the CT image and blurring of edges that occur due to the point spread function of the CT scanner. It has been shown that airway quantification using FWHM method



overestimates the airway wall and underestimated airway lumen.<sup>286,287</sup> To overcome such problems several other methods for quantitative analysis of airways were developed which included ‘maximum-likelihood method’,<sup>287</sup> whereby the attenuation threshold along each ray is matched to an ideal calculated ray, ‘energy driven contour estimation method’,<sup>288,289</sup> which incorporates shape independent quantification and ‘phase congruency method’,<sup>292,293</sup> which uses multiple reconstruction algorithms to localise airway wall. In addition, volumetric acquisition of the CT scan with near isotropic voxel allows reconstruction of the airway in any plane and measurement of the airway dimension in a plane orthogonal to its central axis thereby reducing errors due to oblique orientation. However, CT scanner non-conformity between different centres may also cause variation in airway dimensions in a multi-centre study.

Several lung density parameters have been developed to quantify pulmonary diseases, most common applications being assessment of emphysema in COPD<sup>314,510</sup> and air-trapping in asthma.<sup>319</sup> ‘Density mask’ technique was first described by Muller *et al.*<sup>314</sup> which relies on the principle that CT scanner, if adequately calibrated, reconstructs air with a HU of -1000, water as 0 HU, and blood / tissue as approximately +50 HU. Lungs are composed of either air or blood / tissue densities therefore assessment of percentage of air and percentage of blood/tissue in each reconstructed CT voxel can be made, thereby providing us with a tool to quantify emphysema and air-trapping. CT VI is defined as percentage of lung volume below a certain threshold value. VI on an inspiratory CT scan at a threshold value of -950 HU corresponds best with microscopic and macroscopic morphometry in emphysema.<sup>479</sup> VI at a threshold of -850 HU at FRC<sup>302</sup> is used to quantify air-trapping in asthma. Perc15, defined as cut-off value in HU below which 15% of all lung voxels are distributed, is

another measure to quantify emphysema.<sup>478,479,511</sup> It is important to perform CT imaging without contrast agent when using CT densitometry as a measure of emphysema or air-trapping as demonstrated by Adam and coworkers.<sup>512</sup> CT scanner miscalibration, differences in reconstruction algorithms and CT scanner non-conformity cause variations in densitometry measurements.<sup>513-516</sup> Although the use of a uniform protocol will reduce some of the variation between scanners and centres, exact equivalence is unlikely to be achieved when scanners of different design or manufacturer are used.

Researchers have used variety of airway and densitometry phantoms for correction of CT quantification errors. Airway phantoms of known dimensions constructed from materials such as plexiglass and sweet potato<sup>283,284,287</sup> as well as polycarbonate and foam<sup>517</sup> have been utilised to validate CT airway morphometry using customised computer-analysis algorithms. Explanted inflated animal lungs have also been used as calibration standards for validation of airway dimensions.<sup>518,519</sup> Steps to reduce densitometry errors include scanner air calibration (within 3 hours of the first patient scan and every 3 hours during CT list) and scanner water calibration (using manufacturers' water phantom every 3 months) performed in accordance with manufacturers' guidelines. In addition, internal calibration of CT image sequences may be performed using measured blood density in thoracic aorta and extra-thoracic air density ventral to patient.<sup>520</sup> Statistical<sup>521</sup> and physiological<sup>514</sup> model have also been employed for volume adjustment of the densitometry measures to account for variation in the inspiratory level. Stoel *et al.*<sup>513</sup> used densitometry phantom made of Perspex cylinder containing foam pieces to compare sensitivity of 5 different CT scanners and found significant differences in densitometry despite using standardised acquisition protocols.

In this study we investigated different sources of error in the airway morphometry and lung densitometry. We also sought to assess the variability in airway morphometry and lung densitometry measures arising from scanner non-conformity. Furthermore, we aimed to develop novel airway and densitometry phantoms and assess their validity for standardisation of quantitative CT measures in multicentre studies as well as correction of different errors associated with airway morphometry and lung densitometry.

### **3.2.3 Materials and Methods**

#### **3.2.3.1 Phantom models for validation of quantitative CT airway morphometry**

##### **3.2.3.1.1 Leicester Airway Phantom (LAP)**

A phantom model was constructed consisting of a polystyrene block embedded with 9 cylindrical plastic tubes of varying dimensions [Figure 3.3]. The wall and lumen measurements of various tubes were chosen so as to simulate dimensions of RB1 bronchus, a 3<sup>rd</sup> generation airway, in healthy and asthmatic subjects,<sup>75</sup> as well as airways down to 12<sup>th</sup> generation.<sup>522</sup> Mean (SEM) attenuation of polystyrene was -965 (9.3) HU.

##### **3.2.3.1.2 CTP674 Phantom, The Phantom Laboratory<sup>523</sup>**

This phantom consists of an outer ring (Catphan Uniformity Material Ring) that simulates soft tissue attenuation with an electron density just above water, and a central oval insert that simulates lung attenuation. The central oval insert contains 6 tubes made of

polycarbonate (CTP666, 1-6) simulating airways of different dimensions, air holes of varying dimensions, an acrylic reference material and an insert for a small bottle filled with sterile water.<sup>524</sup> [Figure 3.4, Table 3.4]. The manufacturer measured the polycarbonate tubes using a micrometer and the dimensions were provided. Measured CT attenuation of the polycarbonate material used to fabricate the tubes provided by the manufacturer was 95HU. The CTP674 Phantom was used as a surrogate ‘patient’ to assess the inter-scanner variability in CT airway measurements and the efficacy of the standardisation methodology.

### **3.2.3.2 Stereomicroscopy and micro-CT**

Stereomicroscopy was used to determine the cross-sectional dimensions of the LAP tubes. Leading face of all tubes was imaged using an Olympus SZX12 stereomicroscope and tube geometry determined [Figure 3.5]. Measurements were made using Aquis Pro software (Syncroscopy, Cambridge, United Kingdom). Calibration was performed using a standard calibration block, which gave an accuracy of  $\pm 1\mu\text{m}$ . The stereomicroscope measurement for the tubes ranged from: WA ( $2.42 - 47.02 \text{ mm}^2$ ) and LA ( $0.95 - 20.42 \text{ mm}^2$ )[Table 3.5]. Vernier caliper was used to measure the length of the phantom tubes. The mean (range) length of the tubes was 51.91 (31.48 – 60.32) mm.

Micro CT was used to confirm the stereomicroscope measurements for LAP tube dimensions, due to the inherent variability in wall thickness and cross sectional LA across the length of the tubes. WV, LV and length of LAP tubes were determined using the micro CT analysis. The WV/length was used to give a mean cross sectional WA of the phantom tube. The 3D tomographic volumes were reconstructed using a cone beam extension of the

filtered back projection algorithm for fan beams from 370 radiographs acquired using a sample rotation step of 0.5°, with 32 frames averaged for acquisition of each projection (using an exposure time for each frame of 120ms).

### **3.2.3.3 CT scanning of airway phantoms**

CT imaging of both LAP and CTP674 phantoms was performed with Siemens Sensation 16 scanner at Glenfield Hospital, Leicester. CT scans were acquired with dose modulation switched off at 16 x 0.75 mm collimation, 1.1 mm pitch, 120 kVp, 50 mAs, 0.5 seconds rotation time and scanning field of view of 500 mm. Images were reconstructed with slice thickness 0.75 mm and slice interval 0.5 mm, using a high (B70f) and low (B35f), spatial frequency algorithm through a 512 X 512 matrix, with a field of view of 350 mm. Both phantoms were scanned at nine additional centres across 5 European Union countries (Germany, UK, Italy, Hungary and Poland). Scanning at two UK centres and all centres outside UK was performed as part of the Emphysema versus Airways disease (EvA) study.<sup>525</sup> The scanning parameters devised were as close as possible to the Siemens Sensation 16 scanner at Glenfield Hospital, Leicester. All CT scans were acquired with dose modulation switched off, utilising scanner –specific protocols as shown in Table 3.6.

### **3.2.3.4 Two-dimensional quantitative analysis of airway phantom tubes using EmphylxJ software.**

All LAP and CTP674 phantom imaging series were analysed with a semi-automated software, EmphylxJ as described in [Section 2.3.2.1]. Dimensions were measured at three

locations (leading face, middle and lagging end) across the length of each tube and averaged.

#### **3.2.3.4.1 Accuracy of airway morphometry assessed using EmphylxJ**

Additional reconstruction of LAP CT images at FOV of 139 was performed, as the three tubes with smallest dimensions were not measurable at reconstruction FOV of 350 mm. Accuracy of FWHM method was assessed from CT airway morphometry (LA, WA and %WA) of the LAP tubes. Tube dimensions measured using EmphylxJ were compared with the stereomicroscope tube measurements. Intra-observer and inter-observer repeatability of CT morphometry using EmphylxJ was also assessed.

#### **3.2.3.4.2 Influence of oblique orientation on CT airway morphometry assessed using EmphylxJ**

The leading face of LAP was reconstructed (FOV 139 mm) at angular increments of 10°, from 0° to 60° [Figure 3.6]. Cross-sectional measurements were made at the leading face using FWHM principle with EmphylxJ software.

#### **3.2.3.4.3 Correction methodology for size and oblique orientation associated errors in CT airway morphometry assessed using EmphylxJ**

We derived correction equations by looking at the best parabolic planar 3D fit of the phantom tube measured WA/LA, the maximum air way lumen diameter (Dmax)/minimum airway lumen diameter (Dmin) ratio [a marker of oblique orientation] and the true WA/LA measured by stereomicroscopy to the nearest micron. For each tube 7 values of

Dmax/Dmin ratio and corresponding geometry (WA and LA) measured using the FWHM method were derived based upon reconstructing each phantom tube at 10° increments from 0° (perpendicular to the long axis of the tube) to 60° corresponding to a ratio of largest to smallest diameter of 1.0 to 2.0. The final correction equations were derived using all 63 measurements of the 9 phantom tubes. Correction equations were generated using a custom program (LeoStatistic, Version 14.5, [www.leokrut.com](http://www.leokrut.com)).

#### **3.2.3.4.4 Effect of varying tube current-time product (mAs) on CT airway morphometry assessed using EmphylyxJ**

The LAP was scanned four times with Siemens Sensation 16 scanner using protocol as described before, but with mAs values of 40, 70, 100 and 140 respectively [Table 3.7]. The images were reconstructed using a high spatial frequency algorithm, through a 512 X 512 matrix, with a field of view of 350 mm. Tubes 1-3 were excluded from analysis as they were below the limit of resolution obtained with the applied image reconstruction parameters. Other six tubes (tubes 4-9) were assessed using EmphylyxJ software using the FWHM technique. Dimensions were measured at three locations across the length of each tube and averaged.

#### **3.2.3.4.5 Inter-scanner variability in CT airway morphometry assessed using EmphylyxJ and validation of proposed standardisation methodology**

Inter-scanner variability was assessed from CT airway morphometry (LA, WA and %WA) of the CTP674 phantom tubes [Table 3.8]. Three tubes with smallest dimensions in the LAP were not measurable at reconstruction FOV of 350 mm, therefore only tube 4-9 were

used. Linear regression equations were derived using LAP tubes measurements obtained from the CT scanner at each EvA centre and the reference scanner [Table 3.8]. Standardisation of airway morphometry of the CTP674 phantom at each EvA centre was achieved by regression towards the airway measurements of the CTP674 phantom obtained at the reference centre. Standardised % WA was derived from standardised LA and WA [ $\%WA = WA/(WA+LA) \times 100$ ]. The efficacy of the standardisation method was assessed by percentage error reduction in %WA measurements of the CTP674 phantom following standardisation [Table 3.8].

#### **3.2.3.4.6 Inter-software variability in CT airway morphometry assessed using EmphylxJ and MedView**

LAP tubes reconstructed at FOV of 139 mm were analysed with another semi-automated software, MedView beta release version 1.0 (Department ARTEMIS, Institut TELECOM, Evry, France) [Section 2.3.2.2.1.2], to assess inter-software difference in CT airway morphometry.

Tube 1 dimensions could not be measured using MedView. Comparison was made between CT morphometry of LAP tube 2-9 assessed using EmphylxJ and MedView software programs.



### **3.2.3.5 Three-dimensional quantitative analysis of airway phantom tubes using Pulmonary Workstation 2 software.**

Volumetric CT scan of LAP tubes 4-9 and all CTP674 phantom tubes were analysed using fully automated software, PW2 [Vida Diagnostics, Coralville, Iowa, <http://www.vidadiagnostics.com/>]. CT imaging of both LAP and CTP674 phantoms was performed with Siemens Sensation 16 scanner at Glenfield Hospital, Leicester using the protocol as described in [section3.2.3.3]. Low spatial frequency algorithm (B35) reconstruction was used for analysis by PW2 software, as recommended by VIDA Diagnostics. Morphological measurements of the phantom tubes were obtained along each centreline voxel of the lumen perpendicular to the long axis on each tube, and averaged over the middle third of the tube. LA, TA and length of all the phantom tubes were measured [Figure 3.7].

#### **3.2.3.5.1 Accuracy of airway morphometry assessed using PW2**

Tube dimensions measured using PW2 were compared with the stereomicroscope tube measurements. Intra-observer repeatability of CT morphometry using PW2 was also assessed.

#### **3.2.3.5.2 Inter-scanner variability in CT airway morphometry assessed using PW2**

Inter-scanner variability between Siemens Sensation 16 and General Electric Lightspeed 64 scanners, was assessed from CT airway morphometry (LA, WA and length) of the CTP674 phantom tubes.

### **3.2.3.6 Phantom models for validation of quantitative CT densitometry analysis**

#### **3.2.3.6.1 Warwick densitometry phantom (WDP)**

The WDP [Figure 3.8] was constructed of a milled housing of ‘solid water’ (Gammex – RMI Ltd, Nottingham, UK) that contained a series of synthetic lung cores designed to mimic the structure and heterogeneous density of lung tissue. Nine cores were made to provide a range of density measurements comparable to lungs with a range of emphysema severity. The lung cores were modelled on data from volumetric lung CT imaging of patients with a range of emphysema severity. These images were imported into a software package (Mimics, Materialise, Belgium) and used to construct a laser-sintered (EOS P380i - EOS GmbH, Munich, Germany) polyamide-12 polymer (PA2200 - EOS GmbH, Munich, Germany) ‘skeleton’ of high-density structures, equivalent to airway walls and blood vessels. The open volumes of the cores were subsequently filled with stiff polyurethane (PU) expanding foam (DRF002, Tiranti Ltd, Thatcham, UK) of different densities, generated by using pure PU foam and PU foam mixed with 5% or 10 % acetone ( $\text{CH}_3\text{O}$ ) prior to casting.

#### **3.2.3.6.2 Electron density Rods**

Three EDR (two rods with density values equivalent to lung tissue (LN300, LN450), and one rod with equivalent density to water ('solid water')) from an RMI467 electron density CT phantom (Gammex – RMI Ltd, Nottingham, UK) were also used [Figure 2.3, Section 2.4].

### **3.2.3.6.3 Anthropomorphic lung phantom**

An Anthropomorphic phantom was used which was loaned from King's College Hospital, London (KCARE) and was made up of human bony thorax within a soft tissue equivalent torso.<sup>526</sup> Inside the thorax was a pair of canine lungs fixed in preservative with their pulmonary vasculature filled with epoxy resin to simulate normal sanguination. The mediastinum was made up of a porcine heart and great vessels. The anthropometric lung phantom was used as a surrogate 'patient' to assess the inter-scanner variability in CT lung densitometry measurements and the efficacy of the standardisation methodology.

### **3.2.3.7 CT lung densitometry**

#### **3.2.3.7.1 Inter-scanner variability in CT lung densitometry and validation of proposed standardisation methodology**

Inter-scanner variability was assessed by imaging an anthropomorphic lung phantom (KCARE, Kings College Hospital, London, UK), containing fixed whole dog lungs in a GE Lightspeed VCT 64 scanner using a reference imaging series protocol [Protocol 1, Table 3.9] and five other scanners using the closest equivalent scanner settings. In addition, other scanning protocols were employed in each scanner in order to generate a total of twenty-five imaging protocols with a wide range of parameters [see Table 3.9]. A semi-automated software program, Pulmo-CMS (Medis Medical Imaging, Leiden, Netherlands) was used for densitometry analysis as previously described.<sup>527</sup> Analysis consisted of 2 parts: threshold-based lung segmentation and derivation of lung densitometric indices from the voxel frequency distribution histogram. Whole lung densitometry (Perc15) of the dog lung

was assessed for each imaging series using Pulmo-CMS (Pulmo) and variability assessed as mean and standard deviation.

A method for standardisation of densitometric indices was explored using density measurements obtained from a number of ‘standards’, including WDP and EDR that were imaged synchronously with the dog lung phantom. Three EDR were secured by a *Velcro* strap to the sternal region of the dog lung phantom for all imaging series. Density measurements of these rods and the WDP ‘solid water’ housing were obtained using the ROI facility of Pulmo. In addition, density measurements of air ventral to the phantom sternal region were obtained using the ROI sampling facility of Pulmo and used for internal air calibration, as previously described.<sup>526,528</sup>

Regression equations were calculated from measurements of the densitometry standards (all WDP cores, three EDR, WDP ‘solid water’ housing and air ventral to phantom) for each of the scanning protocols in relation to the reference protocol [Protocol 1, Table 3.9]. Each regression equation was used to adjust the density measurements of the lung phantom to standardize towards the lung densitometry value obtained using the reference protocol on the reference scanner. The efficacy of the standardisation procedures was assessed by comparison of the mean and standard deviation.

#### **3.2.3.7.2 Inter-software variability in CT lung densitometry**

Inter-software variability was assessed by comparing the CT lung densitometry of 10 COPD subjects assessed using two software programs; Pulmo and PW2. Five COPD

subjects were scanned with Siemens Sensation 16 scanner and other 5 were scanned with General Electric Lightspeed VCT 64 scanner as part of the EVA study.<sup>525</sup>

#### **3.2.3.7.3 Inter-observer and intra-observer variability in CT lung densitometry**

CT densitometry of nine cores in WDP, representing lung density with different degree of emphysema, was measured using PW2 by two observers as well as single observer two months apart. Inter-observer and intra-observer repeatability of CT densitometry using PW2 was assessed.

#### **3.2.3.8 Statistical Analysis**

Statistical analysis was performed using GraphPad Prism version 5.00 for Windows, GraphPad Software, San Diego California USA, [www.graphpad.com](http://www.graphpad.com) and SPSS for Windows, Rel. 16.0.1.2008. Chicago: SPSS Inc. Data were expressed as mean (SEM). One-way analysis of variance with Tukey correction was used to compare multiple groups. Unpaired and paired t-tests were used to compare data between two groups. Pearson correlation coefficient (Pearson R) was used to assess linear dependence between two variables. Intraclass correlation (ICC) and Bland-Altman plots were used to assess repeatability. Two-way random effect model with absolute agreement ICC was used to assess single measure reliability. A p value of  $<0.05$  was taken as statistically significant.

### **3.2.4 Results**

#### **3.2.4.1 Comparison of cross sectional geometry using micro CT and stereomicroscopy**

There was a close correlation between micro CT and stereomicroscopy of the leading face of phantom tubes 1-9 [Table 3.5] for the WA ( $r^2=0.99$ ) and LA ( $r^2=0.99$ ). The mean (SEM) unsigned % difference in WA and LA between stereomicroscopy and micro CT was 6.44 (1.0) % and 9.70 (3.53) % respectively.

#### **3.2.4.2 Accuracy of airway morphometry assessed using EmphylxJ**

There was excellent repeatability between two observers for LA and WA measurements of tubes 1-9 of LAP; LA, ICC = 1 (95% CI, 1 – 1;  $p<0.005$ ) and; WA, ICC = 1 (95% CI, 0.992 – 1;  $p<0.005$ ) [two-way random effect model, absolute agreement, single measure reliability]. Bland-Altman plots for inter-observer repeatability are shown in [Figure 3.9].

Repeatability analysis for LA and WA measurements of tubes 1-9 of LAP by single observer two-weeks apart also showed almost perfect results; LA, ICC = 1 (95% CI, 1 – 1;  $p<0.005$ ) and; WA, ICC = 1 (95% CI, 0.996 – 1;  $p<0.005$ ) [two-way random effect model, absolute agreement, single measure reliability].

Measures of LA and WA of all LAP tubes made using FWHM method was compared with stereomicroscope measures. There was excellent correlation with near perfect linear relationship between the two measures [LA and WA, Pearson  $r = 0.99$ ,  $p < 0.0001$ ; [Figure

3.10 A and C]. Bland-Altman plots comparing the difference versus the mean of two measures show a systematic bias based on size [Figure 3.10 B and D].

#### **3.2.4.3 .Influence of oblique orientation on CT airway morphometry assessed using EmphylxJ**

Statistically significant errors were demonstrated in measurement of mean LA and mean WA of LAP tubes when incident angle (IA) of oblique orientation was 30° or more compared to measurement at 0° IA (perpendicular to the CT plane) [Figure 3.11 A and Figure 3.12 A]. Mean %WA of the LAP tubes was not influenced by oblique orientation and did not show any significant difference when oriented obliquely in comparison to the scan at 0° IA [Figure 3.13].

Relationship between IA and LA or WA of the LAP tubes was non-linear which was best described by second-degree polynomial equations [Figure 3.11 B and Figure 3.12 B].

#### **3.2.4.4 Correction methodology for size and oblique orientation associated errors in CT airway morphometry assessed using EmphylxJ**

We found that a 3D plot of the Dmax/Dmin (representing degree of oblique orientation), measured LA/WA and true LA/WA demonstrated a close parabolic planar fit between plotted points [Figure 3.14].

The correction equations were generated using a custom software program [LeoStatistic, Version 14.5, [www.leokrut.com](http://www.leokrut.com)]. The correction equations derived from multivariate analysis using parabolic approximation were:

$$\text{True LA} = 20 - 0.014 (\text{Measured LA} - 20)^2 + 3.7(\text{Dmax/Dmin} - 2.1)^2 \quad [R^2=0.85]$$

$$\text{True WA} = 50 - 0.0073 (\text{Measured WA} - 92)^2 + 7.5(\text{Dmax/Dmin} - 2.3)^2 \quad [R^2=0.80]$$

#### **3.2.4.5 Effect of varying tube current-time product (mAs) on CT airway morphometry assessed using EmphylxJ**

No significant difference between dimensions of phantom airway model tubes was found when scanned at varying mAs [Table 3.7].

#### **3.2.4.6 Inter-scanner variability in CT airway morphometry assessed using EmphylxJ and validation of proposed standardisation methodology**

Mean tube measurements of the CTP674 phantom imaged at each EvA centre, and the regression equations used for standardisation of the tube measurements, are shown in [Table 3.8].

A mean (SEM) difference of 2.9 (0.6) was observed in the %WA dimensions prior to standardisation [see Figure 3.15]. Mean differences (SEM) in %WA measurement across all centres following standardisation was 0.6 (0.2),  $p=0.002$ . The mean (SEM) %WA of the



CTP674 phantom tubes were significantly lower on the Siemens-derived imaging compared to the GE-derived imaging [62.0 (0.6) versus 66.4 (0.4),  $p=0.001$ ].

#### **3.2.4.7 Inter-software variability in CT airway morphometry**

There were significant differences between the mean (SEM) LAP tubes dimensions assessed using EmphylxJ and MedView [Table 3.10], LA (paired t-test,  $p=0.003$ ); WA (paired t-test,  $p=0.02$ ); and %WA (paired t-test,  $p<0.0001$ ).

#### **3.2.4.8 Accuracy of airway morphometry assessed using PW2**

Repeatability analysis for LA, WA and length measurements of LAP tubes 4-9 by single observer two-months apart showed excellent correlation; LA, ICC = 1 (95% CI, 0.3 – 1;  $p<0.005$ ); WA, ICC = 0.99 (95% CI, 0.3 – 1;  $p<0.005$ ); Length, ICC = 1 (95% CI, 0.97 – 1;  $p<0.005$  [two-way random effect model, absolute agreement, single measure reliability]. Bland-Altman plots for intra-observer repeatability are shown in [Figure 3.16 A, B and C].

Measures of LA and WA of LAP tubes 4-9 made using PW2 software was compared with stereomicroscope measures. Length measurements of LAP tubes 4-9 made using PW2 software were compared with Vernier caliper measures. No significant difference was found when WA measures obtained using PW2 were compared with measures made using stereomicroscope [paired t test; mean (SEM) WA, 20.3 (4.6) vs 21.1 (6.3),  $p=0.7$ ]. Mean (SEM) LA was underestimated by PW2 when compared to stereomicroscope measures although the difference did not reach statistical significance [paired t test; mean (SEM) LA, 11.1 (2.8) vs 11.9 (2.7),  $p=0.06$ ]. Mean (SEM) tube length was underestimated by PW2

compared to Vernier caliper [paired t test; 48.1 (3.4) vs 49.4 (3.7),  $p=0.01$ ]. Repeatability analysis for LA/WA and length measurements of LAP tubes 4-9 by stereomicroscope and Vernier caliper respectively, compared to PW2 measurements showed excellent correlation; LA, ICC = 0.99 (95% CI, 0.82 – 1;  $p<0.005$ ); WA, ICC = 0.95 (95% CI, 0.7 – 0.99;  $p<0.005$ ); Length, ICC = 0.99 (95% CI, 0.52 – 1;  $p<0.005$  [two-way random effect model, absolute agreement, single measure reliability]. Bland-Altman plots of LA and length do not show any systematic bias. Bland-Altman plot of WA shows that PW2 overestimates and underestimates dimensions of smaller and larger tubes respectively compared to stereomicroscope [Figure 3.17 A, B, C, D, E and F].

#### **3.2.4.9 Inter-scanner variability in CT airway morphometry assessed using PW2**

No significant difference was found in PW2 assessed CT airway morphometry (LA, WA and length) of CTP674 phantom tubes scanned in General Electric Lightspeed 64 and Siemens Sensation 16 scanners [paired t test; mean (SEM) LA, 20.5 (4.5) vs 20.0 (4.5),  $p=0.2$ ; mean (SEM) WA, 25.7 (4.7) vs 26.3 (4.6),  $p=0.6$  and; mean (SEM) length, 48.0 (0.7) vs 49.0 (0.9),  $p=0.2$ ] [Figure 3.18 A, B and C].

#### **3.2.4.10 Inter-scanner variability in CT lung densitometry and validation of proposed standardisation methodology**

Figure 3.19 shows the difference between Perc15 values of the dog lung phantom using protocols 2-25 [Table 3.9], and the value obtained from the reference imaging series

[Protocol 1, Table 3.9] for unstandardised and standardised data. A mean difference of 26.2 HU (SD 13.4) was observed in the unstandardised data. Standardisation reduced the mean difference to 4.1 HU (SD 2.3 HU), representing an error reduction of 84 %. When standardisation was performed using just the EDR, air and water there was a reduction in mean difference to 19.6 HU (SD 12.6 HU).

#### **3.2.4.11 Inter-software variability in CT lung densitometry**

Small but statistically significant differences were observed in CT densitometry indices assessed by Pulmo and PW2 [Table 3.10]. There was excellent linear correlation between the MLD measured by the two software programs (Pearson  $r = 0.99$ ,  $p < 0.0001$ ) [Figure 3.20 A]. Bland-Altman plot comparing the difference versus the mean of two measures did not show any systematic bias [Figure 3.20 B]. Other CT densitometry indices also demonstrated excellent correlation between the two measures with no systematic bias.

#### **3.2.4.12 Inter-observer and intra-observer variability in CT lung densitometry**

There was excellent repeatability between two observers for MLD measurements of nine cores of WDP, ICC = 0.95 (95% CI, 0.8 – 0.99;  $p < 0.005$ ; two-way random effect model, absolute agreement, single measure reliability). Graphical representation of paired t test ( $p=0.9$ ) and Bland-Altman analysis for inter-observer repeatability are shown in [Figure 3.21 A and B].

Repeatability analysis for MLD measurements of nine cores of WDP by single observer two-months apart also showed almost perfect results, ICC = 1 (95% CI, 0.997 – 1;  $p < 0.005$ ; two-way random effect model, absolute agreement, single measure reliability). Graphical representation of paired t test ( $p = 0.5$ ) and Bland-Altman analysis for inter-observer repeatability are shown in [Figure 3.22 A and B].

### 3.2.5 Discussion

In this study we have shown the importance of airway and densitometry phantom models in standardising airway morphometry and lung densitometry measures in quantitative studies.

We determined the accuracy and repeatability of airway morphometry assessed using the FWHM method employed by a semi-automated software programme, EmphylxJ. Our study has demonstrated that FWHM method leads to significant size dependent errors. LA is consistently under-estimated by FWHM method and the error becomes greater as the airway size decreases. WA is over-estimated for smaller airways and under-estimated for larger airway, error being least for mid-sized airways. This is consistent with findings of others who have shown that airway quantification using FWHM method overestimates the airway wall and underestimated airway lumen.<sup>286,287</sup> There is linear relationship between the LA or WA measured using FWHM method and SM, suggesting that these errors can be corrected. We have also shown that there is excellent intra-observer and inter-observer repeatability of airway morphometry using FWHM method. Similarly Niimi *et al.* demonstrated good inter-observer and intra-observer repeatability of airway dimension measurement.<sup>75</sup>

We confirmed the findings of others<sup>529</sup> that oblique orientation of the LAP tubes lead to significant errors in LA and WA measurements. The error became statistically significant compared to LA and WA measurement at 0° (plane perpendicular to CT scanner axis), when the angle of oblique orientation was  $\geq 30^\circ$ . Importantly, mean %WA of LAP tubes was not affected by oblique orientation, suggesting that %WA area can be used as a measure of airway remodelling where measurement of airway dimension in plane orthogonal to airway axis is not possible. We endeavoured to correct the size dependent and oblique orientation associated errors in airway morphometry as, (1) EmphylyxJ software measures the airway dimensions on two-dimensional CT slices and is unable to reconstruct the airway in a plane perpendicular to airway axis, and (2) some of our CT studies utilised retrospective high-resolution CT scans which are not acquired in a volumetric fashion and therefore are not amenable to 3D analysis of airway dimensions using more recent software programs. Corrections in airway morphometry were performed using equations derived from multivariate analysis using parabolic approximation on a 3D plots of true LA/WA, measured Dmax/Dmin, and measured LA/WA. Similar techniques for overcoming the influence of oblique orientation on airway morphometry have been utilised by other researchers.<sup>284,294</sup> However the correction technique applied by us accounted for errors due to oblique orientation as well as errors dependent on airway size. Retrospective scans analysed in our clinical studies were acquired with dose modulation switched on resulting in variable mAs in CT xy-plane as well as in the z-axis. We have shown using the LAP that no significant difference in airway morphometry was observed with mAs ranging from 40 to 140. Airway morphometry of the LAP tubes determined using two different two-dimensional software programs using FWHM and EDCE approaches respectively, showed significant differences between measures. Our findings are congruent with those of Brillet

and colleagues<sup>297</sup> who have shown that FWHM and EDCE methods of airway morphometry result in significant differences in airway dimensions most likely attributable to intrinsic properties and the method employed to determine location of the outer bronchial wall boundary by the two morphometry methods. We have demonstrated that airway morphometry using FWHM method is significantly influenced by scanner make and model, and for the first time devised and validated a standardisation method using a purpose built airway phantom.

In our study we also determined the accuracy and repeatability of airway morphometry determined using PW2, a fully automated software programme, using a model-based approach for airway wall detection.<sup>530,531</sup> This approach was shown to be more accurate than the other wall detection methods based on phantom studies.<sup>530</sup> In our analysis no significant differences were found in LAP tubes WA measured using PW2 and stereomicroscope, demonstrating greater accuracy of PW2 than FWHM method in airway wall morphometry. LAP tubes LA was underestimated with PW2 compared to stereomicroscope, although the difference was not statistically significant. We also demonstrated excellent intra-observer repeatability and no significant inter-scanner variability (GE Lightspeed 64 and Siemens Sensation 16) of airway morphometry using PW2.

CT lung densitometry is influenced by different imaging protocols and scanner models.<sup>513,528,532,533</sup> We have confirmed this finding in our study and have demonstrated that a significant reduction in variability can be achieved using a densitometry phantom. The WDP cores used heterogeneous material to generate a complex structure of similar morphology and density to emphysematous lung. This ensured that the densitometric values reflect the influence of the variable image artefacts known to occur with different

image reconstruction algorithms.<sup>534,535</sup> WDP is designed using a novel approach to capture the influence of such artifacts on densitometry, which is less evident in uniform density materials. Kemerink and colleagues<sup>533</sup> in their study concluded that CT numbers for air and water could be used for densitometry standardisation. In contrast, our results show that use of WDP and EDR in addition to air and water CT numbers resulted in greater reduction in variability. On comparison of two softwares, Pulmo-CMS and PW2, differences in CT densitometry observed were small with excellent liner correlation. In addition, intra-observer and inter-observer variability in PW2 determined CT densitometry was excellent. This suggests that the standardisation methodology developed and validated could be applied to both software programs although the results obtained from PW2 and Pulmo-CMS are not interchangeable for CT densitometry.

Our study has a number of potential limitations. The airway phantom tubes have a uniform dimension and do not truly reflect the human airway tree *in vivo*. Explanted inflated animal lungs have also been used as calibration standards for validation of airway dimensions,<sup>518,519</sup> however the majority of these demonstrate large absolute errors in airway morphometry, probably secondary to tissue shrinkage *ex vivo*. Moreover, the human bronchial tree morphometry has been shown to be substantially different to that of other mammalian species used to validate airway geometry in explanted inflated lung models.<sup>536</sup> In our study majority of CT scans were acquired using General Electric and Siemens scanners. The standardisation of airway morphometry and lung densitometry cannot therefor be extrapolated to CT scans acquired using other scanner manufacturers. Further investigation of quantitative CT standardisation is required for assessment of other CT scanners.

In conclusion our study shows the critical importance of using airway and densitometry phantoms to reduce various errors encountered in quantitative computed tomography assessment of asthma and COPD.



### 3.2.6 Figures and Tables

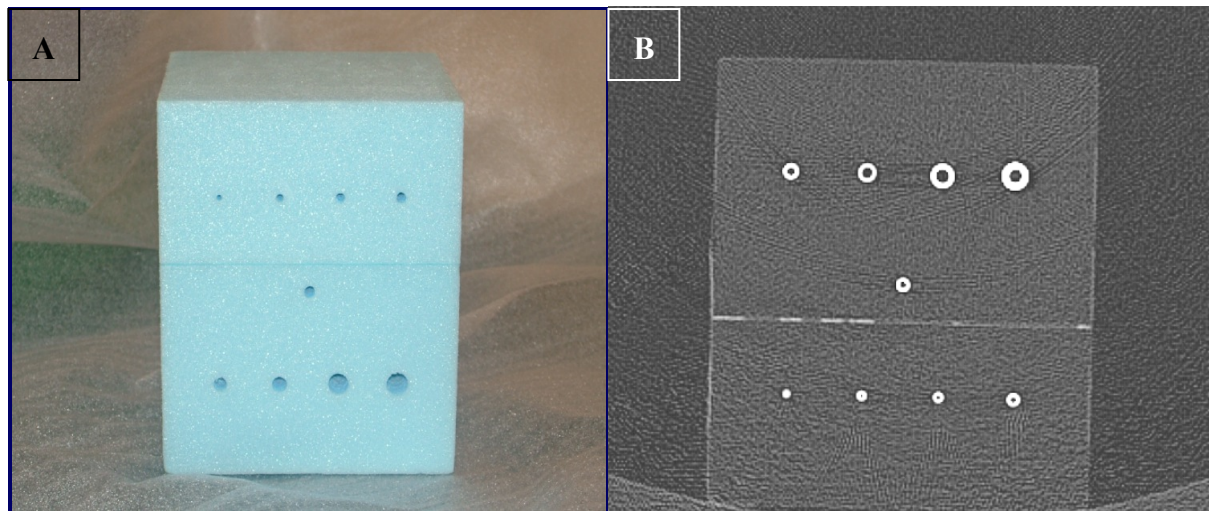


**Figure 3.3: Leicester Airway Phantom**

(A) Leicester Airway Phantom made of polystyrene block embedded with 9 cylindrical plastic tubes of varying dimensions.

(B) CT image of Leicester Airway Phantom

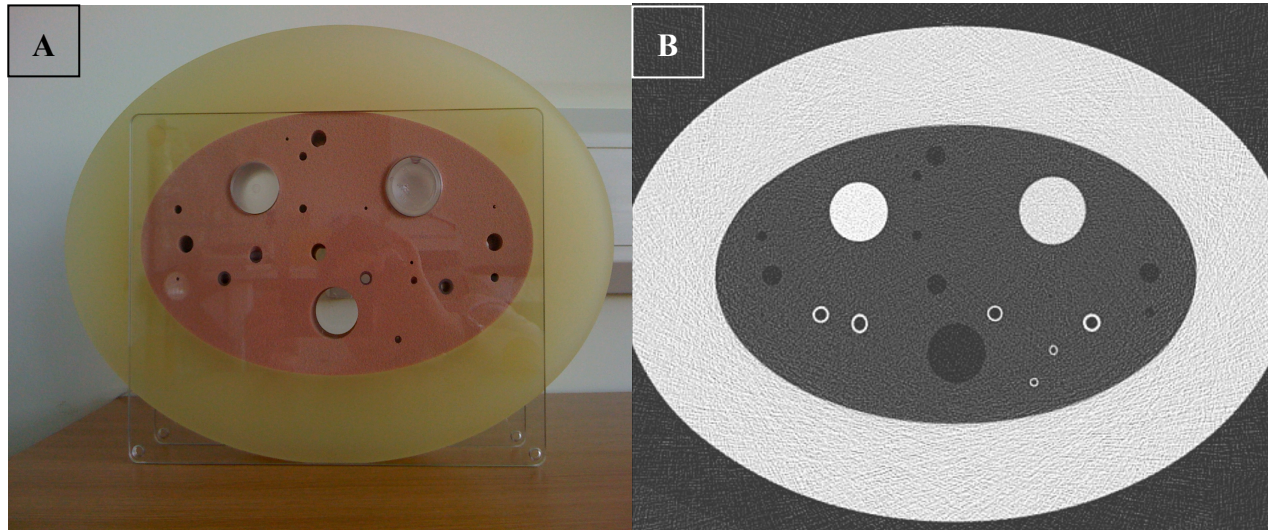


**Figure 3.4: CTP674 Phantom, The Phantom Laboratory**

(A) CTP674 Phantom consisting of outer ring, central oval insert and 6 tubes made of polycarbonate within the central insert simulating airways of different dimensions

(B) CT image of CTP674 Phantom

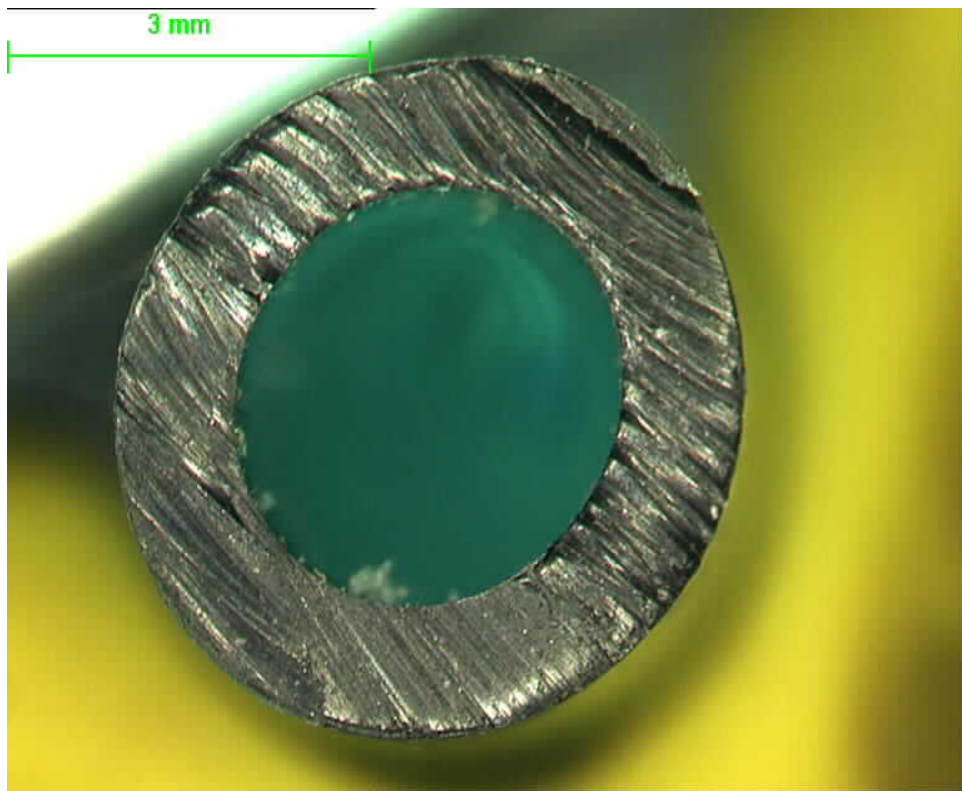


**Figure 3.5: Stereomicroscope image of LAP tube**

Stereomicroscope image showing the leading face of Leicester Airway Phantom, tube 6.

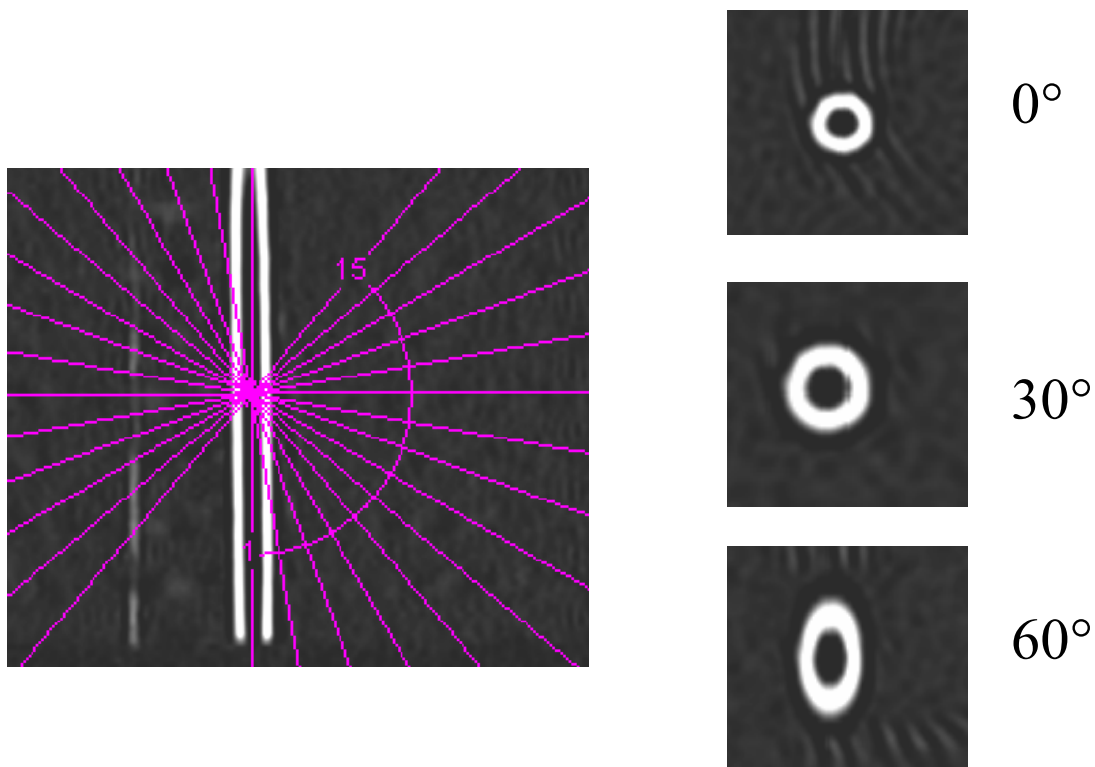


**Figure 3.6: Oblique orientation of LAP tube**

Figure illustrates a LAP tube in long axis view and the leading face of the tube reconstructed perpendicular to the CT plane ( $0^\circ$ ), with  $30^\circ$  and  $60^\circ$  oblique orientation.

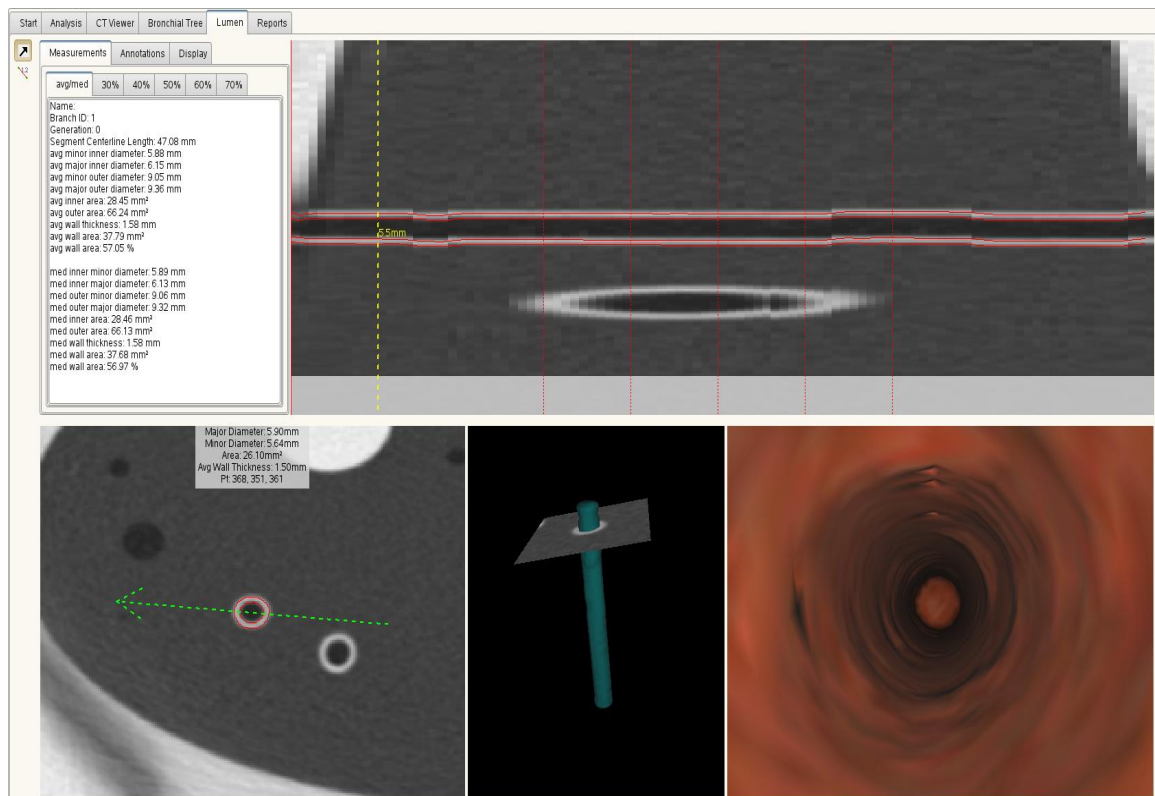


**Figure 3.7: Phantom tube morphometry using PW2 software**

Figure illustrates 3D segmentation of one of the CTP674 phantom tubes using PW2 software for determination of tube dimensions.



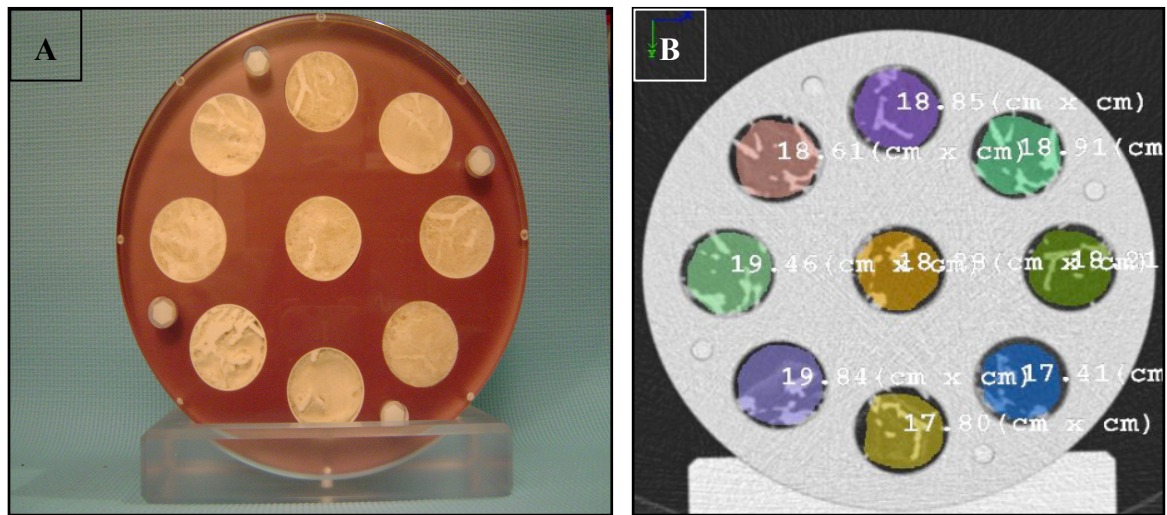


**Figure 3.8: Warwick densitometry phantom**

- (A) Picture of the Warwick densitometry phantom, housing the nine fabricated lung cores.  
 (B) Cross-sectional CT image following densitometric analysis using region of interest (ROI) tool of PW2 software.

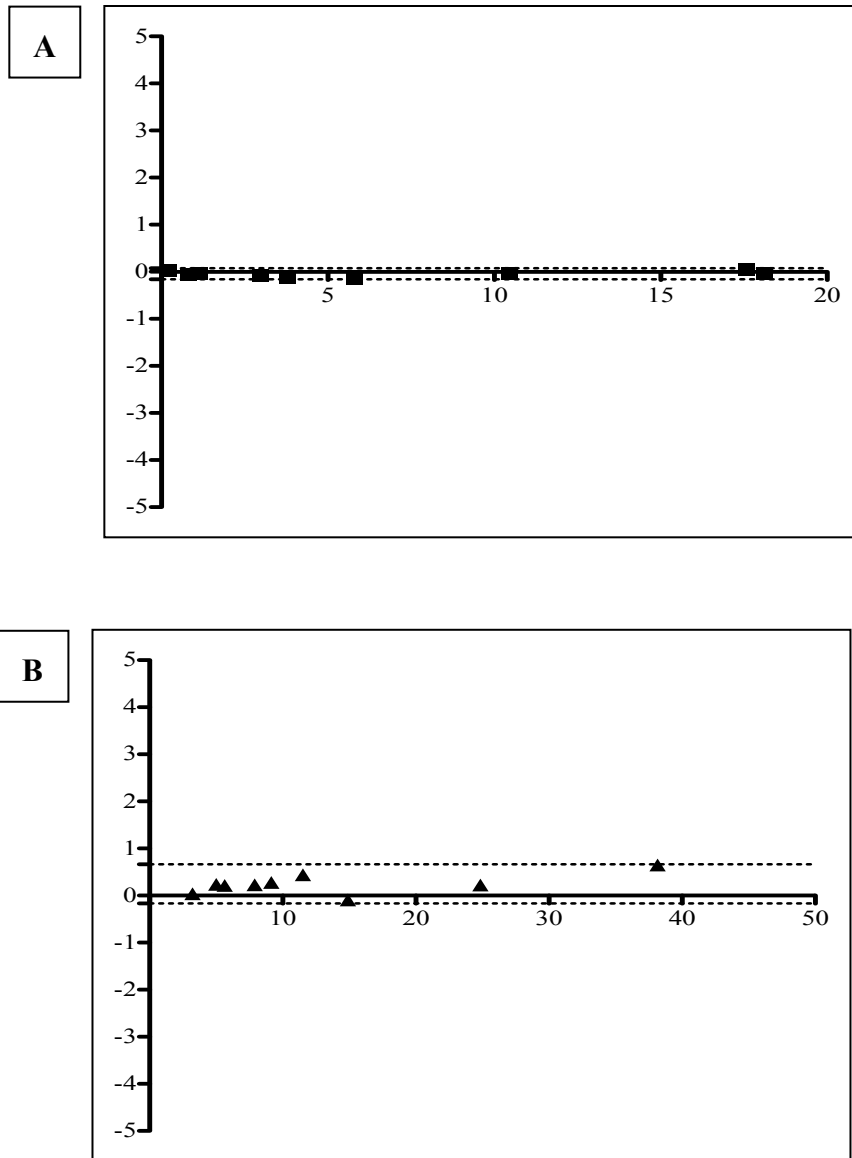


**Figure 3.9: Bland-Altman Plots, inter-observer repeatability using EmphylxJ**

Difference between measures of LA (A) and WA (B) by two observers (y-axis) is plotted against the average of LA (A) and WA (B) measures by two observers (x-axis).

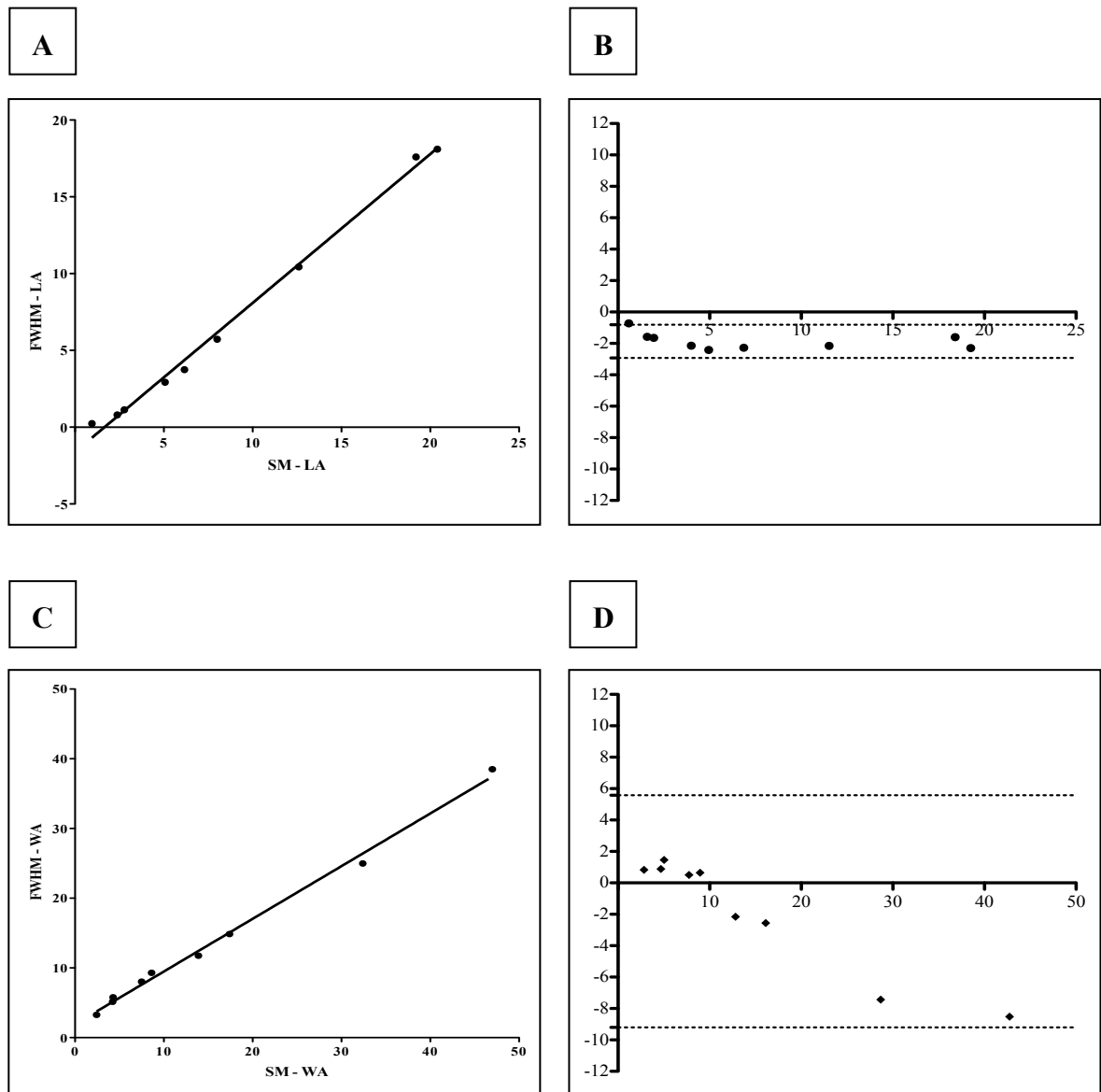


**Figure 3.10: Comparison of LAP tube morphometry using FWHM method and stereomicroscope**

Correlation between LAP tubes LA (A) and WA (C) using stereomicroscope (x-axis) and FWHM (y-axis) method. Bland-Altman plots comparing the difference (y-axis) versus the average (x-axis) measure of LAP tubes LA (B) and WA (D) using the two methods.



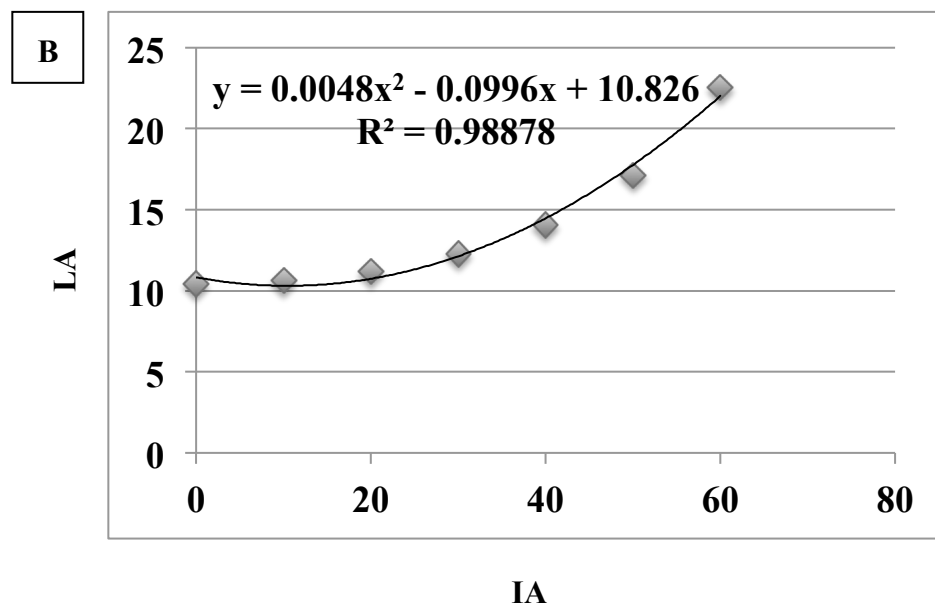
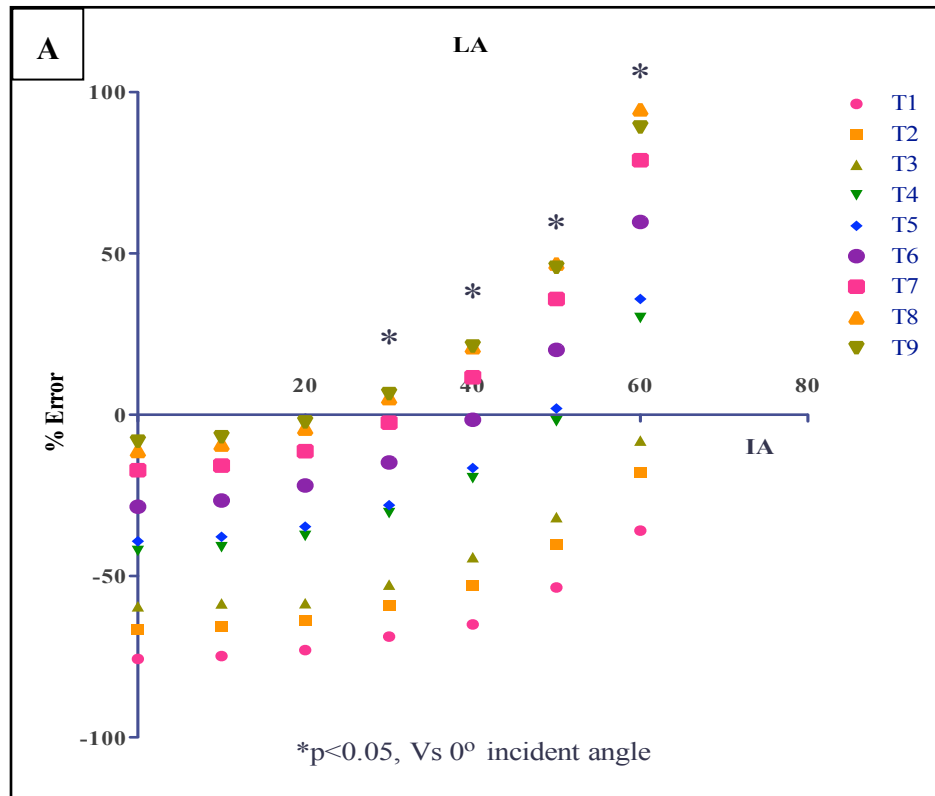


**Figure 3.11: Influence of oblique orientation on lumen area**

(A) Percent error in LA for each LAP tube at incident angle (IA) of oblique orientation 0-60°. (B) Relationship between LA of LAP tube 6 and IA of oblique orientation

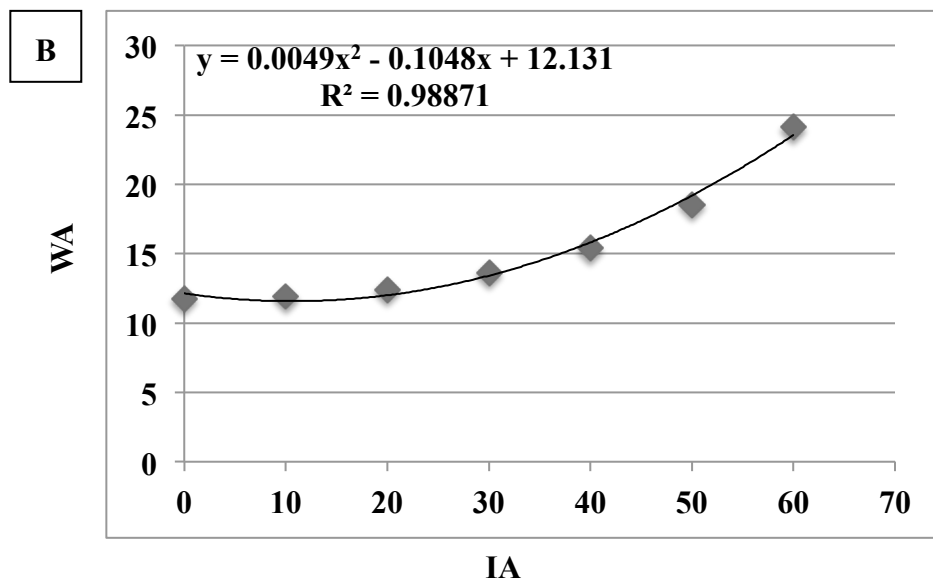
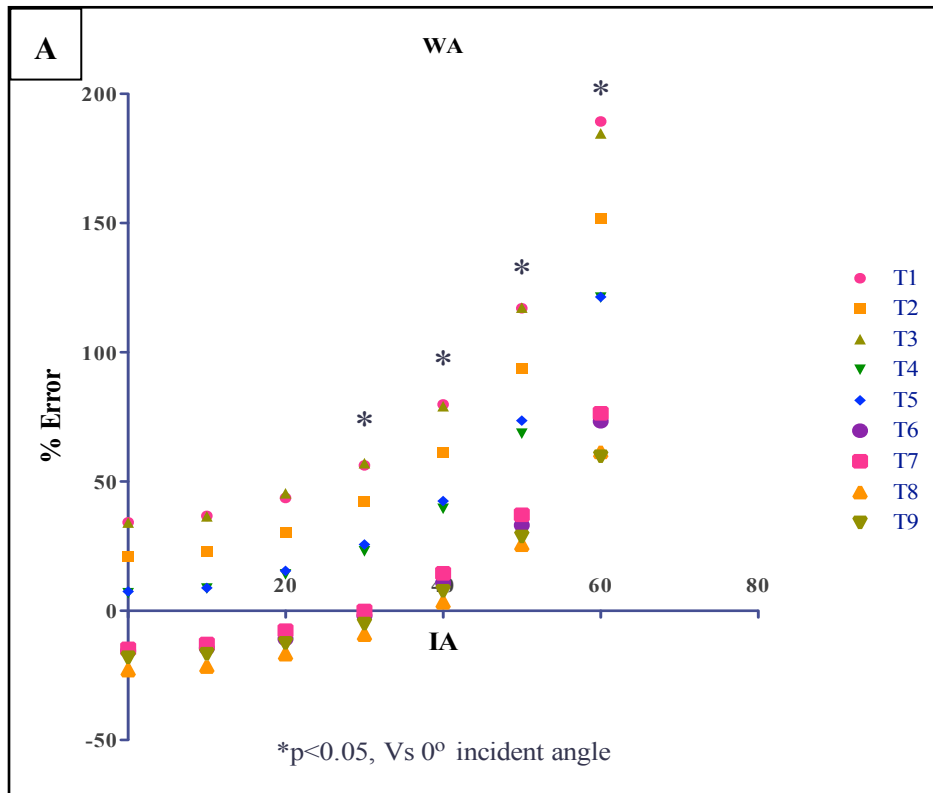


**Figure 3.12: Influence of oblique orientation on wall area**

(A) Percent error in WA for each LAP tube at incident angle (IA) of oblique orientation 0-60°. (B) Relationship between WA of LAP tube 6 and IA of oblique orientation

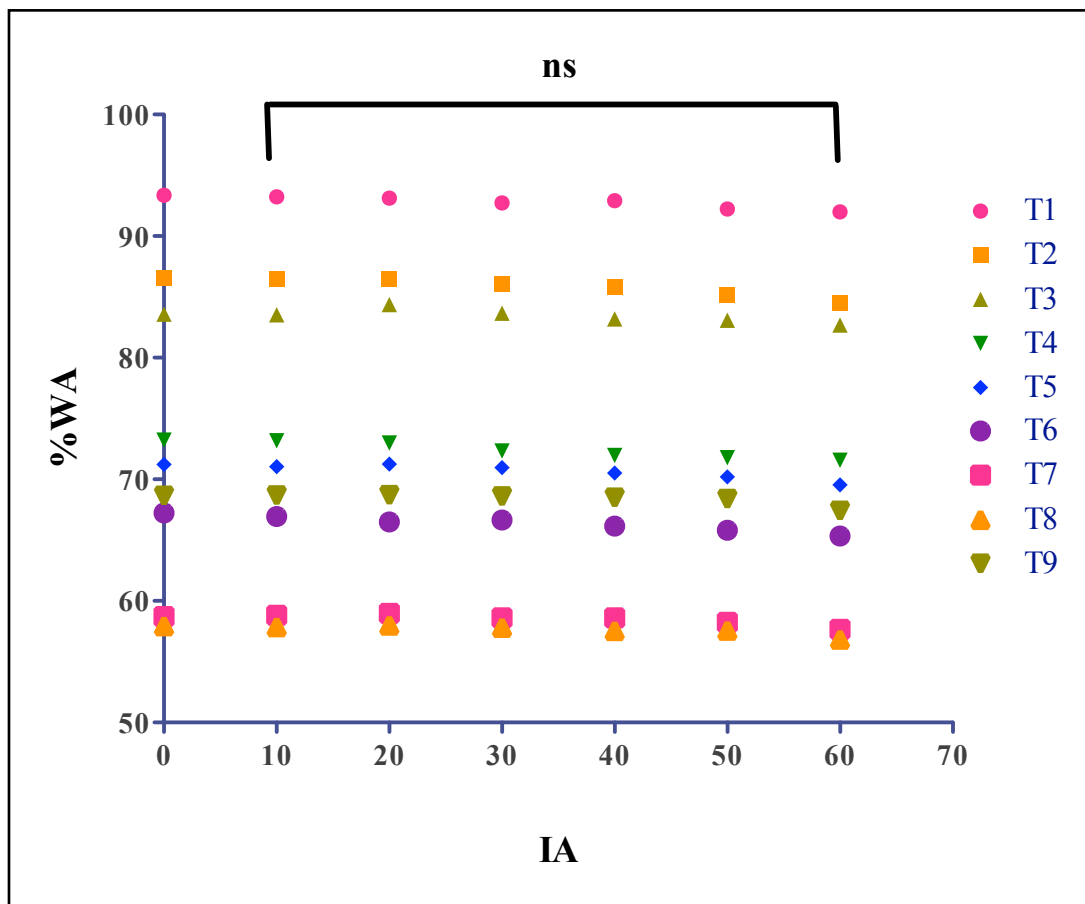


**Figure 3.13: Influence of oblique orientation on percent wall area**

Percent error in percent WA for each LAP tube at incident angle (IA) of oblique orientation 0-60°.

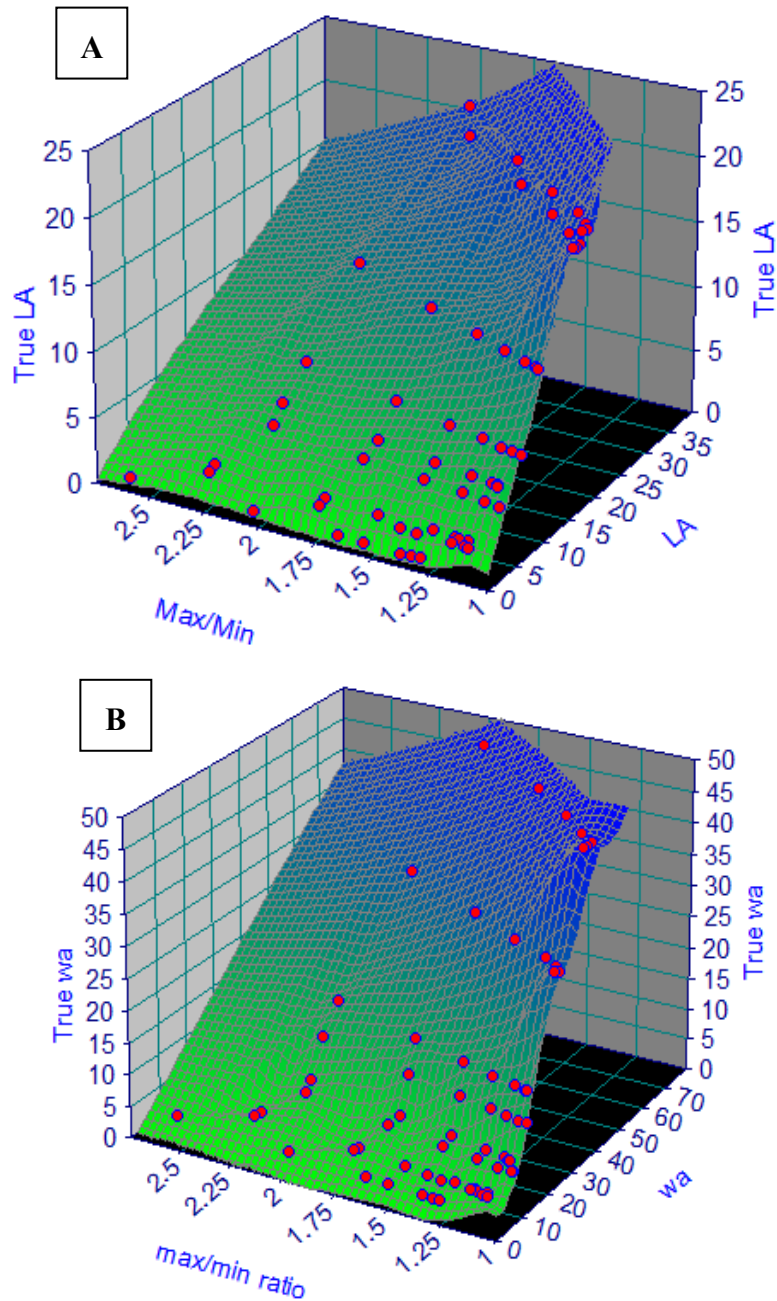


**Figure 3.14: Correction of size and oblique orientation associated errors in CT airway morphometry**

Three-dimensional plot of the  $D_{max}/D_{min}$  ratio (representing degree of oblique orientation), measured LA/WA and true LA/WA for all LAP tubes reconstructed at oblique orientation of  $0-60^\circ$  with parabolic planar fit between plotted points.

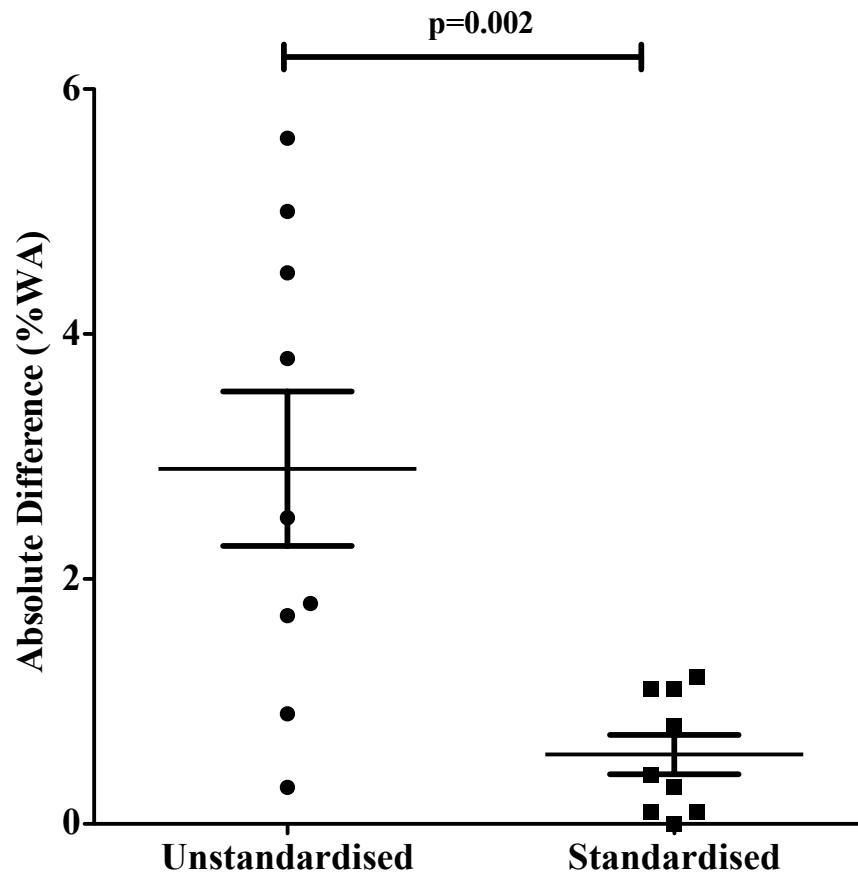


**Figure 3.15: Influence of standardisation on inter-scanner variability in %WA**

Scanner variability is expressed as the absolute difference in mean %WA values of the CTP674 phantom between each of the 9 image series acquired from each EvA centre compared to the airway reference image series

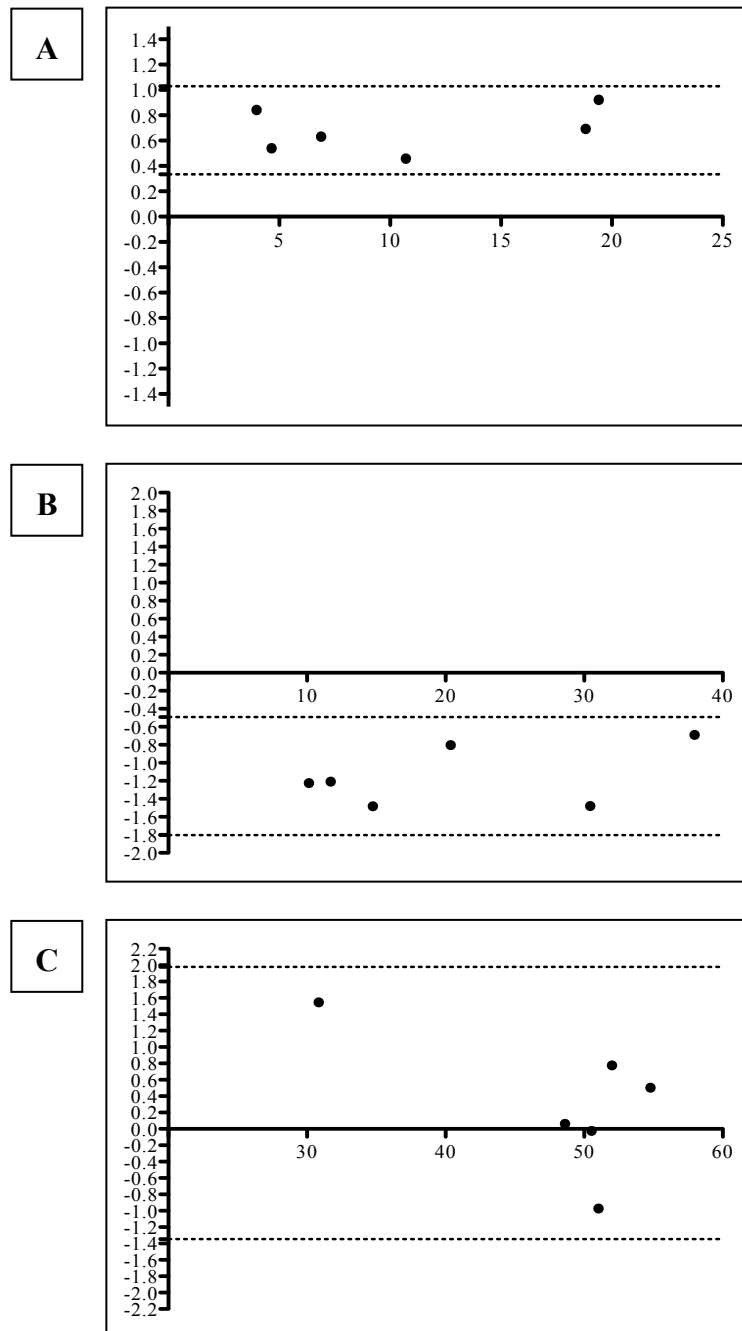


**Figure 3.16: Bland-Altman Plots, intra-observer repeatability using PW2**

Difference between measures of LA (A), WA (B) and length (C) by single observers 2 months apart (y-axis) is plotted against the average of LA (A), WA (B) and length (C) measurements (x-axis).

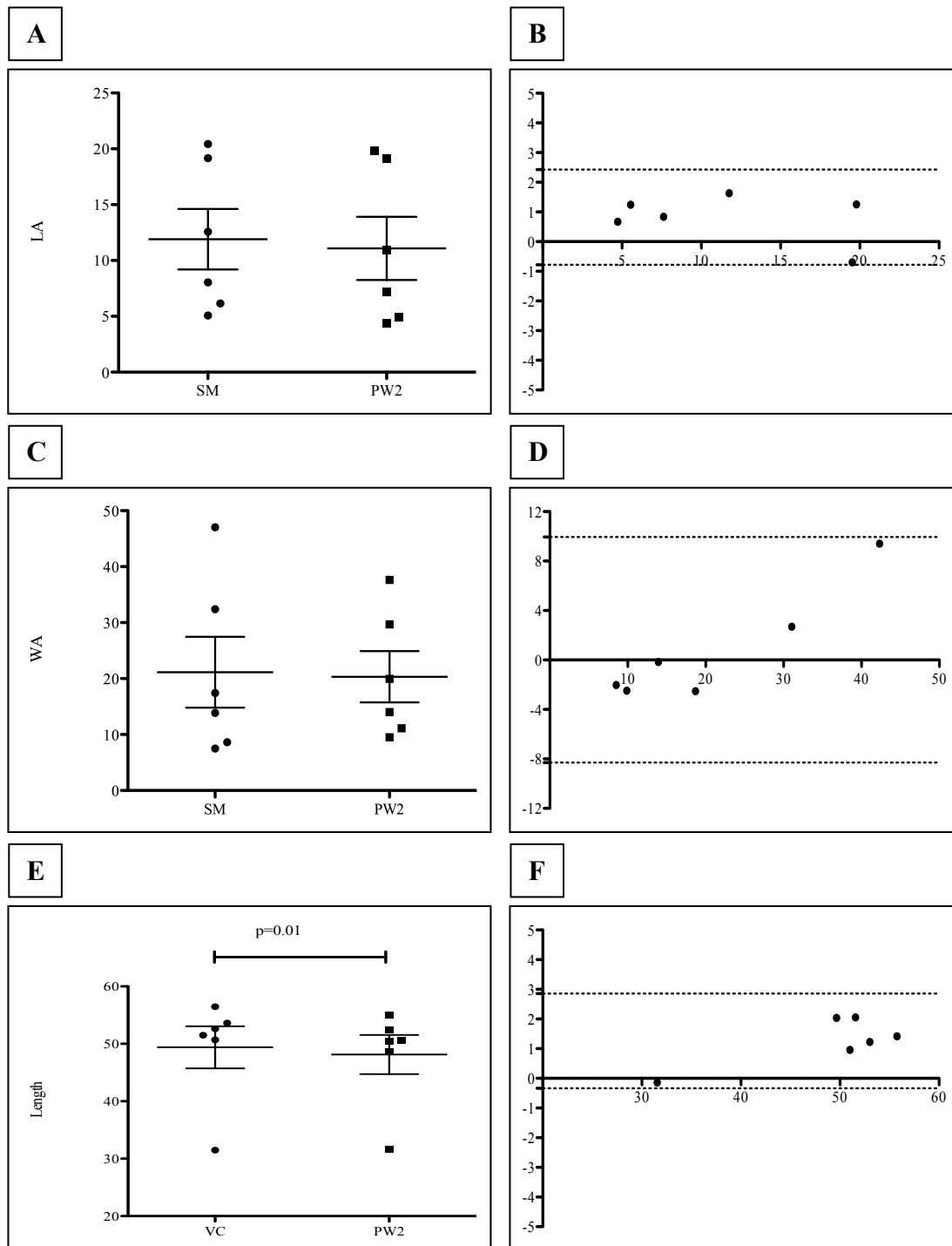


**Figure 3.17:Accuracy of airway morphometry assessed using PW2**

Comparison of PW2 and stereomicroscope measures of LA (A and B), WA (C and D) and length (E and F) using paired t-test and Bland-Altman plots [difference (y-axis) versus the average (x-axis) measure using the two methods is plotted]

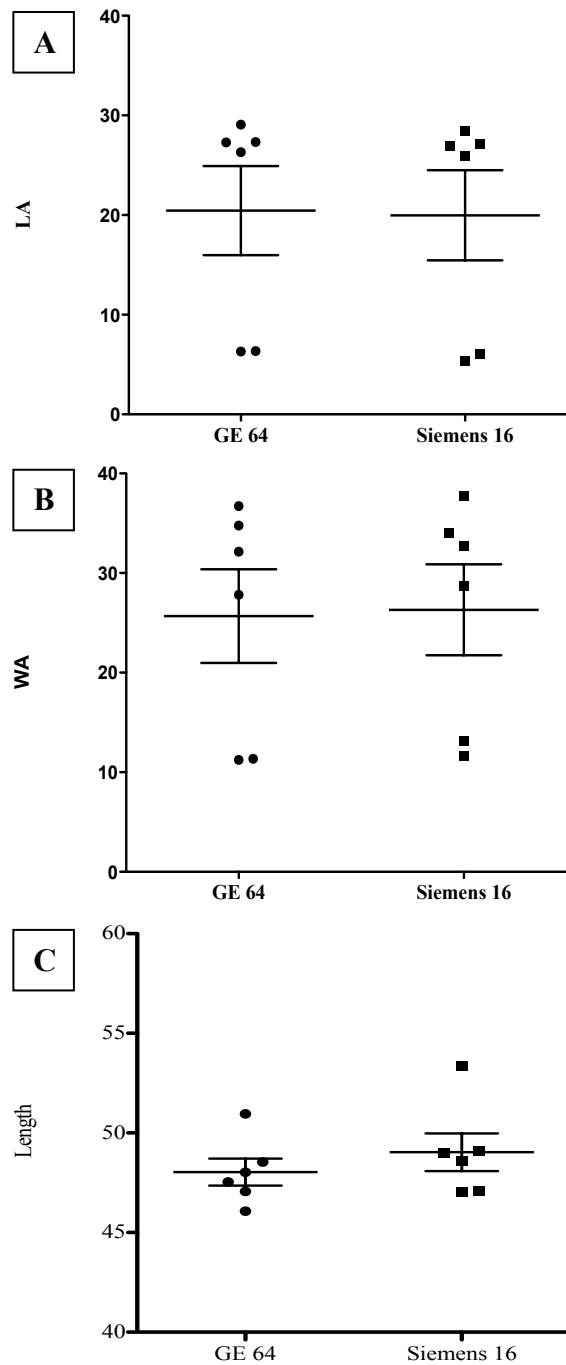


**Figure 3.18: Inter-scanner variability in airway morphometry assessed using PW2**

Comparison of PW2 measures of LA (A), WA (B) and length (C) of CTP674 phantom tubes scanned in two different CT scanners.



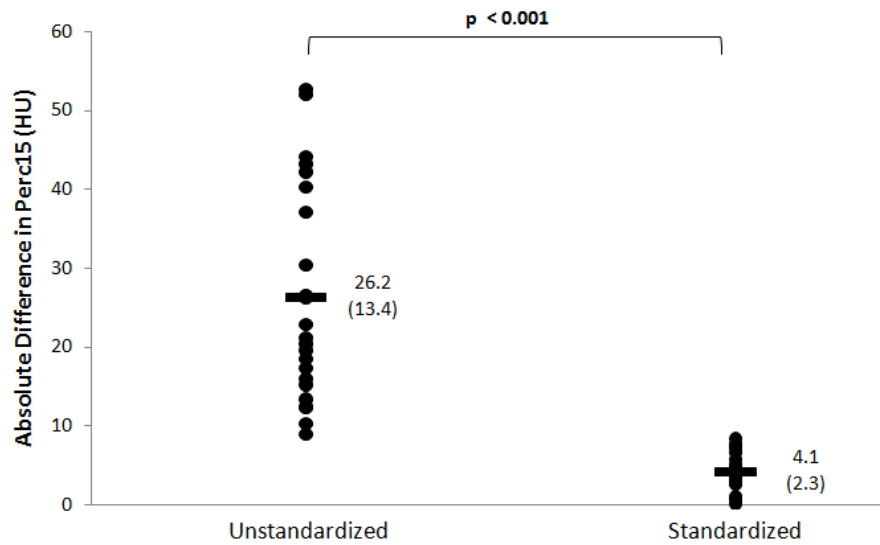


**Figure 3.19: Influence of standardisation on inter-scanner variability in Perc15**

Scanner variability is expressed as the absolute difference in mean (and standard deviation) Perc15 values of the dog lung phantom between each of the 24 image series compared to the reference image series (protocol 1, table 6)

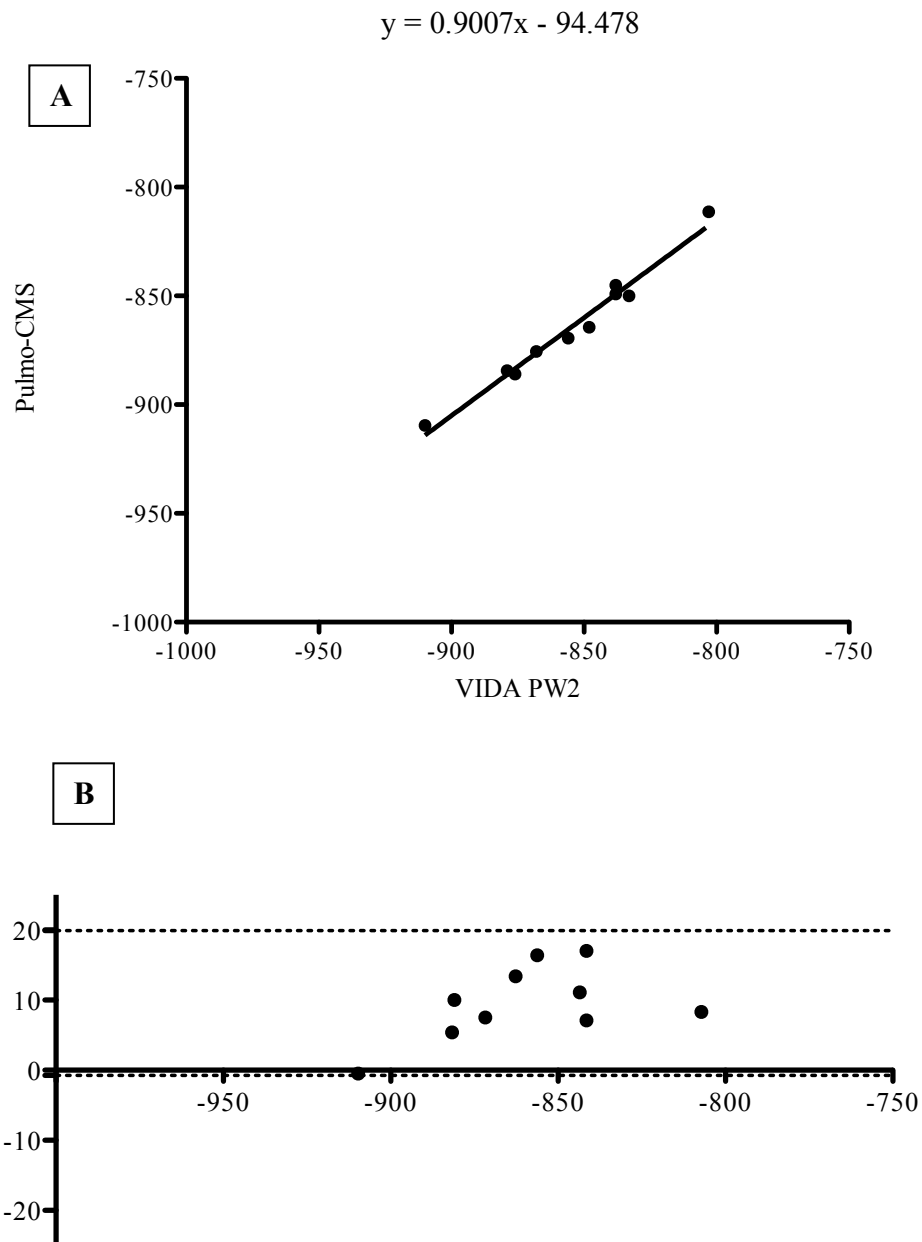


**Figure 3.20: Comparison of lung densitometry using PW2 and Pulmo**

(A) Correlation between MLD of 10 COPD subjects measured using PW2 (x-axis) and Pulmo (y-axis) software. (B) Bland-Altman plots comparing the difference (y-axis) versus the average (x-axis) measure of MLD using the two methods.

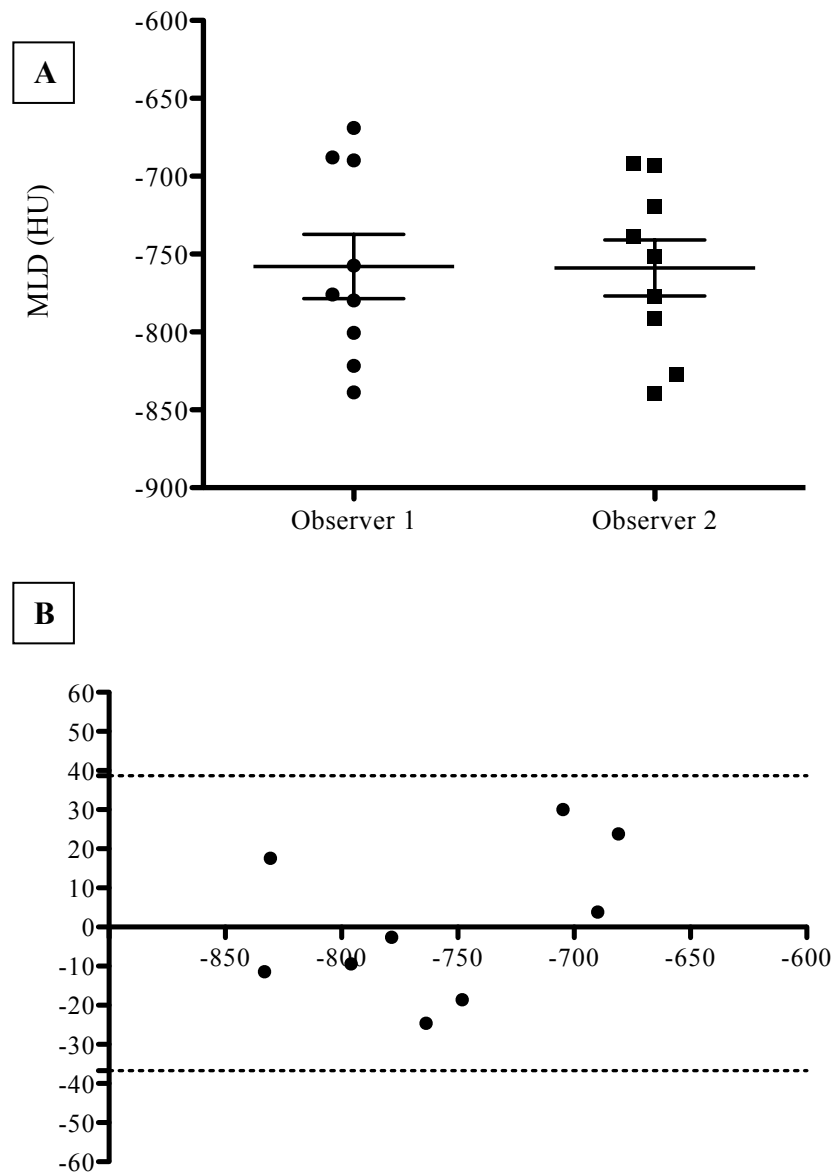


**Figure 3.21: Inter-observer variability in CT lung densitometry**

(A) Comparison of MLD measures of nine WDP cores using PW2 by two observers with paired t-test. (B) Difference between MLD measures of nine WDP cores by two observers using PW2 (y-axis) is plotted against the average of MLD measures by two observers (x-axis).

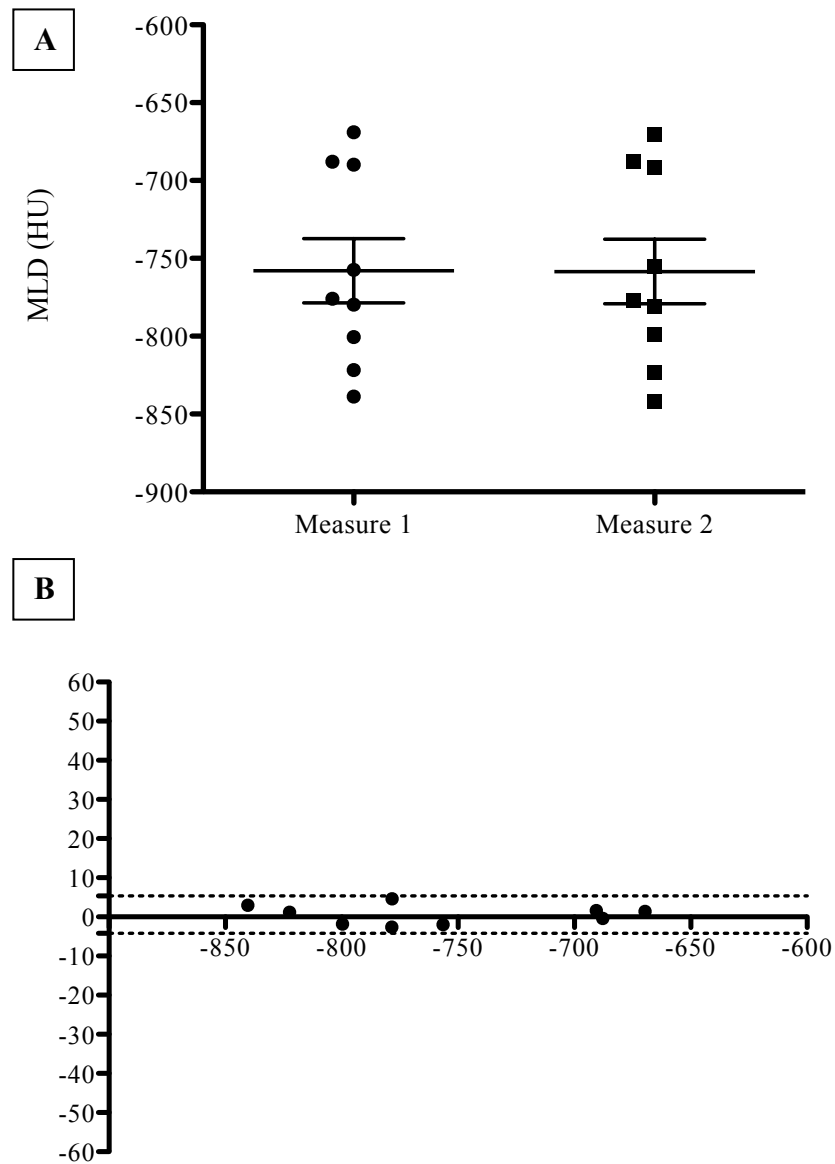


**Figure 3.22: Intra-observer variability in CT lung densitometry**

(A) Comparison of MLD measure of nine WDP cores with PW2 by single observer two months apart using paired t-test. (B) Difference between MLD measures of nine WDP cores by single observer two months apart using PW2 (y-axis) is plotted against the average of MLD measures (x-axis).

**Table 3.4: CTP674 Phantom tube measurements**

<b>Tubes</b>	<b>WA (mm<sup>2</sup>)</b>	<b>LA (mm<sup>2</sup>)</b>	<b>%WA</b>	<b>Tube length</b>
CTP666-1	6.79	7.07	48.98	55.6
CTP666-2	6.79	7.07	48.98	50.0
CTP666-3	19.51	28.27	40.83	50.0
CTP666-4	27.14	28.27	48.98	53.5
CTP666-5	27.14	28.27	48.98	50.0
CTP666-6	35.34	28.27	55.56	50.0

Micrometer measurements of the CTP674 Phantom tubes provided by the manufacturer

**Table 3.5: Leicester Airway Phantom tube measurements**

<b>Tubes</b>	<b>WA (mm<sup>2</sup>)</b>	<b>LA (mm<sup>2</sup>)</b>	<b>%WA</b>	<b>Length</b>
1	2.42	0.95	71.8	58.78
2	4.23	2.38	64	60.32
3	4.29	2.78	60.68	51.74
4	7.5	5.07	59.67	52.6
5	8.63	6.16	58.35	56.46
6	13.86	8.04	63.29	51.48
7	17.43	12.57	58.1	50.68
8	32.39	20.42	61.33	31.48
9	47.02	19.17	71	53.62

Steromicroscope (LA, WA and %WA) and Vernier calipre (length) measurements of Leicester Airway Phantom tubes

*Defenitions of abbreviations:* WA = wall area, LA = lumen area, %WA = percent wall area

**Table 3.6: Scanner-specific imaging protocols**

Scanner model					
	GE Brightspeed 16	GE Lightspeed VCT 64	Siemens Sensation 16	Siemens Emotion 16	Sensation 64 and Definition 64
Scan type	Helical	VCT Helical	Spiral	Spiral	Spiral
Scan field of view (mm)	500	500	500	500	500
Reconstruction field of view (mm)	350	350	350	350	350
Matrix	512 x 512	512 x 512	512 x 512	512 x 512	512 x 512
Rotation time (s)	0.5	0.5	0.5	0.5	0.5
Detector Rows	16	64	16	16	64
Detector width (mm)	0.625	0.625	0.75	0.6	0.6
Pitch	0.983	0.983	1.1	1.1	1.1
kVp	120	120	120	110	120
mAs	50	50	50	50	50
Algorithm	BONE	BONE	B70f	B70f	B70f
Thickness (mm)	0.625	0.625	0.75	0.75	0.75
Interval (mm)	0.5	0.5	0.5	0.5	0.5

*Defenitions of abbreviations:* GE = General Electric, kVp = tube voltage; mAs = milliamperere-second

**Table 3.7: Effect of varying tube current-time product (mAs) on airway dimensions**

	<b>40 mAs</b>	<b>70mAs</b>	<b>100mAs</b>	<b>140mAs</b>
<b>%Wall Area</b>	75.7(3.8)	74.4(3.4)	74.8(3.5)	75.4(3.3)
<b>Wall Area (mm<sup>2</sup>)</b>	17.8(0.9)	17.5(4.5)	17.6(4.5)	17.8(4.6)
<b>Lumen Area (mm<sup>2</sup>)</b>	7.0(2.4)	7.1(2.4)	7.0(2.4)	6.9(2.4)
<b>Total Area (mm<sup>2</sup>)</b>	24.7(6.8)	24.6(6.8)	24.7(6.8)	24.7(6.8)

Data expressed as mean (SEM). Intergroup comparisons: no significant difference (one-way repeated measure ANOVA with Tukey test to compare all pairs of columns) between dimensions of phantom airway model was found.



**Table 3.8: Mean airway measurements of the CTP674 phantom imaged at each EvA centre.**

Centre and Scanner Type	Mean (SEM) airway measurement CTP674 <sup>®</sup> phantom		Significant difference in airway measurements compared to reference scanner (p value)	Regression equations for standardisation (LA and WA)	Error reduction in %WA following standardisation (%)
<b>1</b> GE Brightspeed 16	LA	15.4 (4.1)	0.03	(LA*1.0724)-0.0831	
	WA	23.5 (4.1)	0.01	(WA*0.914)+0.4753	
	%WA	65.5 (5.4)	0.005		69
<b>2 *</b> Siemens Sensation 16	LA	16.4 (4.3)	na	na	
	WA	21.5 (3.7)	na	na	
	%WA	61.7 (5.0)	na		na
<b>3</b> GE Lightspeed VCT 64	LA	14.8 (4.0)	0.02	(LA*1.0602)+0.3644	
	WA	24.5 (4.3)	0.008	(WA*0.9259)-0.4496	
	%WA	67.3 (5.2)	<0.001		77
<b>4</b> Siemens Emotion 16	LA	15.8 (4.1)	0.07	(LA*1.0027)+0.2722	
	WA	22.5 (3.9)	0.003	(WA*0.9816)-0.4388	
	%WA	63.5 (5.0)	0.001		89
<b>5</b> Siemens Sensation 64	LA	16.6 (4.3)	0.55	(LA*0.9429)+0.229	
	WA	20.8 (3.6)	0.008	(WA*1.0128)-0.0892	
	%WA	60.8 (5.1)	0.03		99
<b>6</b> GE Lightspeed VCT 64	LA	15.0 (4.0)	0.01	(LA*1.052)+0.4666	
	WA	24.2 (4.2)	0.005	(WA*0.9298)-0.3498	
	%WA	66.7 (5.3)	<0.001		84
<b>7</b> Siemens Sensation 16	LA	16.2 (4.2)	0.4	(LA*0.9873)+0.063	
	WA	21.6 (3.8)	0.3	(WA*0.9985)-0.2161	
	%WA	62.0 (4.9)	0.2		41
<b>8</b> Siemens Emotion 16	LA	15.8 (4.2)	0.02	(LA*1.0457)-0.1652	
	WA	22.8 (3.9)	0.002	(WA*0.9782)-0.3254	
	%WA	64.2 (5.3)	0.004		52
<b>9</b> Siemens Definition 32	LA	16.8 (4.4)	0.2	(LA*0.9837)-0.2005	
	WA	20.5 (3.6)	0.02	(WA*1.008)+0.1707	
	%WA	60.1 (5.1)	0.1		81
<b>10</b> GE Lightspeed VCT 64	LA	15.2 (4.0)	0.008	(LA*1.0572)+0.3667	
	WA	24.3 (4.3)	0.007	(WA*0.9297)-0.2666	
	%WA	66.2 (5.0)	<0.001		89

\* Airway reference scanner.

*Defenitions of abbreviations:* LA = lumen area, na = not applicable, SEM = standard error of mean, WA = wall area.

**Table 3.9: Imaging protocols used for validation of inter-scanner densitometry standardisation.**

Scanner model	Protocol number	kV	mAs	Slice thickness (mm)	Slice interval (mm)	FOV (mm)	Reconstruction Filter
<b>GE Lightspeed VCT 64</b>	1*	120	40	5.0	2.5	360	Soft
<b>GE Lightspeed 16</b>	2*	120	40	5.0	2.5	360	Soft
	3	120	20	2.5	1.25	360	Soft
	4	120	20	2.5	1.25	360	Standard
	5	120	20	5.0	2.5	360	Soft
	6	120	40	2.5	1.25	360	Soft
	7	120	40	5.0	2.5	500	Standard
	8	120	80	5.0	2.5	360	Soft
	9	120	80	2.5	1.25	450	Soft
	10	120	80	5.0	2.5	450	Soft
<b>Siemens Sensation 16</b>	11*	120	40	5.0	2.5	360	b30f
	12	120	80	3.0	1.5	360	b30f
	13	120	80	1.5	1.5	360	b30f
	14	120	80	3.0	3.0	360	b30f
	15	120	80	5.0	5.0	360	b41f
<b>GE Lightspeed 8</b>	16*	120	40	5.0	2.5	360	Soft
	17	120	40	2.5	1.25	360	Soft
	18	120	40	1.25	1.25	360	Soft
<b>GE Lightspeed 16</b>	19*	120	40	5.0	2.5	360	Soft
	20	120	40	5.0	2.5	360	Soft
	21	120	40	2.5	1.25	360	Soft
<b>Toshiba Aquilion 32</b>	22*	120	40	5.0	2.5	360	FC12
	23	120	80	5.0	2.5	360	FC12
	24	120	80	3.0	1.5	360	FC12
	25	120	80	1.0	0.8	360	FC12

\* indicates the protocol used in each scanner that was closest to the reference imaging series protocol.

*Defenitions of abbreviations:* FOV = field of view, GE = General Electric, kVp = tube voltage, mAs = milliampere-second

**Table 3.10: Inter-software variability in CT airway morphometry**

<b>LAP tubes</b>	<b>Lumen Area (mm<sup>2</sup>)</b>		<b>Wall Area (mm<sup>2</sup>)</b>		<b>% Wall Area</b>	
	<b>EmphylxJ</b>	<b>MedView</b>	<b>EmphylxJ</b>	<b>MedView</b>	<b>EmphylxJ</b>	<b>MedView</b>
<b>2</b>	0.7952439	0.345742	5.115631	8.05582	86.54609	95.88479
<b>3</b>	1.130678	0.568948	5.75582	9.63591	83.58124	94.42474
<b>4</b>	2.928827	1.998990	8.008857	13.0357	73.22260	86.70415
<b>5</b>	3.746401	2.735740	9.275079	14.155	71.22906	83.80331
<b>6</b>	5.721550	4.124580	11.74348	19.0497	67.23997	82.20190
<b>7</b>	10.439060	9.955180	14.8416	18.5129	58.70734	65.03038
<b>8</b>	18.106230	14.676300	24.96263	38.2359	57.95981	72.26292
<b>9</b>	17.598600	13.339900	38.47862	53.0538	68.61720	79.90788
<b>Mean (SEM)</b>	7.6 (2.5)	6.0 (2.1)	14.8 (4.1)	21.7 (5.6)	70.9 (3.6)	82.5 (3.7)

**Table 3.11: Inter-software variability in CT lung densitometry**

	<b>PW2</b>	<b>Pulmo</b>	<b>Mean Difference (PW2 – Pulmo)</b>	<b>Paired t test (p value)</b>
<b>Lung volume (mls)</b>	6279 (366)	6257 (361)	22	0.01
<b>MLD (HU)</b>	-854.9 (9.4)	-864.5 (8.6)	9.6	0.0003
<b>VI-950 (%)</b>	18.5 (3.6)	18.8 (3.6)	-0.3	0.0004
<b>VI-910 (%)</b>	38.4 (4.5)	40.2 (4.5)	-1.8	<0.0001
<b>Perc15 (HU)</b>	-953.7 (7.9)	-954.4 (7.9)	0.7	0.0006

Data expressed as mean (SEM)

*Defenitions of abbreviations:* PW2 = Pulmonary workstation 2 software, Pulmo = Pulmo-CMS software, MLD = mean lung density, HU = Hounsfield Unit, VI = Volex index, Perc15 = percentile 15

### **3.3 STUDY 3: Quantitative Analysis of Airway Remodelling Using High Resolution Computed Tomography Scans in Severe Asthma.**

#### **3.3.1 Abstract**

##### **Background**

Severe asthma is a heterogeneous condition. Airway remodelling is a feature of severe asthma and can be determined by the assessment of HRCT scans. Our aim was to assess whether airway remodelling is restricted to specific phenotypes of severe asthma.

##### **Methods**

A retrospective analysis was performed of HRCT scans from subjects that had attended a single-centre severe asthma clinic between 2003 and 2008. The RB1 bronchus cross-sectional geometry was measured using the FWHM method. The clinical and sputum inflammatory characteristics associated with RB1 geometry were assessed by univariate and multivariate regression analyses. Longitudinal sputum data were available and were described as area under the time curve (AUC). Comparisons were made in RB1 geometry across subjects in 4 sub-groups determined by cluster analysis, between smokers versus non-smokers and subjects with and without persistent airflow obstruction.

## Results

Ninety-nine subjects with severe asthma and 16 healthy controls were recruited. In the subjects with severe asthma the RB1 % WA was increased ( $p=0.009$ ) and LA/BSA was decreased ( $p=0.008$ ) compared to controls, but was not different across the clusters. Airway geometry was not different between smokers and non-smokers and RB1 %WA was increased in those with persistent airflow obstruction. %WA of RB1 in severe asthma was best associated with post-bronchodilator FEV<sub>1</sub>% predicted and sputum neutrophils AUC (Model  $R^2=0.27$ ,  $p=0.001$ ).

## Conclusions

Airway remodelling of proximal airways occurs in severe asthma and is associated with impaired lung function and neutrophilic airway inflammation.

### 3.3.2 Introduction

Asthma, a common complex inflammatory disorder, affects ~5% of adults in the general population, of which approximately 5-10% suffer from severe and/or difficult-to-treat asthma.<sup>10</sup> This severe asthma group is important as these patients suffer severe morbidity and consume a disproportionately high amount of healthcare resources attributed to asthma.<sup>12</sup> Airway remodelling, characterised by changes such as increase in airway smooth muscle mass due to both hyperplastic and hypertrophic changes, mucous gland hyperplasia, thickening of RBM, dysregulated ECM deposition and increased vasculature, is important and considered fundamental to the chronicity of the asthma disease complex.<sup>69</sup> Remodelling of airway structure in asthma has been associated with airflow limitation,<sup>73,537</sup> AHR,<sup>76,77</sup> and eosinophilic inflammation.<sup>33,56,78</sup>

Airway wall changes in severe asthma are common and impossible to predict without imaging.<sup>537</sup> CT has emerged as a repeatable and accurate tool for non-invasive quantitative assessment of proximal airway structural changes in patients with asthma.<sup>72,75,76</sup> Thickening of the RB1 bronchus has been shown to correlate with airflow limitation,<sup>72</sup> AHR<sup>300</sup> in asthma, and air trapping on expiratory CT.<sup>74</sup> In addition to RB1 bronchus, the right lower lobe posterior basal segmental (RB10) bronchus is also oriented perpendicular to the axial CT scanning plane with paucity of surrounding structures and is therefore ideal for quantitative analysis.<sup>538</sup> Remodelling in RB1 bronchus has also been shown to correlate well with non-RB1 proximal airways in severe asthma.<sup>72,76</sup>

The heterogeneity of asthma is highlighted by different phenotypes identified using cluster analysis.<sup>21</sup> Dividing a multi-dimensional disease complex like asthma into distinct

phenotypes may help target treatment more effectively which is exemplified by success of corticosteroid or anti-interleukin-5 (IL-5) treatment [also see Section 3.4]<sup>57,250</sup> in EA and anti-immunoglobulin E treatment<sup>539,540</sup> in allergic asthma to prevent asthma exacerbations. A critical gap in improving our understanding of severe asthma phenotypes is identification of remodelling patterns in various subtypes of severe asthma and the ability to relate airway structure to important clinical outcomes.

We hypothesised that airway remodelling assessed by CT does not differ between severe asthma phenotypes. Our study aims were (1) to compare CT derived dimensions of RB1 between severe asthma phenotypes and (2) to assess whether clinical features relating to patients' demographic profiles, symptoms, pulmonary functions or airway inflammation are associated with geometry of RB1 bronchus.

### **3.3.3 Methods**

#### **3.3.3.1 Subjects**

We performed a single centre retrospective cross-sectional study based upon the DAC at Glenfield hospital, Leicester, UK. Out of 364 patients attending DAC between April 2003 and April 2008, 173 had HRCT scans and were considered for inclusion in the study. Six severe asthma patients, who had moved out of the area, could not be contacted for consent and were excluded. RB1 bronchus could not be quantitatively analysed in sixty-eight severe asthma patients, who were also excluded. Subjects attending the DAC undergo an extensive re-evaluation, as part of their routine clinical care including an extensive history, skin prick tests for common aeroallergens, spirometry, methacholine challenge tests, sputum



induction<sup>51</sup> and asthma control questionnaire.<sup>461</sup> Clinical methods are described in [Section 2.1]. Longitudinal sputum data were available in 91% of subjects (>2 sputum samples over period of at least 3 months; median [IQR] number of samples, 5 [3 – 9] and duration, 22 [11 – 38] months) and were described as area under the time curve expressed as the differential cell count/unit of time (AUC %). The diagnosis of asthma is confirmed by a respiratory physician based on history and one or more of the following objective criteria (maximum diurnal PEF variability >20% over a 2 week period, significant bronchodilator reversibility defined as an increase in FEV<sub>1</sub> of >200mls post bronchodilator or a PC<sub>20</sub>MCh of <8mg/ml). Severe asthma was defined in accordance with the ATS workshop on refractory asthma.<sup>9</sup> The non-asthmatic control subjects (n=16) were non-smokers (never smokers or ex-smokers with smoking history <10 pack years) with normal spirometry. Consent for analysis of previously collected, clinical and CT data was obtained from all patients and control subjects. The consent was obtained by, either one of the respiratory physicians in difficult asthma clinic or myself. None of the patients declined to consent for retrospective analysis of their clinical and CT data as part of this study. The study was approved by the Leicestershire, Northamptonshire and Rutland Research Ethics Committee.

### **3.3.3.2 HRCT scanning protocol and quantitative airway morphometry**

HRCT scanning protocol is described in [Section 2.3.1.1]. Two-dimensional quantitative analysis of proximal airway geometry was performed using semi-automated software, EmphyxJ, delineated in [Section 2.3.2.2]. Dimensions of RB1 bronchus were used for the purpose of this study. Quantitative airway morphometry on HRCT scans was validated by evaluating inter-observer variability in assessment of RB1 dimensions and determination of

RB1 variability across its length. To further validate findings from RB1 we also assessed the right B10 (RB10) bronchus.

#### **3.3.3.2.1 Assessment of inter-observer variability of right apical segmental bronchus (RB1) dimensions**

Inter-observer repeatability was assessed for RB1 dimension in subgroup (n=55) of severe asthmatics. Two observers [Dr Sumit Gupta (SG) and Dr Salman Siddiqui (SS)] blinded to the clinical characteristics of the subjects measured RB1 dimensions with EmphylxJ software as described in [Section 2.3.2.2]. RB1 %WA variability between two observers was assessed using Pearson correlation and Bland-Altman plot.

#### **3.3.3.2.2 Variability of RB1 dimensions across its length**

HRCT chest does not capture the RB1 bronchus across its entire length and therefore measurement of RB1 dimensions may take place at varying distance from its origin. We therefore assessed the variability in measurement of RB1 across its length at three different levels in 10 separate severe asthmatics, who as part of another study [Section 3.4] had high resolution, low collimation, limited CT scans to capture the RB1 bronchus. Limited thoracic CT scanning and image reconstruction protocol was as described in [Section 2.3.1.2]. RB1 bronchus on the CT image of each subject was identified, cross sectional geometry was measured, and %WA derived at three different levels across the length of RB1 with EmphylxJ software. Variability in RB1 %WA across its length at three levels was assessed and comparison was made with variability in RB1 %WA between subjects.

### 3.3.3.2.3 Assessment of RB10 bronchus

Amongst the subjects included in the study, 71 severe asthmatics and 11 control subjects had a measurable RB10 bronchus. RB10 dimensions were determined using EmphylyxJ software as described in [Section 2.3.2.2].

### 3.3.3.3 Data analysis

Data analysis was performed in three steps. First, *a priori* analysis was performed in patients with severe asthma dichotomised into clinically relevant groups based on (i) presence or absence of chronic persistent airflow obstruction ( $FEV_1$  of less than 70% of predicted value and  $FEV_1/FVC < 70\%$ ),<sup>85</sup> (ii) smoking history (smokers defined as subjects with  $\geq 10$  pack-years smoking history), (iii) gender, and (iv) eosinophilic airway inflammation (NEA was defined as those subjects with asthma that had a sputum eosinophil count of  $\leq 1.9\%$ <sup>60</sup> on at least 2 occasions with no previous evidence of significant eosinophilia  $> 1.9\%$ , EA was defined as those subjects with asthma and a sputum eosinophil count of  $\geq 3\%$ <sup>57</sup> on at least 2 occasions; 30 and 16 patients qualified as EA and NEA respectively). Unbiased phenotyping of subjects with severe asthma was then undertaken using factor and cluster analysis techniques as described previously.<sup>21</sup> Briefly, a two-step cluster analysis methodology was employed using representative variables identified on factor analysis.<sup>21</sup> Number of likely clusters was estimated using hierarchical cluster analysis. This estimate was prespecified in a k-means cluster analysis that was used as the principal clustering technique. Finally, univariate and multiple regression analysis was performed to explore structure and function relationship in severe asthma.

### **3.3.3.4 Statistical analysis**

Statistical analysis was performed using GraphPad Prism version 5.00 for Windows, GraphPad Software, San Diego California USA, [www.graphpad.com](http://www.graphpad.com) and standard multiple regression using SPSS for Windows, Rel. 16.0.1.2008. Chicago: SPSS Inc. Parametric data were expressed as mean (SEM) and non-parametric data were described as median (IQR). Chi-squared tests were used for categorical data analysis. Unpaired t-test was used to compare clinical characteristics and RB1 dimensions of dichotomised severe asthma subjects. Mann Whitney U-test was used to compare sputum characteristics of dichotomised severe asthma subjects. One-way analysis of variance with Tukey correction (clinical characteristics and RB1 dimensions) and Kruskal-Wallis test with Dunn's intergroup comparison (sputum characteristics) was used to compare severe asthma phenotypes determined by cluster analysis. One-way analysis of variance with Tukey correction was used to assess effect of varying mAs on airway phantom dimensions. Two-way analysis of variance was used to assess variability in dimension of RB1 across its length at three levels and between subjects.

Pearson correlation coefficient was used to determine the relationship between RB1 dimensions (LA/BSA, WA/BSA, TA/BSA and %WA) and clinical indices. Relationship between RB1 %WA and clinical indices was further explored using standard multiple regression. A p value of  $<0.05$  was taken as statistically significant.

### **3.3.4 Results**

Patients with severe asthma, measurable RB1 bronchus, and sufficient baseline data to perform cluster analysis as described previously<sup>21</sup> (n=99) were included in the study. Seventy-three of the patients included in this study had also participated in a previous study.<sup>537</sup> Longitudinal sputum data, obtained at scheduled clinic visits, were available in 91% of subjects (>2 sputum samples over period of at least 3 months; median [IQR] number of samples, 5 [3 – 9] and duration, 22 [11 – 38] months) and were described as area under the time curve expressed as the differential cell count/unit of time (AUC %).

#### **3.3.4.1 Assessment of inter-observer variability of RB1 dimensions**

There was excellent agreement between observers for the measurement of % WA of the RB1 bronchus  $r=0.9$ ;  $p<0.0001$  (n=55) [Figure 3.23 (A)]. Bland-Altman plot [Figure 3.23 (B)] shows that the fold-difference between observers was small [bias (95% limits of agreement) = 1.0 (0.85 – 1.12)] and the variability is consistent across the graph without any specific trend.

#### **3.3.4.2 Variability of RB1 dimensions across its length**

On analysis of % WA using two-way ANOVA, there was a significant main effect of subject [ $F(9,18) = 10.5$ ,  $p<0.0001$ ] but non-significant main effect of level of RB1 assessment [ $F(2,18) = 1.4$ ,  $p=0.3$ ]. Between subject difference accounted for 82% of the total variance in %WA as opposed to level of RB1 assessment, which accounted for 2% of the total variance in %WA.

### **3.3.4.3 Severe asthma patients dichotomised into clinically relevant groups.**

In the severe asthma group as a whole we found that mean (SEM) RB1 %WA was significantly greater in subjects with persistent airflow obstruction compared with those without [73.8 (1.5) vs 69.0 (0.7),  $p=0.006$ , Table 3.12]. There was no significant difference in RB1 dimensions between smokers and non-smokers [71.9 (1.5) vs 69.7 (0.8),  $p=0.2$ , Table 3.13]. Women had greater RB1 LA/BSA ( $\text{mm}^2/\text{m}^2$ ) [5.8(0.4) vs 4.8(0.3),  $p=0.05$ ] and RB1 WA/BSA ( $\text{mm}^2/\text{m}^2$ ) [13.0(0.6) vs 11.2(0.5),  $p=0.03$ ] than men, but no significant difference was found in RB1 %WA [Table 3.14]. There was no difference in RB1 %WA between those with EA ( $n=30$ ) versus NEA ( $n=16$ ) [70.5(1.2)% vs 70.6(1.3)%,  $p=0.2$ , Table 3.15].

### **3.3.4.4 Unbiased phenotyping of severe asthma subjects using cluster analysis.**

Clinical characteristics of the four severe asthma phenotypes (groups A-D) determined by cluster analysis and controls are as shown in [Table 3.16]. No significant differences were found between groups with regards to age. The severe asthma phenotypes were similar with regards to FEV<sub>1</sub>% predicted, FEV<sub>1</sub>/FVC ratio and treatment with long-acting beta-agonist and inhaled or oral corticosteroid. Group A represents severe asthmatics with concordant asthma control score and eosinophilic inflammation with significantly greater bronchodilator response. Group B consisted of severe asthmatics who were predominantly females with high body mass index (BMI) and evidence of high asthma control score but

very little eosinophilic airway inflammation. Group C and D both demonstrated discordant asthma control score and eosinophilic inflammation with Group C predominantly having high asthma control score and Group D predominantly having eosinophilic airway inflammation. The clinical characteristics of the 99 subjects in this study were not significantly different to the remaining 74 severe asthmatic subjects that underwent HRCT but were not included (data not shown).

The mean (SEM) LA/BSA ( $\text{mm}^2/\text{m}^2$ ) of RB1 was significantly smaller in all severe asthma phenotypes compared to the control group [Table 3.17, Figure 3.24]. The mean (SEM) RB1 %WA was significantly increased in all severe asthma phenotypes compared to the control group [Table 3.17, Figure 3.25]. There was no difference in WA between phenotypes. RB10 results were akin to that of RB1.

RB10 and RB1 %WA correlated significantly [ $r = 0.6$ ;  $p = 0.001$ ]; [Figure 3.26]. The mean (SEM) LA/BSA ( $\text{mm}^2/\text{m}^2$ ) of RB10 was significantly smaller in Group A [5.8(0.7)  $\text{mm}^2/\text{m}^2$ ], Group B [4.8(0.6)  $\text{mm}^2/\text{m}^2$ ], Group C [6.3(0.5)  $\text{mm}^2/\text{m}^2$ ] and Group D [6.7(0.5)  $\text{mm}^2/\text{m}^2$ ] compared to the control group [9.4(0.5)  $\text{mm}^2/\text{m}^2$ ] ( $p < 0.001$ , ANOVA). RB10 %WA [mean (SEM)] results were similar to RB1, Group A [68.2(2.0)%], Group B [68.9(1.7)%], Group C [66.6(1.5)%], and Group D [66.5(1.0)%] vs. control group [61.7(0.9)%] ( $p = 0.03$ , ANOVA).

### **3.3.4.5 Univariate and multiple regression analysis to explore structure and function relationship in severe asthma**

Univariate analysis of relationship between RB1 dimensions and clinical indices is detailed in [Table 3.18, Figure 3.27 and Figure 3.28]. RB1 %WA correlated significantly with disease duration, post bronchodilator FEV<sub>1</sub> percent predicted, post bronchodilator FEV<sub>1</sub>/FVC, JACQ and sputum neutrophils AUC (%). Standard multiple regression was performed using 'Enter' method between RB1 %WA as the dependent variable and disease duration, post bronchodilator FEV<sub>1</sub>% predicted, sputum neutrophils AUC and Modified JACQ (6 point score without FEV<sub>1</sub>% predicted)<sup>462</sup> as the independent variables, selected based upon the univariate analysis. With the use of a  $p < 0.001$  criterion for Mahalanobis distance no outliers among the cases were found. No multicollinearity or singularity was detected. Normality, linearity, homoscedasticity and independence of residuals was confirmed. [Table 3.19] displays the unstandardised correlation coefficients (B), the standardised correlation coefficient ( $\beta$ ), the semipartial correlations,  $R^2$  and adjusted  $R^2$ .

Post bronchodilator FEV<sub>1</sub> % predicted and sputum neutrophils AUC (%) made statistically significant contribution to the regression model for prediction of RB1 % WA with the former making the strongest unique contribution to explaining the dependent variable as indicated by standardised coefficients.



### 3.3.5 Discussion

We found in severe asthma that the RB1 bronchus, a proximal third generation airway, was remodelled with luminal narrowing and increased %WA. The degree of airway remodelling was similar across clinical phenotypes determined by cluster analysis and was independent of smoking status. Importantly, we confirmed that %WA was associated with lung function impairment and was significantly greater in severe asthmatics with persistent airflow obstruction compared with those without. For the first time we demonstrated that %WA was associated with the burden of neutrophilic airway inflammation over time suggesting that this component of the airway inflammatory profile may be particularly important in the development of airway remodelling.

Airway remodelling is an established feature of asthma, particularly in those with severe disease. Our findings confirm that airway wall thickening and reduced luminal patency are features of severe asthma. This altered geometry in patients with severe asthma compared with healthy controls may be important in determining physiological characteristics such as AHR and airflow obstruction. However, there is increasing recognition that severe asthma is a heterogeneous condition and the relationship between clinical, physiological, and inflammatory features of disease and remodelling is poorly understood.

Whether subjects with airway remodelling represent a distinct asthma phenotype is unknown. Cluster analysis has been applied to determine asthma subgroups.<sup>21,22</sup> Using a combination of factor and cluster analysis Haldar *et al.* have previously reported 4 novel phenotypes in severe asthma.<sup>21</sup> Here we used the same approach to categorise our severe asthmatics into distinct groups. The four groups identified had very similar characteristics

to the report by Haldar and colleagues. Importantly, airway remodelling was a feature of all the 4 groups and there were no between group differences. RB1 luminal narrowing observed in severe asthma subjects may be secondary to airway wall remodelling with encroachment of the airway lumen. Bronchoconstriction may also cause airway luminal narrowing without change in wall area.<sup>299</sup> Despite all severe asthma subjects in our study being on long-acting beta-agonists, bronchoconstriction may partly contribute to the narrowing of the airway lumen observed in these subjects.

In addition to this unbiased approach to phenotyping, we pre-specified criteria to stratify our subjects into those with or without persistent airflow obstruction, smoking status, and presence or absence of a sputum eosinophilia. Those with persistent airflow limitation had the most marked CT evidence of remodelling. Whereas altered airway geometry was independent of smoking status. Our observation that RB1 %WA was associated with the post-bronchodilator FEV<sub>1</sub>% predicted is in keeping with previous reports in asthma<sup>72,75</sup> and COPD.<sup>291,466</sup> In addition, we have previously identified that in asthma the RB1 %WA is associated with AHR.<sup>76</sup> Taken together these findings support the view that the changes in airway geometry are functionally important.

To date there has been a paucity of studies exploring the associations between remodelling assessed by CT and airway inflammation. Sputum analysis provides a non-invasive, safe tool to assess airway inflammation and has been widely applied in the study of severe asthma. Indeed, the identification of eosinophilic airway inflammation in severe asthma has evolved as a powerful diagnostic tool to predict response to corticosteroids<sup>541</sup> and to prevent exacerbations.<sup>57,250</sup> In addition to eosinophilic airway inflammation the existence of a distinct subgroup exhibiting neutrophilic airway inflammation in severe<sup>33,138,542</sup> as well as

mild-to-moderate<sup>36</sup> asthma is well recognised. Both eosinophilic<sup>58,59,543</sup> and neutrophilic<sup>59,63</sup> inflammation has been implicated in the development of persistent airflow obstruction. ten Brinke *et al.*<sup>58</sup> showed that the only independent factor associated with persistent airflow limitation was a differential sputum eosinophilia, whereas Shaw *et al.*<sup>63</sup> and others<sup>59</sup> demonstrated that raised differential sputum eosinophil and neutrophil counts were both associated with a lower pre-bronchodilator FEV<sub>1</sub>. In addition Shaw *et al.* demonstrated that the sputum total neutrophil, but not the differential eosinophil count was associated with lower post-bronchodilator FEV<sub>1</sub>. Here we report for the first time that the RB1 %WA was increased in subjects with and without eosinophilic inflammation and is associated with the preceding burden of neutrophilic inflammation over time measured by repeated sputum analysis. Our observation that airway wall thickening in severe asthma can be present in both EA and NEA, but is not related to the degree of airway inflammation measured cross-sectionally is in keeping with other imaging studies in mild-moderate disease. Little *et al.* failed to find an association between airway wall geometry and sputum neutrophils or E<sub>NO</sub>.<sup>144</sup> Similarly Niimi *et al.* failed to find an association between sputum eosinophilia or serum ECP and airway wall geometry in two quantitative airway imaging studies.<sup>75,300</sup> Paradoxically low serum ECP levels were associated with a greater degree of wall thickening on CT than those patients that had high ECP levels during exacerbations in one study.<sup>544</sup> However, in contrast De Blic *et al.* demonstrated in a childhood asthma cohort that bronchoalveolar lavage ECP levels were related to airway wall thickening in asthma.<sup>146</sup> No correlation was found between intraepithelial neutrophils or eosinophils and airway wall thickness. These studies have been cross-sectional in design and have not captured the temporal relationship between inflammation and remodelling. Our study findings supporting a role for persistent neutrophilic inflammation in the development of airway

remodelling is in contrast to our recent report [Section 3.4] that the RB1 WA decreased after 1 year of treatment with anti-IL-5 compared to placebo providing strong evidence in favour of the eosinophils playing a key role in airway remodelling determined by CT. One possible explanation for this apparent paradox is that eosinophilic and neutrophilic inflammation may both contribute to airway remodelling, but they may exert different effects upon airway geometry and lung function. In this report the changes in RB1 %WA are largely driven by the luminal narrowing, which may be more closely related to neutrophilic inflammation whereas, in our study of anti-IL-5 [Section 3.4], the WA was decreased without affecting the LA. Importantly, the change in WA in response to anti-IL5 was small, albeit significant, suggesting that additional components of airway inflammation play a role in remodelling. This view is supported by the association of other markers of airway inflammation in sputum such as TGF- $\beta$ <sup>305</sup> or the MMP-9/TIMP-1 ratio<sup>143</sup> and airway wall thickening.

This recognition of the complexity of the interactions of different aspects of the airway inflammation underlying asthma and their temporal course provides an explanation for the apparent discrepancy between some CT studies. Methodological variations or difficulties in measurement of airway dimensions and inability of CT to dissect out various individual components of airway remodeling may also contribute to apparent discrepancy between CT studies. This highlights the need for further prospective interventional and longitudinal studies.

In addition to FEV<sub>1</sub> % predicted and neutrophilic inflammation, our univariate analysis also demonstrated that disease duration was associated with thickening of the airway wall in severe asthma. This is in keeping with previous reports that have shown that vascular

remodelling of the airway wall is related to disease duration<sup>49</sup> and that duration of disease was associated with increased ASM mass and luminal narrowing in patients with fatal asthma.<sup>545</sup> However, this feature together with the univariate association between asthma control and %WA were not found to be independent predictors in the multiple regression model.

Our study has a number of potential limitations. The HRCT scan was part of the clinical assessment of the subjects, was not undertaken in all subjects and in some subjects the CT scan did not adequately capture the RB1 and therefore these subjects were excluded. We are confident that our findings can be extended to those subjects that underwent CT, but were excluded (n= 74) as there were no differences in the clinical characteristics between these groups (data not shown). However, our findings cannot be simply extrapolated to our severe asthma population as a whole as we have previously described that subjects in our Difficult Asthma Clinic that undergo HRCT are older, had longer disease duration, poorer lung function, were treated with higher dose of inhaled corticosteroids and oral corticosteroids, and had increased neutrophilic airway inflammation.<sup>537</sup> There is therefore a need to undertake multi-centre prospective studies that include the full spectrum of severe asthmatics. In addition, we analysed images of the RB1 bronchus from standard HRCT scans and not narrow collimation CT scans, which capture the RB1 bronchus across its entire length. We found that the variability of RB1 dimensions across its length was small and considerably less than the between subject variability. Thus this was unlikely to impact upon our findings. Our analysis was limited to third bronchial generation airways unlike other studies,<sup>150</sup> where differences between asthmatics and control subjects, was only found in airways of higher generations. We and others have established that the measurement of

RB1 is closely associated with the measurement of multiple airways.<sup>72,76</sup> RB10 dimensions were correlated with that of RB1, and more importantly the degree of RB10 remodelling in severe asthmatics and control subjects reflected remodelling changes observed in RB1 bronchus suggesting that despite disease heterogeneity RB1 dimensions serve as a good surrogate for airway wall remodelling in this disease cohort as previously described. FWHM technique, used for quantitative assessment in this study, is known to cause errors in airway wall estimation due to CT scanner point spread function. To overcome such problems various techniques<sup>150,287,288</sup> have been developed. Most of the newer software platforms that utilise such techniques are designed to work on volumetric CT scans and not the standard sequential HRCT scans. We used an airway phantom model with gold standard measures obtained using high-precision micro-CT as previously described [Section 3.2] to correct potential size and oblique orientation related errors in quantification of airway dimensions. Moreover we have measured and compared the 3<sup>rd</sup> generation proximal airway in all subjects. We are therefore confident that the potential errors associated with FWHM technique are unlikely to affect our results.

In conclusion we have shown for the first time that airway wall remodelling assessed by CT is associated with neutrophilic inflammation. The degree of airway wall remodelling was also associated with airflow limitation. Longitudinal studies are required in severe asthma to assess the natural history of remodelling, its association with airway inflammation and function and its response to current and novel therapies.

### 3.3.6 Figures and Tables

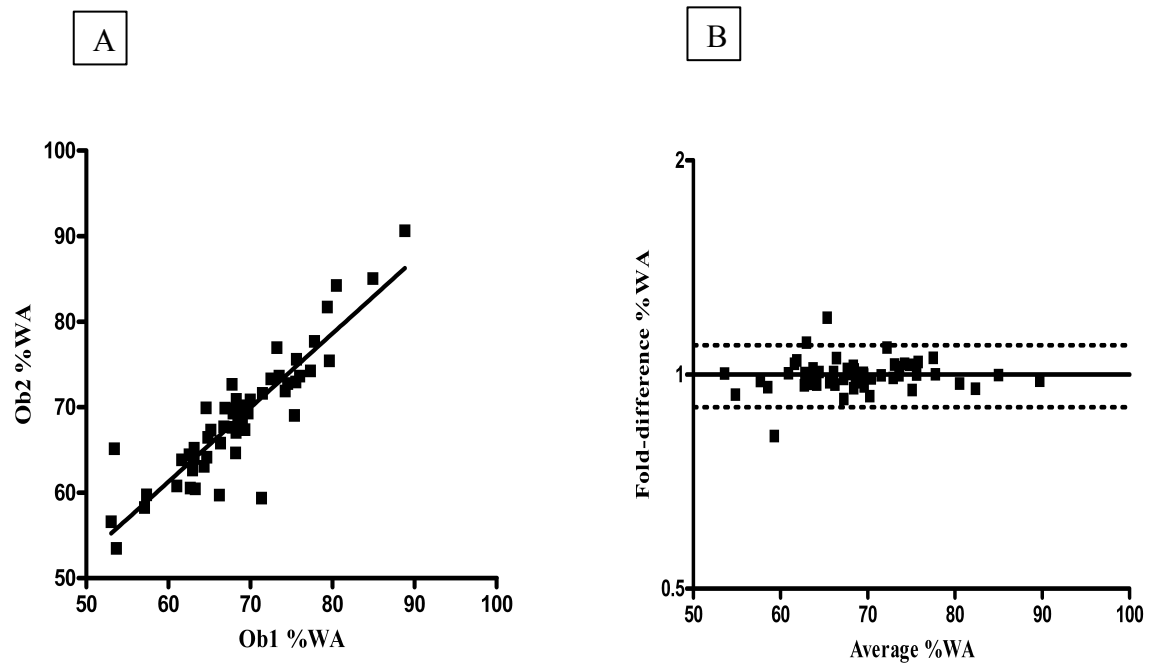


**Figure 3.23: Inter-observer variability of RB1 %WA**

(A) Correlation between RB1 %WA measures by two blinded observers (Ob1: SG, Ob2: SS) in severe asthmatics (n=55,  $r=0.9$ ;  $p<0.0001$ ).

(B) Bland-Altman plot to assess inter-observer variability of RB1 %WA measurement in severe asthmatics (n=55) [fold-difference between observers, bias (95% limits of agreement) = 1.0 (0.85 – 1.12)].

Identity of Observers: SG – Dr Sumit Gupta, SS – Dr Salman Siddiqui

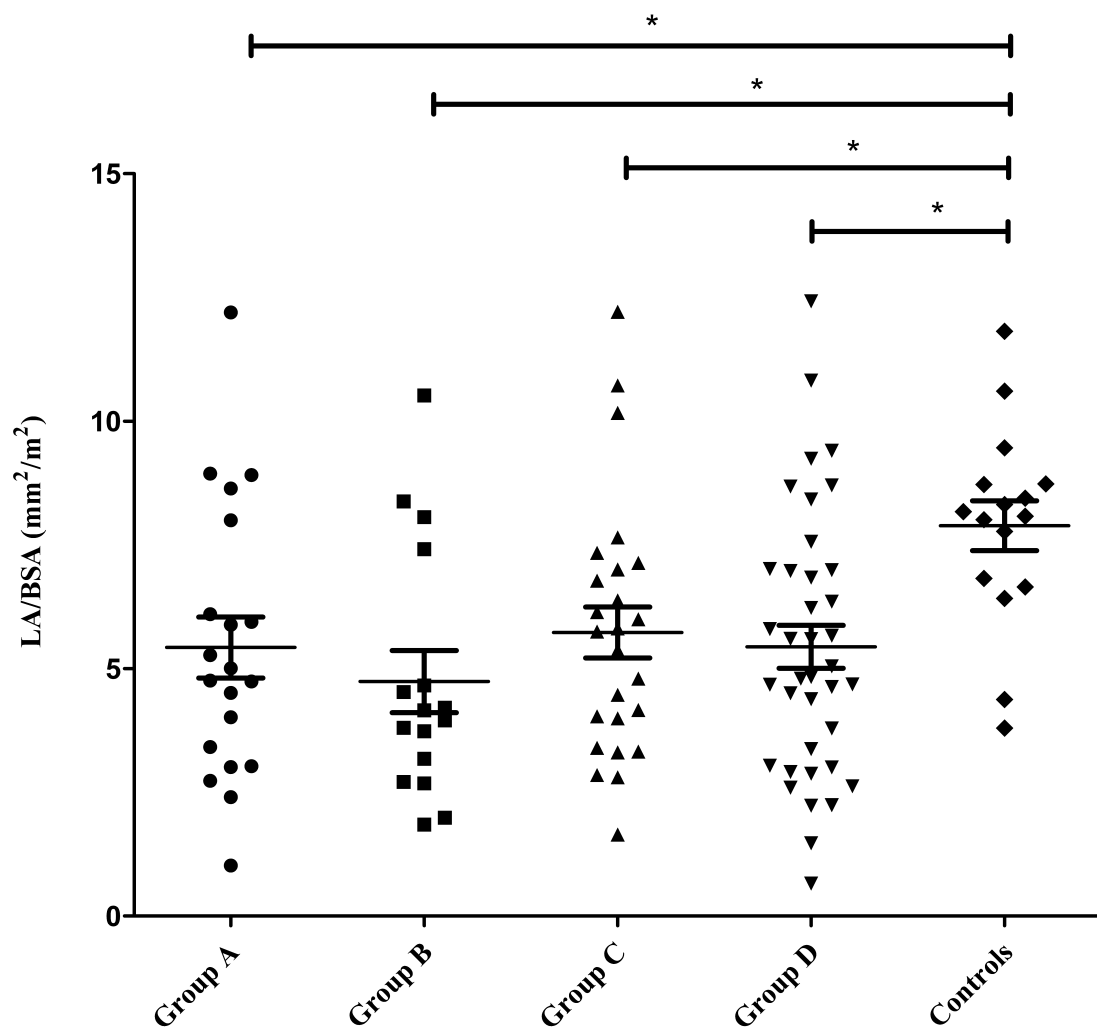


**Figure 3.24: RB1 LA/BSA**

Comparison of RB1 LA/BSA (mm<sup>2</sup>/m<sup>2</sup>) of four severe asthma phenotypes and control subjects (p=0.008, ANOVA).

\* p < 0.05



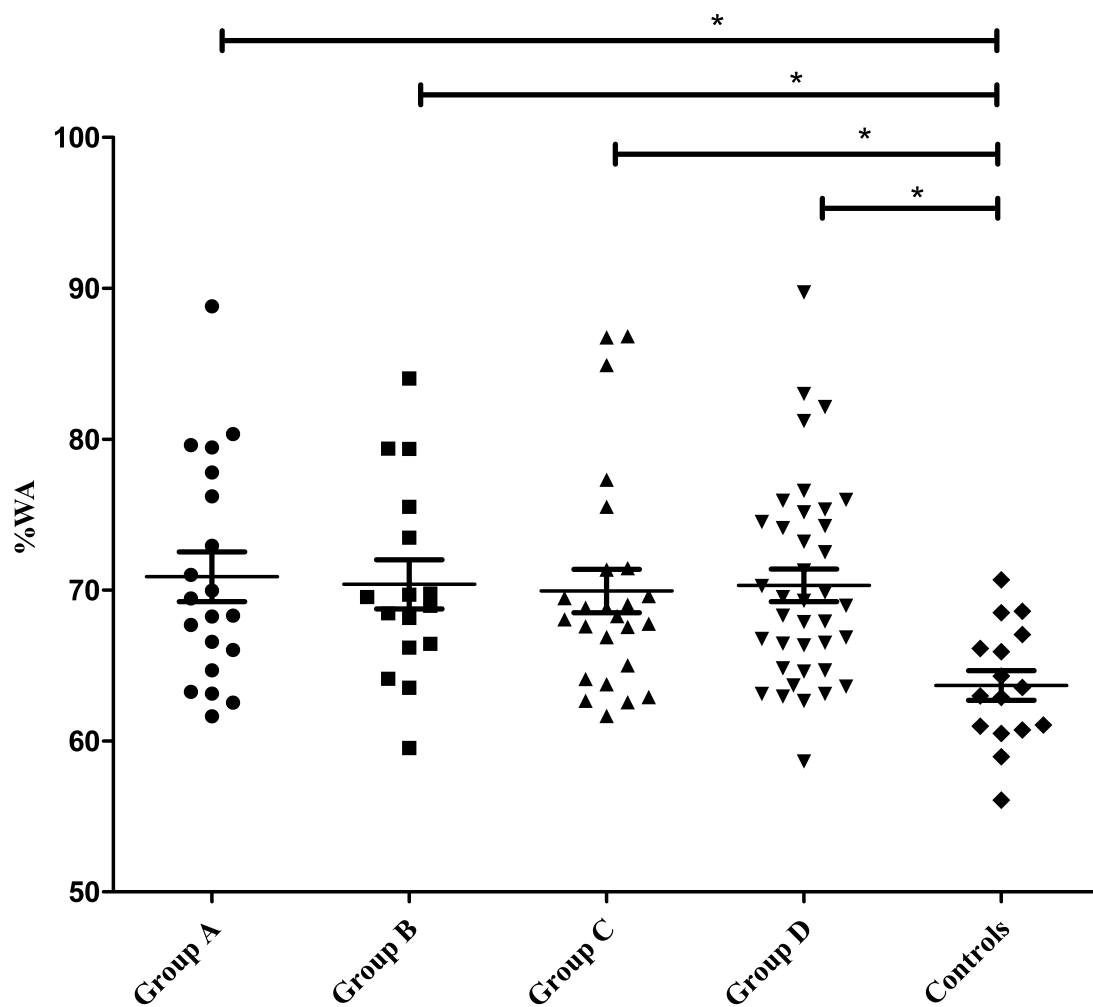


**Figure 3.25: RB1 %WA**

Comparison of RB1 %WA of four severe asthma phenotypes and control subjects (p=0.009, ANOVA).

\* p < 0.05

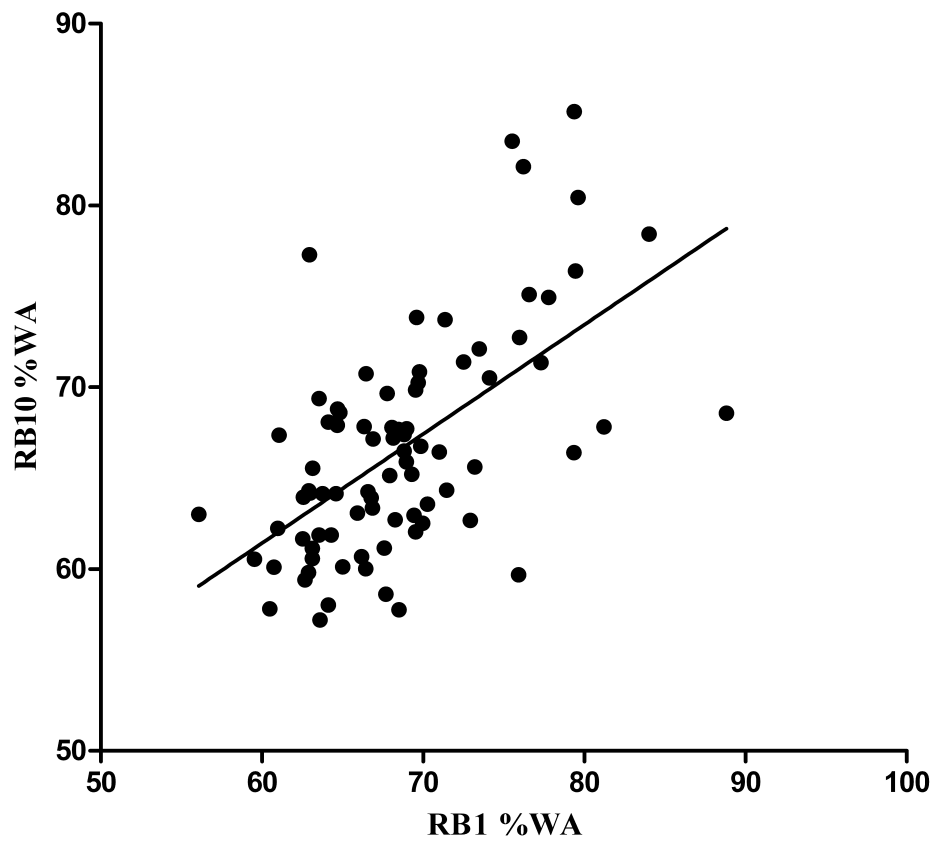


**Figure 3.26: RB1 %WA and RB10 %WA**

Correlation between RB1 %WA and RB10 %WA in severe asthmatics (n=71) and control subjects (n=11) [ $r = 0.6$ ;  $p=0.001$ ].

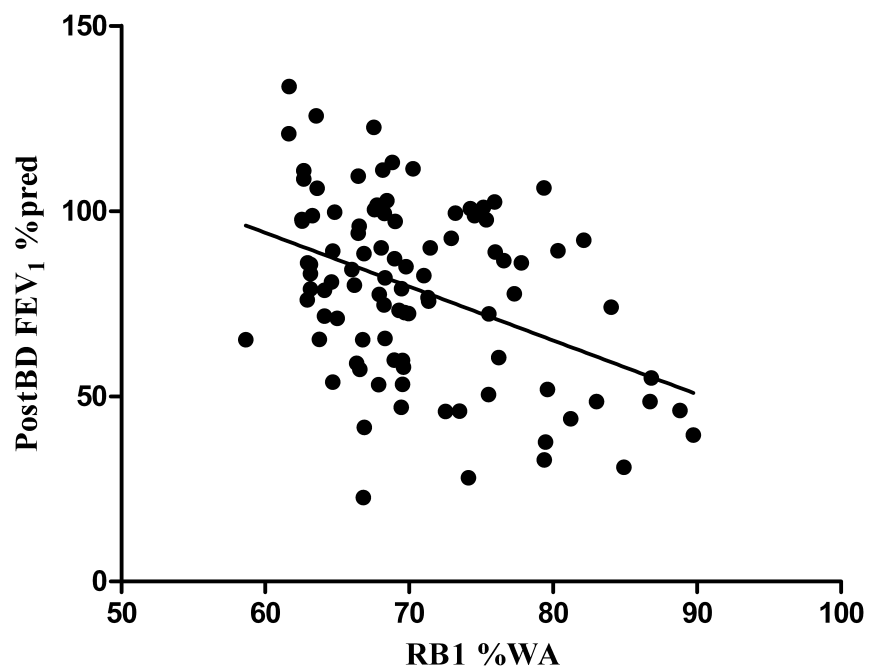


**Figure 3.27: RB1 %WA and post bronchodilator FEV<sub>1</sub> %predicted**

Correlation between RB1 %WA and post bronchodilator FEV<sub>1</sub> %predicted in severe asthmatics ( $r=0.41$ ,  $p<0.0001$ ).

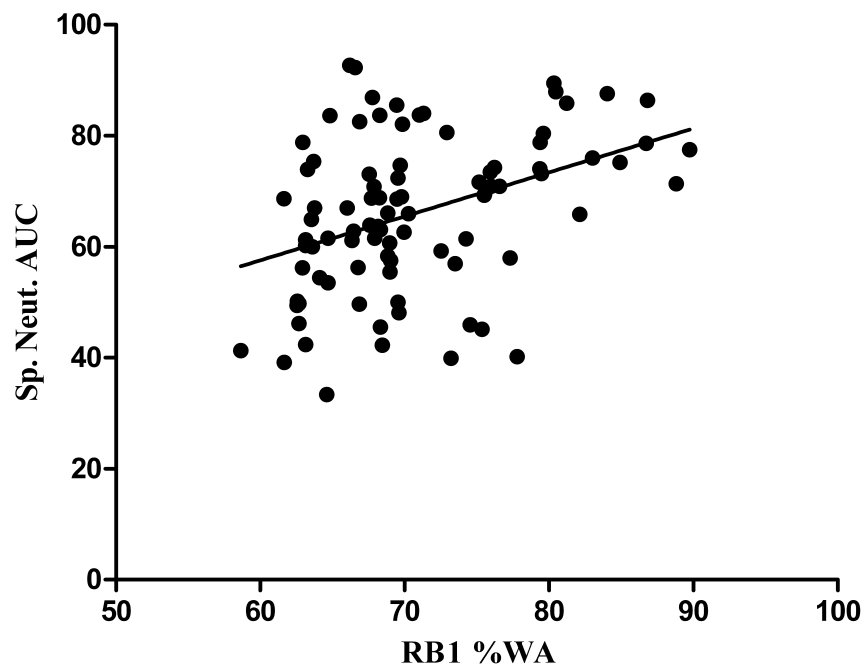


**Figure 3.28: RB1 %WA and sputum neutrophils AUC (%)**

Correlation between RB1 %WA and sputum neutrophils AUC (%) in severe asthmatics ( $r=0.36$ ,  $p<0.005$ ).

**Table 3.12: Severe asthma with or without chronic persistent airflow obstruction**

	<b>Persistent Airflow Obstruction present (n=34)</b>	<b>Persistent Airflow Obstruction absent (n=65)</b>
<b>Age (yrs)</b>	53.7 (1.6)	47.9 (1.9)
<b>Gender M:F</b>	15:19	25:40
<b>Disease Duration (yrs)*</b>	28.6 (2.9)	19.3 (2.1)
<b>Post Bronchodilator FEV<sub>1</sub> % predicted<sup>∞</sup></b>	49.7 (2.1)	92.2 (1.8)
<b>Post Bronchodilator FEV<sub>1</sub>/FVC (%)*</b>	60.4 (2.4)	74.8 (1.1)
<b>Inhaled BDP equivalent/24 hrs (mcg)</b>	1890 (148)	1916 (135)
<b>Oral prednisolone use (% of subjects)</b>	50	40
<b>Oral prednisolone dose (mg)</b>	10.2 (0.9)	9.9 (1.2)
<b>Sputum eosinophils AUC (%) ^</b>	4.1 [2.0 – 15.8]	4.7 [1.1 – 8.7]
<b>Sputum neutrophils AUC (%) ^#</b>	71.9 [59.6 – 78.8]	63.8 [53.4 – 73.2]
<b>RB1 % Wall Area*</b>	73.8 (1.5)	69.0 (0.7)
<b>RB1 Lumen Area/BSA (mm<sup>2</sup>/m<sup>2</sup>)</b>	4.7 (0.5)	5.6 (0.3)

Chronic persistent airflow obstruction defined as post bronchodilator FEV<sub>1</sub> of less than 70% predicted and FEV<sub>1</sub>/FVC <70%. Data expressed as mean (SEM); ^Median [IQR]. Intergroup comparison: parametric data, unpaired t-test, \*p<0.05, <sup>∞</sup>p<0.0001; non-parametric data, Mann Whitney U-test, #p=0.06

BDP equivalents; Fluticasone 2:1, Budesonide 1.25:1, Mometasone 1.25:1, QVAR 2:1, Ciclesonide 2.5:1.

*Definitions of abbreviations:* BDP = beclometasone dipropionate, FEV<sub>1</sub> = forced expiratory volume in 1 second, FVC = forced vital capacity, AUC = area under the time curve, BSA = body surface area.

**Table 3.13: Severe asthma subjects dichotomised based on smoking history**

	<b>Smokers (n=30)</b>	<b>Non-smokers (n=69)</b>
<b>Age (yrs)</b>	51.4 (2.5)	49.4 (1.7)
<b>Gender M:F</b>	16:14	26:43
<b>Disease Duration (yrs)</b>	22.5 (3.7)	23.9 (2.2)
<b>Post Bronchodilator FEV<sub>1</sub> % predicted</b>	73.1 (5.4)	81.9 (2.8)
<b>Post Bronchodilator FEV<sub>1</sub>/FVC (%)*</b>	64.5 (2.9)	71.5 (1.5)
<b>Inhaled BDP equivalent/24 hrs (mcg)</b>	1854 (199)	2004 (122)
<b>Oral prednisolone use (% of subjects)</b>	28	49
<b>Oral prednisolone dose (mg)</b>	11.3 (2.2)	9.7 (0.9)
<b>Sputum eosinophils AUC (%) ^#</b>	2.0 [0.8 – 6.3]	5.3 [1.5 – 14.5]
<b>Sputum neutrophils AUC (%) ^</b>	64.9 [59.3 – 76.3]	66.5 [55.7 – 75.2]
<b>RB1 %Wall Area</b>	71.9 (1.5)	69.7 (0.8)
<b>RB1 Lumen Area/BSA (mm<sup>2</sup>/m<sup>2</sup>)</b>	5.2 (0.6)	5.5 (0.3)

Smokers defined as subjects with  $\geq 10$  pack-years smoking history. Data expressed as mean (SEM); ^Median [IQR]. Intergroup comparison: parametric data, unpaired t-test, \* $p < 0.05$ ; non-parametric data, Mann Whitney U-test, # $p = 0.05$

BDP equivalents; Fluticasone 2:1, Budesonide 1.25:1, Mometasone 1.25:1, QVAR 2:1, Ciclesonide 2.5:1.

*Definitions of abbreviations:* BDP = beclometasone dipropionate, FEV<sub>1</sub> = forced expiratory volume in 1 second, FVC = forced vital capacity, AUC = area under the time curve, BSA = body surface area.

**Table 3.14: Severe asthma subjects dichotomised based on gender**

	<b>Females (n=58)</b>	<b>Males (n=41)</b>
<b>Age (yrs)*</b>	46.5 (1.8)	55.5 (2.0)
<b>Disease Duration (yrs)</b>	20.4 (1.9)	27.8 (3.4)
<b>Post Bronchodilator FEV<sub>1</sub> % predicted</b>	81.4 (3.2)	74.9 (3.8)
<b>Post Bronchodilator FEV<sub>1</sub>/FVC (%)<sup>∞</sup></b>	71.6 (1.6)	66.2 (2.3)
<b>Inhaled BDP equivalent/24 hrs (mcg)</b>	1840 (125)	2106 (168)
<b>Oral prednisolone use (% of subjects)</b>	41	46
<b>Oral prednisolone dose (mg)</b>	10.3 (1.1)	10.0 (1.1)
<b>Sputum eosinophils AUC (%) ^</b>	3.6 [0.8 – 8.1]	5.4 [2.3 – 12.4]
<b>Sputum neutrophils AUC (%) ^</b>	64.9 [57.5 – 74.9]	66.5 [56.8 – 77.8]
<b>RB1 %Wall Area</b>	70.0 (0.8)	71.0 (1.2)
<b>RB1 Wall Area/BSA (mm<sup>2</sup>/m<sup>2</sup>)*</b>	13.0 (0.6)	11.2 (0.5)
<b>RB1 Lumen Area/BSA (mm<sup>2</sup>/m<sup>2</sup>)*</b>	5.8 (0.4)	4.8 (0.3)

Data expressed as mean (SEM); ^Median [IQR]. Intergroup comparison: parametric data, unpaired t-test, \*p<0.05, <sup>∞</sup>p=0.05; non-parametric data, Mann Whitney U-test, #p=0.05 BDP equivalents; Fluticasone 2:1, Budesonide 1.25:1, Mometasone 1.25:1, QVAR 2:1, Ciclesonide 2.5:1.

*Definitions of abbreviations:* BDP = beclometasone dipropionate, FEV<sub>1</sub> = forced expiratory volume in 1 second, FVC = forced vital capacity, AUC =area under the time curve, BSA = body surface area.

**Table 3.15: Eosinophilic and Non-eosinophilic severe asthma**

	<b>Eosinophilic Asthma (n=30)</b>	<b>Non-Eosinophilic Asthma (n=16)</b>
<b>Age (yrs)</b>	49.9 (2.4)	50.1 (5.2)
<b>Gender M:F</b>	15:15	5:11
<b>Disease Duration (yrs)</b>	20.1 (3.2)	31.4 (5.6)
<b>Post Bronchodilator FEV<sub>1</sub> % predicted</b>	81.4 (3.5)	77.8 (7.9)
<b>Post Bronchodilator FEV<sub>1</sub>/FVC (%)</b>	71.7 (1.8)	71.1 (4.0)
<b>Inhaled BDP equivalent/24 hrs (mcg)</b>	1907 (162)	2115 (246)
<b>Oral prednisolone use (% of subjects)</b>	53	44
<b>Oral prednisolone dose (mg)</b>	11.9 (1.4)	9.0 (2.1)
<b>Sputum eosinophils (%) ^#</b>	6.2 [3.0 – 18.1]	0.25 [0.25 – 1.0]
<b>Sputum neutrophils (%) ^</b>	55.9 [32.3 – 86.2]	84.0 [49.5 – 90.8]
<b>Sputum eosinophils AUC (%) ^#</b>	7.9 [4.8 – 19.0]	0.78 [0.28 – 1.5]
<b>Sputum neutrophils AUC (%) ^∞</b>	58.0 [47.7 – 69.8]	74.4 [63.3 – 81.4]
<b>RB1 %Wall Area</b>	70.5 (1.2)	70.6 (1.3)
<b>RB1 Lumen Area/BSA (mm<sup>2</sup>/m<sup>2</sup>)</b>	5.6 (0.5)	6.0 (0.6)

Data expressed as mean (SEM); ^Median [IQR]. Intergroup comparison: parametric data, unpaired t-test, \*p<0.05; non-parametric data, Mann Whitney U-test, #p<0.001, ∞p=0.006. BDP equivalents; Fluticasone 2:1, Budesonide 1.25:1, Mometasone 1.25:1, QVAR 2:1, Ciclesonide 2.5:1.

*Definitions of abbreviations:* BDP = beclometasone dipropionate, FEV<sub>1</sub> = forced expiratory volume in 1 second, FVC = forced vital capacity, AUC =area under the time curve, BSA = body surface area.



**Table 3.16: Clinical characteristics of severe asthma clinical phenotypes and healthy controls**

		<b>Group A (n=20)</b>	<b>Group B (n=16)</b>	<b>Group C (n=25)</b>	<b>Group D (n=38)</b>	<b>Control (n=16)</b>
<b>Clinical Characteristics</b>						
<b>Age (yrs)</b>		52 (3)	43 (3)	51 (3)	51 (2)	54 (4)
<b>Gender M:F</b>		6:14	3:13	11:14	20:18	9:7
<b>BMI (kg/m<sup>2</sup>)</b>		29 (1)	38 (1)*	26 (1)	28 (1)	27 (2)
<b>Age of onset(yrs)</b>		24 (3)	20 (4)	28 (4)	31 (4)	x
<b>Disease duration(yrs)</b>		28 (4)	23 (4)	24 (4)	20 (3)	x
<b>Smoking status (%)</b>	<b>Never</b>	58	56	71	46	56
	<b>Ex</b>	26	38	21	41	44
	<b>Current</b>	16	6	8	13	0
<b>Atopy (%)</b>		45	75	48	71	x
<b>Severe exacerbations/year</b>		3.1 (0.7)	3.6 (0.9)	1.4 (0.5)	2.1 (0.4)	x
<b>JACQ</b>		2.9 (0.2)	2.8 (0.2)	2.6 (0.2)	1.7 (0.1)*	x
<b>Pre Bronchodilator FEV<sub>1</sub> % predicted</b>		64 (5)	75 (6)	75 (6)	76 (4)	x
<b>Pre Bronchodilator FEV<sub>1</sub>/FVC (%)</b>		67 (3)	74 (3)	69 (3)	68 (3)	x
<b>Post Bronchodilator FEV<sub>1</sub> % predicted</b>		74 (5)	81 (7)	81 (5)	80 (4)	106 (4)*
<b>Post Bronchodilator FEV<sub>1</sub>/FVC (%)</b>		66 (3)	77 (2)	70 (3)	70 (2)	78 (2)#
<b>Bronchodilator response (BDR) %</b>		25 (3)*	10 (2)	6 (2)	3 (2)	x
<b>Inhaled CS (%)</b>		100	100	100	100	x
<b>Inhaled CS dose BDP (µg/24hrs)</b>		2066 (220)	1943 (301)	2071 (218)	1761 (145)	x
<b>LABA (%)</b>		100	100	100	100	x
<b>Oral Prednisolone use (% of subjects)</b>		50	36	44	42	x
<b>Oral Prednisolone dose (mg)</b>		12.8 (1.5)	10.8 (2.4)	10.3 (2.0)	8.1 (0.8)	x
<b>Sputum Characteristics</b>						
<b>Eosinophils (%) ^</b>		3.9 [1.8-13.7]	0.3 [0.3-1.3]	0.3 [0.3-0.4]	6.6 [2.7-14.2]**	x
<b>Eosinophils AUC (%) ^</b>		4.7 [3.6-11.7]	0.9 [0.2-1.5]	1.2 [0.3-6.7]	9.4 [1.2-16.1]~	x
<b>Neutrophils (%) ^</b>		77 [48-87]	83 [27-90]	84 [43-93]	56 [30-78]	x
<b>Neutrophils AUC (%)^</b>		71 [60-82]	69 [56-79]	63 [51-81]	61 [50-75]	x

Data expressed as mean (SEM); ^Median [IQR]. Intergroup comparison: parametric data, one-way ANOVA with Tukey test to compare all pairs of columns, \* $p < 0.05$ , # $p < 0.05$  Control vs Group A; non-parametric data, Kruskal-Wallis test with Dunn's multiple comparison test to compare all pairs of columns, \*\* $p < 0.05$ , ~ $p < 0.05$  Group D vs Group B. BDP equivalents; Fluticasone 2:1, Budesonide 1.25:1, Mometasone 1.25:1, QVAR 2:1, Ciclesonide 2.5:1.

*Definitions of abbreviations:* BDP = beclometasone dipropionate, BMI = body mass index, JACQ = Juniper Asthma Control Questionnaire Score, FEV<sub>1</sub> = forced expiratory volume in 1 second, FVC = forced vital capacity, CS = corticosteroid, LABA = long acting beta agonist, AUC = area under the time curve.

**Table 3.17: RB1 dimensions**

	<b>Group A (n=20)</b>	<b>Group B (n=16)</b>	<b>Group C (n=25)</b>	<b>Group D (n=38)</b>	<b>Controls (n=16)</b>	<b>p value</b>
<b>%Wall Area</b>	70.9(1.6)	70.4(1.6)	69.9(1.4)	70.3(1.1)	63.7(1.0)	<b>0.009</b>
<b>Wall Area/BSA (mm<sup>2</sup>/m<sup>2</sup>)</b>	12.5(0.9)	11.1(1.3)	13.1(0.8)	12.1(0.6)	13.9(1.1)	0.35
<b>Lumen Area/BSA (mm<sup>2</sup>/m<sup>2</sup>)</b>	5.4(0.6)	4.7(0.6)	5.7(0.5)	5.4(0.4)	7.9(0.5)	<b>0.008</b>
<b>Total Area/BSA (mm<sup>2</sup>/m<sup>2</sup>)</b>	17.9(1.4)	15.9(1.8)	18.8(1.2)	17.5(1.0)	21.8(1.5)	0.10

Data expressed as mean (SEM). Intergroup comparisons: one-way ANOVA with Tukey test to compare all pairs of columns.

Definitions of abbreviations: BSA = Body Surface Area.

**Table 3.18: Univariate analysis of relationship between RB1 dimensions and clinical indices.**

	<b>LA/BSA (mm<sup>2</sup>/m<sup>2</sup>)</b>	<b>WA/BSA (mm<sup>2</sup>/m<sup>2</sup>)</b>	<b>TA/BSA (mm<sup>2</sup>/m<sup>2</sup>)</b>	<b>%WA</b>
<b>Disease duration(yrs)</b>	<b>-0.16</b>	<b>-0.003</b>	<b>-0.08</b>	<b>0.21*</b>
<b>Post Bronchodilator FEV<sub>1</sub> % predicted</b>	<b>0.24*</b>	<b>-0.006</b>	<b>0.09</b>	<b>-0.41Ω</b>
<b>Post Bronchodilator FEV<sub>1</sub>/FVC (%)</b>	<b>0.22*</b>	<b>0.17</b>	<b>0.20*</b>	<b>-0.23*</b>
<b>JACQ</b>	<b>-0.03</b>	<b>0.12</b>	<b>0.07</b>	<b>0.23*</b>
<b>Sp. Eosinophils (%)</b>	<b>0.10</b>	<b>0.01</b>	<b>0.05</b>	<b>-0.08</b>
<b>Sp. Eosinophils AUC (%)</b>	<b>0.16</b>	<b>0.02</b>	<b>0.08</b>	<b>-0.16</b>
<b>Sp. Neutrophils (%)</b>	<b>-0.09</b>	<b>0.04</b>	<b>-0.01</b>	<b>0.12</b>
<b>Sp. Neutrophils AUC (%)</b>	<b>-0.31*</b>	<b>-0.08</b>	<b>-0.18</b>	<b>0.36#</b>

Data expressed as pearson correlation coefficient, \*p<0.05, #p<0.005, Ωp<0.001

*Definitions of abbreviations:* BSA = body surface area, LA = lumen area, WA = wall area, JACQ = Juniper Asthma Control Questionnaire score, FEV<sub>1</sub> = forced expiratory volume in 1 second, FVC = forced vital capacity, AUC =area under the curve per unit time.

**Table 3.19: Standard Multiple Regression**

Dependent variable – RB1 %WA (n=91)					
Independent variables	Unstandardised Coefficients B(SE)	95% CI	Standardised Coefficients Beta	Semipartial Correlations	Sig.
Post Bronchodilator FEV <sub>1</sub> % predicted	-0.09(0.03)	-0.16 to -0.02	-0.32	-0.28	0.008
Sp. Neutrophils AUC (%)	0.12(0.05)	0.01 to 0.22	0.26	0.28	0.03
Disease duration(yrs)	0.02(0.04)	-0.07 to 0.10	0.05	0.04	0.70
Modified JACQ	0.55(0.69)	-0.82 to 1.92	0.09	0.09	0.42
Model R <sup>2</sup> = 0.27*, Adjusted R <sup>2</sup> = 0.23, R = 0.52, p = 0.001  *Unique variance = 0.16; shared variance = 0.11  Model equation: RB1 %WA = 66.02 – 0.09(Post Bronchodilator FEV <sub>1</sub> %predicted) + 0.12 (Sp. Neutrophils AUC[%])					

Standard multiple regression using enter method.

*Definitions of abbreviations:* WA = wall area, JACQ = Juniper Asthma Control Questionnaire Score, FEV<sub>1</sub> = forced expiratory volume in 1 second, FVC = forced vital capacity, AUC = area under the curve per unit time, SE = standard error.

## **3.4 STUDY 4: Mepolizumab (Anti-IL-5) and Exacerbations of Refractory Eosinophilic Asthma**

### **3.4.1 Abstract**

#### **Background**

Exacerbations of asthma are associated with substantial morbidity and mortality and with considerable use of healthcare resources. Preventing exacerbations remains an important goal of therapy. There is evidence that eosinophilic inflammation of the airway is associated with risk of exacerbations.

#### **Methods**

We conducted a randomised, double blind, placebo-controlled, parallel-group study of sixty-one subjects who had refractory eosinophilic asthma and a history of recurrent severe exacerbations. Subjects received infusions of either mepolizumab, an anti-interleukin-5 monoclonal antibody (29 subjects) or placebo (n=32) at monthly intervals for one year. The primary outcome measure was number of severe exacerbations per subject during the 50-week treatment phase. Secondary outcomes included a change in asthma symptoms, scores on the Asthma Quality of Life Questionnaire (AQLQ, in which scores range from 1 to 7, with lower values indicating more severe impairment and a change of 0.5 unit considered to be clinically important), FEV<sub>1</sub> after use of a bronchodilator, AHR, eosinophil counts in the blood and sputum, and CT assessed airway dimensions.

## Results

Mepolizumab was associated with significantly fewer severe exacerbations than placebo over the 50 weeks (2.0 vs 3.4 mean exacerbations per subject; relative risk 0.57, 95% confidence interval [CI] 0.32 – 0.92;  $p=0.02$ ), a significant improvement in the score on the AQLQ (mean increase from baseline, 0.55 vs 0.19; mean difference between groups, 0.35; 95% CI, 0.08 – 0.62;  $p=0.02$ ) and a significant between-group difference in the change from baseline for airway WA (mean between-group difference, 1.1 mm<sup>2</sup> per square meter of BSA; 95% CI, 0.2 – 2.1;  $p=0.02$ ). Mepolizumab significantly lowered eosinophil counts in blood ( $p<0.001$ ) and sputum ( $p=0.002$ ). There were no significant differences between the groups with respect to symptoms, FEV<sub>1</sub> after bronchodilator use, or airway hyperresponsiveness. The only serious adverse effects reported were hospitalisations for acute severe asthma.

## Conclusions

Mepolizumab therapy reduces exacerbations, improves AQLQ and modulates CT assessed airway remodelling in patients with refractory eosinophilic asthma. The results of our study suggest that eosinophils have a role as important effector cells in the pathogenesis of severe exacerbations of asthma in this patient population.

### 3.4.2 Introduction

Asthma is a complex chronic inflammatory disorder of the bronchial tree that presents clinically with variable symptoms of cough, breathlessness and wheeze, punctuated by periods of more severe and sustained deterioration in control requiring emergency treatment, termed exacerbations. Exacerbations are associated with significant morbidity, mortality and health care costs.<sup>5</sup>

Exacerbations differ from day-to-day symptoms in that they respond poorly to usual inhaled therapy and are more closely linked to increased airway inflammation.<sup>244</sup> The link to eosinophilic airway inflammation may be particularly important, since infiltration of the airway mucosa with activated eosinophils is seen in post-mortem examinations of patients who have died of acute severe asthma,<sup>246</sup> and markers of eosinophilic airway inflammation increase well before the onset of exacerbations induced by withdrawal of corticosteroid treatment.<sup>546,547</sup> Moreover, management strategies that control eosinophilic airway inflammation as well as the clinical manifestations of asthma are associated with a reduction in exacerbation frequency.<sup>57,250</sup>

A study of asthma therapy involving, mepolizumab, a humanised monoclonal antibody against IL-5, offers the prospect of clarifying the role of eosinophils in exacerbations, since mepolizumab is a selective and effective inhibitor of eosinophilic inflammation.<sup>190,191,548,549</sup> Results of clinical trials of this agent among persons with asthma has been disappointing,<sup>548,549</sup> although these studies have focused on outcome measures that are not closely associated with eosinophilic airway inflammation and have included populations



selected on the basis of clinical and physiological characteristics rather than the presence of eosinophilic airway inflammation.<sup>550</sup>

We hypothesised that specific inhibition of eosinophilic inflammation will not reduce asthma exacerbations in refractory eosinophilic asthma patients and will not modulate the airway remodelling as assessed by computed tomography. We tested the hypothesis by studying the effect of treatment with mepolizumab for 12 months on frequency of exacerbation and airway structure as assessed with the use of CT among subjects who had refractory asthma and evidence of eosinophilic airway inflammation despite treatment with high doses of corticosteroids. Secondary aims included assessments of the effects of treatment on airway inflammation, asthma symptoms, asthma related quality of life, FEV<sub>1</sub> and, since chronic eosinophilic airway inflammation may be associated with airway remodeling.<sup>190</sup>

### **3.4.3 Methods**

#### **3.4.3.1 Subjects**

All subjects were older than 18 years of age and had a clinical diagnosis of asthma supported by one or more of the following criteria: variability in the maximum diurnal PEF of more than 20% over the course of 14 days, an increase in FEV<sub>1</sub> of more than 15% after inhalation of 200 µg salbutamol, and a PC<sub>20</sub>MCh of less than 8 mg/ml. Subjects were recruited among patients attending a Refractory Asthma Clinic, that provided secondary asthma care for a mixed urban and rural population of 1 million people and tertiary care for 4 million people. Patients who attend this clinic undergo a standardised assessment, which

includes non-invasive assessment of airway inflammation every 2 to 4 months by means of an analysis of induced-sputum specimens. Inclusion criteria were a diagnosis of refractory asthma according to ATS criteria,<sup>9</sup> a sputum eosinophil percentage of more than 3% on at least one occasion in the previous two years despite high dose corticosteroid treatment, and at least two exacerbations requiring rescue prednisolone treatment in the previous twelve months. Additional criteria for inclusion were stable treatment requirements and an absence of exacerbation for more than 6 weeks before enrolment in the study. Exclusion criteria were current smoking, serological evidence of parasitic infection, a serious co-existing illness, the possibility of conception, and poor adherence to treatment.

All subjects provided written informed consent. The study protocol was approved by the local research ethics committee and the United Kingdom Medicines and Healthcare Products Regulatory Agency.

### **3.4.3.2 Design of the study**

The study was a single-centre, randomized, double-blind, placebo-controlled, parallel-group clinical trial conducted from April 2006 through August 2008. The study measurements are described in [Section 2] and the protocol is summarised in [Figure 3.29].

At a baseline visit, information on demographic characteristics was collected from all subjects, and spirometry was performed before and after use of bronchodilator. Regular treatment was kept constant from this point until completion of the study. After a two week run-in period, baseline PC<sub>20</sub>MCh was measured; a day later, the FE<sub>NO</sub> was measured, symptoms were assessed, and the AQLQ<sup>551</sup> were administered. Symptoms were assessed

with the use of three 100-mm visual analogue score scales – one assessing cough, one assessing breathlessness and one assessing wheeze – each of which had “no symptoms” at one end and the “the worst symptoms ever” at the other end, and with the use of the modified JACQ.<sup>462</sup> The minimal clinically important difference of the JACQ and AQLQ is 0.5.<sup>462</sup>

To assess the responsiveness of symptoms, FE<sub>NO</sub>, and FEV<sub>1</sub> to treatment with oral corticosteroids and the way in which the responsiveness was influenced by mepolizumab therapy, subjects were treated with oral prednisolone for 2 weeks at a dose of 0.5 mg per kilogram of body weight per day, with a maximum dose of 40 mg per day at the beginning and end of the study. For the subgroup of participants who consented to have a bronchoscopic examination, the procedure was performed before treatment with prednisolone. At visit 3, after completing the 2-week course of prednisolone and before receiving the first study treatment, subjects underwent a further assessment of symptom scores, measurement of FE<sub>NO</sub>, spirometry before and after bronchodilator use, as well as CT scanning in subgroup of patients (n=52) who provided consent for this examination.

Subjects were randomly assigned with the use of minimisation<sup>552</sup> method to receive twelve infusions of either 750mg of mepolizumab delivered intravenously or matched placebo (150mls 0.9% saline) at monthly intervals between visit 3 and 14. The criteria used for minimization were the frequency of exacerbation in previous 12 months, the baseline eosinophil count in the sputum and the number of subjects taking oral corticosteroids. FE<sub>NO</sub>, spirometry before and after use of bronchodilator, and symptom scores were recorded at each visit; the AQLQ was administered at visits 5, 8, 11 and 14; and PC<sub>20</sub>MCh was measured the day before visits 8 and 14. The treatment phase ended 2 weeks after visit

14 – that is 50 weeks after treatment was started. At this time, bronchoscopy was performed in subjects who consented to the procedure, and all subjects were given an additional 2-week course of oral prednisolone. After the course of oral prednisolone was completed, FE<sub>NO</sub> and symptom scores were assessed, and spirometry and, in the sub-group of patients who provided consent, CT scanning were performed.

Exacerbations events during the treatment phase of the study were managed in accordance with standard clinical guidelines.<sup>553</sup> Subjects who initiated treatment at home did so with guidance from their personalised management plan. In all cases, subjects were instructed to seek medical advice as soon as possible after starting therapy. Oral prednisolone therapy was prescribed at a dose of 0.5 mg/kg/day, with a maximum dose of 40 mg/day. Decisions about whether to use adjunctive therapy such as antibiotics and about the need for hospitalisation were led by the study physician or the subject's general practitioner. For subjects who were assessed by the study team within 72 hours of an exacerbation, assessments included symptom scores, FE<sub>NO</sub>, PEF and spirometry performed before and after use of a bronchodilator. In addition, sputum samples were obtained for cell counts and microbial analysis.

Because of the expected anti-eosinophil effects of mepolizumab, results of FE<sub>NO</sub> measurements, sputum analysis and blood leucocyte differential counts obtained during scheduled and unscheduled visits were not disclosed to investigators. Exacerbations requiring hospitalisation were managed by the admitting clinical team, whose members were unaware of the treatment assignments and of the results of the inflammatory factors.

### **3.4.3.3 Safety Assessment**

Safety was assessed on the basis of laboratory tests, physical examinations, measurement of vital signs before and after infusion, and adverse event reports. Serious adverse events were also reported to GlaxoSmithKline as part of their ongoing collection of data.

### **3.4.3.4 Statistical analysis**

The primary outcome measure of the study was the number of severe asthma exacerbations per subject; exacerbations were defined as periods of deterioration in asthma control in subjects who had been treated with high dose oral prednisolone for at least five days.<sup>462</sup> Exacerbations that occurred in the 50 weeks between completion of the first treatment visit and two weeks after the final treatment visit were included in the analysis. A recurrence in asthma symptoms shortly after completing a course of prednisolone was recorded as a separate exacerbation event if the subject had a prior return to baseline control for a period of at least five days. Secondary outcome measures were changes in the differential blood and percent sputum eosinophil counts, FE<sub>NO</sub>, FEV<sub>1</sub> % predicted after bronchodilator use, PC<sub>20</sub>MCh, AQLQ score, symptom scores; CT assessment of airway geometry, and bronchoscopic assessment of eosinophilic airway inflammation.

All subjects who completed at least one treatment visit were included in an intention-to-treat analysis of the primary outcome. In the case of subjects who withdrew from the study, the adjusted number of exacerbation was calculated with the use of the following equation: recorded number of exacerbations + [(visits remaining / total visits) x mean exacerbation frequency in the study group]. Exacerbation frequency was compared between the study

groups using a negative binomial model and verified with the Mann Whitney U-test, as previously described.<sup>554</sup> In a study of a similar cohort<sup>57</sup> the mean (SD) exacerbation number was 3.2 (2.1) per subject per year. Assuming a mean of two exacerbations per subject per year, we needed to include sixty subjects in order to have 80% power to detect a 50% reduction in exacerbation frequency. Secondary outcome parameters were log transformed where appropriate. Between-group and within-group comparisons were made for mean change between baseline values and the mean or geometric mean of the post-treatment values with the use of unpaired and paired t-tests respectively, for parametric distributions and the Mann Whitney U-test for non-parametric distributions. Proportions were compared with use of Fisher's exact test. Statistical software packages used for various analyses included SPSS version 13, STATA version 7 and Graph Pad Prism version 4.

### **3.4.4 Results**

#### **3.4.4.1 Enrolment and baseline characteristics**

Figure 3.30 shows the number of subjects who were screened, enrolled, and randomly assigned to a study group and who completed the study. Total of 61 of the 63 subjects who were screened started treatment and constituted the modified intention-to-treat population. Thirty-two subjects were randomly assigned to receive placebo. Overall, 94.9% of treatment visits were completed. Subjects who withdrew completed a mean of 4.6 treatment visits (38.3%). Subjects in two groups were well matched for baseline characteristics [Table 3.20].

### **3.4.4.2 Efficacy**

#### **3.4.4.2.1 Frequency of Severe Exacerbations**

The median treatment period was 348 days in the mepolizumab group and 340 days in the placebo group ( $p=0.3$ ). During this period, a total of 57 exacerbations occurred in the group of subjects who were assigned to receive mepolizumab and 109 in the group assigned to receive placebo [Figure 3.31A]. The mean number of severe exacerbations per subject was 2.0 in the mepolizumab group and 3.4 in the placebo group (relative risk 0.57; 95% confidence interval [CI] 0.32 – 0.92;  $p=0.02$ ; [Figure 3.31 A and B]. The difference in exacerbation number remained significant with non-parametric analysis ( $p=0.04$ ). Thirty-one percent of subjects in the mepolizumab group had no exacerbations during the study period, as compared with 16% in the placebo group ( $p=0.23$ ; Figure 3.31 B). The mean duration of prednisolone therapy per exacerbation was similar between the two groups (10.9 days in the mepolizumab group and 11.7 days in the placebo group;  $p=0.31$ ). There were 3 hospital admissions for exacerbations of asthma in the mepolizumab group, as compared with 11 admissions in the placebo group ( $p=0.07$ ). The total number of days in hospital was significantly less in subjects receiving mepolizumab treatment than for those receiving placebo (12 days vs. 48 days;  $p<0.001$ ).

Treatment for an exacerbation was initiated by the subject in 20% of cases, by the primary care physician or by the physician at a hospital other than the study site in 25 % and by the study team on 55%. In 77% of cases in which exacerbations were assessed within 72 hours after the initiation of prednisolone therapy, there were no significant differences between the groups in PEF, FEV<sub>1</sub> before and after bronchodilator use, symptom scores, or rescue

bronchodilator use. Sputum samples were obtained from patients during 61% of the exacerbations. The geometric mean eosinophil percentage in the sputum during an exacerbation was significantly lower in the mepolizumab group than in the placebo group (1.5 % vs. 4.4%), with the values differing by a factor of 2.9 (95% CI, 1.4 – 6.1;  $p=0.005$ ), but the mean total neutrophil count in the sputum did not differ significantly between the two groups (3846 cells per milligram of sputum in the mepolizumab group and 4122 cells per milligram in the placebo group,  $p=0.80$ ). The sputum eosinophil count was  $>3\%$  in 59.3% of the episodes in placebo group and in 35.7% of the episodes of the mepolizumab group ( $p=0.04$ ).

#### **3.4.4.2.2 Inflammatory markers**

Mepolizumab therapy was associated with a significant between-group and within-group reduction in eosinophil counts both blood and sputum [Figure 3.32 A]. The geometric mean of eosinophil counts in blood during the treatment phase, as compared with the baseline value, was reduced by a factor of 6.6 in the mepolizumab group and by a factor of 1.1 in the placebo group, with the changes from baseline differing between the groups by a factor of 6.1 (95% CI, 4.1 – 8.9;  $p<0.001$ ). Sputum induction at 90 % of visits resulted in cytopsin preparations that could be assessed for eosinophil counts. The geometric mean eosinophil count in sputum was reduced by a factor of 7.1 in the mepolizumab group and by a factor of 1.9 in the placebo group, with the changes from baseline differing between the groups by a factor of 3.7 (95% CI, 1.6 – 8.4;  $p=0.002$ ). There was no significant between-group difference in the change in  $FE_{NO}$  ( $p=0.29$ ) or the total neutrophil count in sputum ( $p=0.68$ ) [Figure 3.32 and Table 3.21].



Paired bronchial-biopsy specimens (specimens obtained before and after the study treatment) were available for 14 subjects (of whom 9 were in the mepolizumab group), paired bronchoalveolar-lavage specimens for 11 subjects (8 in the mepolizumab group) and paired bronchial-wash specimens for 10 subjects (7 in the mepolizumab group). Changes in eosinophil counts after infusions of mepolizumab, as compared with changes after placebo infusions, were reduced by a factor of 2.1 (95% CI, 0.6 – 68.1;  $p=0.68$ ) in bronchial-biopsy specimens, by a factor of 8.2 (95% CI, 0.9 – 75.4;  $p=0.06$ ) in bronchoalveolar-lavage specimens, and by a factor of 16 fold (95% CI, 1.8 – 140;  $p=0.02$ ) in bronchial-wash specimens [Table 3.21].

#### **3.4.4.2.3 Other outcomes**

There were no significant differences between the groups in the change from baseline symptom scores, whether they were assessed with the use of visual-analogue scales or JACQ [Figure 3.32 and Table 3.21]. The mean improvement in AQLQ score was 0.55 in the mepolizumab group, as compared with 0.19 in the placebo group (mean difference between the groups, 0.35; 95% CI 0.08 – 0.63;  $p=0.02$ ; Figure 3.32). There were no significant between-group differences in changes from baseline values for FEV<sub>1</sub> after bronchodilator use or PC<sub>20</sub>MCh (Figure 3.32 and Table 3.21).

There were no significant between-group differences in the changes in FEV<sub>1</sub> or symptom scores after prednisolone treatment given at the end of the study period, as compared with prednisolone given at the beginning of the study period [Figure 3.32]. Nine subjects who were assigned to mepolizumab group had more than 0.5 point decrease in JACQ scores after 2-week course of prednisolone that was given before the initiation of mepolizumab

therapy. These subjects had a similar within-group decrease in JACQ scores after the prednisolone treatment that was given at the end of the study (mean reduction, 1.2 points before mepolizumab therapy and 0.9 points afterward; mean difference, -0.3; 95% CI, -1.0 – 0.4;  $p=0.32$ ).

CT scans were obtained before and after the treatment phase of the study in 26 patients in each group. The results of all CT assessments are shown in Figure 3.33 and Table 3.21. There was a significant between-group difference in the change from baseline for airway WA (mean between-group difference, 1.1 mm<sup>2</sup> per square meter of body surface area; 95% CI, 0.2 – 2.1;  $p=0.02$ ) and in change in total area (mean between-group difference 1.5 mm<sup>2</sup> per square meter of BSA; 95% CI, 0.12 – 2.8;  $p=0.03$ ).

At the completion of the study, subjects were asked to guess their treatment assignment. Forty-five percent of subjects were unsure of their treatment assignment, 36% guessed correctly and 19% guessed incorrectly. There was no significant difference between the study groups in the proportions of patients choosing each response ( $p=0.42$ ).

#### **3.4.4.2.4 Safety**

Intravenous mepolizumab had an acceptable adverse event and side effect profile throughout the 12 months of treatment. The only serious adverse events reported were hospitalisations for acute severe asthma [Table 3.22]. No local effects of infusion were observed. One subject was withdrawn from the study after developing a transient maculopapular rash 24 hours after receiving the first infusion of mepolizumab.

### 3.4.5 Discussion

We found that mepolizumab treatment significantly reduced the number of asthma exacerbations that resulted in the prescription of corticosteroid therapy and increased asthma-related quality of life in subjects with refractory eosinophilic asthma and a history of recurrent exacerbations. There was no significant improvement in symptoms or FEV<sub>1</sub>, measures that are commonly used for quantifying asthma control. Treatment effectively lowered eosinophil counts in blood and was well tolerated over the course of the 12-month study period.

Previous studies of mepolizumab in less severe asthma have been too short to evaluate the effect of treatment on exacerbation frequency although the largest study to date, like ours, showed a reduction in severe exacerbations, which approached significance.<sup>549</sup> The lack of effect of mepolizumab on symptoms, FEV<sub>1</sub>, and airway responsiveness in our study is also consistent with the results of previous studies investigating less severe asthma.<sup>190,191,548,549</sup> Treatment had a larger effect on blood and sputum than biopsy eosinophil numbers, findings that are consistent with earlier work,<sup>191</sup> although sputum eosinophilia was present in 36% of exacerbations, despite mepolizumab therapy. Further studies are required to investigate the mechanisms underlying heterogeneity in the biological response to mepolizumab and the relative resistance of eosinophils in tissue to anti-IL-5.

Green *et al.* have previously shown that the main effect of a management strategy that suppresses eosinophilic airway inflammation is a reduction in exacerbation frequency and have suggested a causal link between eosinophilic airway inflammation and

exacerbations.<sup>57</sup> This view is strongly supported by the results of the current study, since mepolizumab is a selective inhibitor of eosinophilic airway inflammation.

Mepolizumab treatment had no effect on asthma symptoms, FE<sub>NO</sub> or lung function although these measures did improve in some subjects with prednisolone treatment, even when the prednisolone was administered after mepolizumab treatment, when eosinophilic airway inflammation was suppressed. This finding suggests that symptoms, FE<sub>NO</sub> and lung function can be dissociated from eosinophilic inflammation and are improved by corticosteroid treatment through another mechanism. Modulation of the interaction between ASM and infiltrating mast cells<sup>45</sup> is a possible explanation for the effect of prednisolone on lung function and symptoms. . The absence of an association between exacerbations and eosinophilic airway inflammation, on one hand, and lung function and day-to-day clinical manifestations of asthma, on the other, has important implications for the way asthma is managed and assessed in patients with refractory asthma. There was a small but statistically significant improvement in asthma quality of life with mepolizumab therapy, perhaps reflecting the value to patients of the prevention of exacerbations.

We found that airway WA and TA, as measured by CT, were reduced in subjects who were treated with mepolizumab as compared with those who were given placebo. The CT scans were obtained after a 2-week course of prednisolone and after administration of bronchodilators, so the findings are unlikely to be confounded by bronchomotor tone and acute airway inflammation. Whether the changes in airway dimensions translate to important long-term clinical effects requires further investigation.

The therapeutic effect that was seen with mepolizumab treatment shows how we can learn more about the pathogenesis of different airway responses with selective inhibitors of inflammation. The patients who were included in this study had refractory eosinophilic asthma despite maximum tolerated therapy, which in many cases included regular oral corticosteroids. Their asthma resembled the exacerbation-prone phenotype of severe asthma described by Moore *et al.*<sup>206</sup> and the phenotype of asthma with predominant eosinophilic inflammation, which Haldar *et al.*<sup>21</sup> have described. Our results should not be extrapolated beyond the highly selected group of patients we recruited for this study. However, further clinical trials should be performed to establish more clearly the risk and benefits of treatment in a wider population of patients. Many patients with fluctuating respiratory symptoms and eosinophilic airway inflammation do not meet current criteria for a diagnosis of asthma,<sup>45,555-557</sup> and it has been previously argued that new ways of classifying airway disease are needed to allow proper evaluation of new therapies.<sup>558</sup> Investigators planning future trials should be mindful of disease characteristics that suggest a response to therapy and select patients with airways disease and eosinophilic airway inflammation rather than those that meet arbitrary physiological criteria.

### 3.4.6 Figures and Tables

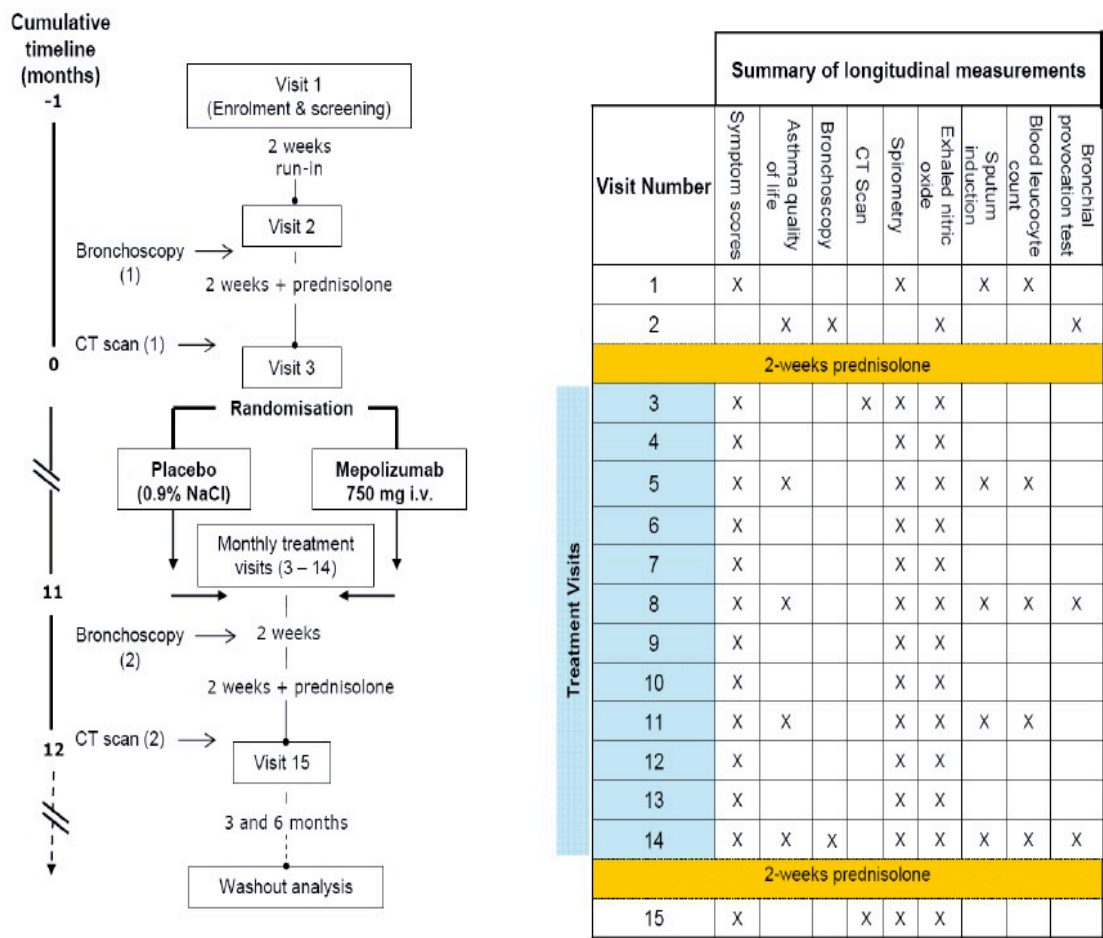


**Figure 3.29: Design of the study**

Study design and summary of the measurements performed at each study visit

Bronchial provocation testing was performed a day before visits 2, 8 and 14.

Limited thoracic CT scans were performed very soon after the scheduled two-week prednisolone trials.

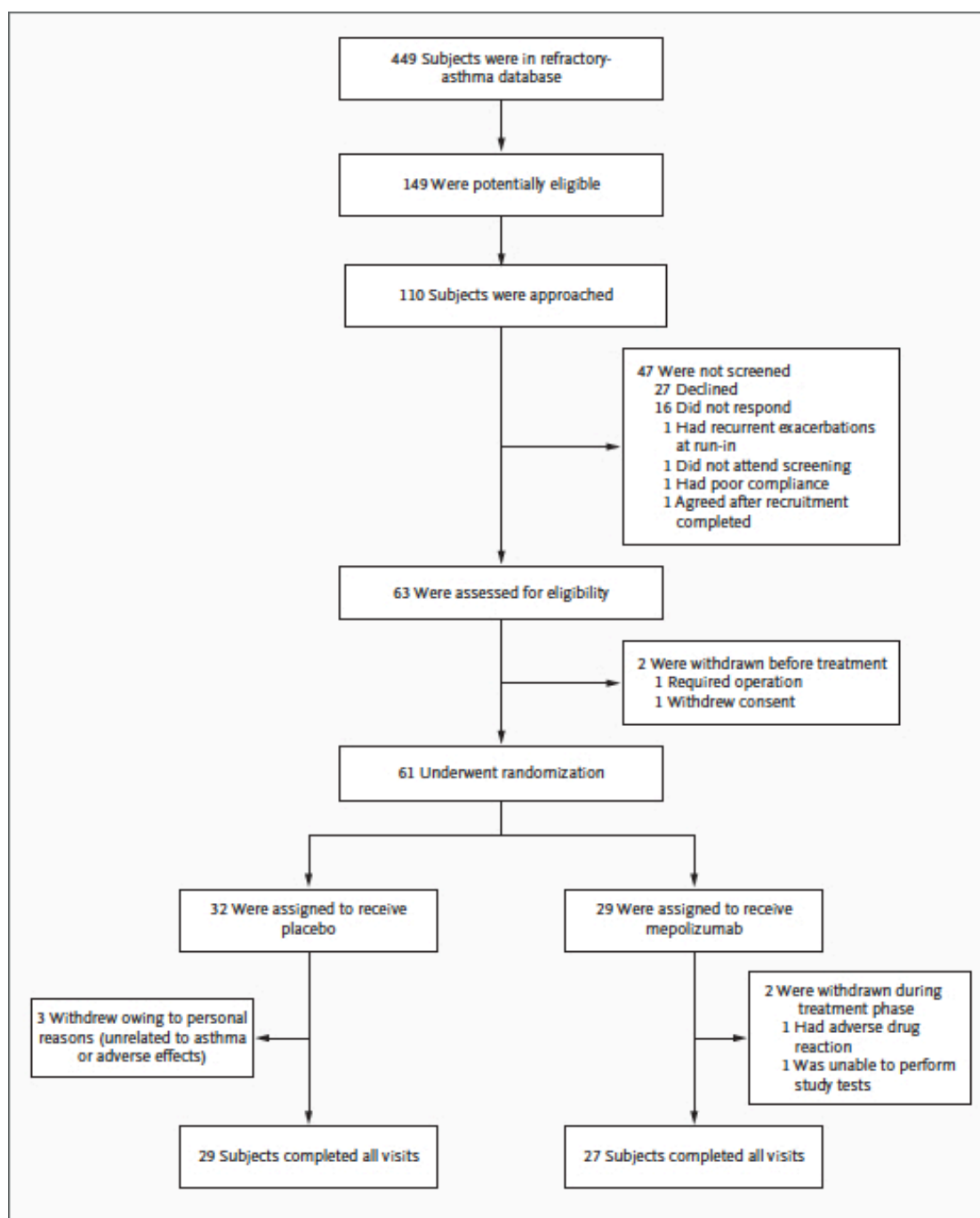


**Figure 3.30: Screening, enrolment and randomisation of study subjects**

Paired limited CT scans were performed in 52 subjects (n=26, placebo arm; n=26, mepolizumab arm).

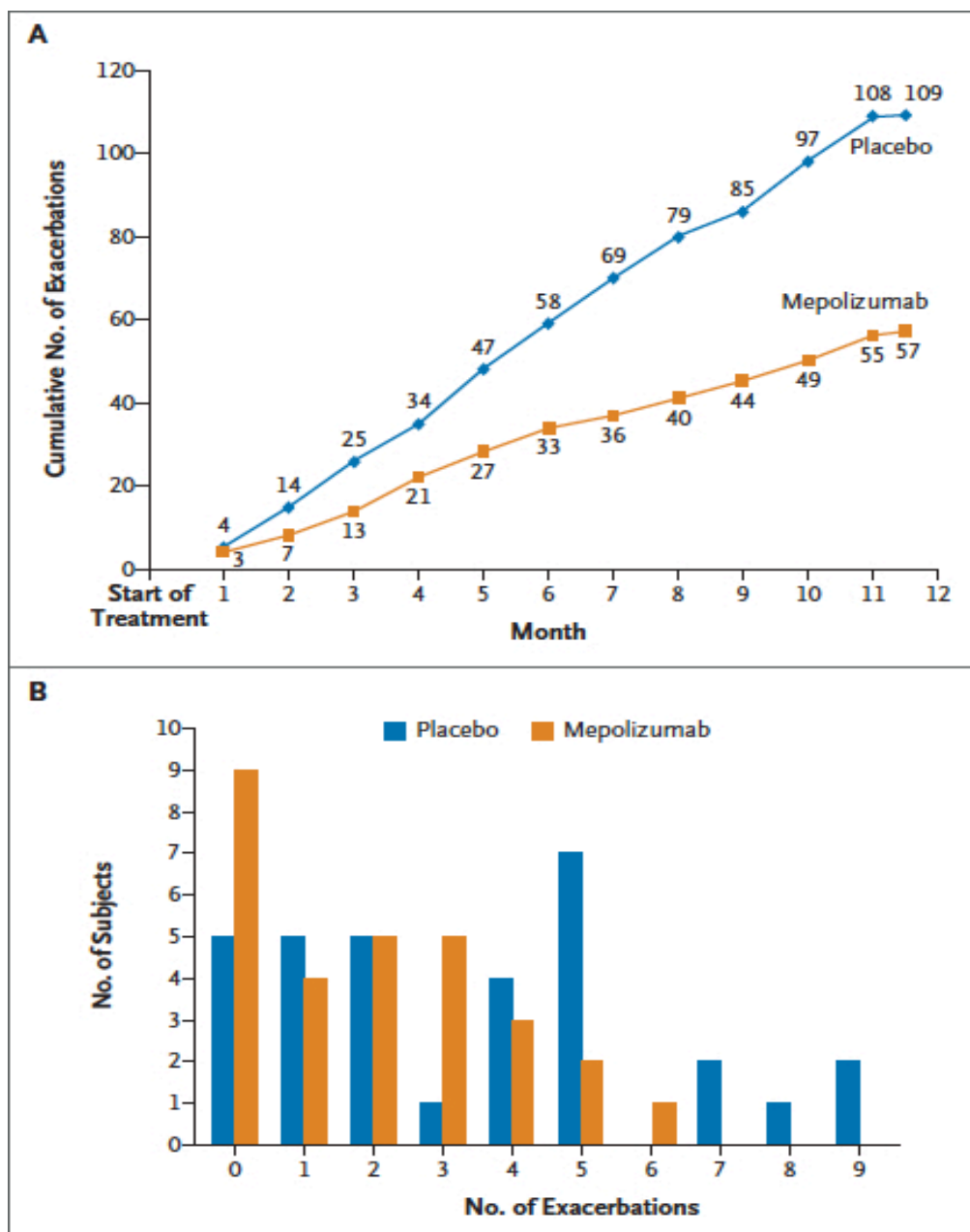


**Figure 3.31: Severe Exacerbations during the course of the study**

(A) Cumulative number of severe exacerbations that occurred in each study group over the course of 50 weeks.

(B) Distribution of the number of exacerbations among subjects in each study group during the treatment period of the study.



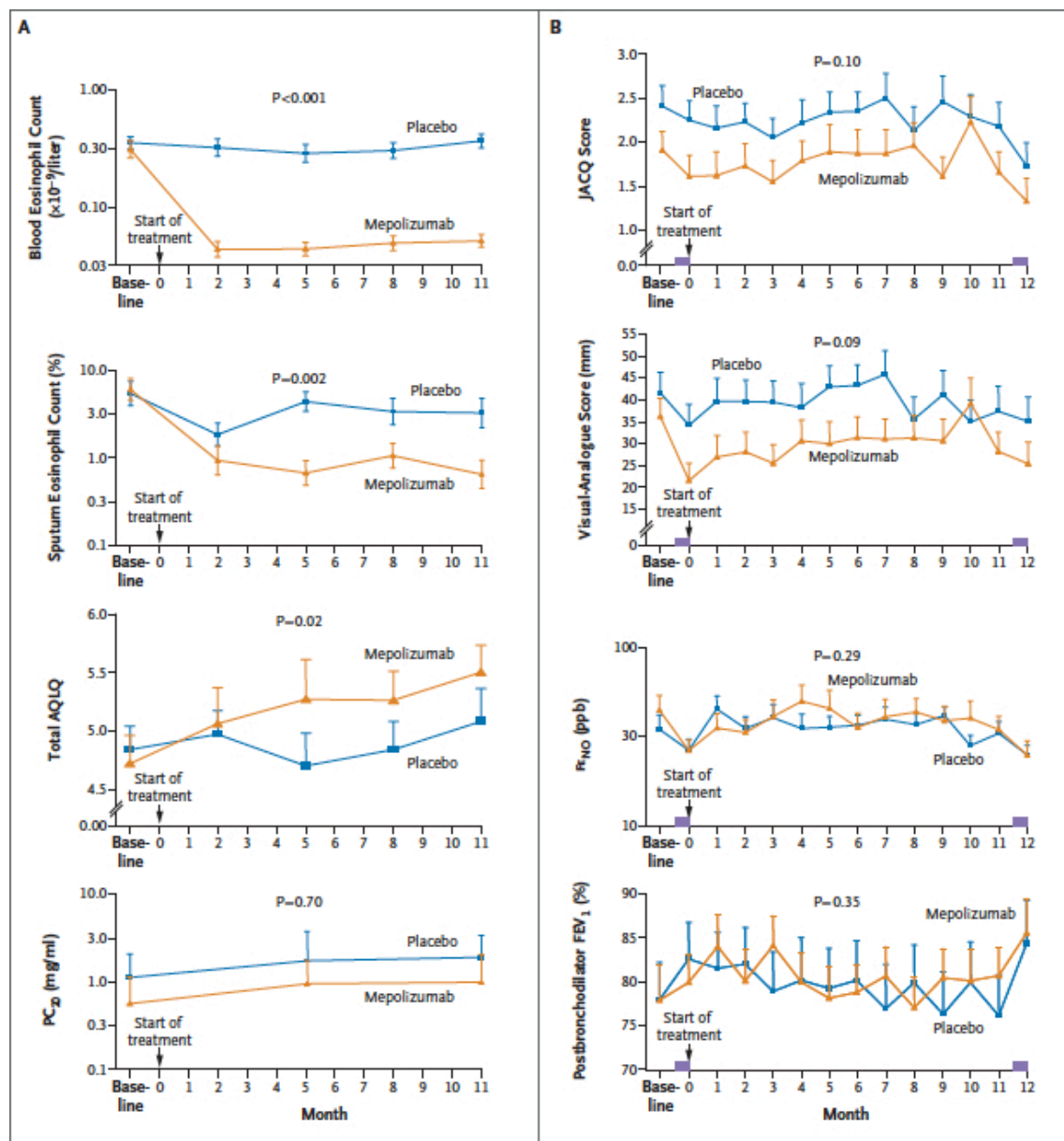


**Figure 3.32: Comparison of study outcomes between study groups**

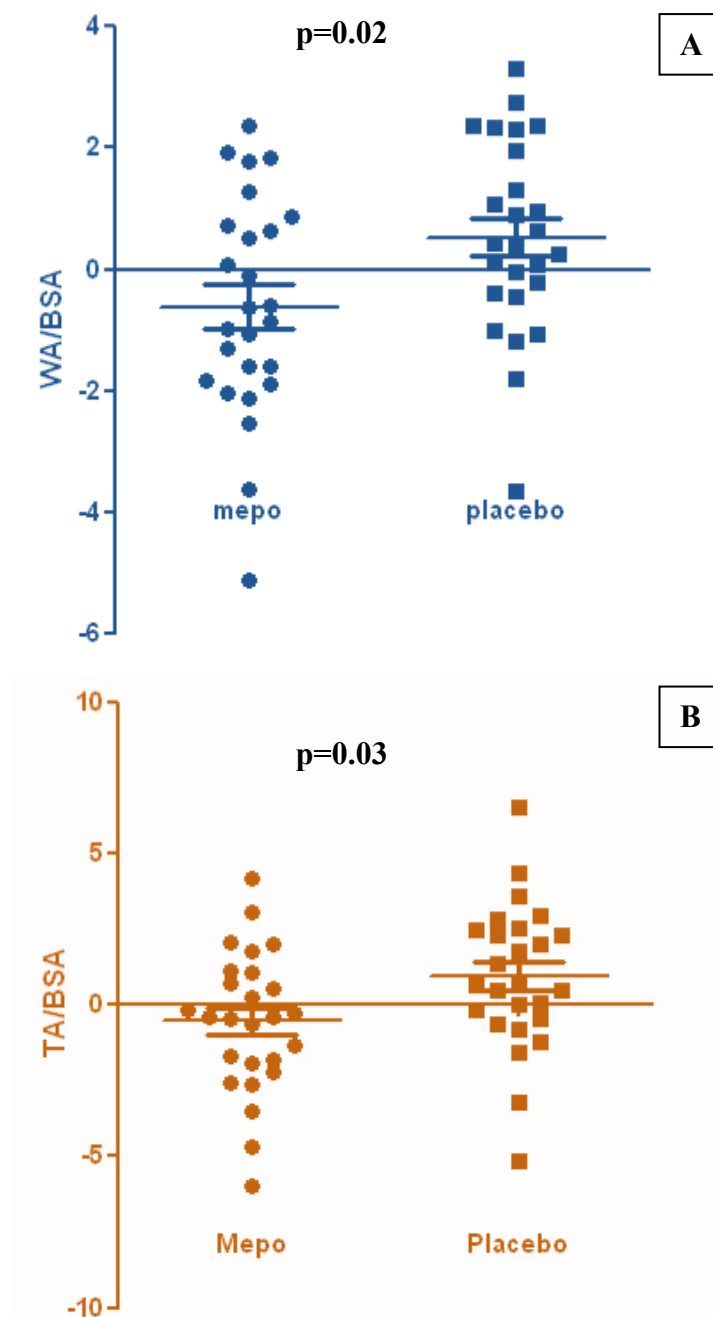


**Figure 3.33: Comparison CT assessed study outcomes between study groups**

Mean change in CT measured wall area (WA) and total area (TA), corrected for body surface area (BSA) after 12 months therapy with mepolizumab or placebo  
Horizontal bars represent mean change from baseline and error bars  $\pm$  SEM.

**Table 3.20: Baseline characteristics of subjects in the intention-to-treat population**

	<b>Mepolizumab (N=29)</b>	<b>Placebo (N=32)</b>	<b>P value</b>
<b>Gender - male/female</b>	14/15	18/14	0.80
<b>Age - yrs (Range)</b>	48 (21-63)	50 (24-72)	0.34
<b>Age of onset - yrs (Range)</b>	26 (2-53)	26 (2-57)	0.99
<b>Body Mass Index - kg m<sup>-2</sup></b>	29.4 ± 7.3	29.2 ± 5.9	0.92
<b>Atopic Status - %positive ^</b>	67.9	68.8	0.78
<b>Total IgE - kU l<sup>-1</sup> *</b>	177.8 ± 2.47	195 ± 2.64	0.75
<b>Nasal polyps - % positive</b>	34.4	31.2	0.59
<b>‡Severe exacerbations in previous year</b>	5.5	5	0.71
<b>Previous ITU admission for asthma - %</b>	27.5	31.25	0.78
<b>PC<sub>20</sub>MCh - mg ml<sup>-1</sup> *</b>	0.6 ± 1.24 (N=16)	1.1 ± 1.1 (N=18)	0.38
<b>Post bronchodilator FEV1 - % predicted</b>	78.1 ± 20.9	77.6 ± 24.1	0.93
<b>FEV1/FVC ratio - %</b>	72.2 ± 9.6	67.7 ± 13.5	0.15
<b>FEV1 Bronchodilator responsiveness - %</b>	9.1 ± 14.2	7.0 ± 13.1	0.57
<b>‡Baseline sputum eosinophil count - % *</b>	6.84 ± 0.64	5.46 ± 0.75	0.60
<b>Baseline blood eosinophil count - x10<sup>9</sup> l<sup>-1</sup> *</b>	0.32 ± 0.38	0.35 ± 0.30	0.57
<b>FE<sub>NO</sub> - ppb *</b>	44.4 ± 0.40	35.5 ± 0.40	0.31
<b>Juniper asthma control score ‡</b>	1.98 ± 1.07	2.38 ± 1.35	0.28
<b>Asthma Quality of Life Score</b>	4.72 ± 1.26	4.84 ± 1.13	0.71
<b>BDP equivalent Inhaled corticosteroid dose - µg per day (Range)</b>	2038 (1000-4000)	1711 (1000-4000)	0.03
<b>Long acting beta agonist use - % using</b>	92.9	90.6	0.99
<b>‡Regular oral prednisolone - % using</b>	57.1	53.1	0.80
<b>Mean (range) daily dose of maintenance prednisolone - mg</b>	9 (5-20)	10 (2-40)	0.72
<b>Monteleukast use - % using</b>	21.4	25	0.76
<b>Methotrexate use for asthma – no. of subjects</b>	0	2	0.49

Plus-minus figures are means  $\pm$  standard deviation unless otherwise stated

p-values obtained by performing a two-sided independent t-test for variables with a parametric distribution, the Fisher exact test for comparison of proportions and a Mann Whitney U-test for comparison of non-parametric variables

‡ Parameters used for stratifying randomisation with minimisation. Minimisation was performed by an independent clinician (CEB)

^ Positive atopic status defined on the basis of a positive skin test to any of four specified aeroallergens

\* Figures presented are the geometric mean  $\pm$  log10 (standard deviation)

‡ Score ranges from 0-6 with higher scores indicating worse symptoms

Definitions of Abbreviations: BDP = beclomethasone dipropionate, FENO = Fraction exhaled nitric oxide (measured at a flow of 50ml/sec), FEV1 = Forced expiratory volume in 1 second, FVC = Forced vital capacity, PC20MCh = provocative concentration of methacholine causing 20% fall in FEV1

**Table 3.21: Overview and comparison of changes in secondary outcomes after treatment with mepolizumab or placebo**

	Mepolizumab		Placebo		Between group difference in change† (95% CI)	Significance ‡
	Baseline	Change from baseline §	Baseline	Change from baseline §		
Fraction exhaled nitric oxide (ppb) *	44.4 ± 0.4	0.85 (0.67 to 1.04)	35.5 ± 0.4	0.99 (0.80 to 1.19)	0.9 (0.6 to 1.1)	0.29
Total sputum neutrophil count (cells per mg selected sputum)	2534 ± 4890	-1291 (-3363 to 779)	1062 ± 1210	370 (-417 to 1157)	-1662 (-4410 to 1085)	0.22
Modified Juniper Asthma Control Score	1.98 ± 1.07	-0.17 (-0.47 to 0.13)	2.38 ± 1.35	-0.21 (-0.52 to 0.11)	0.04 (-0.38 to 0.46)	0.65
Visual analogue symptom score	36.2 ± 22.0	-7.7 (-15.2 to -0.3)	40.6 ± 26.2	-3.2 (-9.0 to 2.7)	-4.6 (-13.9 to 4.7)	0.36
Asthma quality of life score	4.61 ± 1.21	0.55 (0.14 to 0.97)	4.77 ± 0.99	0.19 (-0.06 to 0.44)	0.35 (0.08 to 0.63)	0.02
Post bronchodilator FEV1 (litres)	2.31 ± 0.82	0.06 (-0.09 to 0.21)	2.39 ± 0.85	0.12 (-0.03 to 0.26)	-0.05 (-0.26 to 0.15)	0.61
^Methacholine PC <sub>20</sub> (mg/ml <sup>-1</sup> ) *	0.6 ± 1.2	0.9 (-1.5 to 2.1)	1.1 ± 1.1	0.4 (-0.6 to 1.5)	2.3 (-0.5 to 0.3)	0.70
Blood eosinophil count (x10 <sup>9</sup> l <sup>-1</sup> ) *	0.32 ± 0.38	0.15 (0.11 to 0.20)	0.35 ± 0.30	0.9 (0.7 to 1.17)	0.17 (0.11 to 0.24)	<0.001
Sputum eosinophil count (%) *	6.8 ± 0.6	0.14 (0.07 to 0.25)	5.46 ± 0.75	0.51 (0.28 to 0.91)	0.27 (0.12 to 0.63)	0.002
Bronchial wash eosinophil count (%) *	3.1 ± 0.8	0.19 (0.04 to 0.81)	3.1 ± 0.1	3.0 (0.2 to 45.7)	0.06 (0.01 to 0.56)	0.02
Bronchoalveolar lavage eosinophil count (%) *	5.5 ± 0.7	0.1 (0.02 to 0.50)	5.6 ± 0.3	0.8 (0.05 to 12)	0.13 (0.01 to 1.1)	0.06
Bronchial subepithelial eosinophil count (number per unit area) *	47.6 ± 0.4	0.41 (0.03 to 5.3)	10.9 ± 0.5	0.85 (0.04 to 19.1)	0.48 (0.01 to 16.7)	0.68
CT % Wall Area	66.3 ± 4.5	-1.2 (-2.5 to 0.1)	65.0 ± 5.3	-0.4 (-2.1 to 1.4)	-0.8 (-2.9 to 1.3)	0.43
Wall area/ BSA (mm <sup>2</sup> m <sup>-2</sup> )	12.1 ± 3.9	-0.6 (-1.3 to 0.1)	11.6 ± 3.9	0.5 (-0.1 to 1.2)	-1.1 (-2.1 to -0.2)	0.02
Luminal area/ BSA (mm <sup>2</sup> m <sup>-2</sup> )	6.4 ± 2.8	0.08 (-0.2 to 0.4)	6.5 ± 2.7	0.4 (-0.1 to 0.9)	-0.3 (-0.9 to -0.3)	0.26
Total area/ BSA (mm <sup>2</sup> m <sup>-2</sup> )	18.4 ± 6.5	-0.5 (-1.5 to 0.4)	18.0 ± 6.4	0.9 (-0.04 to 1.9)	-1.5 (-2.8 to -0.2)	0.03

Mean (SD) pre-treatment values and post-treatment change within and between groups with 95% confidence intervals (CI).

\* Geometric mean (log SD) with mean fold change and 95% CI. ^ For methacholine PC<sub>20</sub>, the change from baseline is expressed as doubling doses.

§ Change was calculated as a difference between the mean or geometric mean of the post treatment values and the baseline values. For parameters expressed as geometric mean, the change is expressed as a fold change.

‡ Significance refers to the between group difference in change.

† The between group difference was calculated as the difference in change from baseline with placebo and mepolizumab.

*Definitions of abbreviations:* FEV<sub>1</sub> = Forced expiratory volume in 1 second, Methacholine PC<sub>20</sub> = Provocative concentration of methacholine required to induce a fall in the FEV<sub>1</sub> of 20% from baseline, CT = Computed tomography, WA = Wall area, BSA = Body surface area, LA = Lumen area, TA = Total area

**Table 3.22: Reported adverse events during the 50-week treatment phase of the study**

Event	Mepolizumab (N=29)	Placebo (N=32)
	<i>Number of patients (percent)</i>	
Serious adverse event		
Hospitalisation for asthma	3 (10)	11 (34)
Adverse event		
Chest pain	1 (3)	0
Facial flushing	2 (7)	1 (3)
Erectile or ejaculatory dysfunction	2 (7)	0
Rash	2 (7)	4 (13)
Pruritis	2 (7)	0
Sub conjunctival haemorrhage	0	1 (3)
Conjunctivitis	1 (3)	1 (3)
Upper respiratory tract infection	1	4 (13)
Shingles	1 (3)	0
Fatigue	2 (7)	1 (3)
Night sweats	0	1 (3)
Nasal ulcer	0	1 (3)
Nasal polypectomy (elective)	0	1 (3)
Musculoskeletal pain	1 (3)	2 (6)
Gout	0	1 (3)
Delayed wound healing	0	1 (3)
Paraesthesiae hands	1 (3)	0
Loss of taste	0	1 (3)
Abdominal pain	0	1 (3)
Diarrhoea	0	1 (3)
Syncope	0	1 (3)
Dizziness	1 (3)	0

## **3.5 Study 5: Asthma Phenotypes based on Quantitative Computed Tomography Analysis of Proximal and Distal Airway Remodelling**

### **3.5.1 Abstract**

#### **Background**

Asthma heterogeneity is multi-dimensional and requires additional tools to unravel its complexity. Proximal and distal airway remodelling in asthma can be assessed with quantitative CT analysis. The aim of this study was to explore novel quantitative CT determined asthma phenotypes.

#### **Methods**

Forty-eight severe asthma, 17 mild / moderate asthma and 30 healthy subjects underwent detailed clinical and physiological characterisation as well as quantitative analysis of paired inspiratory and expiratory thoracic CT including fractal analysis of the segmented airway tree and lung parenchymal low attenuation clusters. Two retrospective limited CT scans of the RB1 bronchus over a mean duration of 2.6 years, were available for 22 severe asthma subjects enabling temporal analysis of proximal airway remodelling. Factor and cluster analysis techniques were utilised to determine three novel asthma phenotypes based on quantitative proximal and distal airway remodelling indices.

## Results

Severe and mild / moderate asthma subjects demonstrated smaller mean (SEM) RB1 LV in comparison to healthy controls (272.3 (16.4); 259.0 (12.9); 366.4 (35.6),  $p = 0.007$ ) but no significant difference in RB1 WV. Air trapping measured by MLD E/I was significantly greater in severe and mild / moderate asthma subjects compared to healthy controls (0.861 (0.01); 0.866 (0.02); 0.830 (0.01),  $p = 0.04$ ). Fractal dimension of the segmented airway tree was significantly lower in asthma subjects compared to control subjects ( $p = 0.007$ ). All three novel quantitative CT determined asthma clusters demonstrate air trapping. Cluster 1 demonstrates increased RB1 WV and RB1 LV, but decreased RB1 %WV. On the contrary cluster 3 asthma subjects have smallest RB1 WV and LV but highest RB1 %WV in comparison to other clusters. Temporal assessment revealed significant increase in RB1 WA/BSA over time but no change in RB1 LA/BSA.

## Conclusions

Quantitative CT analysis provides a new perspective in asthma phenotyping, which may prove useful in patient selection for novel therapies.



### 3.5.2 Introduction

Asthma remains a major healthcare burden affecting an estimated population of 300 million people worldwide with an annual premature fatality of 250,000.<sup>18</sup> Clinical presentation of asthma comprises of breathlessness, cough and wheeze with episodic worsening of symptoms in form of an exacerbation.<sup>5</sup> Majority of asthma population can be effectively managed by inhaled corticosteroid and short acting bronchodilators. About 5-10 % patients who do not respond adequately to traditional treatment are known to suffer from severe asthma.<sup>559</sup> These patients have severely impaired quality of life and exert disproportionately high burden on healthcare resources due to high risk of exacerbations, hospitalisation and death.<sup>12,230</sup> Asthma is also characterised by chronic airway inflammation, disordered airway physiology and airway remodelling. Disordered airway physiology constitutes variable airflow obstruction, airway hyper-responsiveness and persistent airflow obstruction in chronic disease. Airway remodelling is asthma disease complex embody changes such as increase in airway smooth muscle mass due to both hyperplastic and hypertrophic changes, mucous gland hyperplasia, thickening of reticular basement membrane, dysregulated ECM deposition and increased vasculature.<sup>69</sup>

MDCT has emerged as a non-invasive, repeatable and reliable tool for quantitative assessment of airway remodelling in asthma<sup>72,75,560</sup> and COPD<sup>467</sup>. Quantitative CT techniques in asthma now enable 3D objective morphometric assessment of the proximal airways<sup>72</sup> as well as indirect assessment of small airways by densitometric assessment of paired inspiratory and expiratory scans.<sup>149</sup> CT assessed proximal airway remodelling in asthma has been shown to correlate with airflow limitation,<sup>72,560</sup> AHR,<sup>76,302</sup> air trapping on

expiratory CT scans<sup>74</sup> and airway epithelial thickness<sup>72</sup> and smooth muscle layer area<sup>150</sup> measured on biopsy specimens. Areas of air trapping, indirect measure of small airway dysfunction, in asthma subjects have also been correlated with lung function abnormalities.<sup>298,302,319</sup>

There is increasing recognition that asthma is heterogeneous and comprises of distinct phenotypes.<sup>21,138,251,561</sup> Statistical techniques such as factor and cluster analysis have been employed to tease out asthma heterogeneity and identify distinct clinical phenotypes.<sup>21,22</sup> The benefits of phenotyping are evident in targeted treatment of eosinophilic airway inflammation using corticosteroids and anti-IL-5 to successfully reduce asthma exacerbations.<sup>57,250,562</sup> To address the complexity of structure-function relationship in asthma understanding the natural history and pattern of airway remodelling in asthma phenotypes is critical. Although quantitative CT based disease phenotyping has been used in COPD<sup>467</sup> this has not yet been utilised in asthma.

We hypothesised that asthma phenotypes, determined by quantitative CT measures of proximal and distal airway remodelling, do not have distinct clinical and physiological features. Our study aims were (1) to assess the use of factor and cluster analysis with quantitative proximal and distal airway CT indices in identification of novel asthma phenotypes and compare their clinical and physiological features; (2) to compare quantitative CT measures of proximal and distal airway remodelling from volumetric paired inspiratory and expiratory CT scans between severe asthma, mild / moderate asthma and healthy controls; (3) to compare fractal dimension of segmented airway tree and terminal air space between severe asthma, mild / moderate asthma and healthy controls

and; (4) To assess temporal pattern of proximal airway remodelling in quantitative CT asthma clusters from a subset of severe eosinophilic asthma patients.

### **3.5.3 Methods**

#### **3.5.3.1 Study Design**

Data presented here is part of the Longitudinal Quantitative CT Analysis of Airway Remodelling in Airway Disease study. This single-centre study aims to acquire baseline full thoracic paired inspiratory and expiratory CT scan with detailed clinical and physiological characterisation in airway disease and healthy subjects. Further limited CT scans to image the RB1 bronchus with clinical and physiological data will be acquired at interval of one year for up to three years in subjects with airway disease. Low dose CT scans are performed for the purpose of this study and the upper limit of radiation dose that will be imparted to subjects is 5 mSv. If any of the study participants had taken part in research study involving CT scans prior to the current study, this was taken into account to ensure that the upper limit of radiation dose due to research CT scans did not exceed 5 mSv. The first ninety-five subjects (48 severe asthma, 17 mild / moderate asthma and 30 healthy) who had completed their first visit between January 2009 and January 2011 were included in the current study.

### **3.5.3.2 Subjects**

#### **3.5.3.2.1 Cross-sectional assessment of subjects with eosinophilic severe asthma, mild / moderate asthma and healthy controls**

All subjects recruited were greater than 18 years with female subjects at least 30 years or older. The diagnosis of asthma is confirmed by a respiratory physician based on history and one or more of the following objective criteria (maximum diurnal PEF variability >20% over a 2 week period, significant bronchodilator reversibility defined as an increase in FEV<sub>1</sub> of >200mls post bronchodilator or a PC<sub>20</sub>MCh of <8mg/ml). Severe asthma was defined in accordance with the ATS workshop on refractory asthma.<sup>9</sup> Healthy subjects enrolled were in good overall health, asymptomatic and had no known respiratory illness with normal spirometry. It was ensured that subjects recruited did not have any previous lung surgery or any metal prosthesis or wires in vicinity of their thorax that may affect the quantitative CT analysis. All subjects enrolled in the study underwent clinical characterisation including an extensive history, skin prick tests for common aeroallergens, peripheral blood test, spirometry, full pulmonary function test, methacholine challenge tests, and sputum induction.<sup>51</sup> In asthma subjects, quality of life and asthma control was assessed using the standardised Juniper asthma quality of life questionnaire<sup>563</sup> and Juniper asthma control questionnaires.<sup>461,462</sup> Informed consent for clinical characterisation and CT was obtained from all subjects and the study was approved by the Leicestershire, Northamptonshire and Rutland Research Ethics Committee.

#### **3.5.3.2.2 Temporal assessment of airway remodelling pattern in subset of eosinophilic severe asthma subjects**

A subset of severe eosinophilic asthma patients (n=22) were included in this analysis who had two limited CT scans (imaging the RB1 bronchus) with a mean (range) duration of 1.6 (0.9 – 2.7) and 2.6 (1.9 – 3.7) years prior to the current scan. The limited CT scans were acquired as part of another study<sup>562</sup> evaluating the effect of anti-IL-5 treatment on exacerbations of severe eosinophilic asthma where this subset of patients were assigned to the placebo arm.

#### **3.5.3.3 Computed tomography imaging**

CT scans were acquired using multi-detector CT scanner, Siemens Sensation 16, at Glenfield Hospital, Leicester. Volumetric whole-lung scans were acquired at full inspiration (near TLC) and at the end of normal expiration (near FRC), the details for which are described in [Section 2.3.1.3].

Assessment of radiation exposure due to research CT scans was performed as described in [Section 2.3.3]

#### **3.5.3.4 Quantitative airway and air trapping analysis using automated software**

Fully automated software, PW2 was used for quantitative airway and densitometry analysis.

Quantitative airway morphometry and air trapping analysis was performed as described in [Section 2.3.2.2.2]. Fractal dimension of the airway tree and low attenuation areas in the lungs were also determined, which is detailed in [Section 2.3.2.2.3].

Ninety-five percent CI of MLD E/I among healthy controls was considered as normal range for CT air trapping. CT air trapping in asthma subjects was graded based on value of MLD E/I ratio: (1) Severe: greater than upper limit of 99.5 % CI of MLD E/I ratio in healthy controls, (2) Moderate: greater than upper limit of 98 % CI of MLD E/I ratio in healthy controls, and (3) Mild: greater than upper limit of 95 % CI of MLD E/I ratio in healthy controls.

### **3.5.3.5 Statistical Analysis**

Statistical analysis was performed using GraphPad Prism version 5.00 for Windows, GraphPad Software, San Diego California USA, [www.graphpad.com](http://www.graphpad.com) and standard multiple regression using SPSS for Windows, Rel. 16.0.1.2008. Chicago: SPSS Inc. Parametric data were expressed as mean (SEM) and non-parametric data were described as median (IQR). Log transformed data is presented as geometric mean (95% CI). Pearson Chi-squared test and Fisher's exact tests were used to compare ratios. One-way analysis of variance with Tukey correction (parametric data) and Kruskal-Wallis test with Dunn's intergroup comparison (non-parametric data) was used to compare multiple groups.

Pearson correlation coefficient was used to determine the relationship between proximal airway, distal airway and clinical indices.

CT data was subjected to unsupervised multivariate modelling using principal component analysis (orthogonal varimax rotation method) to extract factors that best describe the underlying relationship among the quantitative CT variables in all asthma patients. Prior to performing principal component analysis the suitability of data for factor analysis was assessed. Inspection of correlation matrix revealed the presence of many coefficients of 0.3 or above. The Kaiser-Mayer-Olkin measure<sup>564,565</sup> for sampling adequacy was 0.6, recommended value being 0.6 or above. The Barlett's Test of Sphericity<sup>566</sup> reached statistical significance ( $p < 0.0005$ ) supporting factorability of the correlation matrix. Independent components reflecting different asthma CT phenotypes, were identified using factor analysis of eleven quantitative CT variables that encompassed a broad range of proximal and distal airway measures; RB1 LA/BSA, RB1 WA/BSA, RB1 TA, RB1 LV, RB1 WV, RB1 %WV, Expiratory VI -850, MLD E/I ratio, VI<sub>-850-950</sub> E-I, Expiratory LAC-D -850 and Inspiratory  $D_{av}$ . Factor analysis identified three components that contributed to the dataset in accordance with the Kaiser criterion<sup>567</sup> (Eigen values  $> 1$ ). After identification of three 'quantitative CT' components we employed cluster analysis to classify patients with asthma into phenotypes based on quantitative CT indices. The highest loading variable from each component (namely RB1 LA/BSA, MLD E/I ratio and Expiratory LAC-D -850) was used for cluster analysis. Two steps were involved in statistical cluster analysis: (1) Hierarchical cluster analysis was performed using Ward's method (uses squared Euclidean distance as the interval measure) which generated a dendrogram to determine the number of likely clusters. Period of large change between successive fusion levels in the dendrogram were used to define likely cluster boundaries.<sup>21</sup> Three clusters were estimated by hierarchical cluster analysis of the predominant variable from each component that had been identified by principal component analysis; (2) k-means cluster analysis was used as

the principal clustering technique with a pre-specified number of clusters to determine cluster membership of asthma patients.<sup>568</sup> Clinical and quantitative CT characteristics for the asthma clusters were tabulated.

For temporal assessment of airway remodelling pattern in subset of eosinophilic severe asthma subjects, analysis of between and within asthma cluster change was performed to compare RB1 LA/BSA and RB1 WA/BSA at three time points (baseline limited CT scan, second limited CT scan and current full CT scan). Within-cluster change in variables at each time point was analysed by paired t-test and data was expressed as mean (SEM) change from baseline. Between-cluster change in variables at the time of second and current CT scan was analysed by independent t-test and data expressed as mean (SEM) difference in mean change from baseline for each cluster at the time of second and current CT. Intraclass correlation (ICC) was used to assess repeatability of airway dimension over time. Two-way random effect model with absolute agreement ICC was used to assess single measure reliability.

A p value of <0.05 was taken as statistically significant.

### **3.5.4 Results**

Baseline demographics and clinical characteristics of subjects with severe (n=48) or mild / moderate (n=17) asthma and healthy controls (n=30) are shown in Table 3.23. Forty-eight severe asthma subjects included in this study have previously taken part in another study.<sup>562</sup> [Section 3.4]. Among the three groups no significant difference was found in age, gender, BSA and smoking status.



#### **3.5.4.1 Adequacy of breath-hold on inspiratory and expiratory CT scans**

On assessment of all study subjects there was no significant difference between expiratory CT lung volume and FRC calculated on full lung function tests (mean (SEM), 3.0 (0.1) vs 2.9 (0.1),  $p=0.2$ ). Inspiratory CT lung volume was less than TLC assessed by full lung function tests (mean (SEM), 5.2 (0.1) vs 6.0 (0.2),  $p<0.0005$ ).

#### **3.5.4.2 Proximal airway remodelling**

On inspiratory CT scan mean (SEM) RB1 %WV was significantly higher in severe asthma and mild / moderate asthma group as compared to healthy controls (62.4 (0.5); 61.4 (0.7); 58.5 (0.7),  $p<0.0005$ ). Severe and mild / moderate asthma subjects had smaller mean (SEM) RB1 LV in comparison to healthy controls (272.3 (16.4); 259.0 (12.9); 366.4 (35.6),  $p = 0.007$ )[Figure 3.34]. No significant difference in RB1 dimension was found amongst the two asthmatic groups [Table 3.24].

Assessment of three other segmental bronchi (RB10, LB1+2 and LB10) on inspiratory CT scan revealed results similar to RB1. Mean (SEM) LV or LA/BSA of all the additional segmental bronchi assessed was significantly smaller in asthmatic subjects compared to healthy controls [Table 3.25]. RB10 and LB10 (but not LB1+2) %WV was significantly greater in asthma subjects compared to healthy controls [Table 3.25].

Pi<sub>10</sub> WA and Po<sub>20</sub> %WA was greater in severe asthma subjects compared to healthy control subjects [Table 3.26].

### **3.5.4.3 Air-trapping as indirect measure of distal airway remodelling**

CT assessed lung volumes on inspiratory and expiratory scans were similar amongst the three groups [Table 3.27]. Air-trapping indices, MLD E/I and  $VI_{.850}$  E-I, were significantly greater in asthmatic subjects compared to healthy controls [Table 3.27]. Upper limit of 99.5 % CI, 98 % CI and 95 % CI of MLD E/I ratio in healthy controls was 0.862, 0.853 and 0.849 respectively.

### **3.5.4.4 Fractal dimension**

On inspiratory CT, fractal dimensions ( $D_{av}$ ,  $D_{sc}$ ,  $D_e$  and  $D_{sce}$ ) of the segmented airway tree were significantly lower in asthma subjects compared to control subjects, indicating decreased complexity of the branching airway tree in asthma [Table 3.28, Figure 3.35].

Fractal dimension of LAC at threshold of -950 HU (LAC-D -950) on inspiratory scan and fractal dimension of LAC at threshold of -850 HU (LAC-D -850) on expiratory scan were not different across the three groups [Table 3.28].

### **3.5.4.5 Univariate analysis to explore structure-function relationship and proximal–distal airway remodelling relationship in asthma**

Good correlation was observed between air-trapping indices and hypothetical airway measurements,  $Pi_{10}$  WA or  $PO_{20}$  %WA [Table 3.29], but not between air-trapping indices and RB1 dimensions.

Pi<sub>10</sub> WA inversely correlated with post bronchodilator FEV<sub>1</sub>/FVC (Pearson  $r = -0.27$ ,  $p < 0.05$ ) and mid expiratory flow rate (Pearson  $r = -0.34$ ,  $p < 0.05$ ). A significant inverse correlation was also found between RB1 %WV and % RV/TLC (Pearson  $r = -0.35$ ,  $p < 0.05$ ) [Table 3.30].

MLD E/I ratio positively correlated with RV/TLC (Pearson  $r = 0.46$ ,  $p < 0.001$ ) and negatively correlated with post bronchodilator FEV<sub>1</sub> % predicted (Pearson  $r = -0.4$ ,  $p < 0.001$ ), post bronchodilator FEV<sub>1</sub>/FVC ratio (Pearson  $r = -0.48$ ,  $p < 0.001$ ) and MEF (Pearson  $r = -0.6$ ,  $p < 0.001$ ). Other CT indices of air trapping also demonstrated similar correlation with lung function tests [Table 3.31]. Disease duration, JACQ score, sputum eosinophil and neutrophil counts also showed correlations with CT air trapping indices.

### **3.5.4.6 Unbiased CT phenotyping of asthma subjects using factor and cluster analysis**

#### **3.5.4.6.1 Factor analysis of radiological variables**

Factor analysis identified three components that contributed to the dataset in accordance with the Kaiser criterion (Eigen values  $> 1$ ) [Figure 3.36] and which accounted for 75.2 % of the total population variance. Component loading for the selected variables of the three independent components are shown in Table 3.32. Component 1 which accounted for 42.6 % of total variance, correlated with RB1 LA/BSA and RB1 LV and inversely correlated with RB1 %WV. Component 2 (23.3 % of total variance) correlated with MLD E/I ratio and VI<sub>850-950</sub> E-I. Component 3 (9.3 % of total variance) correlated with Expiratory LAC-D-850 and Inspiratory D<sub>av</sub>.

#### **3.5.4.6.2 Asthma phenotypes based on quantitative CT variables delineated by cluster analysis**

Clinical and quantitative CT characteristics of three asthma phenotypes determined by cluster analysis are shown in Table 3.33 and Table 3.34 respectively. All three asthma clusters demonstrate air trapping suggesting presence of small airway disease. Cluster 1 and 3 demonstrate severe CT air trapping compared to moderate CT air trapping seen in cluster 2. Normal range of expiratory VI -850, calculated from 95 % confidence interval of the variable in healthy control subjects, was 12.1 % - 20.3 %. Proportion of subjects with expiratory VI -850 above 20.3% was higher in cluster 1 and cluster 3 compared to cluster 2. Asthma patients in cluster 1 in addition to severe air trapping had increased RB1 wall volume and lumen volume, but decreased RB1 %WV. On the contrary cluster 3 asthma patients in addition to severe air trapping has smallest RB1 wall volume and lumen volume but highest RB1 %WV in comparison to other clusters [Figure 3.37]. Fractal dimension of the segmented airway tree was highest in cluster 1.

No significant differences were found between the three clusters with regards to age, gender distribution, disease duration, smoking status, symptom score, severe exacerbation frequency, atopy, aspergillus sensitisation, sputum eosinophilic or neutrophilic inflammation. Significantly greater number of subjects in cluster 1 and 3 were on LABA treatment compared to cluster 2. Proportion of patients with severe asthma were greater in cluster 1 and 3. Cluster 1 and 3 had significantly higher RV/TLC% and lower pre and post bronchodilator FEV<sub>1</sub> % predicted compared to cluster 2. Patients in cluster 3 had increased

BMI compared to other groups. Bronchodilator response was significantly lower in cluster 2 patients in comparison to other clusters.

### **3.5.4.7 Temporal assessment of subset of eosinophilic severe asthma subjects**

#### **3.5.4.7.1 Assessment of airway remodelling**

When all asthmatic subjects in this subset (n=22) were assessed as a single group, RB1 WA/BSA demonstrated significant increase over time (mean (SEM); baseline CT, 14.3 (0.9); second CT, 14.7 (0.9); current CT, 16.5 (1.3); repeated measure ANOVA,  $p=0.008$ ). No significant change was seen in RB1 LA/BSA (mean (SEM); baseline CT, 9.1 (1.0); second CT, 9.6 (1.0); current CT, 9.9 (0.9); repeated measure ANOVA,  $p=0.4$ ) [Figure 3.38 and Figure 3.39]. RB1 LA/BSA and RB1 WA/BSA showed good repeatability between three time points (baseline limited CT scan, second limited CT scan and current full CT scan); RB1 LA/BSA, ICC = 0.82 (95% CI, 0.68 – 0.91;  $p<0.0005$ ) and; RB1 WA/BSA, ICC = 0.75 (95% CI, 0.56 – 0.88;  $p<0.0005$ ) [two-way random effect model, absolute agreement, single measure reliability]. Within-group change and between-group change in RB1 LA/BSA and RB1 WA/BSA at three time points (baseline limited CT scan, second limited CT scan and current full CT scan) is shown in Table 3.35 and Figure 3.40. Significant between-group differences in change from baseline of the RB1 WA/BSA were seen over the 2.6 years mean duration. Significant within-group change in RB1 WA/BSA and RB1 LA/BSA was seen in cluster 1 between second and the current CT. Cluster 2

showed a significant within-group change in RB1 WA/BSA between current and baseline CT scan. No significant within-group change in RB1 dimensions was seen in cluster 3.

Mean (SEM) change in interval normalised RB1 WA/BSA and LA/BSA respectively was: Cluster 1, 3.6 (0.8) mm<sup>2</sup>/m<sup>2</sup>/year, 1.7 (1.1) mm<sup>2</sup>/m<sup>2</sup>/year; Cluster 2, 1.0 (0.5) mm<sup>2</sup>/m<sup>2</sup>/year, -0.02 (0.4) mm<sup>2</sup>/m<sup>2</sup>/year; Cluster 3, -0.1 (0.3) mm<sup>2</sup>/m<sup>2</sup>/year, 0.1 (0.4) mm<sup>2</sup>/m<sup>2</sup>/year.

#### **3.5.4.7.2 Assessment of airflow limitation, symptoms and airway inflammation**

Asthmatic subjects (n=22) did not show any significant change in post bronchodilator FEV<sub>1</sub> % predicted [mean (SEM) change from baseline, -1.8 (2.7), p=0.5], post bronchodilator FEV<sub>1</sub>/FVC (%) [mean (SEM) change from baseline, -0.7 (1.3), p=0.6], AQLQ score [mean (SEM) change from baseline, 0.07 (1.3), p=0.7] and sputum neutrophils [mean (SEM) change from baseline, 5.4 (7.1), p=0.5] at the time of current CT scan compared to baseline. There was a statistically significant increase in the modified (symptoms only) JACQ score [mean (SEM) change from baseline, 0.4 (0.2), p=0.03].

#### **3.5.4.8 Effective radiation dose for research CT scans**

Using ImPACT CT dosimetry calculator the estimated ED for limited and full thoracic CT scan was 0.42 mSv and 1.5 mSv respectively. The estimated ED using the scanner determined CTDI<sub>vol</sub> for limited and full thoracic CT scan was 0.33 (=19.7 x 0.017) mSv and 1.6 (=93.6 x 0.017) mSv respectively. Radiation dose associated with common radiological examinations and research CT scans is presented in Table 3.36.

Using ImPACT CT dosimetry calculator the estimated breast tissue absorbed dose for limited and full thoracic CT scan was 1.5 mGy and 3.3 mGy respectively.

### **3.5.5 Discussion**

We found that in asthma patients irrespective of disease severity, there was airway remodelling with reduced luminal volume and increased percentage wall volume compared to healthy subjects. The increase in %WV was largely driven by reduction in LV with no significant difference in WV between asthma and healthy subjects. Thus suggesting that airway remodeling reflects complex changes in the airway geometry rather than simply an increase in wall volume. Air trapping was increased in asthmatics compared to healthy subjects, with no significant difference seen between severe and mild / moderate asthma subjects. Fractal dimension of the segmented airway tree was significantly lower in asthma subjects compared to healthy subjects on inspiratory scan indicating a loss of complexity and decrease in the space filling ability of these airways. Assessment of a subset of asthmatics who had 3 CT scans over a mean duration of 2.6 years demonstrated a small increase in wall area, but no significant change in luminal area. Using CT indices of proximal and distal airway remodeling, we present three novel asthma phenotypes with distinct clinical and radiological features.

Proximal airway remodelling, though an established feature of asthma,<sup>72,150</sup> is heterogeneous with variable changes in wall and lumen dimensions reported by several authors.<sup>72,75,298,560</sup> Few authors have also reported pathological correlation of CT assessed proximal airway remodelling.<sup>72,150,296</sup> We have confirmed in this study that proximal airway

lumen is narrow in asthmatic subjects compared to healthy controls. Airway narrowing in asthma subjects may be due to ASM shortening, thickening of the airway wall encroaching upon the lumen, decreased compliance of the airway wall due to change in its composition or architecture leading to reduced distensibility<sup>569,570</sup> and changes in the parenchymal tethering of the airway wall (airway-parenchymal interdependence). Moreno *et al.*<sup>571</sup> and others<sup>229,572</sup> have used mathematical modelling to demonstrate that thickening of the inner airway wall and consequent luminal narrowing can amplify the increase in airway resistance for a given degree of smooth muscle shortening. Our results demonstrate lumen narrowing as a predominant feature of proximal airway remodelling in asthmatic subjects in keeping with our previous observation.<sup>560</sup> Recently Williamson and coworkers<sup>445</sup> have also shown a reduced lumen area in asthma subjects compared to controls using optical coherence tomography. Taken together these findings suggest that lumen narrowing may be critical in functional and physiological manifestations of asthma. Despite the heterogeneity of airway remodelling, RB1 has been shown to emulate changes in other proximal airways.<sup>72,76,560</sup> In our study the differences in RB1 dimensions between asthma and healthy groups were reflected in airway remodelling pattern of three other proximal airways and two hypothetical airways, confirming that RB1 is a good surrogate for proximal airway remodelling.

Air-trapping indices were derived from paired inspiratory and expiratory scans after calibration using air, blood and electron density rods. X-ray tube ageing and replacement may introduce errors in densitometry measures<sup>526,532</sup> despite standard CT scanner quality assurance procedures.<sup>573</sup> Densitometry calibration is therefore critical and our study is the first to apply this for assessment of air trapping in asthma subjects. The air trapping indices,



MLD E/I ratio and  $VL_{850}$  E-I were significantly higher in asthma patients compared to healthy subjects in keeping with observations by other authors.<sup>74,302,319</sup> In our study CT indices of air trapping correlated with Pi10 and Po20 but not with any other proximal airway dimensions. Similarly Gono and colleagues<sup>74</sup> had also shown correlation between CT assessed proximal airway dimension and indices of air trapping. Univariate analysis of CT air trapping indices, in contrast to proximal airway remodelling, showed a much stronger correlation with lung functions and disease duration. Previous studies<sup>72,74,75,302,319,560</sup> have also demonstrated correlation between CT and clinical indices, thus highlighting the importance of structure-function relationship in asthma.

For the first time, we have used an unbiased method to determine asthma phenotypes based on CT measures of proximal and distal airway remodelling. Previous we did not find any difference in proximal airway remodelling in 4 clinical severe asthma phenotypes,<sup>560</sup> which prompted the current analysis. Both CT and physiological measures demonstrate more severe air trapping in clusters 1 and 3 compared to cluster 2. Cluster 1 and 3 demonstrate poorer lung function compared to cluster 2. Moreover, lack of proximal airway remodelling in cluster 2 implies that this phenotype represents asthma subjects with mild disease. Similarly, others report<sup>72,282</sup> no significant difference in airway dimensions between the mild/moderate asthma patients and healthy subjects. Wagner *et al.*<sup>310</sup> have shown a seven-fold increase in distal airway resistance in asthmatic patients with mild disease and normal spirometry, compared to healthy subjects. Taken together these findings perhaps suggest that small airway involvement in asthma precedes proximal airway remodelling. Cluster 1, with significantly increased RB1 lumen and wall dimensions may represent bronchiectasis phenotype of asthma, described previously,<sup>262,267,537</sup> which

correlates negatively with  $FEV_1$ <sup>574</sup> and positively with air trapping.<sup>575</sup> There is emerging evidence that ciliary dysfunction with profound ultrastructural abnormality is a feature of severe asthma<sup>37</sup> which may contribute to development of bronchiectasis.<sup>576</sup> Bronchiectasis in a subset of severe asthma subjects may also be explained by increased airway malacia<sup>577,578</sup> and collapsibility<sup>33</sup> resulting from on-going inflammation, structural alteration in ECM, cartilage degradation and elastolysis.<sup>579</sup> Cluster 3 patients have marked airway luminal narrowing along with severe air trapping and lack of airway wall thickening. This suggests that remodelling of airway wall alone cannot account for the structural changes observed in these patients. Therefore, one could speculate, that additional mechanisms such as decreased airway wall compliance and/or loss of parenchymal tethering on the airway wall may contribute to lumen narrowing this group of patients. Mathematical modelling studies<sup>580,581</sup> have also shown that thickening of the adventitia can uncouple the airway smooth muscle from the lung's elastic recoil forces abating the airway-parenchymal interdependence. Numerous CT studies have also demonstrated an increased %WA or percent wall thickness in severe asthmatics compared to healthy subjects,<sup>72,74-76,295,560</sup> findings similar to cluster 3 asthma subjects in our study. Whether the CT-derived phenotypes we describe here represent distinct asthma endotypes<sup>251,582</sup> with discrete pathogenic pathways, or indicate towards a progressive disease captured at different stages of airway remodeling is uncertain and warrants further study.

There is paucity of studies in asthma investigating longitudinal aspects of airway remodelling. Three different studies have demonstrated a significant decrease in airway wall thickness / WA after use of inhaled corticosteroids.<sup>185-187</sup> Recently, in a study of 30

patients with severe persistent asthma randomised to conventional therapy with or without Omalizumab, an anti-Immunoglobulin E antibody, a significant decrease in WA/BSA and %WA over a period of 16 weeks in patients receiving Omalizumab therapy was demonstrated along with significant improvement in FEV<sub>1</sub> and AQLQ scores.<sup>583</sup> On the contrary, Brillet *et al.* found no change in CT assessed airway dimensions in 12 patients with poor asthma control treated for 12 weeks with inhaled LABA and inhaled corticosteroids despite improvement in physiological measures of airway obstruction and air trapping.<sup>307</sup> Moreover, a further follow up of asthma subjects on inhaled corticosteroids from a previous study<sup>185</sup> for a mean duration of 4.2 years did not show any significant change in airway dimensions with reported mean (SEM) change in RB1 WA/BSA normalised by interval of -0.27 (0.59) mm<sup>2</sup>/m<sup>2</sup>/year.<sup>306</sup> We have previously shown a decrease in RB1 WA/BSA in severe asthma subjects after one-year treatment with anti-IL-5 compared to placebo with approximately 10% between-group change.<sup>562</sup> Twenty-two of these severe asthma patients (from placebo arm) after a further follow-up CT in our current study demonstrate small, albeit significant temporal increase in RB1 WA/BSA but no change in the RB1 LA/BSA. These varied patterns of airway remodelling modulation exhibited by asthma subjects may be explained by heterogeneous nature of the disease, differences in patient selection and duration of treatment and/or follow up. Asthma CT phenotypes in our study show a differential temporal pattern of airway remodelling, particularly patients in cluster 3, where no significant change in airway wall or lumen dimensions was demonstrated over a period of 2.6 years. CT based phenotyping could thus help us unravel novel asthma subtypes which may have distinct pathophysiological mechanisms.

Our finding of decreased fractal dimension of the segmented airway tree in asthmatic patients compared to healthy subjects is consistent with similar analyses of bronchial tree,<sup>342</sup> peak expiratory flow time series<sup>343</sup> and, fluctuation in daily fraction of exhaled nitric oxide<sup>344</sup> in asthma patients. To determine the fractal dimension we used the digital picture of the segmented airway tree obtained from CT scans using PW2 software, in contrast to Boser *et al.*<sup>342</sup> who used digital picture of silicone rubber cast of airways made using autopsy material from post-mortem subjects. Despite these differences in the method used by Boser *et al.* and our group, the values of fractal dimension obtained were similar. Reduced fractal dimension and hence the complexity of the airway tree may be fundamental in understanding the disordered physiology<sup>584</sup> and exacerbation events<sup>394</sup> associated with asthma. Fractal dimension of LAC at threshold of -950 HU on inspiratory scans can help detect early emphysema.<sup>333</sup> In our study there was no evidence of emphysema in asthma subjects as both VI -950 and LAC-D -950 were not significantly different compared to healthy subjects. This is in keeping with results from our previous study<sup>537</sup> as well as other studies.<sup>262,263,265,268</sup> Although degree of air trapping is higher in asthmatics compared to healthy subjects, no difference was found in fractal dimension of LAC at threshold of -850 HU on expiratory scans, representing distribution of areas of low attenuation. In addition we did not find any significant difference in LAC-D -850 on expiratory scans between mild / moderate and severe asthma suggesting that air trapping in asthma is not associated with alveolar wall destruction as is the case in emphysema. In concert with our results, Mitsunobu and colleagues,<sup>328</sup> on analysis of inspiratory CT scans, did not find any difference in fractal dimension of LAC at -950 HU between non-smoking asthma and healthy subjects. Although, in the same study Mitsunobu *et al.* demonstrated that fractal dimension of LAC at -950 HU was significantly lower in severe asthma in

comparison to mild and moderate asthma. However, fractal analysis of LAC by Mitsunobu *et al.* in asthma subjects most likely represent emphysematous regions as their analysis was at -950 HU threshold on inspiratory CT scans. Hyperpolarised gas MRI studies have also confirmed that apparent diffusion coefficient, which is increased in emphysema due to enlarged airspaces caused by breakdown of the alveoli,<sup>405,585</sup> does not differ significantly between asthma and healthy never-smoker subjects.<sup>586</sup>

Major concern with longitudinal CT studies is radiation dose accrued by study subjects.<sup>587,588</sup> Moreover, children are more sensitive to radiation than adults and it has been shown that risk in females is approximately twice that of males for the same level of radiation exposure.<sup>356,357</sup> Field of radiation for thoracic CT includes radiosensitive breast tissue in females, increasing the risk of breast cancer in younger females exposed.<sup>358,359</sup> In our study we ensured that only male and female subjects with age greater than 18 and 30 years respectively were recruited. We devised low dose CT scanning protocols for this study ensuring that no subject was exposed to total estimated effective dose of more than 5 mSv and radiation exposure due to any previous CT research studies was taken into account. In comparison, estimated effective dose for single clinical cancer staging chest CT is 6.8 mSv [Table 3.36]. The risk due to radiation exposure from research CT scans was considered low and it was estimated that additional radiation dose of 5 mSv would add an additional 0.025% to a person's 25% risk of dying from cancer.<sup>366</sup> Estimated breast tissue absorbed dose due to limited and full thoracic research CT scan was 1.5 mGy and 3.3 mGy respectively. In comparison, radiation dose to breast tissue from CT scans performed on 16 slice MDCT for pulmonary embolism protocol ranged from 40-60 mGy.<sup>359</sup> The average glandular dose for standard two-view screening mammography is 3 mGy,<sup>358</sup> which is

comparable to breast tissue absorbed dose secondary to low dose full thoracic CT scan in our study.

Our study has a number of potential limitations. Inspiratory and expiratory CT scans obtained were not spirometrically gated. We are confident that the differences observed in airway dimensions between asthma and healthy subjects in our study are not due to differences in lung volume as all subjects practiced breath-hold prior to CT scan and no significant differences were found in inspiratory or expiratory lung volumes between groups. Expiratory CT assessed lung volume was not significantly different from physiologically assessed FRC. Inspiratory CT assessed lung volume, though lower than physiologically assessed TLC, was similar in healthy, mild / moderate asthma and severe asthma subjects. Studies have shown that it is unlikely that spirometric gating will further improve quantitative CT repeatability.<sup>589</sup> Moreover, animal studies have demonstrated that airways do not distend isotropically with the lung and following elimination of bronchial tone airway lumen reaches a plateau at low trans-pulmonary pressure with trivial changes in lumen area on further elevation of trans-pulmonary pressure.<sup>590-592</sup> Temporal assessment of airway remodelling was performed only on eosinophilic severe refractory asthma subjects and therefore we may not be able to extrapolate our findings to non-eosinophilic severe asthma and mild / moderate asthma population. However, no significant difference in CT assessed proximal or distal airway remodelling was found between mild / moderate and severe asthma groups. Additionally, we have previously demonstrated that there is no significant difference in proximal airway remodelling between eosinophilic and non-eosinophilic severe asthma patients.<sup>560</sup> Moreover, there is emerging evidence that macrophage eosinophil protein content in addition to sputum eosinophil count reflects

actual eosinophil load in asthmatic subjects and absence of both is uncommon in moderate to severe asthma suggesting that true non-eosinophilic asthma is probably less common than previously estimated.<sup>593</sup> CT determined asthma clusters were determined based on full thoracic paired inspiratory and expiratory CT scans acquired as part of the current study and temporal CT data was obtained from retrospective scans. We therefore are unable to assess the stability of CT derived clusters over time. However, good ICC was demonstrated for three measures of RB1 LA/BSA and WA/BSA over a mean duration of 2.6 years indicating phenotype stability of severe asthma subjects in our study. Temporal assessment was possible in small number of subjects in each cluster, therefore further verification of this finding is required by large longitudinal studies. Despite this limitation, temporal analysis may provide useful insight into natural history of airway remodelling.

Our study has further extended the tools to investigate asthma heterogeneity and for the first time utilized CT indices of proximal and distal airway remodelling to determine distinct asthma phenotypes. Consequently, our findings challenge the paradigm in asthma that airway wall remodelling is characterized by increased wall volume, but rather suggests that in asthma there is an important component of small airway disease coupled with distinct and polarised phenotypes of proximal airway dilatation or narrowing. Whether these changes occur in parallel or as a consequence of small airways disease needs to be further investigated. Additionally, fractal analysis of the segmented airway tree and low attenuation clusters in asthma accentuates the traditional Euclidian geometry methods for assessment of structural changes in airway and lung parenchyma. Structural basis of phenotyping asthma may prove invaluable in patient stratification to inform underlying

mechanisms of disease and for novel pharmacological and non-pharmacological<sup>594</sup> treatments.



3.5.6 Figures and Tables

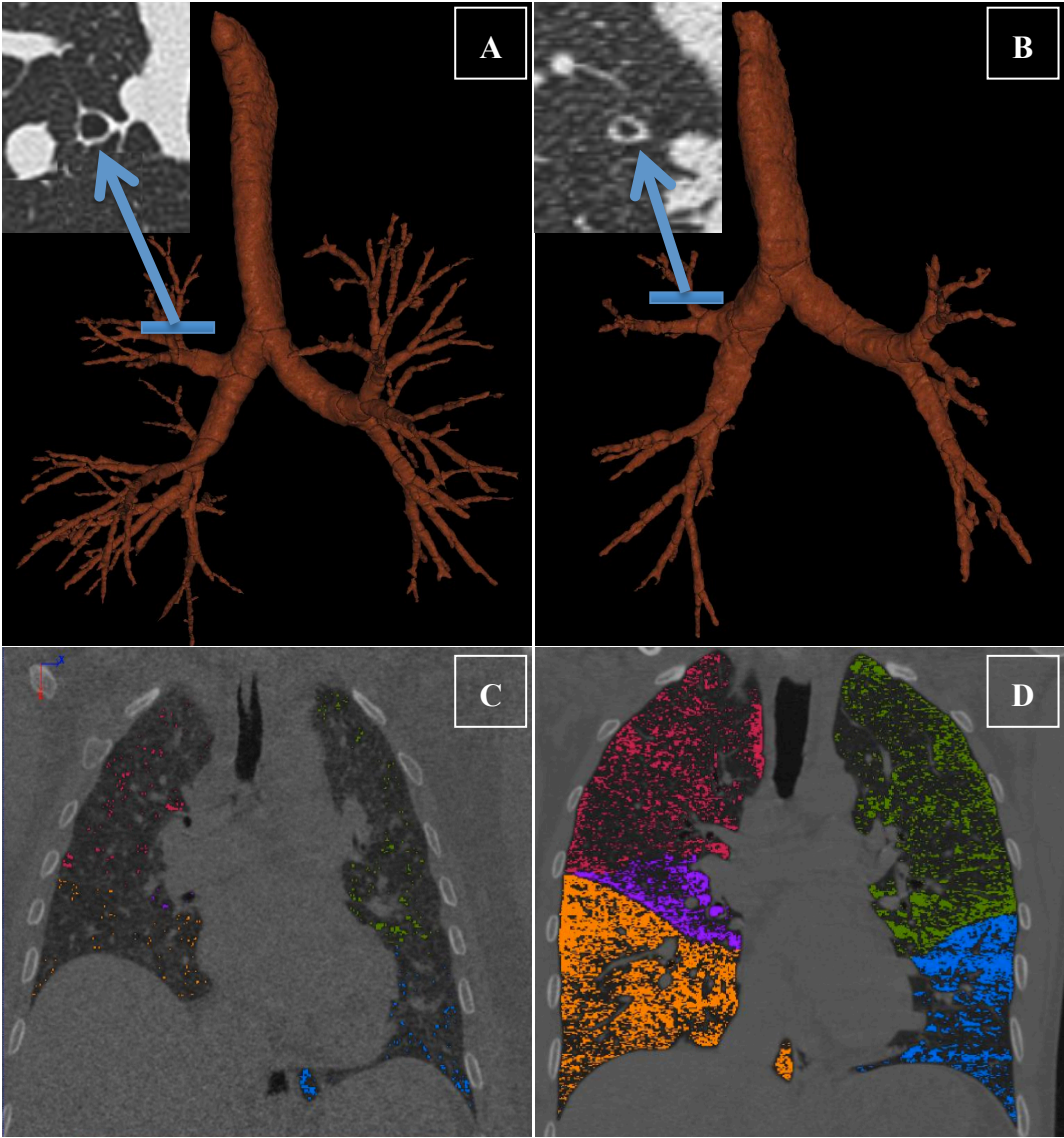


### **Figure 3.34: Quantitative CT in healthy and severe asthma subjects**

Three-dimensional reconstruction of an airway tree from (A) a healthy subject and (B) a severe asthmatic subject using PW2 software illustrating that in healthy subjects sub-segmental airways can be reconstructed to more generations than in asthma. This is due to increased airway narrowing and closure in asthma. The insets illustrate the cross-section of RB1 in health and severe asthma showing that the lumen is narrowed in asthma with a decrease in total area and an increase in percentage wall area, but with a relatively preserved wall area. Coronal section of expiratory CT from (C) a healthy subject and (D) a severe asthma subject showing increased low attenuation areas (colour coded according to lung lobes) in severe asthma compared to healthy subject

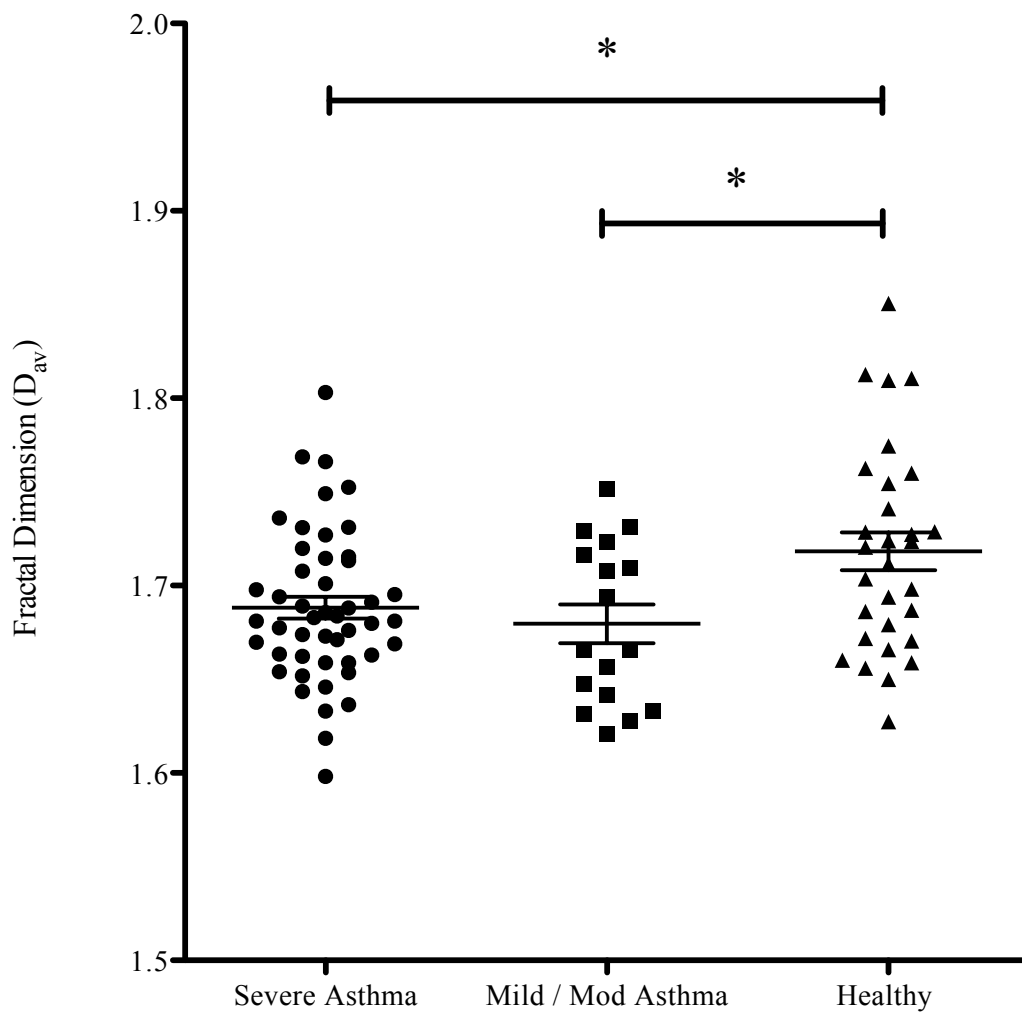


**Figure 3.35: Fractal Dimension of segmented airway tree**

Fractal dimension of segmented airway tree on an inspiratory CT scan in asthmatic and healthy subjects ( $p < 0.05$ , ANOVA)

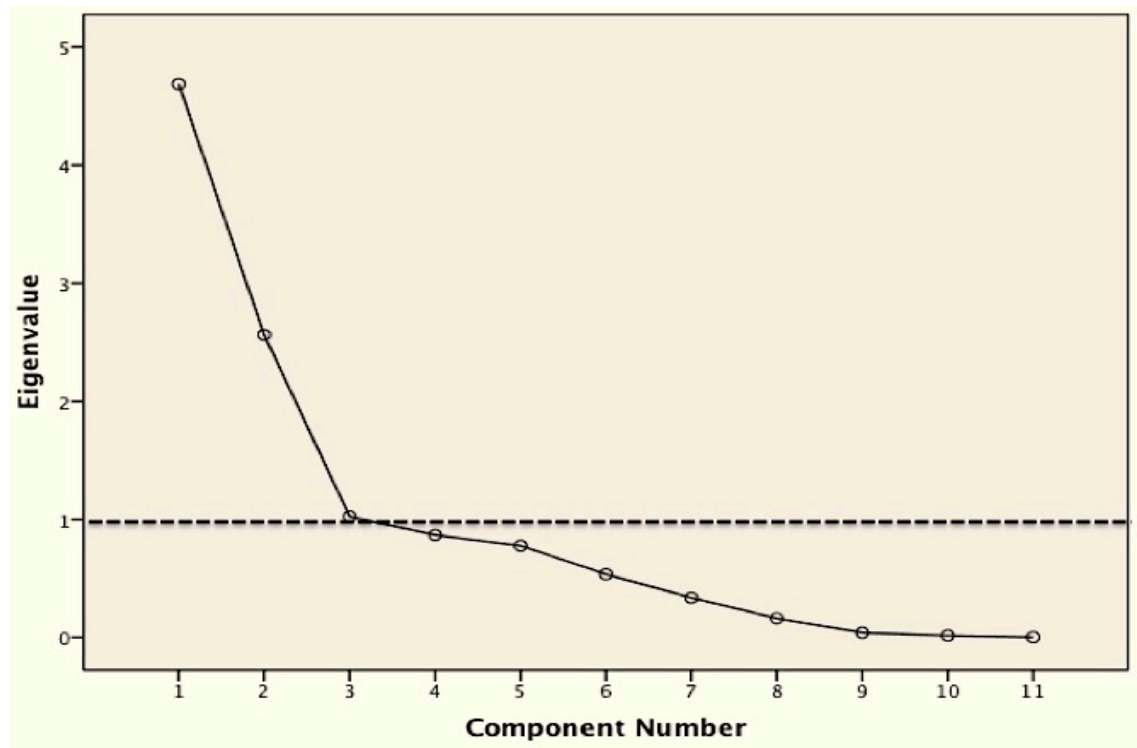


**Figure 3.36: Component number based on Kaiser criterion**

Scree plot showing Eigenvalues for components; reference line at Eigenvalue 1.

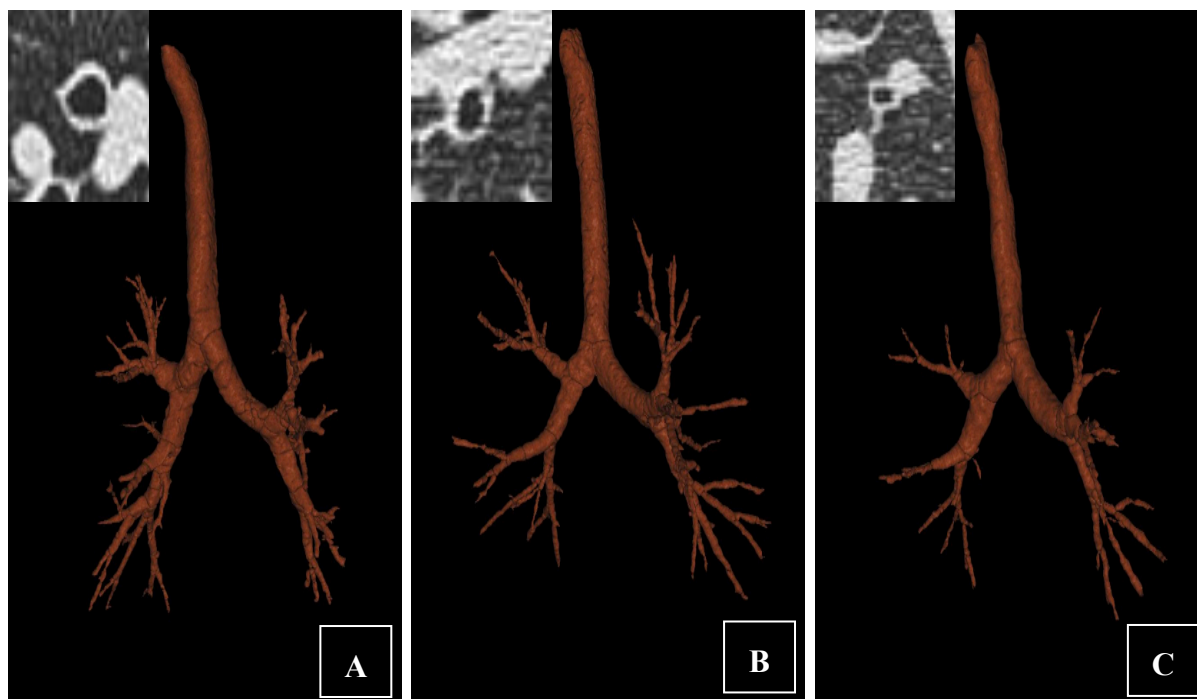


**Figure 3.37: Proximal airway remodelling in asthma phenotypes**

Pictures of segmented airway tree and RB1 CT cross-section (insets) of asthma patients from Cluster 1 (A), Cluster 2 (B) and Cluster 3 (C)

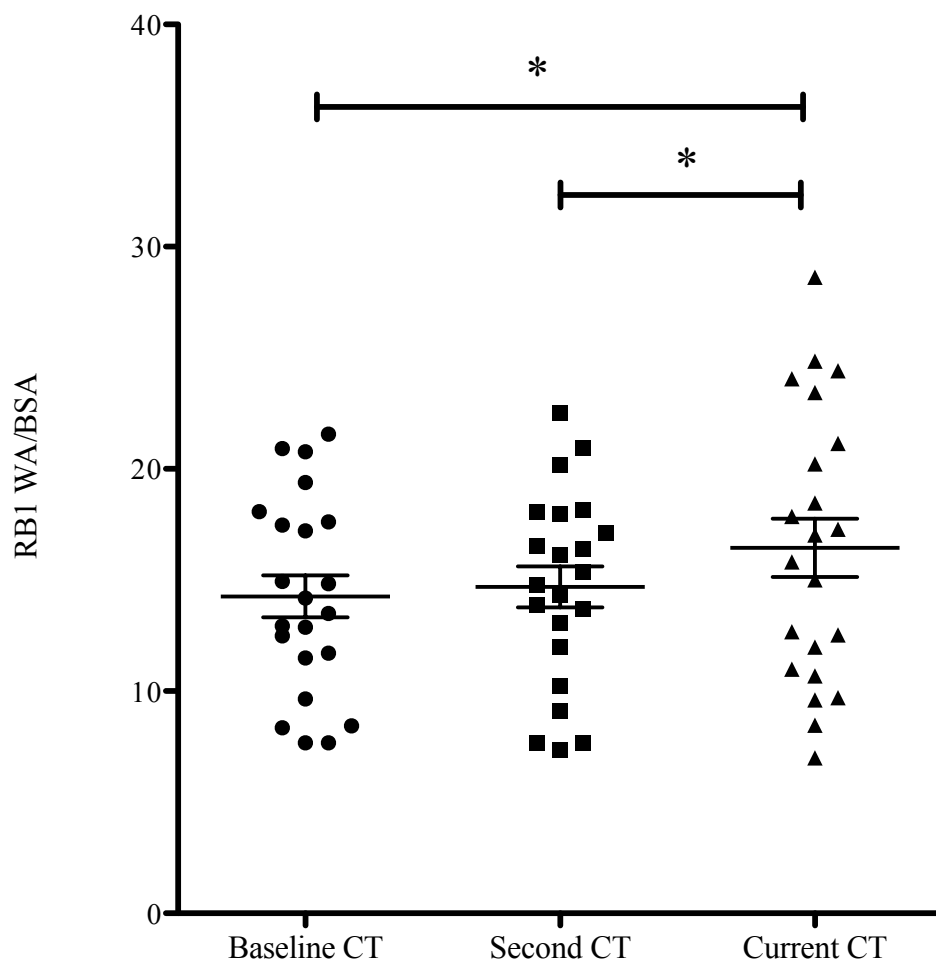


**Figure 3.38: Temporal change in RB1 WA/BSA**

All asthmatic subjects who had two retrospective CT scans available (n=22) showed an increase in mean (SEM) WA/BSA over time (\* $p < 0.05$ , repeated-measure ANOVA)

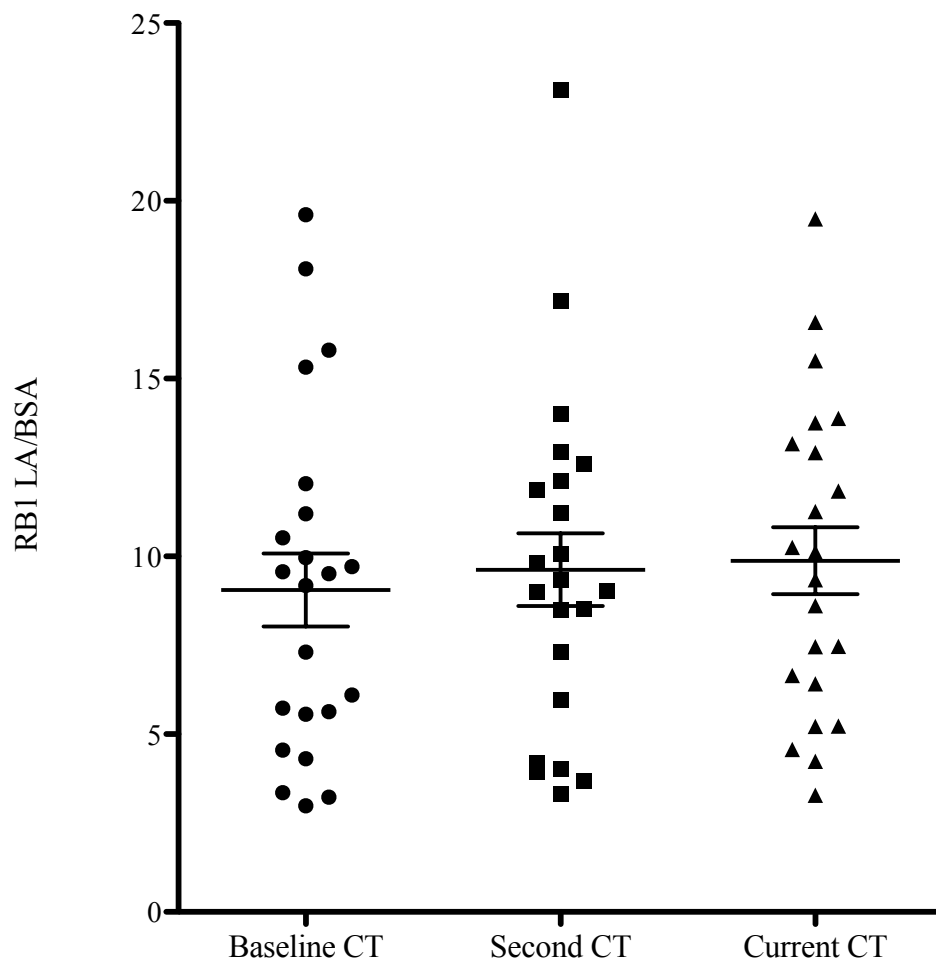


**Figure 3.39: Temporal change in RB1 LA/BSA**

All asthmatic subjects who had two retrospective CT scans available (n=22) showed no significant change in mean (SEM) LA/BSA over time ( $p = 0.4$ , repeated-measure ANOVA)

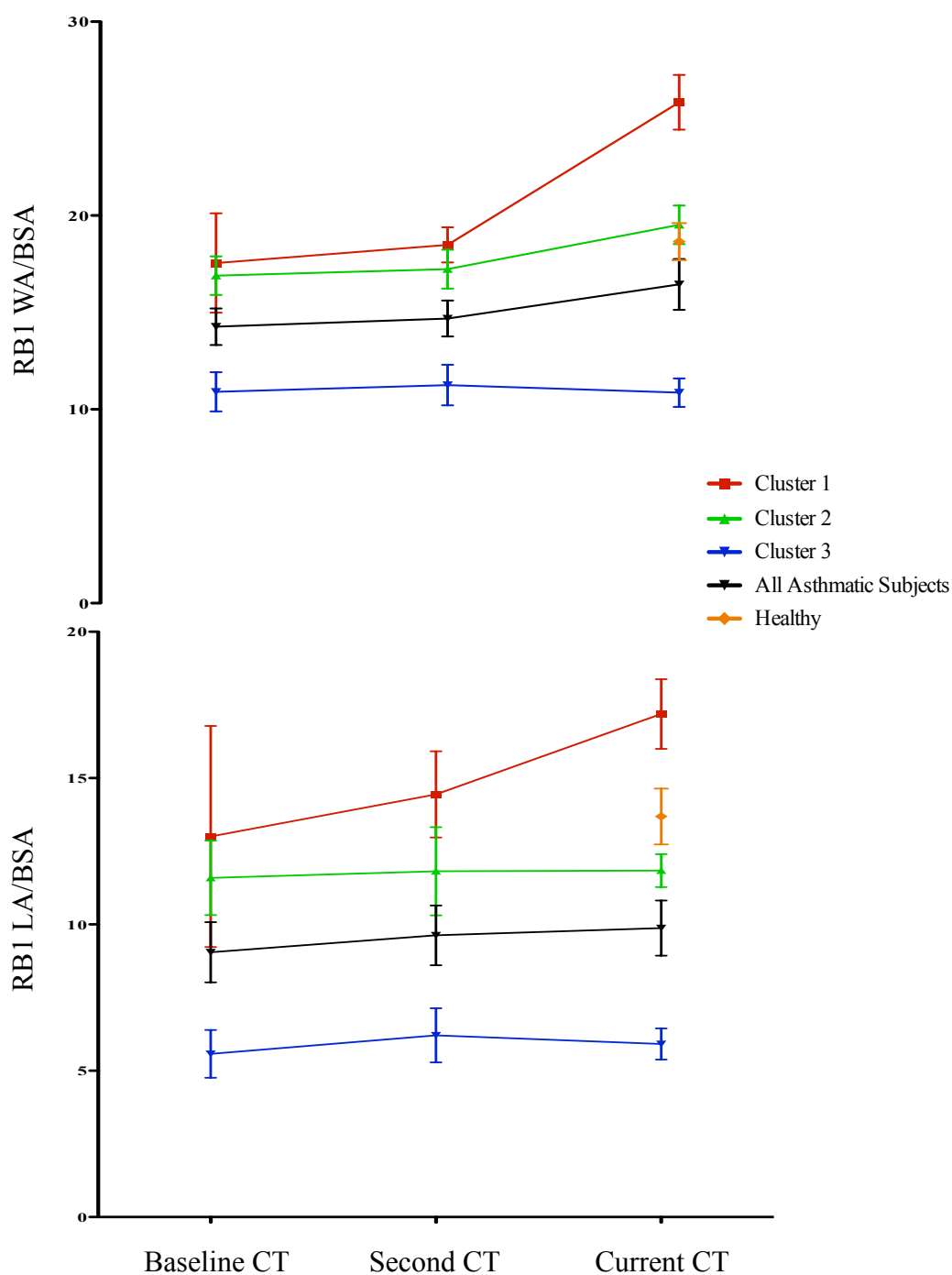


**Figure 3.40: Temporal assessment of airway remodelling in asthma clusters**

Asthma clusters were determined based on current CT data. Retrospective scans were available for temporal assessment of RB1 remodelling



**Table 3.23: Clinical characteristics of asthmatic and healthy subjects**

	Severe Asthmatics (n=48)	Mild/Moderate Asthmatics (n=17)	Healthy Controls (n=30)	Significance (p value)
Age (yrs)	50.7 (1.4)	53.0 (3.9)	56.9 (2.3)	0.09
Gender M:F	24:24	10:7	16:14	0.8
BMI (kg/m <sup>2</sup> )	28.8 (0.9)	28.3 (1.3)	28.3 (1.0)	0.9
BSA (m <sup>2</sup> )	1.9 (0.04)	1.9 (0.05)	1.9 (0.03)	1.0
Disease duration(yrs)	26.8 (2.2)	33.2 (3.3)	x	0.2
Smoking status (%)	Never	77	59	0.2
	Ex	21	35	
	Current	2	6	
Atopy (%)	67	82	18	<0.0005
Aspergillus sensitisation (%)	23	36	7	0.08
Severe exacerbations/year ^	3.0 [1.0 – 5.3]	1.0 [0 – 2.5]	x	0.007
Modified JACQ score (symptoms only)	2.6 (0.2)	1.8 (0.4)	x	0.04
AQLQ score	8.3 (3.7)	5.2 (0.3)	x	0.6
Pre Bronchodilator FEV <sub>1</sub> % predicted	69.2 (2.9)	79.0 (5.7)	110.9 (2.9)	<0.0005* <sub>∞</sub>
Pre Bronchodilator FEV <sub>1</sub> /FVC (%)	67.9 (1.8)	69.7 (2.6)	78.3 (1.0)	<0.0005* <sub>∞</sub>
Post Bronchodilator FEV <sub>1</sub> % predicted	74.4 (2.8)	81.3 (5.5)	112.7 (3.2)	<0.0005* <sub>∞</sub>
Post Bronchodilator FEV <sub>1</sub> /FVC (%)	69.9 (1.8)	69.8 (2.6)	79.9 (1.1)	<0.0005* <sub>∞</sub>
Bronchodilator response (BDR) %	9.6 (2.1)	3.5 (1.6)	1.6 (0.6)	0.0007*
Mid Expiratory Flow (L/s)	2.0 (0.2)	1.8 (0.3)	3.2 (0.2)	<0.0005* <sub>∞</sub>
Vital Capacity (L)	3.7 (0.2)	4.0 (0.2)	4.2 (0.2)	0.2
Functional Residual Capacity (L)	3.0 (0.2)	2.9 (0.3)	3.1 (0.2)	0.9
Residual Volume (L)	2.1 (0.2)	2.0 (0.3)	2.2 (0.2)	0.8
Total Lung Capacity (L)	5.8 (0.3)	5.9 (0.4)	6.3 (0.3)	0.6
Residual Volume / Total Lung Capacity (%)	35.7 (1.5)	31.2 (2.8)	33.6 (3.1)	0.7
Methacholine PC20 (mg/ml) #	2.0 (0.7 – 6.0)	2.4 (0.8 – 7.3)	24.4 (17.6 – 33.7)	<0.0005* <sub>∞</sub>
FE <sub>NO</sub> (ppb) #	36.1 (27.7 – 47.0)	26.4 (18.6 – 37.5)	27.2 (21.1 – 34.7)	0.2
Total IgE (kU/L) #	179.0 (128.7 – 248.9)	137.0 (68.5 – 273.8)	25.5 (15.8 – 41.0)	<0.0005* <sub>∞</sub>
Inhaled CS (%)	100	82	x	0.02
Inhaled CS dose BDP (µg/24hrs) ^	2000 [1600 – 2000]	1000 [600 -2000]	x	0.004
LABA (%)	94	71	x	0.03
Oral CS (%)	68	0	x	<0.0005
Montelukast (%)	32	0	x	0.007
Theophylline (%)	40	24	x	0.3
Sputum Eosinophils (%) #	4.3 (2.5 – 7.5)	2.0 (0.8 – 4.8)	0.7 (0.4 -1.1)	<0.0005*
Sputum Total Neutrophils X 10 <sup>6</sup> (cells/g)	2.8 (1.1)	4.0 (1.8)	2.9 (0.8)	0.9

Data expressed as mean (SEM); # Geometric mean (95% CI); ^Median [IQR]. Intergroup comparison:

parametric data, one-way ANOVA with Tukey test to compare all pairs of columns, \* $p < 0.05$  SA vs HC,  $\infty p < 0.005$  MA vs HC, § $p < 0.05$  SA vs MA;

non-parametric data, Kruskal-Wallis test with Dunn's multiple comparison test to compare all pairs of columns, \* $p < 0.05$  SA vs HC,  $\infty p < 0.005$  MA vs HC, § $p < 0.05$  SA vs MA; Mann-Whitney U test.

Pearson Chi-square and Fisher's exact test to compare ratios

BDP equivalents; Fluticasone 2:1, Budesonide 1.25:1, Mometasone 1.25:1, QVAR 2:1, Ciclesonide 2.5:1.

*Definitions of abbreviations:* SA = Severe asthmatics, MA = Mild/moderate asthmatics, HC = Healthy controls, BDP = beclometasone dipropionate, BMI = body mass index, JACS = Juniper Asthma Control Score, FEV<sub>1</sub> = forced expiratory volume in 1 second, FVC = forced vital capacity, CS = corticosteroid, LABA = long acting beta agonist

**Table 3.24: RB1 dimensions of asthmatic and healthy subjects**

	Severe Asthmatics	Mild/Moderate Asthmatics	Healthy Controls	Significance (p value)
Inspiratory	(n=48)	(n=17)	(n=30)	
Wall Area/BSA (mm <sup>2</sup> /m <sup>2</sup> )	18.2 (0.8)	18.5 (0.9)	18.7 (1.0)	0.9
Lumen Area/BSA (mm <sup>2</sup> /m <sup>2</sup> )	11.3 (0.6)	11.7 (0.7)	13.7 (1.0)	<u>0.08</u>
Total Area/BSA (mm <sup>2</sup> /m <sup>2</sup> )	29.5 (1.4)	30.2 (1.6)	32.3 (1.9)	0.4
Wall Area (mm <sup>2</sup> )	34.8 (1.5)	35.6 (2.0)	36.1 (2.0)	0.8
Lumen Area (mm <sup>2</sup> )	21.6 (1.2)	22.6 (1.6)	26. (1.9)	<u>0.06</u>
Total Area (mm <sup>2</sup> )	58.7 (1.9)	58.2 (3.4)	62.6 (3.8)	0.4
Length (mm)	12.8 (0.4)	11.8 (0.6)	13.7 (0.8)	0.2
Wall Volume (mm <sup>3</sup> )	437.6 (21.0)	412.9 (21.5)	496.3 (40.5)	0.2
Lumen Volume (mm <sup>3</sup> )	272.3 (16.4)	259.0 (12.9)	366.4 (35.6)	<b>0.007*</b> <sup>∞</sup>
Total Volume (mm <sup>3</sup> )	709.9 (36.8)	672.0 (32.7)	862.8 (75.7)	<b>0.05</b>
%Wall Volume	62.4 (0.5)	61.4 (0.7)	58.5 (0.7)	<b>&lt;0.0005*</b> <sup>∞</sup>

Data expressed as mean (SEM). Intergroup comparisons: one-way ANOVA with Tukey test to compare all pairs of columns. \*p<0.05 SA vs HC, <sup>∞</sup>p<0.005 MA vs HC, §p<0.05 SA vs MA

Definitions of abbreviations: SA = Severe asthmatics, MA = Mild/moderate asthmatics, HC = Healthy controls, BSA = Body Surface Area.

**Table 3.25: Other proximal airway dimensions**

Inspiratory CT scans	Severe Asthmatics	Mild/Moderate Asthmatics	Healthy Controls	Significance (p value)
RB10	(n=45)	(n=15)	(n=30)	
Wall Area/BSA (mm <sup>2</sup> /m <sup>2</sup> )	17.6 (0.6)	18.2 (1.5)	19.2 (0.6)	0.3
Lumen Area/BSA (mm <sup>2</sup> /m <sup>2</sup> )	11.8 (0.6)	12.7 (1.2)	14.0 (0.7)	<b>0.05*</b>
Total Area/BSA (mm <sup>2</sup> /m <sup>2</sup> )	29.7 (1.1)	30.9 (2.6)	33.2 (1.3)	0.1
Wall Area (mm <sup>2</sup> )	33.8 (1.1)	34.4 (2.6)	37.1 (1.1)	0.2
Lumen Area (mm <sup>2</sup> )	22.4 (1.0)	24.0 (2.0)	27.1 (1.3)	<b>0.02*</b>
Total Area (mm <sup>2</sup> )	56.3 (2.0)	58.4 (4.5)	64.2 (2.4)	<u>0.06</u>
Length (mm)	15.4 (1.1)	12.2 (1.2)	12.8 (0.9)	0.1
Wall Volume (mm <sup>3</sup> )	504.5 (32.5)	411.4 (44.2)	465.9 (31.5)	0.3
Lumen Volume (mm <sup>3</sup> )	332.5 (22.5)	284.5 (31.4)	334.7 (22.5)	0.5
Total Volume (mm <sup>3</sup> )	837.0 (54.5)	696.0 (74.7)	800.6 (53.0)	0.4
%Wall Volume	60.5 (0.5)	59.1 (0.7)	58.2 (0.6)	<b>0.008*</b>
LB1+2	(n=43)	(n=15)	(n=26)	
Wall Area/BSA (mm <sup>2</sup> /m <sup>2</sup> )	21.9 (0.8)	20.5 (1.2)	20.1 (0.9)	0.3
Lumen Area/BSA (mm <sup>2</sup> /m <sup>2</sup> )	14.7 (1.0)	13.1 (0.9)	14.0 (0.8)	0.6
Total Area/BSA (mm <sup>2</sup> /m <sup>2</sup> )	36.6 (1.8)	33.6 (2.1)	34.1 (1.7)	0.5
Wall Area (mm <sup>2</sup> )	41.5	38.5 (2.0)	39.7 (1.8)	0.5
Lumen Area (mm <sup>2</sup> )	27.8 (1.1)	24.5 (1.6)	27.7 (1.7)	0.6
Total Area (mm <sup>2</sup> )	69.3 (3.4)	62.9 (3.5)	67.3 (3.5)	0.6
Length (mm)	10.9 (0.5)	11.3 (1.1)	12.6 (0.8)	0.2
Wall Volume (mm <sup>3</sup> )	431.6 (16.8)	418.0 (35.8)	506.7 (47.5)	0.1
Lumen Volume (mm <sup>3</sup> )	280.7 (13.2)	265.0 (22.7)	359.6 (39.6)	<b>0.03*</b>
Total Volume (mm <sup>3</sup> )	712.3 (28.4)	683.0 (57.8)	866.3 (86.9)	<u>0.07</u>
%Wall Volume	60.9 (0.7)	61.3 (0.5)	59.5 (0.6)	0.2
LB10	(n=42)	(n=14)	(n=27)	
Wall Area/BSA (mm <sup>2</sup> /m <sup>2</sup> )	19.2 (0.6)	19.6 (1.5)	20.6 (0.9)	0.4
Lumen Area/BSA (mm <sup>2</sup> /m <sup>2</sup> )	13.0 (0.7)	12.7 (1.3)	15.9 (1.1)	<b>0.03*</b>
Total Area/BSA (mm <sup>2</sup> /m <sup>2</sup> )	32.2 (1.2)	32.2 (2.7)	36.6 (1.9)	0.1
Wall Area (mm <sup>2</sup> )	36.0 (0.9)	37.3 (2.4)	40.0 (1.5)	0.08
Lumen Area (mm <sup>2</sup> )	24.4 (1.1)	24.1 (2.1)	30.7 (1.8)	<b>0.004*</b> <sub>∞</sub>
Total Area (mm <sup>2</sup> )	60.4 (1.9)	61.4 (4.4)	70.8 (3.3)	<b>0.02*</b>
Length (mm)	15.5 (1.0)	15.4 (1.2)	14.1 (1.0)	0.6
Wall Volume (mm <sup>3</sup> )	553.4 (37.5)	561.3 (51.5)	557.1 (41.0)	1.0
Lumen Volume (mm <sup>3</sup> )	372.8 (28.0)	361.3 (38.2)	430.1 (40.3)	0.4
Total Volume (mm <sup>3</sup> )	926.2 (64.3)	922.6(88.5)	987.2 (80.0)	0.8
%Wall Volume	60.2 (0.7)	61.2 (1.0)	57.2 (0.7)	<b>0.003*</b> <sub>∞</sub>

parametric data, one-way ANOVA with Tukey test to compare all pairs of columns, \*p<0.05 SA vs HC, ∞p<0.005 MA vs HC, §p<0.05 SA vs MA

Definitions of abbreviations: SA = Severe asthmatics, MA = Mild/moderate asthmatics, HC = Healthy controls, BSA = Body Surface Area.

**Table 3.26: Dimensions of hypothetical airways (Pi10, Po20)**

	<b>Severe Asthmatics (n=48)</b>	<b>Mild/Moderate Asthmatics (n=17)</b>	<b>Healthy Controls (n=30)</b>	<b>Significance (p value)</b>
<b>Inspiratory</b>				
<b>Pi<sub>10</sub>WA (mm<sup>2</sup>)</b>	16.5 (0.3)	16.1 (0.4)	15.2 (0.2)	<b>0.002*</b>
<b>Po<sub>20</sub>%WA</b>	65.2 (0.3)	64.6 (0.6)	63.4 (0.3)	<b>0.002*</b>

Data expressed as mean (SEM). Intergroup comparisons: one-way ANOVA with Tukey test to compare all pairs of columns. \*p<0.05 SA vs HC, ∞p<0.005 MA vs HC, §p<0.05 SA vs MA

*Definitions of abbreviations:* Pi10 = inner perimeter of 10 mm, Po20 = outer perimeter of 20 mm, SA = Severe asthmatics, MA = Mild/moderate asthmatics, HC = Healthy controls

**Table 3.27: Densitometry Indices in asthmatic and healthy subjects**

	Severe Asthmatics (n=48)	Mild/Moderate Asthmatics (n=17)	Healthy Controls (n=30)	Significance (p value)
<b>Inspiratory</b>				
Lung Volume (L)	5.15	5.02	5.49	0.4
Mean Lung Density (HU)	-830.9 (6.0)	-831.5 (10.4)	-837.8 (4.8)	0.7
VI -950 (%)	11.2 (0.9)	11.9 (1.8)	10.1 (1.0)	0.6
Percentile 15 (HU)	-932.8 (4.5)	-934.3 (6.8)	-930.1 (4.1)	0.9
VI -850 (%)	59.1 (2.3)	59.9 (4.2)	61.8 (2.4)	0.8
<b>Expiratory</b>				
Lung Volume (L)	2.9 (0.1)	2.9 (0.3)	2.8 (0.1)	0.9
Mean Lung Density (HU)	-713.3 (7.8)	-719.5 (15.2)	-695.6 (10.0)	0.3
<b>Air-trapping Indices</b>				
Expiratory VI -850 (%)	19.7 (1.7)	22.0 (4.4)	16.2 (2.1)	0.3
MLD E/I ratio	0.861 (0.01)	0.866 (0.02)	0.830 (0.01)	<b>0.04</b>
VI <sub>-850</sub> E-I (%)	-30.4 (1.4)	-29.1 (4.6)	-36.9 (1.9)	<b>0.04</b>
VI <sub>-850-950</sub> E-I (%)	-39.1 (1.7)	-37.8 (4.9)	-45.6 (2.2)	<u>0.08</u>

Data expressed as mean (SEM). Intergroup comparisons: one-way ANOVA with Tukey test to compare all pairs of columns. All densitometry indices were standardised for extra-thoracic air, blood and three electron density rods as described in [section 3.2.3.7].

*Definitions of abbreviations:* VI<sub>-850-950</sub> E-I = Voxel index change of % voxels between -950 HU and -850 HU on paired expiratory and inspiratory scans, VI<sub>-850</sub> E-I = Voxel index change of % voxels below -850 HU on paired expiratory and inspiratory scans

**Table 3.28: Fractal Dimensions**

	Severe Asthmatics (n=48)	Mild/Moderate Asthmatics (n=17)	Healthy Controls (n=30)	Significance (p value)
<b>Airway Tree</b>				
<i>Inspiratory</i>				
<b>D<sub>av</sub></b>	1.688 (0.01)	1.680 (0.01)	1.718 (0.01)	<b>0.007*</b> <sup>∞</sup>
<b>D<sub>sc</sub></b>	1.649 (0.01)	1.637 (0.01)	1.677 (0.01)	<b>0.001*</b> <sup>∞</sup>
<b>D<sub>e</sub></b>	1.794 (0.01)	1.777 (0.01)	1.824 (0.01)	<b>0.02</b> <sup>∞</sup>
<b>D<sub>sce</sub></b>	1.745 (0.01)	1.731 (0.01)	1.764 (0.01)	<b>0.03</b> <sup>∞</sup>
<b>Terminal Airspace</b>				
<b>Inspiratory LAC-D -950</b>	1.972 (0.02)	1.956 (0.03)	1.987 (0.02)	0.7
<b>Expiratory LAC-D -850</b>	1.812 (0.01)	1.802 (0.02)	1.813 (0.02)	0.8

Data expressed as mean (SEM). Intergroup comparisons: one-way ANOVA with Tukey test to compare all pairs of columns. \*p<0.05 SA vs. HC, <sup>∞</sup>p<0.005 MA vs. HC, §p<0.05 SA vs. MA

D<sub>av</sub>: fractal dimension, which is averaged over all 10 global scan locations.

D<sub>sc</sub>: same as D<sub>av</sub> but corrected for periods of no change for the log-log plot of box size and count.

D<sub>e</sub>: same as D<sub>av</sub>, but for each grid size the box-count that required the lowest number of boxes was used.

D<sub>sce</sub>: combination of all the above

*Definitions of abbreviations:* D<sub>av</sub> = Averaged D, D<sub>sc</sub> = Slope-corrected D, D<sub>e</sub> = Most-efficient covering D, D<sub>sce</sub> = Slope-corrected most-efficient covering D, LAC = Low attenuation clusters, LAC-D -950 = Fractal dimension of LAC at threshold of -950 HU, LAC-D -850 = Fractal dimension of LAC at threshold of -850 HU

**Table 3.29: Univariate analysis of relationship between proximal airway dimensions on inspiratory scan and CT air-trapping indices.**

<b>n=65</b>	<b>Expiratory Mean Lung Density (HU)</b>	<b>Expiratory VI -850 (%)</b>	<b>MLD E/I ratio</b>	<b>VI<sub>-850-950</sub> E-I (%)</b>	<b>VI<sub>-850</sub> E-I (%)</b>
<b>RB1 LA/BSA (mm<sup>2</sup>/m<sup>2</sup>)</b>	-0.13	0.07	0.1	-0.07	-0.01
<b>RB1 WA/BSA (mm<sup>2</sup>/m<sup>2</sup>)</b>	-0.07	-0.02	0.11	-0.09	-0.01
<b>RB1 TA/BSA (mm<sup>2</sup>/m<sup>2</sup>)</b>	-0.1	0.02	0.11	-0.09	-0.01
<b>RB1 Lumen Volume (mm<sup>3</sup>)</b>	-0.15	0.16	0.03	-0.04	-0.04
<b>RB1 Wall Volume (mm<sup>3</sup>)</b>	-0.01	0.14	0.04	-0.04	-0.04
<b>RB1 Total Volume (mm<sup>3</sup>)</b>	-0.14	0.15	0.04	-0.04	-0.04
<b>RB1 %WV</b>	0.14	-0.2	0.002	0.04	0.03
<b>Pi<sub>10</sub> WA (mm<sup>2</sup>)</b>	-0.16	0.29*	0.28*	0.40**	0.35**
<b>Po<sub>20</sub> %WA</b>	-0.05	0.17	0.28*	0.47**	0.42**

Data expressed as pearson correlation coefficient, \*p<0.05, \*\*p<0.001

*Definitions of abbreviations:* BSA = body surface area, LA = lumen area, WA = wall area



**Table 3.30: Univariate analysis of relationship between proximal airway dimensions on inspiratory scan and clinical indices.**

n=65	Post-BD FEV <sub>1</sub> % predicted	Post-BD FEV <sub>1</sub> /FVC (%)	Mid Expiratory Flow (L/s)	RV/TLC (%)	Disease Duration (years)	Sputum Neutrophils (%)	Log Sputum Eosinophil count	JACQ score
RB1 LA/BSA (mm <sup>2</sup> /m <sup>2</sup> )	-0.10	-0.06	-0.02	0.30	-0.02	0.13	0.08	-0.17
RB1 WA/BSA (mm <sup>2</sup> /m <sup>2</sup> )	-0.07	-0.04	-0.05	0.20	0.08	0.10	0.08	-0.13
RB1 TA/BSA (mm <sup>2</sup> /m <sup>2</sup> )	-0.09	-0.06	-0.04	0.25	0.03	0.11	0.08	-0.15
RB1 Lumen Volume (mm <sup>3</sup> )	-0.01	-0.06	0.08	0.21	-0.04	0.10	-0.03	-0.18
RB1 Wall Volume (mm <sup>3</sup> )	0.05	-0.05	0.08	0.11	0.05	0.06	-0.04	-0.16
RB1 Total Volume (mm <sup>3</sup> )	0.03	-0.06	0.08	0.15	0.01	0.08	-0.04	-0.17
RB1 %WV	0.08	0.05	-0.02	-0.35*	0.19	-0.11	-0.06	0.19
Pi <sub>10</sub> WA (mm <sup>2</sup> )	-0.21	-0.27*	-0.34*	0.21	-0.07	0.04	-0.10	0.17
Po <sub>20</sub> %WA	-0.11	-0.10	-0.14	0.02	0.05	0.03	-0.22	0.19

Data expressed as pearson correlation coefficient, \*p<0.05, \*\*p<0.001

*Definitions of abbreviations:* BSA = body surface area, LA = lumen area, WA = wall area, JACQ = Juniper Asthma Control Questionnaire, FEV<sub>1</sub> = forced expiratory volume in 1 second, FVC = forced vital capacity, BD = bronchodilator, RV = residual volume, TLC = total lung capacity

**Table 3.31: Univariate analysis of relationship between CT air-trapping indices and clinical indices.**

n=65	Post-BD FEV <sub>1</sub> % predicted	Post-BD FEV <sub>1</sub> /FVC (%)	Mid Expiratory Flow (L/s)	RV/TLC (%)	Disease Duration (years)	Sputum Neutrophils (%)	Log Sputum Eosinophil count	JACQ score
Expiratory Mean Lung Density (HU)	0.45**	0.64**	0.47**	-0.63**	-0.35*	0.03	-0.38*	-0.10
Expiratory VI -850 (%)	-0.48**	-0.68**	-0.48**	0.64**	0.27	0.10	0.23	0.15
MLD E/I ratio	-0.40**	-0.48**	-0.60**	0.46**	0.29*	0.17	0.02	0.23
VI <sub>-850-950</sub> E-I (%)	-0.30*	-0.32*	-0.41**	0.34*	0.03	0.34*	-0.23	0.30*
VI <sub>-850</sub> E-I (%)	-0.22	-0.15	-0.33*	0.25	-0.03	0.37*	-0.27	0.28*

Data expressed as pearson correlation coefficient, \*p<0.05, \*\*p<0.001

*Definitions of abbreviations:* BSA = body surface area, LA = lumen area, WA = wall area, JACQ = Juniper Asthma Control Questionnaire, FEV<sub>1</sub> = forced expiratory volume in 1 second, FVC = forced vital capacity, BD = bronchodilator, RV = residual volume, TLC = total lung capacity

**Table 3.32: Component loading of selected variables**

	<b>Components</b>		
	<b>1</b>	<b>2</b>	<b>3</b>
<b>RB1 LA/BSA</b>	.949*	.020	.117
<b>RB1 LV</b>	.935	.021	-.024
<b>RB1 TA</b>	.905	.050	.231
<b>RB1 WA/BSA</b>	.876	.021	.249
<b>RB1 WV</b>	.831	.045	.049
<b>RB1 %WV</b>	-.682	.035	.180
<b>MLD E/I ratio</b>	.054	.937*	-.101
<b>VI<sub>-850-950</sub> E-I</b>	-.102	.901	.090
<b>Expiratory VI -850</b>	.138	.757	-.427
<b>Expiratory LAC-D -850</b>	-.063	-.301	.745*
<b>Inspiratory D<sub>av</sub></b>	.244	.054	.610

Rotated Component Matrix

Extraction Method: Principal Component Analysis.

Rotation Method: Varimax with Kaiser Normalization

Component loading of the eleven original variables with the three main components derived by factor analysis in the 62 subjects with asthma (\* indicates the predominant variable in each component).

**Table 3.33: Clinical characteristics of asthma phenotypes**

		Asthma Cluster 1 Severe air trapping, bronchial wall thickening and bronchial lumen dilatation]	Asthma Cluster 2 [Moderate air trapping]	Asthma Cluster 3 [Severe air trapping and bronchial lumen narrowing]	Significance (p value)
		(n=11)	(n=34)	(n=17)	
Age (yrs)		51.9 (2.9)	49.3 (2.2)	54.7 (2.5)	0.3
Gender M:F		4:7	17:17	9:8	0.7
BMI (kg/m <sup>2</sup> )		25.0 (1.0)	28.3 (0.9)	31.5 (1.8)	<b>0.02</b> <sub>∞</sub>
BSA (m <sup>2</sup> )		1.9 (0.1)	1.9 (0.03)	2.0 (0.1)	0.3
Subjects with severe asthma (%)		81.8	58.8	94.1	<b>0.02</b>
Disease duration(yrs)		26. 3 (5.1)	26.4 (3.4)	27. 2 (4.4)	1.0
Smoking status (%)	Never	60	74	82	0.6
	Ex	40	23	18	
	Current	0	3	0	
Atopy (%)		73	69	69	1.0
Aspergillus sensitisation (%)		36	17	29	0.4
Severe exacerbations/year ^		2.5 [1 – 4.25]	1.5 [0 – 5.0]	2 [1.0 – 6.5]	0.6
Modified JACQ score (symptoms only)		2.1 (0.3)	2.0 (0.3)	2.8 (0.3)	0.1
AQLQ score		4.9 (0.3)	5.0 (0.2)	4.1 (0.3)	<u>0.09</u>
Pre Bronchodilator FEV <sub>1</sub> % predicted		58.0 (5.4)	80.7 (3.4)	64.0 (4.7)	<b>0.001</b> *§
Pre Bronchodilator FEV <sub>1</sub> /FVC (%)		64.8 (4.1)	71.1 (1.7)	67.0 (3.5)	0.2
Post Bronchodilator FEV <sub>1</sub> % predicted		63.8 (5.6)	83.8 (3.4)	70.6 (4.0)	<b>0.005</b> *§
Post Bronchodilator FEV <sub>1</sub> /FVC (%)		67.0 (4.4)	72.8 (1.8)	67.2 (2.9)	0.2
Bronchodilator response (%)		11.1 (3.7)	4.4 (1.2)	13.9 (5.0)	<b>0.04</b> §
Mid Expiratory Flow (L/s)		2.0 (0.6)	2.1 (0.2)	1.9 (0.3)	0.8
Vital Capacity (L)		3.5 (0.3)	4.0 (0.2)	3.6 (0.4)	0.4
Functional Residual Capacity (L)		3.6 (0.4)	2.7 (0.2)	2.7 (0.4)	<u>0.06</u>
Residual Volume (L)		2.7 (0.3)	1.7 (0.1)	2.1 (0.3)	<b>0.02</b> *
Total Lung Capacity (L)		6.2 (0.5)	5.7 (0.3)	5.8 (0.6)	0.8
Residual Volume / Total Lung Capacity (%)		43.5 (4.0)	29.1 (1.4)	35.5 (3.3)	<b>0.001</b> *
Methacholine PC20 (mg/ml) #		1.5 (0.1 – 16.4)	3.7 (1.2 – 11.5)	0.7 (0.07 – 5.6)	0.2
FE <sub>NO</sub> (ppb) #		37.5 (20.0 – 70.2)	30.5 (22.6 – 41.3)	38.8 (24.5 (61.4)	0.6
Total IgE (kU/L) #		227.2 (81.3 – 634.9)	139.2 (97.3 – 199.1)	217.9 (110.0 – 432.4)	0.3
Inhaled CS (%)		100	91	100	0.3
Inhaled CS dose BDP (µg/24hrs) ^		2000 [1450 – 2000]	2000 [1000 – 2000]	2000 [1500 – 2000]	0.2
LABA (%)		100	77	100	<b>0.03</b>
Oral CS (%)		60	41	53	0.5
Montelukast (%)		10	24	29	0.5
Theophylline (%)		40	29	35	0.8
Sputum Eosinophils (%) #		2.8 (0.9 – 8.4)	3.3 (1.6 – 6.7)	5.7 (1.5 – 20.6)	0.6
Sputum Total Neutrophils X 10 <sup>6</sup> (cells/g)		2.0 (0.6)	2.4 (0.8)	2.4 (0.6)	0.9

Data expressed as mean (SEM); # Geometric mean (95% CI); ^Median [IQR].

Intergroup comparisons:

Parametric data, one-way ANOVA with Tukey test to compare all pairs of columns.

\* $p < 0.05$  AC 1 vs AC 2,  $\infty p < 0.05$  AC 1 vs AC 3, § $p < 0.05$  AC 2 vs AC 3.

non-parametric data, Kruskal-Wallis test with Dunn's multiple comparison test to compare all pairs of columns, \* $p < 0.05$  AC 1 vs AC 2,  $\infty p < 0.05$  AC 1 vs AC 3, § $p < 0.05$  AC 2 vs AC 3

Pearson Chi-square and Fisher's exact test to compare ratios.

BDP equivalents; Fluticasone 2:1, Budesonide 1.25:1, Mometasone 1.25:1, QVAR 2:1, Ciclesonide 2.5:1.

*Definitions of abbreviations:* AC = asthma cluster, BSA = body surface area, JACQ = Juniper Asthma Control Questionnaire, AQLQ = asthma quality of life questionnaire, FEV<sub>1</sub> = forced expiratory volume in 1 second, FVC = forced vital capacity, FE<sub>NO</sub> = fraction of exhaled nitric oxide, CS = corticosteroid, BDP = beclometasone dipropionate, LABA = Long acting  $\beta$ 2 agonist

**Table 3.34: Quantitative CT indices of asthma phenotypes**

	Cluster 1 [Severe air-trapping, bronchial wall thickening and bronchial lumen dilatation]	Cluster 2 [Moderate air- trapping]	Cluster 3 [Severe air- trapping and bronchial lumen narrowing]	Significance (p value)
	(n=11)	(n=34)	(n=17)	
<b>Proximal airway dimensions (Inspiratory)</b>				
RB1 %Wall Volume	58.1 (0.8)	62.0 (0.4)	64.8 (0.7)	<0.005*∞§
RB1 Wall Area/BSA (mm <sup>2</sup> /m <sup>2</sup> )	25.0 (1.0)	19.2 (0.4)	12.3 (0.8)	<0.005*∞§
RB1 Lumen Area/BSA (mm <sup>2</sup> /m <sup>2</sup> )	18.0 (0.6)	11.7 (0.3)	6.7 (0.4)	<0.005*∞§
RB1 Total Area/BSA (mm <sup>2</sup> /m <sup>2</sup> )	42.9 (1.5)	30.9 (0.7)	18.9 (1.2)	<0.005*∞§
RB1 Length (mm)	11.6 (0.8)	12.5 (0.4)	13.5 (0.7)	0.2
RB1 Wall Volume (mm <sup>3</sup> )	540.5 (28.0)	453.1 (20.6)	324.2 (25.0)	<0.005∞§
RB1 Wall Volume (% above upper 95% CI of Healthy Controls)	27	15	6	0.3
RB1 Lumen Volume (mm <sup>3</sup> )	392.2 (23.7)	278.0 (13.4)	176.1 (13.1)	<0.005*∞§
RB1 Lumen Volume (% below lower 95% CI of Healthy Controls)	9	65	94	<0.005
RB1 Total Volume (mm <sup>3</sup> )	932.7 (49.2)	731.2 (33.4)	500.3 (37.4)	<0.005*∞§
Pi <sub>10</sub> WA (mm <sup>2</sup> )	16.9 (0.6)	16.2 (0.3)	16.2 (0.3)	0.5
Po <sub>20</sub> %WA	64.7 (0.8)	64.8 (0.4)	65.5 (0.6)	0.6
<b>Air-trapping</b>				
Expiratory VI -850 (%)	23.7 (4.8)	17.2 (2.0)	24.8 (3.4)	0.1
Expiratory VI -850 (% above upper 95% CI of Healthy Controls)	64	29	59	<b>0.045</b>
VI <sub>850-950</sub> E-I (%)	-28.6 (3.9)	-31.7 (2.3)	-27.6 (2.8)	0.5
VI <sub>850</sub> E-I (%)	-35.9 (4.3)	-39.9 (2.7)	-38.3 (3.0)	0.7
MLD E/I ratio	0.876 (0.02)	0.857 (0.01)	0.864 (0.01)	0.6
MLD E/I ratio (% above upper 95% CI of Healthy Controls)	73	53	65	0.5
<b>Fractal Dimension</b>				
Inspiratory Dav	1.712 (0.01)	1.686 (0.01)	1.671 (0.01)	<b>0.04</b> ∞
Inspiratory Dav (% below lower 95% CI of Healthy Controls)	46	65	77	0.2
Expiratory LAC-D -850	1.838 (0.03)	1.814 (0.02)	1.794 (0.01)	0.4

Data expressed as mean (SEM). Intergroup comparisons: one-way ANOVA with Tukey test to compare all pairs of columns. \* $p < 0.05$  AC 1 vs AC 2,  $\infty p < 0.005$  AC 1 vs AC 3, § $p < 0.05$  AC 2 vs AC 3.

Definitions of abbreviations: AC = asthma cluster, BSA = body surface area

**Table 3.35: Between-group and within-group changes in RB1 dimensions at three time points**

	Within group change						Between group change								
	Cluster 1  A  N=3			Cluster 2  B  N=9			Cluster 3  C  N=10			2-1		3-2		3-1	
	Second CT	Current CT	p value (second vs current CT)	Second CT	Current CT	p value (second vs current CT)	Second CT	Current CT	p value (second vs current CT)	Second CT	Current CT	Second CT	Current CT	Second CT	Current CT
WA/BSA (change from baseline CT)	0.9 (1.9) [0.7]	8.3 (2.2) [0.07]	0.01	0.3 (0.6) [0.6]	2.6 (1.8) [0.05]	0.07	0.3 (0.3) [0.3]	-0.04 (0.8) [1.0]	0.6	-0.6 (1.4) [0.7]	-5.7 (2.4) [0.04]	0.01 (0.6) [1.0]	-2.7 (1.4) [0.07]	-0.6 (1.1) [0.6]	-8.3 (1.8) [0.001]
LA/BSA (change from baseline CT)	1.4 (2.5) [0.6]	4.2 (2.8) [0.3]	0.01	0.2 (0.6) [0.7]	0.2 (0.9) [0.8]	0.1	0.6 (0.4) [0.2]	0.3 (0.9) [0.7]	0.7	-1.2 (2.6) [0.7]	-3.9 (2.2) [0.1]	0.4 (0.7) [0.6]	0.1 (1.3) [0.9]	-0.8 (1.5) [0.6]	-3.8 (2.2) [0.1]

Within-group change: Mean (SEM) [p value] change from baseline, assessed using paired sample t-test; Between-group change: Mean (SEM) [p value] difference in mean change from baseline, assessed using independent sample t-test

*Definitions of abbreviations:* BSA = body surface area, WA = wall area, LA = lumen area



**Table 3.36: Radiation risk associated with common radiological examinations in UK compared to research CT examinations**

	DLP		ED		Equivalent period of Natural Background Radiation ¶	Lifetime additional risk of fatal cancer per examination Δ
	75 <sup>th</sup> percentile	Mean	75 <sup>th</sup> percentile	Mean		
<b>CXR (single PA radiograph) ^</b>	x	x	x	0.02	3 days	1 in a million
<b>Pelvic x-ray ^</b>	x	x	x	0.7	4 months	1 in 30,000
<b>Barium swallow ^</b>	x	x	x	1.5	8.5 months	1 in 13,000
<b>Head CT ^^</b>	1015	820	2.1	1.7	9.7 months	1 in 11,700
<b>Abdomen CT ^^</b>	399	312	6.0	4.7	2.1 years	1 in 10,000
<b>Chest (Cancer Staging) CT ^^</b>	536	479	7.6	6.8	3.1 years	1 in 6,700
<b>Limited thoracic CT (research)</b>	x	19.7*	x	0.42#	10.4 weeks	1 in 47,600
<b>Full thoracic CT (research)</b>	x	93.6*	x	1.5#	8.5 months	1 in 13,000

^ data based on information from Health Protection Agency, UK<sup>365</sup>; ^^ data based on national survey of doses from CT in UK 2003<sup>595</sup>; \*calculated from scanner CTDI<sub>vol</sub>; #calculated using the ImPACT CT dosimetry calculator<sup>363</sup>; ¶ average natural background radiation in the UK is 2.2 mSv; range [1.5 - 7.5 mSv]<sup>365</sup>; Δ approximate lifetime risk for patients 16 - 69 years old (paediatric patients multiply risks by about 2 and for older patients divide risks by about 5)<sup>365</sup>

*Definitions of abbreviations:* CXR = chest x-ray, CT = computed tomography, ED = effective dose, DLP = dose length product, CTDI<sub>vol</sub> = volume CT dose index.

## 4 CONCLUSIONS

---

## **4.1 Final discussions and critique**

In this section, I have summarised results from this thesis, presented key questions that arise from our data and speculated possible directions imaging research in asthma may take.

### **4.1.1 CT assessed structural changes in severe asthma**

In this thesis I present CT assessment of remodelling in proximal and distal airways in severe asthma. Both, cross-sectional and longitudinal CT assessments of proximal airway remodelling in severe asthma were performed. For cross-sectional assessment, qualitative as well as quantitative methods of analyses were utilised. Moreover, different software programs that employ two-dimensional and three-dimensional methods of proximal airway analysis were explored. Indirect assessment of distal airway remodelling in asthma patients by quantitative densitometric analysis of air trapping, in paired inspiratory and expiratory CT scans, was performed in a cross-sectional study.

This thesis presents one of the largest qualitative study of CT findings in severe asthma patients. In this retrospective cross-sectional study of 185 severe asthmatics, we found that changes in airways and lung parenchyma were common with only 20% scans reported as normal. BE and BWT was present in 40% and 62% of cases, respectively. On logistic regression analysis, disease duration and particularly FEV<sub>1</sub>/FVC ratio emerged as important predictors of BE and BWT. We therefore assessed, using ROC curve, whether a non-radiological test i.e. FEV<sub>1</sub>/FVC ratio would effectively discriminate between severe asthma

patients who did or did not have airway structural changes. FEV<sub>1</sub>/FVC ratio ( $\geq 75\%$ ) identified severe asthma patients with normal airway with a sensitivity and specificity of 67% and 65% respectively, suggesting that it not possible to reliably identify severe asthma patients with airway structural changes without CT scanning.

In our quantitative studies, utilising 2D and 3D software for proximal airway assessment, the RB1 bronchus lumen was narrower compared to healthy subjects with no significant difference in WA (or WV). Percent WA (or %WV) was greater in severe asthmatics compared to healthy controls and this was largely driven by changes in the airway lumen rather than the airway wall. Three-dimensional software segmented the airway tree up to 5<sup>th</sup>-6<sup>th</sup> generation, allowing determination of fractal dimension, which is used to quantitate global description of shapes of objects and is associated with its complexity. Our findings of reduced fractal dimension of the segmented airway tree in asthma patients compared to healthy subjects is concurrent with other studies.<sup>342</sup> Temporal assessment of RB1 dimensions over a mean duration of 2.6 years demonstrate an increased in WA/BSA but no significant change in LA/BSA.

Air trapping indices, which are indirect measure of distal airway remodeling, were found to be significantly higher in asthma patients compared to healthy controls. No difference in quantitative CT indices was demonstrated between severe and mild-moderate asthma.

### **4.1.2 Relationship between structure (assessed by CT), function and inflammation in severe asthma**

Qualitative CT study showed that BE and BWT were associated with increased disease duration and reduced FEV<sub>1</sub>/FVC ratio. Percent WA correlated well with FEV<sub>1</sub> % predicted in our quantitative cross-sectional CT study. In addition, when severe asthma patients were dichotomised based of presence or absence of persistent airflow obstruction, we found that %WA was significantly higher in severe asthma patients in the former group. Quantitative CT indices assessed using 3D software also revealed good association of lung functions with both air-trapping and proximal airway remodelling indices on univariate analysis. Air-trapping indices showed much stronger correlation with lung functions. Taken together, these findings reflect the importance of structural changes in physiological manifestations of severe asthma.

In this thesis, I have also explored the associations between remodelling assessed by CT and airway inflammation. We have shown for the first time that the RB1 %WA was increased in subjects with and without eosinophilic inflammation and is associated with the preceding burden of neutrophilic inflammation over time measured by repeated sputum analysis. There is evidence supporting the role of neutrophils in severe asthma pathogenesis, as it has been shown that neutrophilic airway inflammation is associated with chronic airway narrowing in asthma.<sup>59,63</sup> In this thesis we have also demonstrated a decrease in RB1 WA/BSA after 1 year of treatment with anti-IL-5 compared to placebo providing strong evidence in favour of the eosinophils playing a key role in airway remodelling determined by CT. It has been shown in biopsy studies that reticular basement

membrane is increased in severe asthma subjects with eosinophilic airway inflammation compared to those without.<sup>33</sup> In addition, various other markers of inflammation have been associated with CT assessed airway remodeling, suggesting that various components of airway inflammation including eosinophilic and neutrophilic inflammation contribute to airway remodeling in severe asthma.

### **4.1.3 Standardisation of quantitative CT indices**

In this thesis I have also described airway and densitometry phantom models that were developed to study errors associated with quantitative airway morphometry and lung densitometry. We found that three-dimensional software is more accurate in airway morphometry compared to 2D software with reduced errors due to oblique orientation of airways and inter-scanner variability in airway dimensions. However, 3D software programs are limited by their inability to analyse sequentially acquired HRCT scans used in our retrospective quantitative study. We therefore, devised an airway phantom based correction method for errors due to airway size and oblique orientation in 2D airway morphometry. Moreover, we found that phantom models are critical for reducing between scanner variability in CT assessed quantitative airway morphometry and lung densitometry.

### **4.1.4 Role of CT in phenotyping asthma**

Multi-dimensional phenotyping in severe asthma may potentially generate new insights into disease pathogenesis, predict disease progression and identify responders to current and novel therapies. There are two important studies that have used statistical techniques

such as factor and cluster analysis to phenotype severe asthma.<sup>21,22</sup> We found no significant difference in RB1 dimensions in four severe asthma phenotypes determined based on clinical and physiological indices. Moreover, review of quantitative studies in literature show discrepancies in pattern of proximal airway remodelling in asthma, supporting the existence of different structural phenotypes. In this thesis, I have described for the first time three distinct asthma phenotypes identified based on CT assessed proximal and distal airway remodeling.

#### **4.1.5 Criticisms**

Some potential limitations of the work presented in this thesis are addressed in the discussion section of individual studies. However, few more general issues, which require particular attention, are considered in this section. All severe asthma subjects attending difficult asthma clinic at our centre undergo extensive re-characterisation and confirmation of diagnosis by a chest physician. Standard severe refractory asthma definition based on ATS criteria<sup>9</sup> is used for classification. Despite all efforts to identify ‘true’ severe asthma patients there may potentially be few patients who do not have severe asthma and have other mechanisms for persistent symptoms that have not been addressed. Previous observational studies have suggested that up to 50% of patients referred with difficult to control asthma to specialist clinics do not have refractory disease.<sup>596,597</sup> Severe asthma subjects included in this work were recruited from the difficult asthma clinic at a single centre, which may potentially introduce a population bias. Recent report of severe asthma subjects from four different UK centres, who fulfill the ATS definition of refractory asthma, show important differences in multiple characteristics including prebronchodilator

and postbronchodilator spirometry and degree of airflow obstruction.<sup>20</sup> Such between-centre differences may partly be explained by local patient referral patterns and specialist areas of interest amongst the chest physicians at a particular centre. It is therefore important that future studies are multi-centre in nature to overcome any potential population bias.

Clinical and CT data collection for two cross-sectional CT studies (section 3.1 and 3.3) presented in this thesis was retrospective in nature. One of the major limitations of retrospective data collection is a potentially biased sample from which conclusions are drawn. Moreover, robust standardisation of clinical data collection and CT acquisition can only be achieved in a prospective study. Furthermore, at our centre, CT scans were not undertaken in all severe asthma subjects and therefore our findings cannot be extrapolated to severe asthma population as a whole. Prospective assessment of unselected severe asthma population is required to assess true incidence of CT assessed structural changes.

The study presented in section 3.4 of this thesis was a double-blind study. Despite all efforts to maintain blinding there is a potential of this being compromised, as the results of FE<sub>NO</sub>, sputum and blood leucocyte differential counts are affected due to the anti-eosinophilic effects of mepolizumab. Such a problem with double blinding is particularly relevant in placebo controlled pharmacological trials where the extent of drug response or side effects are dramatically different than placebo.

Multivariate modelling techniques such as factor and cluster analysis are used in two studies (section 3.3 and 3.5) presented in this thesis. Such techniques are designed to identify patterns within a heterogeneous dataset and attempt to form groups of similar observations. Various methods to perform such analyses have been described. As these are



algorithm-based techniques, outputs can be non-unique. Therefore, the results presented in these studies cannot be generalised to whole severe asthma population. Replication of results in different samples and over time is required to establish the validity and stability of clusters presented in the two studies. Another potential limitation of multivariate modelling is that subjects with diseases of distinct pathophysiology may potentially be grouped together based on strong association between a single / few variables. Future longitudinal studies will be helpful in assessing temporal stability and validity of asthma clusters identified in this thesis.

## **4.2 Key questions arising from this thesis and future directions**

From the data presented in this thesis a number of new questions arise:

1. What structural changes constitute remodelling in asthma?

Our finding that proximal airway WV (or WA) measured on CT is not increased in asthma subjects compared to healthy subjects is contrary to the biopsy studies in asthma, which shows an increased in various components of airway wall including ASM and RBM. Our data shows that the increase in %WV (or %WA) in asthma subjects is predominantly influenced by narrowing of the lumen despite adequate bronchodilator therapy. Airway narrowing in asthma subjects may be due to ASM shortening, uncoupling of the  $\beta$ 2-adrenoreceptors from the G protein adenylyl cyclase,<sup>598</sup> decreased compliance of the airway wall due to change in its composition or architecture leading to reduced distensibility<sup>569,570</sup>

and changes in the airway-parenchymal interdependence. More work is required to identify cause for lumen narrowing in asthma sub-groups, which may help target a tailored therapy. Bronchiectasis was found to be common in severe asthma subjects in our qualitative CT study, a finding reinforced by identification of asthma phenotype with proximal airway lumen dilatational on 3D quantitative study. Together these findings suggest that changes in proximal airway lumen dimensions represents an important aspect of airway remodelling in asthma. The importance of proximal airway wall dimensions is demonstrated by our results from the temporal CT assessment of severe asthma subjects with eosinophilic inflammation. Air trapping, a surrogate for distal airway remodelling, was a feature in all asthma phenotypes identified irrespective of the presence of proximal airway structural changes indicating that small airway remodelling precede large airway changes. Furthermore, proximal and distal airway remodelling was unrelated to disease severity.

## 2. Is remodelling a cause or consequence of asthma?

It remains elusive whether these structural changes are consequence of asthma and represent different stages of disease progression or the distinct remodelling changes are fundamental to pathogenesis of asthma and represent distinct asthma endotypes. Future studies should explore ways to identify asthma endotypes from the discerned phenotypes so that asthma disease complex can be dissected into entities with distinct primary disease pathobiology.

## 3. Are CT derived quantitative measures valid and reproducible temporally and between scanners and centres ?

This thesis confirms that CT is a valid and reliable tool for non-invasive assessment of proximal and distal airway remodelling in asthma. We have explored the accuracy and repeatability of quantitative measures using airway and densitometry phantom models. Moreover, we have used phantom models to standardise airway morphometry and lung densitometry indices to account for errors associated with quantitative measures. It is unclear if similar standardisation methods are applicable to various different CT scanner models at different centres. Further work is required to refine the phantom models and the standardisation techniques.

4. What is the minimum detectable structural change using quantitative CT analysis?

Quantitative CT analysis in asthma is still in its infancy and normal values are yet to be established. Large longitudinal studies are required to determine the minimal detectable change in CT airway morphometry and lung densitometry.

5. Can CT or other imaging derived biomarker/s help phenotype severe asthma patients in a more clinically relevant manner to predict mortality, morbidity and treatment response?

Imaging biomarkers to study anatomical, physiological, biochemical or molecular parameters in various diseases are in development.<sup>599,600</sup> This thesis presents data that supports the use of CT derived quantitative measures in severe asthma as imaging biomarkers to monitor disease progression and response to treatment. Whether such imaging biomarkers will predict asthma related mortality, morbidity and response to treatment is currently unknown.

In order to address these and many other critical questions there is a need for both proof-of-concept studies and large clinical trials using multi-modality and multi-disciplinary approach for severe asthma.

Recent advances in pulmonary imaging means, that we are now able to perform detailed analysis of large airways, small airways and lung parenchyma. Distal lung is beyond the conventional resolution of CT and therefore a variety of other imaging modalities can be used to generate information on small airway and alveolar structure or function. Physiological assessment of the distal pulmonary compartment is possible with novel techniques such as impulse oscillation technique and multiple breath nitrogen wash-out, which can complement, refine and validate the imaging-derived measures. The imaging-derived structural and physiological data allow us to study pathophysiological phenomenon in severe asthma using novel methods. Computational fluid dynamics (CFD)<sup>601,602</sup> and Image functional modelling (IFM)<sup>603,604</sup> are two such techniques that amalgamate clinical, physiological, radiological, image processing, bioengineering and computing expertise to develop patient-specific, multi-dimensional and multi-modality tools to study airway disease in detail. Using CFD the air-flow in the pulmonary tree from the large central airways to the acinar regions can be studied in detail.<sup>602,605-607</sup> This may help detect differences in regional airflow and airway resistance in asthmatic subjects before and after bronchodilation.<sup>602</sup> Moreover, at baseline despite normal spirometry, asthmatic subjects had differences in CFD-derived airway resistance.<sup>602</sup> CFD studies, which can help predict deposition of therapeutic particles and pollutants, may prove to be fundamental for improving drug delivery methods in the respiratory system and understanding of pollutant induced lung pathophysiology.<sup>608,609</sup> Image functional models integrating large and small

airway behaviour, ventilation and impedance have demonstrated that large airway narrowing alone cannot account for the AHR seen in asthma.<sup>603</sup> There has been a limited application of these techniques to study severe asthma. These tools integrate a range of imaging techniques along with clinical and physiological data and present us with fresh opportunities to unravel the elusive structure-function relationship and methods to discover novel phenotypes and endotypes in severe asthma.

# REFERENCES

---

1. Keeney EL. The History of Asthma from Hippocrates to Meltzer. *J Allergy* 1964;35:215-26.
2. Cohen SG. Asthma among the famous. Henry Hyde Salter (1823-1871), British physician. *Allergy Asthma Proc* 1997;18:256-8.
3. Girard DE. The history of Osler's Principles and Practice of Medicine. *Med Times* 1981;109:1s-4s, 13s.
4. Kirby JG, Hargreave FE, Gleich GJ, O'Byrne PM. Bronchoalveolar cell profiles of asthmatic and nonasthmatic subjects. *Am Rev Respir Dis* 1987;136:379-83.
5. From the Global Strategy for Asthma Management and Prevention, Global Initiative for Asthma (GINA) 2010., 2010. (Accessed 01/01/2012, at <http://www.ginasthma.org/>.)
6. Masoli M, Fabian D, Holt S, Beasley R. The global burden of asthma: executive summary of the GINA Dissemination Committee Report. *Allergy* 2004;59:469-78.
7. Ford ES. The epidemiology of obesity and asthma. *J Allergy Clin Immunol* 2005;115:897-909; quiz 10.
8. BTS. British Guideline on the Management of Asthma - A national clinical guideline. 2011.
9. ATS. Proceedings of the ATS workshop on refractory asthma: current understanding, recommendations, and unanswered questions. American Thoracic Society. *Am J Respir Crit Care Med* 2000;162:2341-51.
10. Wenzel S. Severe asthma in adults. *American Journal of Respiratory and Critical Care Medicine* 2005;172:149-60.
11. Tough SC, Hessel PA, Ruff M, Green FH, Mitchell I, Butt JC. Features that distinguish those who die from asthma from community controls with asthma. *J Asthma* 1998;35:657-65.
12. Antonicelli L, Bucca C, Neri M, et al. Asthma severity and medical resource utilisation. *Eur Respir J* 2004;23:723-9.

13. The World Health Report 2003, Shaping the Future, the World Health Organization, 2003. (Accessed 12/12/2011, at <http://www.who.int/whr/2003/en/index.html>)
14. The European Lung White Book: The First Comprehensive Survey on Respiratory Health in Europe 2003. In.
15. Chaney P, Wenzel SE, Anderson GP, et al. Severe asthma in adults: What are the important questions? *Journal of Allergy and Clinical Immunology* 2007;119:1337-48.
16. Chung KF, Godard P, Adelroth E, et al. Difficult/therapy-resistant asthma: the need for an integrated approach to define clinical phenotypes, evaluate risk factors, understand pathophysiology and find novel therapies. ERS Task Force on Difficult/Therapy-Resistant Asthma. *European Respiratory Society. EurRespirJ* 1999;13:1198-208.
17. Prys-Picard CO, Campbell SM, Ayres JG, Miles JF, Niven RM, Consensus on Difficult Asthma Consortium UK. Defining and investigating difficult asthma: developing quality indicators. *Respir Med* 2006;100:1254-61.
18. Bousquet J, Mantzouranis E, Cruz AA, et al. Uniform definition of asthma severity, control, and exacerbations: document presented for the World Health Organization Consultation on Severe Asthma. *J Allergy Clin Immunol* 2010;126:926-38.
19. Bel EH, Sousa A, Fleming L, et al. Diagnosis and definition of severe refractory asthma: an international consensus statement from the Innovative Medicine Initiative (IMI). *Thorax* 2011;66:910-7.
20. Heaney LG, Brightling CE, Menzies-Gow A, Stevenson M, Niven RM, British Thoracic Society Difficult Asthma N. Refractory asthma in the UK: cross-sectional findings from a UK multicentre registry. *Thorax* 2010;65:787-94.
21. Haldar P, Pavord ID, Shaw DE, et al. Cluster analysis and clinical asthma phenotypes. *American Journal of Respiratory and Critical Care Medicine* 2008;178:218-24.
22. Moore WC, Meyers DA, Wenzel SE, et al. Identification of Asthma Phenotypes Using Cluster Analysis in the Severe Asthma Research Program. *AmJRespirCrit Care Med* 2010;181:315-23.
23. Berry MA, Parker D, Neale N, et al. Sputum and bronchial submucosal IL-13 expression in asthma and eosinophilic bronchitis. *Journal of Allergy and Clinical Immunology* 2004;114:1106-9.
24. Brightling CE, Symon FA, Birring SS, Bradding P, Pavord ID, Wardlaw AJ. T(H)2 cytokine expression in bronchoalveolar lavage fluid T lymphocytes and bronchial submucosa is a feature of asthma and eosinophilic bronchitis. *Journal of Allergy and Clinical Immunology* 2002;110:899-905.

25. Saha SK, Berry MA, Parker D, et al. Increased sputum and bronchial biopsy IL-13 expression in severe asthma. *Journal of Allergy and Clinical Immunology* 2008;121:685-91.
26. Semlali A, Jacques E, Koussih L, Gounni AS, Chakir J. Thymic stromal lymphopoietin-induced human asthmatic airway epithelial cell proliferation through an IL-13-dependent pathway. *J Allergy Clin Immunol* 2010;125:844-50.
27. Okayama Y, Okumura S, Sagara H, et al. FcepsilonRI-mediated thymic stromal lymphopoietin production by interleukin-4-primed human mast cells. *Eur Respir J* 2009;34:425-35.
28. Zhang KQ, Shan LY, Rahman MS, Unruh H, Halayko AJ, Gounni AS. Constitutive and inducible thymic stromal lymphopoietin expression in human airway smooth muscle cells: role in chronic obstructive pulmonary disease. *American Journal of Physiology-Lung Cellular and Molecular Physiology* 2007;293:L375-L82.
29. Kashyap M, Rochman Y, Spolski R, Samsel L, Leonard WJ. Thymic stromal lymphopoietin is produced by dendritic cells. *J Immunol* 2011;187:1207-11.
30. Ying S, O'Connor B, Ratoff J, et al. Expression and cellular provenance of thymic stromal lymphopoietin and chemokines in patients with severe asthma and chronic obstructive pulmonary disease. *J Immunol* 2008;181:2790-8.
31. Kaur D, Doe C, Woodman L, et al. Mast cell-airway smooth muscle crosstalk: the role of thymic stromal lymphopoietin. *Chest* 2011.
32. Siddiqui S, Mistry V, Doe C, Stinson S, Foster M, Brightling C. Airway wall expression of OX40/OX40L and interleukin-4 in asthma. *Chest* 2010;137:797-804.
33. Wenzel SE, Schwartz LB, Langmack EL, et al. Evidence that severe asthma can be divided pathologically into two inflammatory subtypes with distinct physiologic and clinical characteristics. *American Journal of Respiratory and Critical Care Medicine* 1999;160:1001-8.
34. Brightling CE. Clinical applications of induced sputum. *Chest* 2006;129:1344-8.
35. Barnes PJ. The cytokine network in asthma and chronic obstructive pulmonary disease. *J Clin Invest* 2008;118:3546-56.
36. Green RH, Brightling CE, Woltmann G, Parker D, Wardlaw AJ, Pavord ID. Analysis of induced sputum in adults with asthma: identification of subgroup with isolated sputum neutrophilia and poor response to inhaled corticosteroids. *Thorax* 2002;57:875-9.
37. Thomas B, Rutman A, Hirst RA, et al. Ciliary dysfunction and ultrastructural abnormalities are features of severe asthma. *J Allergy Clin Immunol* 2010;126:722-9 e2.



38. Lai HY, Rogers DF. Mucus hypersecretion in asthma: intracellular signalling pathways as targets for pharmacotherapy. *Curr Opin Allergy Clin Immunol* 2010;10:67-76.
39. Hilty M, Burke C, Pedro H, et al. Disordered microbial communities in asthmatic airways. *PLoS One* 2010;5:e8578.
40. Duvernelle C, Freund V, Frossard N. Transforming growth factor-beta and its role in asthma. *Pulmonary Pharmacology & Therapeutics* 2003;16:181-96.
41. Chetta A, Zanini A, Foresi A, et al. Vascular endothelial growth factor up-regulation and bronchial wall remodelling in asthma. *Clinical and Experimental Allergy* 2005;35:1437-42.
42. Eickelberg O, Kohler E, Reichenberger F, et al. Extracellular matrix deposition by primary human lung fibroblasts in response to TGF-beta1 and TGF-beta3. *AmJPhysiol* 1999;276:L814-L24.
43. Saunders R, Siddiqui S, Kaur D, et al. Fibrocyte localization to the airway smooth muscle is a feature of asthma. *Journal of Allergy and Clinical Immunology* 2009;123:376-84.
44. Wang CH, Huang CD, Lin HC, et al. Increased circulating fibrocytes in asthma with chronic airflow obstruction. *AmJRespirCrit Care Med* 2008;178:583-91.
45. Brightling CE, Bradding P, Symon FA, Holgate ST, Wardlaw AJ, Pavord ID. Mast-cell infiltration of airway smooth muscle in asthma. *New England Journal of Medicine* 2002;346:1699-705.
46. Siddiqui S, Mistry V, Doe C, et al. Airway hyperresponsiveness is dissociated from airway wall structural remodeling. *Journal of Allergy and Clinical Immunology* 2008;122:335-41.
47. Kaur D, Saunders R, Berger P, et al. Airway smooth muscle and mast cell-derived CC chemokine ligand 19 mediate airway smooth muscle migration in asthma. *American Journal of Respiratory and Critical Care Medicine* 2006;174:1179-88.
48. Siddiqui S, Hollins F, Brightling CE. What can we learn about airway smooth muscle from the company it keeps? *European Respiratory Journal* 2008;32:9-11.
49. Siddiqui S, Sutcliffe A, Shikotra A, et al. Vascular remodeling is a feature of asthma and nonasthmatic eosinophilic bronchitis. *Journal of Allergy and Clinical Immunology* 2007;120:813-9.
50. Simcock DE, Kanabar V, Clarke GW, O'Connor BJ, Lee TH, Hirst SJ. Proangiogenic activity in bronchoalveolar lavage fluid from patients with asthma. *Am J Respir Crit Care Med* 2007;176:146-53.

51. Pavord ID, Pizzichini MMM, Pizzichini E, Hargreave FE. The use of induced sputum to investigate airway inflammation. *Thorax* 1997;52:498-501.
52. Pizzichini E, Pizzichini MMM, Efthimiadis A, et al. Indices of airway inflammation in induced sputum: Reproducibility and validity of cell and fluid-phase measurements. *American Journal of Respiratory and Critical Care Medicine* 1996;154:308-17.
53. The ENFUMOSA study group. The ENFUMOSA cross-sectional European multicentre study of the clinical phenotype of chronic severe asthma. European Network for Understanding Mechanisms of Severe Asthma. *Eur Respir J* 2003;22:470-7.
54. Doe C, Bafadhel M, Siddiqui S, et al. Expression of the T helper 17-associated cytokines IL-17A and IL-17F in asthma and COPD. *Chest* 2010;138:1140-7.
55. Al-Ramli W, Prefontaine D, Chouiali F, et al. T(H)17-associated cytokines (IL-17A and IL-17F) in severe asthma. *J Allergy Clin Immunol* 2009;123:1185-7.
56. Berry M, Morgan A, Shaw DE, et al. Pathological features and inhaled corticosteroid response of eosinophilic and non-eosinophilic asthma. *Thorax* 2007;62:1043-9.
57. Green RH, Brightling CE, McKenna S, et al. Asthma exacerbations and sputum eosinophil counts: a randomised controlled trial. *Lancet* 2002;360:1715-21.
58. ten Brinke A, Zwinderman AH, Sterk PJ, Rabe KF, Bel EH. Factors associated with persistent airflow limitation in severe asthma. *American Journal of Respiratory and Critical Care Medicine* 2001;164:744-8.
59. Woodruff PG, Khashayar R, Lazarus SC, et al. Relationship between airway inflammation, hyperresponsiveness, and obstruction in asthma. *Journal of Allergy and Clinical Immunology* 2001;108:753-8.
60. Pavord ID, Brightling CE, Woltmann G, Wardlaw AJ. Non-eosinophilic corticosteroid unresponsive asthma. *Lancet* 1999;353:2213-4.
61. Simpson JL, Scott R, Boyle MJ, Gibson PG. Inflammatory subtypes in asthma: Assessment and identification using induced sputum. *Respirology* 2006;11:54-61.
62. Simpson JL, Grissell TV, Douwes J, Scott RJ, Boyle MJ, Gibson PG. Innate immune activation in neutrophilic asthma and bronchiectasis. *Thorax* 2007;62:211-8.
63. Shaw DE, Berry MA, Hargadon B, et al. Association between neutrophilic airway inflammation and airflow limitation in adults with asthma. *Chest* 2007;132:1871-5.

64. Howarth PH, Babu KS, Arshad HS, et al. Tumour necrosis factor (TNF $\alpha$ ) as a novel therapeutic target in symptomatic corticosteroid dependent asthma. *Thorax* 2005;60:1012-8.
65. Saha S, Mistry V, Siva R, et al. Induced sputum and bronchial mucosal expression of interleukin-13 is not increased in chronic obstructive pulmonary disease. *Allergy* 2008;63:1239-43.
66. Balzar S, Fajt ML, Comhair SA, et al. Mast cell phenotype, location, and activation in severe asthma. Data from the Severe Asthma Research Program. *Am J Respir Crit Care Med* 2011;183:299-309.
67. Balzar S, Chu HW, Strand M, Wenzel S. Relationship of small airway chymase-positive mast cells and lung function in severe asthma. *Am J Respir Crit Care Med* 2005;171:431-9.
68. McParland BE, Macklem PT, Pare PD. Airway wall remodeling: friend or foe? *J Appl Physiol* 2003;95:426-34.
69. Holgate ST. Epithelium dysfunction in asthma. *Journal of Allergy and Clinical Immunology* 2007;120:1233-46.
70. Balzar S, Wenzel SE, Chu HW. Transbronchial biopsy as a tool to evaluate small airways in asthma. *European Respiratory Journal* 2002;20:254-9.
71. O'Sullivan S, Cormican L, Faul JL, et al. Activated, cytotoxic CD8(+) T lymphocytes contribute to the pathology of asthma death. *Am J Respir Crit Care Med* 2001;164:560-4.
72. Aysola RS, Hoffman EA, Gierada D, et al. Airway remodeling measured by multidetector CT is increased in severe asthma and correlates with pathology. *Chest* 2008;134:1183-91.
73. Benayoun L, Druilhe A, Dombret MC, Aubier M, Pretolani M. Airway structural alterations selectively associated with severe asthma. *American Journal of Respiratory and Critical Care Medicine* 2003;167:1360-8.
74. Gono H, Fujimoto K, Kawakami S, Kubo K. Evaluation of airway wall thickness and air trapping by HRCT in asymptomatic asthma. *European Respiratory Journal* 2003;22:965-71.
75. Niimi A, Matsumoto H, Amitani R, et al. Airway wall thickness in asthma assessed by computed tomography - Relation to clinical indices. *American Journal of Respiratory and Critical Care Medicine* 2000;162:1518-23.

76. Siddiqui S, Gupta S, Cruse G, et al. Airway wall geometry in asthma and nonasthmatic eosinophilic bronchitis. *Allergy* 2009;64:951-8.
77. Boulet LP, Turcotte H, Laviolette M, et al. Airway hyperresponsiveness, inflammation, and subepithelial collagen deposition in recently diagnosed versus long-standing mild asthma - Influence of inhaled corticosteroids. *American Journal of Respiratory and Critical Care Medicine* 2000;162:1308-13.
78. Kariyawasam HH, Robinson DS. The role of eosinophils in airway tissue remodelling in asthma. *Current Opinion in Immunology* 2007;19:681-6.
79. Gu L, Pandey V, Geenen DL, Chowdhury SA, Piano MR. Cigarette smoke-induced left ventricular remodelling is associated with activation of mitogen-activated protein kinases. *Eur J Heart Fail* 2008;10:1057-64.
80. Grunewald S, Bodendorf M, Illes M, Kendler M, Simon JC, Paasch U. In vivo wound healing and dermal matrix remodelling in response to fractional CO(2) laser intervention: Clinicopathological correlation in non-facial skin. *Int J Hyperthermia* 2011;27:811-8.
81. Gustafsson T. Vascular remodelling in human skeletal muscle. *Biochem Soc Trans* 2011;39:1628-32.
82. Chabot A, Jiang BH, Shi Y, Tardif JC, Dupuis J. Role of aldosterone on lung structural remodelling and right ventricular function in congestive heart failure. *BMC Cardiovasc Disord* 2011;11:72.
83. Bergeron C, Tulic MK, Hamid Q. Airway remodelling in asthma: from benchside to clinical practice. *Can Respir J* 2010;17:e85-93.
84. Halwani R, Al-Muhsen S, Hamid Q. Airway remodeling in asthma. *Curr Opin Pharmacol* 2010;10:236-45.
85. Kaminska M, Foley S, Maghni K, et al. Airway remodeling in subjects with severe asthma with or without chronic persistent airflow obstruction. *J Allergy Clin Immunol* 2009;124:45-51.
86. Vignola AM, Chanez P, Campbell AM, et al. Airway inflammation in mild intermittent and in persistent asthma. *Am J Respir Crit Care Med* 1998;157:403-9.
87. Montefort S, Roche WR, Holgate ST. Bronchial epithelial shedding in asthmatics and non-asthmatics. *Respir Med* 1993;87 Suppl B:9-11.
88. Demoly P, Simony-Lafontaine J, Chanez P, et al. Cell proliferation in the bronchial mucosa of asthmatics and chronic bronchitis. *Am J Respir Crit Care Med* 1994;150:214-7.

89. Laitinen LA, Heino M, Laitinen A, Kava T, Haahtela T. Damage of the airway epithelium and bronchial reactivity in patients with asthma. *Am Rev Respir Dis* 1985;131:599-606.
90. Beasley R, Roche WR, Roberts JA, Holgate ST. Cellular events in the bronchi in mild asthma and after bronchial provocation. *Am Rev Respir Dis* 1989;139:806-17.
91. Pepe C, Foley S, Shannon J, et al. Differences in airway remodeling between subjects with severe and moderate asthma. *J Allergy Clin Immunol* 2005;116:544-9.
92. Carroll N, Elliot J, Morton A, James A. The Structure of Large and Small Airways in Nonfatal and Fatal Asthma. *American Review of Respiratory Disease* 1993;147:405-10.
93. Woodruff PG, Dolganov GM, Ferrando RE, et al. Hyperplasia of smooth muscle in mild to moderate asthma without changes in cell size or gene expression. *Am J Respir Crit Care Med* 2004;169:1001-6.
94. Payne DN, Rogers AV, Adelroth E, et al. Early thickening of the reticular basement membrane in children with difficult asthma. *Am J Respir Crit Care Med* 2003;167:78-82.
95. Chetta A, Foresi A, Del Donno M, Bertorelli G, Pesci A, Olivieri D. Airways remodeling is a distinctive feature of asthma and is related to severity of disease. *Chest* 1997;111:852-7.
96. Carroll NG, Mutavdzic S, James AL. Increased mast cells and neutrophils in submucosal mucous glands and mucus plugging in patients with asthma. *Thorax* 2002;57:677-82.
97. Minshall EM, Leung DY, Martin RJ, et al. Eosinophil-associated TGF-beta1 mRNA expression and airways fibrosis in bronchial asthma. *Am J Respir Cell Mol Biol* 1997;17:326-33.
98. Chetta A, Zanini A, Torre O, Olivieri D. Vascular remodelling and angiogenesis in asthma: morphological aspects and pharmacological modulation. *InflammAllergy Drug Targets* 2007;6:41-5.
99. Puddicombe SM, Polosa R, Richter A, et al. Involvement of the epidermal growth factor receptor in epithelial repair in asthma. *FASEB J* 2000;14:1362-74.
100. Cohen L, Xueping E, Tarsi J, et al. Epithelial cell proliferation contributes to airway remodeling in severe asthma. *American Journal of Respiratory and Critical Care Medicine* 2007;176:138-45.
101. Shannon J, Ernst P, Yamauchi Y, et al. Differences in airway cytokine profile in severe asthma compared to moderate asthma. *Chest* 2008;133:420-6.

102. Macedo P, Hew M, Torrego A, et al. Inflammatory biomarkers in airways of patients with severe asthma compared with non-severe asthma. *Clin Exp Allergy* 2009;39:1668-76.
103. Tillie-Leblond I, de Blic J, Jaubert F, Wallaert B, Scheinmann P, Gosset P. Airway remodeling is correlated with obstruction in children with severe asthma. *Allergy* 2008;63:533-41.
104. Johnson PR, Roth M, Tamm M, et al. Airway smooth muscle cell proliferation is increased in asthma. *AmJRespirCrit Care Med* 2001;164:474-7.
105. Brightling CE, Symon FA, Holgate ST, Wardlaw AJ, Pavord ID, Bradding P. Interleukin-4 and -13 expression is co-localized to mast cells within the airway smooth muscle in asthma. *Clinical and Experimental Allergy* 2003;33:1711-6.
106. Slats AM, Janssen K, van Schadewijk A, et al. Bronchial inflammation and airway responses to deep inspiration in asthma and chronic obstructive pulmonary disease. *American Journal of Respiratory and Critical Care Medicine* 2007;176:121-8.
107. Bourdin A, Neveu D, Vachier I, Paganin F, Godard P, Chanez P. Specificity of basement membrane thickening in severe asthma. *Journal of Allergy and Clinical Immunology* 2007;119:1367-74.
108. Chakir J, Shannon J, Molet S, et al. Airway remodeling-associated mediators in moderate to severe asthma: effect of steroids on TGF-beta, IL-11, IL-17, and type I and type III collagen expression. *J Allergy Clin Immunol* 2003;111:1293-8.
109. Ueda T, Niimi A, Matsumoto H, et al. Role of small airways in asthma: investigation using high-resolution computed tomography. *Journal of Allergy and Clinical Immunology* 2006;118:1019-25.
110. Sorkness RL, Bleecker ER, Busse WW, et al. Lung function in adults with stable but severe asthma: air trapping and incomplete reversal of obstruction with bronchodilation. *J Appl Physiol* 2008;104:394-403.
111. Campana L, Kenyon J, Zhalehdoust-Sani S, et al. Probing airway conditions governing ventilation defects in asthma via hyperpolarized MRI image functional modeling. *J Appl Physiol* 2009;106:1293-300.
112. Mauad T, Silva LF, Santos MA, et al. Abnormal alveolar attachments with decreased elastic fiber content in distal lung in fatal asthma. *Am J Respir Crit Care Med* 2004;170:857-62.
113. Dolhnikoff M, da Silva LF, de Araujo BB, et al. The outer wall of small airways is a major site of remodeling in fatal asthma. *J Allergy Clin Immunol* 2009;123:1090-7, 7 e1.

114. Matsushita MD, da Silva LFF, dos Santos MA, et al. Airway proteoglycans are differentially altered in fatal asthma. *Journal of Pathology* 2005;207:102-10.
115. Mauad T, Xavier AC, Saldiva PH, Dolnikoff M. Elastosis and fragmentation of fibers of the elastic system in fatal asthma. *Am J Respir Crit Care Med* 1999;160:968-75.
116. de Kluijver J, Schrumpf JA, Evertse CE, et al. Bronchial matrix and inflammation respond to inhaled steroids despite ongoing allergen exposure in asthma. *Clinical and Experimental Allergy* 2005;35:1361-9.
117. Pini L, Hamid Q, Shannon J, et al. Differences in proteoglycan deposition in the airways of moderate and severe asthmatics. *Eur Respir J* 2007;29:71-7.
118. Bergeron C, Hauber HP, Gotfried M, et al. Evidence of remodeling in peripheral airways of patients with mild to moderate asthma: effect of hydrofluoroalkane-flunisolide. *J Allergy Clin Immunol* 2005;116:983-9.
119. van Rensen ELJ, Sont JK, Evertse CE, et al. Bronchial CD8 cell infiltrate and lung function decline in asthma. *American Journal of Respiratory and Critical Care Medicine* 2005;172:837-41.
120. Carroll N, Carello S, Cooke C, James A. Airway structure and inflammatory cells in fatal attacks of asthma. *Eur Respir J* 1996;9:709-15.
121. Jeffery PK, Wardlaw AJ, Nelson FC, Collins JV, Kay AB. Bronchial biopsies in asthma. An ultrastructural, quantitative study and correlation with hyperreactivity. *Am Rev Respir Dis* 1989;140:1745-53.
122. Lozewicz S, Wells C, Gomez E, et al. Morphological integrity of the bronchial epithelium in mild asthma. *Thorax* 1990;45:12-5.
123. Hoshino M, Nakamura Y, Hamid QA. Gene expression of vascular endothelial growth factor and its receptors and angiogenesis in bronchial asthma. *J Allergy Clin Immunol* 2001;107:1034-8.
124. Carroll NG, Perry S, Karkhanis A, et al. The airway longitudinal elastic fiber network and mucosal folding in patients with asthma. *Am J Respir Crit Care Med* 2000;161:244-8.
125. Carroll NG, Cooke C, James AL. Bronchial blood vessel dimensions in asthma. *Am J Respir Crit Care Med* 1997;155:689-95.
126. Synek M, Beasley R, Frew AJ, et al. Cellular infiltration of the airways in asthma of varying severity. *Am J Respir Crit Care Med* 1996;154:224-30.

127. Sur S, Crotty TB, Kephart GM, et al. Sudden-onset fatal asthma. A distinct entity with few eosinophils and relatively more neutrophils in the airway submucosa? *Am Rev Respir Dis* 1993;148:713-9.
128. Azzawi M, Johnston PW, Majumdar S, Kay AB, Jeffery PK. T lymphocytes and activated eosinophils in airway mucosa in fatal asthma and cystic fibrosis. *Am Rev Respir Dis* 1992;145:1477-82.
129. Faul JL, Tormey VJ, Leonard C, et al. Lung immunopathology in cases of sudden asthma death. *Eur Respir J* 1997;10:301-7.
130. Carroll N, Cooke C, James A. The distribution of eosinophils and lymphocytes in the large and small airways of asthmatics. *Eur Respir J* 1997;10:292-300.
131. Carroll N, Lehmann E, Barret J, Morton A, Cooke C, James A. Variability of airway structure and inflammation in normal subjects and in cases of nonfatal and fatal asthma. *Pathol Res Pract* 1996;192:238-48.
132. Kuwano K, Bosken CH, Pare PD, Bai TR, Wiggs BR, Hogg JC. Small airways dimensions in asthma and in chronic obstructive pulmonary disease. *AmRevRespirDis* 1993;148:1220-5.
133. Saglani S, Malmstrom K, Pelkonen AS, et al. Airway remodeling and inflammation in symptomatic infants with reversible airflow obstruction. *Am J Respir Crit Care Med* 2005;171:722-7.
134. Kraft M, Djukanovic R, Wilson S, Holgate ST, Martin RJ. Alveolar tissue inflammation in asthma. *Am J Respir Crit Care Med* 1996;154:1505-10.
135. Hauber HP, Gotfried M, Newman K, et al. Effect of HFA-flunisolide on peripheral lung inflammation in asthma. *J Allergy Clin Immunol* 2003;112:58-63.
136. Jeffery P, Holgate S, Wenzel S, Endobronchial Biopsy W. Methods for the assessment of endobronchial biopsies in clinical research: application to studies of pathogenesis and the effects of treatment. *Am J Respir Crit Care Med* 2003;168:S1-17.
137. Wilson JW, Li X. The measurement of reticular basement membrane and submucosal collagen in the asthmatic airway. *Clin Exp Allergy* 1997;27:363-71.
138. Haldar P, Pavord ID. Noneosinophilic asthma: A distinct clinical and pathologic phenotype. *Journal of Allergy and Clinical Immunology* 2007;119:1043-52.
139. Asai K, Kanazawa H, Kamoi H, Shiraishi S, Hirata K, Yoshikawa J. Increased levels of vascular endothelial growth factor in induced sputum in asthmatic patients. *Clin Exp Allergy* 2003;33:595-9.



140. Kanazawa H, Nomura S, Yoshikawa J. Role of microvascular permeability on physiologic differences in asthma and eosinophilic bronchitis. *Am J Respir Crit Care Med* 2004;169:1125-30.
141. Ko FW, Diba C, Roth M, et al. A comparison of airway and serum matrix metalloproteinase-9 activity among normal subjects, asthmatic patients, and patients with asthmatic mucus hypersecretion. *Chest* 2005;127:1919-27.
142. Vignola AM, Riccobono L, Mirabella A, et al. Sputum metalloproteinase-9/tissue inhibitor of metalloproteinase-1 ratio correlates with airflow obstruction in asthma and chronic bronchitis. *Am J Respir Crit Care Med* 1998;158:1945-50.
143. Matsumoto H, Niimi A, Takemura M, et al. Relationship of airway wall thickening to an imbalance between matrix metalloproteinase-9 and its inhibitor in asthma. *Thorax* 2005;60:277-81.
144. Little SA, Sproule MW, Cowan MD, et al. High resolution computed tomographic assessment of airway wall thickness in chronic asthma: reproducibility and relationship with lung function and severity. *Thorax* 2002;57:247-53.
145. Chae EJ, Kim TB, Cho YS, et al. Airway Measurement for Airway Remodeling Defined by Post-Bronchodilator FEV1/FVC in Asthma: Investigation Using Inspiration-Expiration Computed Tomography. *Allergy Asthma Immunol Res* 2011;3:111-7.
146. de Blic J, Tillie-Leblond I, Ernond S, Mahut B, Duy TLD, Scheinmann P. High-resolution computed tomography scan and airway remodeling in children with severe asthma. *Journal of Allergy and Clinical Immunology* 2005;116:750-4.
147. Marchac V, Emond S, Mamou-Mani T, et al. Thoracic CT in pediatric patients with difficult-to-treat asthma. *AJR AmJ Roentgenol* 2002;179:1245-52.
148. Saglani S, Papaioannou G, Khoo L, et al. Can HRCT be used as a marker of airway remodelling in children with difficult asthma? *Respiratory Research* 2006;7.
149. Ng CS, Desai SR, Rubens MB, Padley SP, Wells AU, Hansell DM. Visual quantitation and observer variation of signs of small airways disease at inspiratory and expiratory CT. *Journal of Thoracic Imaging* 1999;14:279-85.
150. Montaudon M, Lederlin M, Reich S, et al. Bronchial measurements in patients with asthma: comparison of quantitative thin-section CT findings with those in healthy subjects and correlation with pathologic findings. *Radiology* 2009;253:844-53.
151. Soja J, Grzanka P, Sladek K, et al. The use of endobronchial ultrasonography in assessment of bronchial wall remodeling in patients with asthma. *Chest* 2009;136:797-804.

152. Han S, El-Abbadi NH, Hanna N, et al. Evaluation of tracheal imaging by optical coherence tomography. *Respiration* 2005;72:537-41.
153. Hanna N, Saltzman D, Mukai D, et al. Two-dimensional and 3-dimensional optical coherence tomographic imaging of the airway, lung, and pleura. *J ThoracCardiovascSurg* 2005;129:615-22.
154. Whiteman SC, Yang Y, Gey van PD, Stephens M, Parmer J, Spiteri MA. Optical coherence tomography: real-time imaging of bronchial airways microstructure and detection of inflammatory/neoplastic morphologic changes. *Clin Cancer Res* 2006;12:813-8.
155. Coxson HO, Quiney B, Sin DD, et al. Airway wall thickness assessed using computed tomography and optical coherence tomography. *AmJ RespirCrit Care Med* 2008;177:1201-6.
156. Choe MM, Tomei AA, Swartz MA. Physiological 3D tissue model of the airway wall and mucosa. *Nat Protocols* 2006;1:357-62.
157. Huang S, Wiszniewski L, Derouette J-P, Constant S. In vitro organ culture models of asthma. *Drug Discovery Today: Disease Models* 2009;6:137-44.
158. Lange P, Parner J, Vestbo J, Schnohr P, Jensen G. A 15-year follow-up study of ventilatory function in adults with asthma. *NEnglJMed* 1998;339:1194-200.
159. Bumbacea D, Campbell D, Nguyen L, et al. Parameters associated with persistent airflow obstruction in chronic severe asthma. *European Respiratory Journal* 2004;24:122-8.
160. Phelan PD, Robertson CF, Olinsky A. The Melbourne Asthma Study: 1964-1999. *J Allergy Clin Immunol* 2002;109:189-94.
161. Jenkins HA, Cool C, Szeffler SJ, et al. Histopathology of severe childhood asthma: a case series. *Chest* 2003;124:32-41.
162. Rasmussen F, Taylor DR, Flannery EM, et al. Risk factors for airway remodeling in asthma manifested by a low postbronchodilator FEV1/vital capacity ratio: a longitudinal population study from childhood to adulthood. *Am J Respir Crit Care Med* 2002;165:1480-8.
163. de Marco R, Marcon A, Jarvis D, et al. Inhaled steroids are associated with reduced lung function decline in subjects with asthma with elevated total IgE. *J Allergy Clin Immunol* 2007;119:611-7.
164. Holgate ST. Has the time come to rethink the pathogenesis of asthma? *Curr Opin Allergy Clin Immunol* 2010;10:48-53.

165. Marguet C, Jouen-Boedes F, Dean TP, Warner JO. Bronchoalveolar cell profiles in children with asthma, infantile wheeze, chronic cough, or cystic fibrosis. *Am J Respir Crit Care Med* 1999;159:1533-40.
166. de Blic J, Tillie-Leblond I, Tonnel AB, Jaubert F, Scheinmann P, Gosset P. Difficult asthma in children: an analysis of airway inflammation. *J Allergy Clin Immunol* 2004;113:94-100.
167. Krawiec ME, Westcott JY, Chu HW, et al. Persistent wheezing in very young children is associated with lower respiratory inflammation. *Am J Respir Crit Care Med* 2001;163:1338-43.
168. Le Bourgeois M, Goncalves M, Le Clainche L, et al. Bronchoalveolar cells in children < 3 years old with severe recurrent wheezing. *Chest* 2002;122:791-7.
169. Barbato A, Turato G, Baraldo S, et al. Airway inflammation in childhood asthma. *Am J Respir Crit Care Med* 2003;168:798-803.
170. Saglani S, Payne DN, Zhu J, et al. Early detection of airway wall remodeling and eosinophilic inflammation in preschool wheezers. *Am J Respir Crit Care Med* 2007;176:858-64.
171. Payne DN, Qiu Y, Zhu J, et al. Airway inflammation in children with difficult asthma: relationships with airflow limitation and persistent symptoms. *Thorax* 2004;59:862-9.
172. Ward C, Pais M, Bish R, et al. Airway inflammation, basement membrane thickening and bronchial hyperresponsiveness in asthma. *Thorax* 2002;57:309-16.
173. Sont JK, Willems LN, Bel EH, van Krieken JH, Vandenbroucke JP, Sterk PJ. Clinical control and histopathologic outcome of asthma when using airway hyperresponsiveness as an additional guide to long-term treatment. The AMPUL Study Group. *Am J Respir Crit Care Med* 1999;159:1043-51.
174. Jeffery PK, Godfrey RW, Adelroth E, Nelson F, Rogers A, Johansson SA. Effects of treatment on airway inflammation and thickening of basement membrane reticular collagen in asthma. A quantitative light and electron microscopic study. *Am Rev Respir Dis* 1992;145:890-9.
175. Trigg CJ, Manolitsas ND, Wang J, et al. Placebo-controlled immunopathologic study of four months of inhaled corticosteroids in asthma. *Am J Respir Crit Care Med* 1994;150:17-22.
176. Olivieri D, Chetta A, Del Donno M, et al. Effect of short-term treatment with low-dose inhaled fluticasone propionate on airway inflammation and remodeling in mild asthma: a placebo-controlled study. *Am J Respir Crit Care Med* 1997;155:1864-71.

177. Stewart AG. Mediators and receptors in the resolution of inflammation: drug targeting opportunities. *Br J Pharmacol* 2009;158:933-5.
178. Young PG, Skinner SJ, Black PN. Effects of glucocorticoids and beta-adrenoceptor agonists on the proliferation of airway smooth muscle. *Eur J Pharmacol* 1995;273:137-43.
179. Schramm CM, Grunstein MM. Corticosteroid modulation of Na(+)-K<sup>+</sup> pump-mediated relaxation in maturing airway smooth muscle. *Br J Pharmacol* 1996;119:807-12.
180. Fernandes DJ, Mitchell RW, Lakser O, Dowell M, Stewart AG, Solway J. Do inflammatory mediators influence the contribution of airway smooth muscle contraction to airway hyperresponsiveness in asthma? *J Appl Physiol* 2003;95:844-53.
181. Goldsmith AM, Hershenson MB, Wolbert MP, Bentley JK. Regulation of airway smooth muscle alpha-actin expression by glucocorticoids. *Am J Physiol Lung Cell Mol Physiol* 2007;292:L99-L106.
182. Dorscheid DR, Wojcik KR, Sun S, Marroquin B, White SR. Apoptosis of airway epithelial cells induced by corticosteroids. *Am J Respir Crit Care Med* 2001;164:1939-47.
183. Descalzi D, Folli C, Nicolini G, et al. Anti-proliferative and anti-remodelling effect of beclomethasone dipropionate, formoterol and salbutamol alone or in combination in primary human bronchial fibroblasts. *Allergy* 2008;63:432-7.
184. Sabatini F, Silvestri M, Sale R, et al. Concentration-dependent effects of mometasone furoate and dexamethasone on foetal lung fibroblast functions involved in airway inflammation and remodeling. *Pulm Pharmacol Ther* 2003;16:287-97.
185. Niimi A, Matsumoto H, Amitani R, et al. Effect of short-term treatment with inhaled corticosteroid on airway wall thickening in asthma. *American Journal of Medicine* 2004;116:725-31.
186. Lee YM, Park JS, Hwang JH, et al. High-resolution CT findings in patients with near-fatal asthma - Comparison of patients with mild-to-severe asthma and normal control subjects and changes in airway abnormalities following steroid treatment. *Chest* 2004;126:1840-8.
187. Kurashima K, Kanauchi T, Hoshi T, et al. Effect of early versus late intervention with inhaled corticosteroids on airway wall thickness in patients with asthma. *Respirology* 2008;13:1008-13.
188. Kelly MM, Chakir J, Vethanayagam D, et al. Montelukast treatment attenuates the increase in myofibroblasts following low-dose allergen challenge. *Chest* 2006;130:741-53.
189. Zeidler MR, Kleerup EC, Goldin JG, et al. Montelukast improves regional air-trapping due to small airways obstruction in asthma. *Eur Respir J* 2006;27:307-15.

190. Flood-Page P, Menzies-Gow A, Phipps S, et al. Anti-IL-5 treatment reduces deposition of ECM proteins in the bronchial subepithelial basement membrane of mild atopic asthmatics. *J Clin Invest* 2003;112:1029-36.
191. Flood-Page PT, Menzies-Gow AN, Kay AB, Robinson DS. Eosinophil's role remains uncertain as anti-interleukin-5 only partially depletes numbers in asthmatic airway. *Am J Respir Crit Care Med* 2003;167:199-204.
192. Cox G, Thomson NC, Rubin AS, et al. Asthma control during the year after bronchial thermoplasty. *N Engl J Med* 2007;356:1327-37.
193. Castro M, Rubin AS, Laviolette M, et al. Effectiveness and safety of bronchial thermoplasty in the treatment of severe asthma: a multicenter, randomized, double-blind, sham-controlled clinical trial. *Am J Respir Crit Care Med* 2010;181:116-24.
194. Martin AJ, Landau LI, Phelan PD. Lung function in young adults who had asthma in childhood. *Am Rev Respir Dis* 1980;122:609-16.
195. Ulrik CS, Lange P. Decline of lung function in adults with bronchial asthma. *Am J Respir Crit Care Med* 1994;150:629-34.
196. Belousova EG, Haby MM, Xuan W, Peat JK. Factors that affect normal lung function in white Australian adults. *Chest* 1997;112:1539-46.
197. James AL, Palmer LJ, Kicic E, et al. Decline in lung function in the Busselton Health Study: the effects of asthma and cigarette smoking. *Am J Respir Crit Care Med* 2005;171:109-14.
198. Sears MR, Greene JM, Willan AR, et al. A longitudinal, population-based, cohort study of childhood asthma followed to adulthood. *N Engl J Med* 2003;349:1414-22.
199. Lange P, Ulrik CS, Vestbo J. Mortality in adults with self-reported asthma. Copenhagen City Heart Study Group. *Lancet* 1996;347:1285-9.
200. Panizza JA, James AL, Ryan G, de KN, Finucane KE. Mortality and airflow obstruction in asthma: a 17-year follow-up study. *Intern Med J* 2006;36:773-80.
201. Hansen EF, Phanareth K, Laursen LC, Kok-Jensen A, Dirksen A. Reversible and irreversible airflow obstruction as predictor of overall mortality in asthma and chronic obstructive pulmonary disease. *Am J Respir Crit Care Med* 1999;159:1267-71.
202. Cibella F, Cuttitta G, Bellia V, et al. Lung function decline in bronchial asthma. *Chest* 2002;122:1944-8.
203. Ulrik CS, Backer V. Nonreversible airflow obstruction in life-long nonsmokers with moderate to severe asthma. *Eur Respir J* 1999;14:892-6.

204. Ulrik CS, Backer V, Dirksen A. A 10 year follow up of 180 adults with bronchial asthma: factors important for the decline in lung function. *Thorax* 1992;47:14-8.
205. Miranda C, Busacker A, Balzar S, Trudeau J, Wenzel SE. Distinguishing severe asthma phenotypes: role of age at onset and eosinophilic inflammation. *J Allergy Clin Immunol* 2004;113:101-8.
206. Moore WC, Bleecker ER, Curran-Everett D, et al. Characterization of the severe asthma phenotype by the National Heart, Lung, and Blood Institute's Severe Asthma Research Program. *J Allergy Clin Immunol* 2007;119:405-13.
207. Bai TR, Vonk JM, Postma DS, Boezen HM. Severe exacerbations predict excess lung function decline in asthma. *European Respiratory Journal* 2007;30:452-6.
208. O'Byrne PM, Pedersen S, Lamm CJ, Tan WC, Busse WW. Severe exacerbations and decline in lung function in asthma. *AmJRespirCrit Care Med* 2009;179:19-24.
209. Taussig LM, Wright AL, Holberg CJ, Halonen M, Morgan WJ, Martinez FD. Tucson Children's Respiratory Study: 1980 to present. *J Allergy Clin Immunol* 2003;111:661-75; quiz 76.
210. Sherrill DL, Martinez FD, Lebowitz MD, et al. Longitudinal effects of passive smoking on pulmonary function in New Zealand children. *Am Rev Respir Dis* 1992;145:1136-41.
211. Dijkstra A, Vonk JM, Jongepier H, et al. Lung function decline in asthma: association with inhaled corticosteroids, smoking and sex. *Thorax* 2006;61:105-10.
212. Dijkstra A, Howard TD, Vonk JM, et al. Estrogen receptor 1 polymorphisms are associated with airway hyperresponsiveness and lung function decline, particularly in female subjects with asthma. *J Allergy Clin Immunol* 2006;117:604-11.
213. Fairs A, Agbetile J, Hargadon B, et al. IgE sensitization to *Aspergillus fumigatus* is associated with reduced lung function in asthma. *Am J Respir Crit Care Med* 2010;182:1362-8.
214. Denning DW, O'Driscoll BR, Hogaboam CM, Bowyer P, Niven RM. The link between fungi and severe asthma: a summary of the evidence. *Eur Respir J* 2006;27:615-26.
215. Chishimba L, Niven RM, Cooley J, Denning DW. Voriconazole and Posaconazole Improve Asthma Severity in Allergic Bronchopulmonary Aspergillosis and Severe Asthma with Fungal Sensitization. *J Asthma* 2012.
216. Park HW, Kim DI, Sohn SW, et al. Outcomes in occupational asthma caused by reactive dye after long-term avoidance. *Clin Exp Allergy* 2007;37:225-30.

217. Anees W, Huggins V, Pavord ID, Robertson AS, Burge PS. Occupational asthma due to low molecular weight agents: eosinophilic and non-eosinophilic variants. *Thorax* 2002;57:231-6.
218. Vonk JM, Jongepier H, Panhuysen CIM, Schouten JP, Bleecker ER, Postma DS. Risk factors associated with the presence of irreversible airflow limitation and reduced transfer coefficient in patients with asthma after 26 years of follow up. *Thorax* 2003;58:322-7.
219. Brutsche MH, Downs SH, Schindler C, et al. Bronchial hyperresponsiveness and the development of asthma and COPD in asymptomatic individuals: SAPALDIA cohort study. *Thorax* 2006;61:671-7.
220. Little SA, MacLeod KJ, Chalmers GW, Love JG, McSharry C, Thomson NC. Association of forced expiratory volume with disease duration and sputum neutrophils in chronic asthma. *Am J Med* 2002;112:446-52.
221. An SS, Bai TR, Bates JHT, et al. Airway smooth muscle dynamics: a common pathway of airway obstruction in asthma. *European Respiratory Journal* 2007;29:834-60.
222. Wardlaw AJ, Dunnette S, Gleich GJ, Collins JV, Kay AB. Eosinophils and mast cells in bronchoalveolar lavage in subjects with mild asthma. Relationship to bronchial hyperreactivity. *Am Rev Respir Dis* 1988;137:62-9.
223. De Monchy JG, Kauffman HF, Venge P, et al. Bronchoalveolar eosinophilia during allergen-induced late asthmatic reactions. *Am Rev Respir Dis* 1985;131:373-6.
224. Polosa R, Renaud L, Cacciola R, Prosperini G, Crimi N, Djukanovic R. Sputum eosinophilia is more closely associated with airway responsiveness to bradykinin than methacholine in asthma. *Eur Respir J* 1998;12:551-6.
225. Van Den Berge M, Meijer RJ, Kerstjens HA, et al. PC(20) adenosine 5'-monophosphate is more closely associated with airway inflammation in asthma than PC(20) methacholine. *Am J Respir Crit Care Med* 2001;163:1546-50.
226. Rosi E, Ronchi MC, Grazzini M, Duranti R, Scano G. Sputum analysis, bronchial hyperresponsiveness, and airway function in asthma: results of a factor analysis. *J Allergy Clin Immunol* 1999;103:232-7.
227. Brightling CE. Chronic cough due to nonasthmatic eosinophilic bronchitis - ACCP evidence-based clinical practice guidelines. *Chest* 2006;129:116S-21S.
228. Gibson PG, Dolovich J, Denburg J, Ramsdale EH, Hargreave FE. Chronic cough: eosinophilic bronchitis without asthma. *Lancet* 1989;1:1346-8.

229. Lambert RK, Wiggs BR, Kuwano K, Hogg JC, Pare PD. Functional significance of increased airway smooth muscle in asthma and COPD. *J Appl Physiol* 1993;74:2771-81.
230. Taylor DR, Bateman ED, Boulet LP, et al. A new perspective on concepts of asthma severity and control. *EurRespirJ* 2008;32:545-54.
231. Turner MO, Noertjojo K, Vedal S, Bai T, Crump S, Fitzgerald JM. Risk factors for near-fatal asthma. A case-control study in hospitalized patients with asthma. *Am J Respir Crit Care Med* 1998;157:1804-9.
232. Dales RE, Schweitzer I, Kerr P, Gougeon L, Rivington R, Draper J. Risk factors for recurrent emergency department visits for asthma. *Thorax* 1995;50:520-4.
233. Ford JG, Meyer IH, Sternfels P, et al. Patterns and predictors of asthma-related emergency department use in Harlem. *Chest* 2001;120:1129-35.
234. Osborne ML, Pedula KL, O'Hollaren M, et al. Assessing future need for acute care in adult asthmatics: the Profile of Asthma Risk Study: a prospective health maintenance organization-based study. *Chest* 2007;132:1151-61.
235. Miller MK, Lee JH, Miller DP, Wenzel SE, Group TS. Recent asthma exacerbations: a key predictor of future exacerbations. *Respir Med* 2007;101:481-9.
236. Lyell PJ, Villanueva E, Burton D, Freezer NJ, Bardin PG. Risk factors for intensive care in children with acute asthma. *Respirology* 2005;10:436-41.
237. Haselkorn T, Zeiger RS, Chipps BE, et al. Recent asthma exacerbations predict future exacerbations in children with severe or difficult-to-treat asthma. *J Allergy Clin Immunol* 2009;124:921-7.
238. Hamilton LM, Torres-Lozano C, Puddicombe SM, et al. The role of the epidermal growth factor receptor in sustaining neutrophil inflammation in severe asthma. *Clin Exp Allergy* 2003;33:233-40.
239. Wark PA, Johnston SL, Bucchieri F, et al. Asthmatic bronchial epithelial cells have a deficient innate immune response to infection with rhinovirus. *Journal of Experimental Medicine* 2005;201:937-47.
240. Contoli M, Message SD, Laza-Stanca V, et al. Role of deficient type III interferon-lambda production in asthma exacerbations. *Nature Medicine* 2006;12:1023-6.
241. ten Brinke A, van Dissel JT, Sterk PJ, Zwinderman AH, Rabe KF, Bel EH. Persistent airflow limitation in adult-onset nonatopic asthma is associated with serologic evidence of *Chlamydia pneumoniae* infection. *J Allergy Clin Immunol* 2001;107:449-54.



242. Bhavsar P, Hew M, Khorasani N, et al. Relative corticosteroid insensitivity of alveolar macrophages in severe asthma compared with non-severe asthma. *Thorax* 2008;63:784-90.
243. Yamada K, Elliott WM, Brattsand R, Valeur A, Hogg JC, Hayashi S. Molecular mechanisms of decreased steroid responsiveness induced by latent adenoviral infection in allergic lung inflammation. *J Allergy Clin Immunol* 2002;109:35-42.
244. FitzGerald JM, Gibson PG. Asthma exacerbations . 4: Prevention. *Thorax* 2006;61:992-9.
245. Gleich GJ, Motojima S, Frigas E, Kephart GM, Fujisawa T, Kravis LP. The eosinophilic leukocyte and the pathology of fatal bronchial asthma: evidence for pathologic heterogeneity. *J Allergy Clin Immunol* 1987;80:412-5.
246. Houston JC, De Navasquez S, Trounce JR. A clinical and pathological study of fatal cases of status asthmaticus. *Thorax* 1953;8:207-13.
247. Blackie SP, al-Majed S, Staples CA, Hilliam C, Pare PD. Changes in total lung capacity during acute spontaneous asthma. *Am Rev Respir Dis* 1990;142:79-83.
248. Gelb AF, Schein A, Nussbaum E, et al. Risk factors for near-fatal asthma. *Chest* 2004;126:1138-46.
249. Kuyper LM, Pare PD, Hogg JC, et al. Characterization of airway plugging in fatal asthma. *Am J Med* 2003;115:6-11.
250. Jayaram L, Pizzichini MM, Cook RJ, et al. Determining asthma treatment by monitoring sputum cell counts: effect on exacerbations. *European Respiratory Journal* 2006;27:483-94.
251. Anderson GP. Endotyping asthma: new insights into key pathogenic mechanisms in a complex, heterogeneous disease. *Lancet* 2008;372:1107-19.
252. ten Brinke A, Sterk PJ, Masclee AA, et al. Risk factors of frequent exacerbations in difficult-to-treat asthma. *Eur Respir J* 2005;26:812-8.
253. Woodruff PG, Modrek B, Choy DF, et al. T-helper type 2-driven inflammation defines major subphenotypes of asthma. *Am J Respir Crit Care Med* 2009;180:388-95.
254. Lotvall J, Akdis CA, Bacharier LB, et al. Asthma endotypes: a new approach to classification of disease entities within the asthma syndrome. *J Allergy Clin Immunol* 2011;127:355-60.

255. Brasier AR, Victor S, Boetticher G, et al. Molecular phenotyping of severe asthma using pattern recognition of bronchoalveolar lavage-derived cytokines. *J Allergy Clin Immunol* 2008;121:30-7 e6.
256. Dragonieri S, Schot R, Mertens BJ, et al. An electronic nose in the discrimination of patients with asthma and controls. *J Allergy Clin Immunol* 2007;120:856-62.
257. Laprise C, Sladek R, Ponton A, Bernier MC, Hudson TJ, Laviolette M. Functional classes of bronchial mucosa genes that are differentially expressed in asthma. *Bmc Genomics* 2004;5.
258. Yuyama N, Davies DE, Akaiwa M, et al. Analysis of novel disease-related genes in bronchial asthma. *Cytokine* 2002;19:287-96.
259. Kollins SA. Computed tomography of the pulmonary parenchyma and chest wall. *RadiolClinNorth Am* 1977;15:297-308.
260. Bessis L, Callard P, Gotheil C, Biaggi A, Grenier P. High-resolution CT of parenchymal lung disease: precise correlation with histologic findings. *Radiographics* 1992;12:45-58.
261. Carretta A, Ciriaco P, Melloni G, et al. Correlation of computed tomography densitometry and pathological grading of emphysema with the variation of respiratory function after lobectomy for lung cancer. *InteractCardiovascThoracSurg* 2010;10:914-7.
262. Grenier P, MoureyGerosa I, Benali K, et al. Abnormalities of the airways and lung parenchyma in asthmatics: CT observations in 50 patients and inter- and intraobserver variability. *European Radiology* 1996;6:199-206.
263. Paganin F, Trussard V, Seneterre E, et al. Chest Radiography and High-Resolution Computed-Tomography of the Lungs in Asthma. *American Review of Respiratory Disease* 1992;146:1084-7.
264. Paganin F, Seneterre E, Chanez P, et al. Computed tomography of the lungs in asthma: Influence of disease severity and etiology. *American Journal of Respiratory and Critical Care Medicine* 1996;153:110-4.
265. Lynch DA, Newell JD, Tschomper BA, Cink TM, Newman LS, Bethel R. Uncomplicated Asthma in Adults - Comparison of Ct Appearance of the Lungs in Asthmatic and Healthy-Subjects. *Radiology* 1993;188:829-33.
266. Park CS, Muller NL, Worthy SA, Kim JS, Awadh N, Fitzgerald M. Airway obstruction in asthmatic and healthy individuals: Inspiratory and expiratory thin-section CT findings. *Radiology* 1997;203:361-7.

267. Takemura M, Niimi A, Minakuchi M, et al. Bronchial dilatation in asthma - Relation to clinical and sputum indices. *Chest* 2004;125:1352-8.
268. Harmanci E, Kebapci M, Metintas M, Ozkan R. High-resolution computed tomography findings are correlated with disease severity in asthma. *Respiration* 2002;69:420-6.
269. Laurent F, Latrabe V, Raherison C, Marthan R, Tunon-de-Lara JM. Functional significance of air trapping detected in moderate asthma. *European Radiology* 2000;10:1404-10.
270. Yilmaz S, Ekici A, Ekici M, Keles H. High-resolution computed tomography findings in elderly patients with asthma. *European Journal of Radiology* 2006;59:238-43.
271. Menzies D, Holmes L, McCumesky G, Prys-Picard C, Niven R. Aspergillus sensitization is associated with airflow limitation and bronchiectasis in severe asthma. *Allergy* 2011;66:679-85.
272. Kim JS, Muller NL, Park CS, et al. Bronchoarterial ratio on thin section CT: Comparison between high altitude and sea level. *Journal of Computer Assisted Tomography* 1997;21:306-11.
273. Matsuoka S, Uchiyama K, Shima H, Ueno N, Oish S, Nojiri Y. Bronchoarterial ratio and bronchial wall thickness on high-resolution CT in asymptomatic subjects: Correlation with age and smoking. *American Journal of Roentgenology* 2003;180:513-8.
274. Oguzulgen IK, Kervan F, Ozis T, Turktas H. The impact of bronchiectasis in clinical presentation of asthma. *Southern Medical Journal* 2007;100:468-71.
275. Lynch DA. Imaging of asthma and allergic bronchopulmonary mycosis. *Radiologic Clinics of North America* 1998;36:129-+.
276. Park JW, Hong YK, Kim CW, Kim DK, Choe KO, Hong CS. High-resolution computed tomography in patients with bronchial asthma: Correlation with clinical features, pulmonary functions and bronchial hyperresponsiveness. *Journal of Investigational Allergology & Clinical Immunology* 1997;7:186-92.
277. Webb WR. High-resolution computed tomography of obstructive lung disease. *RadiolClinNorth Am* 1994;32:745-57.
278. Webb WR, Gamsu G, Wall SD, Cann CE, Proctor E. CT of a bronchial phantom. Factors affecting appearance and size measurements. *Invest Radiol* 1984;19:394-8.
279. Bankier AA, Fleischmann D, Mallek R, et al. Bronchial wall thickness: Appropriate window settings for thin-section CT and radiologic-anatomic correlation. *Radiology* 1996;199:831-6.

280. McNamara AE, Muller NL, Okazawa M, Arntorp J, Wiggs BR, Pare PD. Airway Narrowing in Excised Canine Lungs Measured by High-Resolution Computed-Tomography. *Journal of Applied Physiology* 1992;73:307-16.
281. Seneterre E, Paganin F, Bruel JM, Michel FB, Bousquet J. Measurement of the Internal Size of Bronchi Using High-Resolution Computed-Tomography (Hrct). *European Respiratory Journal* 1994;7:596-600.
282. Okazawa M, Muller N, McNamara AE, Child S, Verburgt L, Pare PD. Human airway narrowing measured using high resolution computed tomography. *AmJ RespirCrit Care Med* 1996;154:1557-62.
283. McNitt-Gray MF, Goldin JG, Johnson TD, Tashkin DP, Aberle DR. Development and testing of image-processing methods for the quantitative assessment of airway hyperresponsiveness from high-resolution CT images. *J ComputAssistTomogr* 1997;21:939-47.
284. King GG, Muller NL, Whittall KP, Xiang QS, Pare PD. An analysis algorithm for measuring airway lumen and wall areas from high-resolution computed tomographic data. *AmJ RespirCrit Care Med* 2000;161:574-80.
285. de Jong PA, Muller NL, Pare PD, Coxson HO. Computed tomographic imaging of the airways: relationship to structure and function. *European Respiratory Journal* 2005;26:140-52.
286. Nakano Y, Whittall KP, Kalloger SE, et al. Development and validation of human airway analysis algorithm using multidetector row CT. *Medical Imaging 2002: Physiology and Function from Multidimensional Images* 2002;4683:460-9.
287. Reinhardt JM, D'Souza ND, Hoffman EA. Accurate measurement of intrathoracic airways. *Ieee Transactions on Medical Imaging* 1997;16:820-7.
288. Brillet PY, Fetita CI, Beigelman-Aubry C, et al. Quantification of bronchial dimensions at MDCT using dedicated software. *EurRadiol* 2007;17:1483-9.
289. Saragaglia A, Fetita C, Preteux F, Brillet PY, Grenier PA. Accurate 3D quantification of bronchial parameters in MDCT. *Proceedings SPIE* 2005;5916:323-34.
290. Achenbach T, Weinheimer O, Dueber C, Heussel CP. Influence of pixel size on quantification of airway wall thickness in computed tomography. *JComputAssistTomogr* 2009;33:725-30.
291. Achenbach T, Weinheimer O, Biedermann A, et al. MDCT assessment of airway wall thickness in COPD patients using a new method: correlations with pulmonary function tests. *European Radiology* 2008;18:2731-8.

292. Estepar RS, Washko GG, Silverman EK, Reilly JJ, Kikinis R, Westin CF. Accurate airway wall estimation using phase congruency. *MedImage ComputComputAssistInterv* 2006;9:125-34.
293. San Jose ER, Reilly JJ, Silverman EK, Washko GR. Three-dimensional airway measurements and algorithms. *ProcAmThoracSoc* 2008;5:905-9.
294. Saba OI, Hoffman EA, Reinhardt JM. Maximizing quantitative accuracy of lung airway lumen and wall measures obtained from X-ray CT imaging. *JApplPhysiol* 2003;95:1063-75.
295. Awadh N, Muller NL, Park CS, Abboud RT, FitzGerald JM. Airway wall thickness in patients with near fatal asthma and control groups: assessment with high resolution computed tomographic scanning. *Thorax* 1998;53:248-53.
296. Kasahara K, Shiba K, Ozawa T, Okuda K, Adachi M. Correlation between the bronchial subepithelial layer and whole airway wall thickness in patients with asthma. *Thorax* 2002;57:242-6.
297. Brillet PY, Fetita CI, Capderou A, et al. Variability of bronchial measurements obtained by sequential CT using two computer-based methods. *EurRadiol* 2009;19:1139-47.
298. Beigelman-Aubry C, Capderou A, Grenier PA, et al. Mild intermittent asthma: CT assessment of bronchial cross-sectional area and lung attenuation at controlled lung volume. *Radiology* 2002;223:181-7.
299. Kee ST, Fahy JV, Chen DR, Gamsu G. High-resolution computed tomography of airway changes after induced bronchoconstriction and bronchodilation in asthmatic volunteers. *Academic Radiology* 1996;3:389-94.
300. Niimi A, Matsumoto H, Takemura M, Ueda T, Chin K, Mishima M. Relationship of airway wall thickness to airway sensitivity and airway reactivity in asthma. *American Journal of Respiratory and Critical Care Medicine* 2003;168:983-8.
301. Boulet L, Belanger M, Carrier G. Airway responsiveness and bronchial-wall thickness in asthma with or without fixed airflow obstruction. *AmJ RespirCrit Care Med* 1995;152:865-71.
302. Busacker A, Newell JD, Jr., Keefe T, et al. A multivariate analysis of risk factors for the air-trapping asthmatic phenotype as measured by quantitative CT analysis. *Chest* 2009;135:48-56.
303. Brightling CE, Symon FA, Birring SS, Bradding P, Wardlaw AJ, Pavord ID. Comparison of airway immunopathology of eosinophilic bronchitis and asthma. *Thorax* 2003;58:528-32.

304. James AL, Pare PD, Hogg JC. The mechanics of airway narrowing in asthma. *AmRevRespirDis* 1989;139:242-6.
305. Yamaguchi M, Niimi A, Matsumoto H, et al. Sputum levels of transforming growth factor-beta1 in asthma: relation to clinical and computed tomography findings. *JInvestigAllergolClinImmunol* 2008;18:202-6.
306. Matsumoto H, Niimi A, Takemura M, et al. Long-term changes in airway-wall thickness on computed tomography in asthmatic patients. *J Investig Allergol Clin Immunol* 2011;21:113-9.
307. Brillet PY, Attali V, Nachbaur G, et al. Multidetector row computed tomography to assess changes in airways linked to asthma control. *Respiration* 2011;81:461-8.
308. Kraft M. The distal airways: are they important in asthma? *EurRespirJ* 1999;14:1403-17.
309. Yanai M, Sekizawa K, Ohnishi T, Sasaki H, Takishima T. Site of airway obstruction in pulmonary disease: direct measurement of intrabronchial pressure. *JApplPhysiol* 1992;72:1016-23.
310. Wagner EM, Liu MC, Weinmann GG, Permutt S, Bleecker ER. Peripheral lung resistance in normal and asthmatic subjects. *AmRevRespirDis* 1990;141:584-8.
311. Hamid Q, Song Y, Kotsimbos TC, et al. Inflammation of small airways in asthma. *Journal of Allergy and Clinical Immunology* 1997;100:44-51.
312. Kraft M, Martin RJ, Wilson S, Djukanovic R, Holgate ST. Lymphocyte and eosinophil influx into alveolar tissue in nocturnal asthma. *AmJ RespirCrit Care Med* 1999;159:228-34.
313. Guckel C, Wells AU, Taylor DA, Chabat F, Hansell DM. Mechanism of mosaic attenuation of the lungs on computed tomography in induced bronchospasm. *J ApplPhysiol* 1999;86:701-8.
314. Muller NL, Staples CA, Miller RR, Abboud RT. "Density mask". An objective method to quantitate emphysema using computed tomography. *Chest* 1988;94:782-7.
315. Coxson HO, Rogers RM, Whittall KP, et al. A quantification of the lung surface area in emphysema using computed tomography. *AmJ RespirCrit Care Med* 1999;159:851-6.
316. Madani A, Zanen J, de MV, Gevenois PA. Pulmonary emphysema: objective quantification at multi-detector row CT--comparison with macroscopic and microscopic morphometry. *Radiology* 2006;238:1036-43.

317. Gevenois PA, De VP, Sy M, et al. Pulmonary emphysema: quantitative CT during expiration. *Radiology* 1996;199:825-9.
318. Bankier AA, de MV, Keyzer C, Gevenois PA. Pulmonary emphysema: subjective visual grading versus objective quantification with macroscopic morphometry and thin-section CT densitometry. *Radiology* 1999;211:851-8.
319. Newman KB, Lynch DA, Newman LS, Ellegood D, Newell JD. Quantitative Computed-Tomography Detects Air Trapping Due to Asthma. *Chest* 1994;106:105-9.
320. Tunon-de-Lara JM, Laurent F, Giraud V, et al. Air trapping in mild and moderate asthma: effect of inhaled corticosteroids. *Journal of Allergy and Clinical Immunology* 2007;119:583-90.
321. Goldin JG, McNitt-Gray MF, Sorenson SM, et al. Airway hyperreactivity: assessment with helical thin-section CT. *Radiology* 1998;208:321-9.
322. Tanaka N, Matsumoto T, Miura G, et al. Air trapping at CT: high prevalence in asymptomatic subjects with normal pulmonary function. *Radiology* 2003;227:776-85.
323. Grenier PA, Beigelman-Aubry C, Fetita C, Preteux F, Brauner MW, Lenoir S. New frontiers in CT imaging of airway disease. *European Radiology* 2002;12:1022-44.
324. Mitsunobu F, Mifune T, Ashida K, et al. Influence of age and disease severity on high resolution CT lung densitometry in asthma. *Thorax* 2001;56:851-6.
325. Mitsunobu F, Ashida K, Hosaki Y, et al. Decreased computed tomographic lung density during exacerbation of asthma. *EurRespirJ* 2003;22:106-12.
326. Jain N, Covar RA, Gleason MC, Newell JD, Jr., Gelfand EW, Spahn JD. Quantitative computed tomography detects peripheral airway disease in asthmatic children. *PediatrPulmonol* 2005;40:211-8.
327. Goldin JG, Tashkin DP, Kleerup EC, et al. Comparative effects of hydrofluoroalkane and chlorofluorocarbon beclomethasone dipropionate inhalation on small airways: assessment with functional helical thin-section computed tomography. *Journal of Allergy and Clinical Immunology* 1999;104:S258-S67.
328. Mitsunobu F, Ashida K, Hosaki Y, et al. Complexity of terminal airspace geometry assessed by computed tomography in asthma. *AmJ RespirCrit Care Med* 2003;167:411-7.
329. Torigian DA, Geftter WB, Affuso JD, Emami K, Dougherty L. Application of an optical flow method to inspiratory and expiratory lung MDCT to assess regional air trapping: a feasibility study. *AJR AmJ Roentgenol* 2007;188:W276-W80.

330. Mandelbrot BB. The Fractal Geometry of Nature.: Updated and Augmented. Freeman, New York; 1983.
331. Goldberger AL. Non-linear dynamics for clinicians: chaos theory, fractals, and complexity at the bedside. *Lancet* 1996;347:1312-4.
332. Goldberger AL, Amaral LA, Hausdorff JM, Ivanov P, Peng CK, Stanley HE. Fractal dynamics in physiology: alterations with disease and aging. *Proc Natl Acad Sci U S A* 2002;99 Suppl 1:2466-72.
333. Mishima M, Hirai T, Itoh H, et al. Complexity of terminal airspace geometry assessed by lung computed tomography in normal subjects and patients with chronic obstructive pulmonary disease. *Proc Natl Acad Sci U S A* 1999;96:8829-34.
334. Karperien A, Jelinek HF, Leandro JJ, Soares JV, Cesar RM, Jr., Luckie A. Automated detection of proliferative retinopathy in clinical practice. *Clin Ophthalmol* 2008;2:109-22.
335. Goldberger AL, Bhargava V, West BJ, Mandell AJ. On a mechanism of cardiac electrical stability. The fractal hypothesis. *Biophys J* 1985;48:525-8.
336. McNamee JE. Fractal perspectives in pulmonary physiology. *J Appl Physiol* 1991;71:1-8.
337. Kitaoka H, Suki B. Branching design of the bronchial tree based on a diameter-flow relationship. *J Appl Physiol* 1997;82:968-76.
338. Weibel ER. Fractal geometry: a design principle for living organisms. *Am J Physiol* 1991;261:L361-9.
339. Suki B. Fluctuations and power laws in pulmonary physiology. *Am J Respir Crit Care Med* 2002;166:133-7.
340. Cutting JE, Garvin JJ. Fractal curves and complexity. *Percept Psychophys* 1987;42:365-70.
341. Schulze MM, Hutchings N, Simpson TL. The use of fractal analysis and photometry to estimate the accuracy of bulbar redness grading scales. *Invest Ophthalmol Vis Sci* 2008;49:1398-406.
342. Boser SR, Park H, Perry SF, Menache MG, Green FH. Fractal geometry of airway remodeling in human asthma. *Am J Respir Crit Care Med* 2005;172:817-23.
343. Frey U, Brodbeck T, Majumdar A, et al. Risk of severe asthma episodes predicted from fluctuation analysis of airway function. *Nature* 2005;438:667-70.



344. Stern G, de Jongste J, van der Valk R, et al. Fluctuation phenotyping based on daily fraction of exhaled nitric oxide values in asthmatic children. *J Allergy Clin Immunol* 2011;128:293-300.
345. Brenner DJ. Should we be concerned about the rapid increase in CT usage? *Rev Environ Health* 2010;25:63-8.
346. Aldrich JE, Bilawich AM, Mayo JR. Radiation doses to patients receiving computed tomography examinations in British Columbia. *Can Assoc Radiol J* 2006;57:79-85.
347. Pearce MS, Salotti JA, McHugh K, et al. CT scans in young people in Northern England: trends and patterns 1993-2002. *Pediatr Radiol* 2011;41:832-8.
348. Shrimpton PC, Edyvean S. CT scanner dosimetry. *Br J Radiol* 1998;71:1-3.
349. ICRP. The 2007 Recommendations of the International Commission on Radiological Protection. ICRP Publication 103. *Ann. ICRP* 37 (2-4); 2007.
350. Cohen BL. Cancer risk from low-level radiation. *AJR Am J Roentgenol* 2002;179:1137-43.
351. Tubiana M. Dose-effect relationship and estimation of the carcinogenic effects of low doses of ionizing radiation: the joint report of the Academie des Sciences (Paris) and of the Academie Nationale de Medecine. *Int J Radiat Oncol Biol Phys* 2005;63:317-9.
352. Berrington A, Darby SC, Weiss HA, Doll R. 100 years of observation on British radiologists: mortality from cancer and other causes 1897-1997. *Br J Radiol* 2001;74:507-19.
353. Strzelczyk JJ, Damilakis J, Marx MV, Macura KJ. Facts and controversies about radiation exposure, part 2: low-level exposures and cancer risk. *J Am Coll Radiol* 2007;4:32-9.
354. Calabrese EJ, Stanek EJ, 3rd, Nascarella MA, Hoffmann GR. Hormesis predicts low-dose responses better than threshold models. *Int J Toxicol* 2008;27:369-78.
355. Cardis E, Vrijheid M, Blettner M, et al. The 15-Country Collaborative Study of Cancer Risk among Radiation Workers in the Nuclear Industry: estimates of radiation-related cancer risks. *Radiat Res* 2007;167:396-416.
356. Pierce DA, Shimizu Y, Preston DL, Vaeth M, Mabuchi K. Studies of the mortality of atomic bomb survivors. Report 12, Part I. Cancer: 1950-1990. *Radiat Res* 1996;146:1-27.

357. Brenner D, Elliston C, Hall E, Berdon W. Estimated risks of radiation-induced fatal cancer from pediatric CT. *AJR Am J Roentgenol* 2001;176:289-96.
358. Parker MS, Hui FK, Camacho MA, Chung JK, Broga DW, Sethi NN. Female breast radiation exposure during CT pulmonary angiography. *AJR Am J Roentgenol* 2005;185:1228-33.
359. Hurwitz LM, Yoshizumi TT, Reiman RE, et al. Radiation dose to the female breast from 16-MDCT body protocols. *AJR Am J Roentgenol* 2006;186:1718-22.
360. Milne EN. Female breast radiation exposure. *AJR Am J Roentgenol* 2006;186:E24.
361. Allisy-Roberts P, Williams J, Farr RF. *Farr's Physics for Medical Imaging*: Saunders; 2007.
362. Shrimpton PC, Jones DG, Hillier MC, Board GBNRP. Survey of CT practice in the UK. Part 2: Dosimetric aspects: NRPB; 1991.
363. ImPACT's CT dosimetry tool. 2012. (Accessed 04/01/2012, at <http://www.impactscan.org/ctdosimetry.htm>.)
364. Greess H, Lutze J, Nomayr A, et al. Dose reduction in subsecond multislice spiral CT examination of children by online tube current modulation. *Eur Radiol* 2004;14:995-9.
365. Health Protection Agency, UK. 2012 (Accessed 06/01/2012 at [http://www.hpa.org.uk/web/HPAweb&HPAwebStandard/HPAweb\\_C/1195733826941](http://www.hpa.org.uk/web/HPAweb&HPAwebStandard/HPAweb_C/1195733826941))
366. London Health Observatory, UK. 2012 (Accessed 06/01/2012 at [http://www.lho.org.uk/LHO\\_Topics/Health\\_Topics/Determinants\\_of\\_Health/Environment/Radiation.aspx](http://www.lho.org.uk/LHO_Topics/Health_Topics/Determinants_of_Health/Environment/Radiation.aspx))
367. van Beek EJ, Hoffman EA. Functional imaging: CT and MRI. *Clin Chest Med* 2008;29:195-216, vii.
368. Hoffman EA, Chon D. Computed tomography studies of lung ventilation and perfusion. *ProcAmThoracSoc* 2005;2:492-8, 506.
369. Chon D, Simon BA, Beck KC, et al. Differences in regional wash-in and wash-out time constants for xenon-CT ventilation studies. *RespirPhysiol Neurobiol* 2005;148:65-83.
370. Johnson TR, Krauss B, Sedlmair M, et al. Material differentiation by dual energy CT: initial experience. *EurRadiol* 2007;17:1510-7.
371. Herbert DL, Gur D, Shabason L, et al. Mapping of human local pulmonary ventilation by xenon enhanced computed tomography. *J ComputAssistTomogr* 1982;6:1088-93.

372. Bayat S, Porra L, Suhonen H, et al. Imaging of lung function using synchrotron radiation computed tomography: what's new? *Eur J Radiol* 2008;68:S78-S83.
373. Porra L, Monfraix S, Berruyer G, et al. Effect of tidal volume on distribution of ventilation assessed by synchrotron radiation CT in rabbit. *J Appl Physiol* 2004;96:1899-908.
374. Monfraix S, Bayat S, Porra L, et al. Quantitative measurement of regional lung gas volume by synchrotron radiation computed tomography. *Physics in Medicine and Biology* 2005;50:1-11.
375. Bayat S, Porra L, Suhonen H, Nemoz C, Suortti P, Sovijarvi AR. Differences in the time course of proximal and distal airway response to inhaled histamine studied by synchrotron radiation CT. *J Appl Physiol* 2006;100:1964-73.
376. Bayat S, Strengell S, Porra L, et al. Methacholine and ovalbumin challenges assessed by forced oscillations and synchrotron lung imaging. *Am J Respir Crit Care Med* 2009;180:296-303.
377. Adam JF, Nemoz C, Bravin A, et al. High-resolution blood-brain barrier permeability and blood volume imaging using quantitative synchrotron radiation computed tomography: study on an F98 rat brain glioma. *J Cereb Blood Flow Metab* 2005;25:145-53.
378. Chae EJ, Seo JB, Lee J, et al. Xenon ventilation imaging using dual-energy computed tomography in asthmatics: initial experience. *Invest Radiol* 2010;45:354-61.
379. Schenzle JC, Sommer WH, Neumaier K, et al. Dual energy CT of the chest: how about the dose? *Invest Radiol* 2010;45:347-53.
380. Remy-Jardin M, Faivre JB, Pontana F, et al. Thoracic applications of dual energy. *Radiol Clin North Am* 2010;48:193-205.
381. Hodson ME, Simon G, Batten JC. Radiology of uncomplicated asthma. *Thorax* 1974;29:296-303.
382. Woods AQ, Lynch DA. Asthma: an imaging update. *Radiol Clin North Am* 2009;47:317-29.
383. Ismail Y, Loo CS, Zahary MK. The value of routine chest radiographs in acute asthma admissions. *Singapore Med J* 1994;35:171-2.
384. Blair DN, Coppage L, Shaw C. Medical imaging in asthma. *J Thorac Imaging* 1986;1:23-35.
385. Zieverink SE, Harper AP, Holden RW, Klatte EC, Brittain H. Emergency room radiography of asthma: an efficacy study. *Radiology* 1982;145:27-9.

386. Findley LJ, Sahn SA. The value of chest roentgenograms in acute asthma in adults. *Chest* 1981;80:535-6.
387. Tsai TW, Gallagher EJ, Lombardi G, Gennis P, Carter W. Guidelines for the selective ordering of admission chest radiography in adult obstructive airway disease. *Annals of Emergency Medicine* 1993;22:1854-8.
388. Gentile NT, Ufberg J, Barnum M, McHugh M, Karras D. Guidelines reduce x-ray and blood gas utilization in acute asthma. *AmJ EmergMed* 2003;21:451-3.
389. Shaw TJ, Wakely SL, Peebles CR, et al. Endobronchial ultrasound to assess airway wall thickening: validation in vitro and in vivo. *European Respiratory Journal* 2004;23:813-7.
390. Yamasaki A, Tomita K, Sano H, et al. Measuring subepithelial thickness using endobronchial ultrasonography in a patient with asthma: a case report. *Lung* 2003;181:115-20.
391. Musch G, Venegas JG. Positron emission tomography imaging of regional pulmonary perfusion and ventilation. *ProcAmThoracSoc* 2005;2:522-9.
392. Vidal Melo MF, Layfield D, Harris RS, et al. Quantification of regional ventilation-perfusion ratios with PET. *J NuclMed* 2003;44:1982-91.
393. Vidal Melo MF, Harris RS, Layfield JD, Venegas JG. Topographic basis of bimodal ventilation-perfusion distributions during bronchoconstriction in sheep. *AmJ RespirCrit Care Med* 2005;171:714-21.
394. Venegas JG, Winkler T, Musch G, et al. Self-organized patchiness in asthma as a prelude to catastrophic shifts. *Nature* 2005;434:777-82.
395. Anafi RC, Wilson TA. Airway stability and heterogeneity in the constricted lung. *J ApplPhysiol* 2001;91:1185-92.
396. Richard JC, Zhou Z, Ponde DE, et al. Imaging pulmonary gene expression with positron emission tomography. *AmJ RespirCrit Care Med* 2003;167:1257-63.
397. Dharmarajan S, Schuster DP. Molecular imaging of pulmonary gene expression with positron emission tomography. *ProcAmThoracSoc* 2005;2:549-6.
398. Failo R, Wielopolski PA, Tiddens HA, Hop WC, Mucelli RP, Lequin MH. Lung morphology assessment using MRI: a robust ultra-short TR/TE 2D steady state free precession sequence used in cystic fibrosis patients. *Magn ResonMed* 2009;61:299-306.

399. Fan L, Liu SY, Xiao XS, Sun F. Demonstration of pulmonary perfusion heterogeneity induced by gravity and lung inflation using arterial spin labeling. *Eur J Radiol* 2010;73:249-54.
400. Ohno Y, Iwasawa T, Seo JB, et al. Oxygen-enhanced magnetic resonance imaging versus computed tomography: multicenter study for clinical stage classification of smoking-related chronic obstructive pulmonary disease. *Am J Respir Crit Care Med* 2008;177:1095-102.
401. Albert MS, Cates GD, Driehuys B, et al. Biological magnetic resonance imaging using laser-polarized  $^{129}\text{Xe}$ . *Nature* 1994;370:199-201.
402. Morbach AE, Gast KK, Schmiedeskamp J, et al. Diffusion-weighted MRI of the lung with hyperpolarized helium-3: a study of reproducibility. *J Magn Reson Imaging* 2005;21:765-74.
403. Yablonskiy DA, Sukstanskii AL, Leawoods JC, et al. Quantitative in vivo assessment of lung microstructure at the alveolar level with hyperpolarized  $^3\text{He}$  diffusion MRI. *Proc Natl Acad Sci USA* 2002;99:3111-6.
404. Salerno M, Altes TA, Brookeman JR, de Lange EE, Mugler JP, III. Rapid hyperpolarized  $^3\text{He}$  diffusion MRI of healthy and emphysematous human lungs using an optimized interleaved-spiral pulse sequence. *J Magn Reson Imaging* 2003;17:581-8.
405. Fain SB, Panth SR, Evans MD, et al. Early emphysematous changes in asymptomatic smokers: detection with  $^3\text{He}$  MR imaging. *Radiology* 2006;239:875-83.
406. Saam BT, Yablonskiy DA, Kodibagkar VD, et al. MR imaging of diffusion of ( $^3\text{He}$ ) gas in healthy and diseased lungs. *Magn Reson Med* 2000;44:174-9.
407. Chen XJ, Moller HE, Chawla MS, et al. Spatially resolved measurements of hyperpolarized gas properties in the lung in vivo. Part I: diffusion coefficient. *Magn Reson Med* 1999;42:721-8.
408. Conradi MS, Yablonskiy DA, Woods JC, et al.  $^3\text{He}$  diffusion MRI of the lung. *Academic Radiology* 2005;12:1406-13.
409. Woods JC, Yablonskiy DA, Choong CK, et al. Long-range diffusion of hyperpolarized  $^3\text{He}$  in explanted normal and emphysematous human lungs via magnetization tagging. *J Appl Physiol* 2005;99:1992-7.
410. Wang C, Altes TA, Mugler JP, III, et al. Assessment of the lung microstructure in patients with asthma using hyperpolarized  $^3\text{He}$  diffusion MRI at two time scales: comparison with healthy subjects and patients with COPD. *J Magn Reson Imaging* 2008;28:80-8.

411. Wang C, Miller GW, Altes TA, de Lange EE, Cates GD, Jr., Mugler JP, III. Time dependence of  $^3\text{He}$  diffusion in the human lung: measurement in the long-time regime using stimulated echoes. *Magn ResonMed* 2006;56:296-309.
412. Woods JC, Yablonskiy DA, Chino K, Tanoli TS, Cooper JD, Conradi MS. Magnetization tagging decay to measure long-range  $(^3\text{He})$  diffusion in healthy and emphysematous canine lungs. *Magn ResonMed* 2004;51:1002-8.
413. Diaz S, Casselbrant I, Piitulainen E, et al. Validity of apparent diffusion coefficient hyperpolarized  $^3\text{He}$ -MRI using MSCT and pulmonary function tests as references. *EurJ Radiol* 2009;71:257-63.
414. Woods JC, Choong CK, Yablonskiy DA, et al. Hyperpolarized  $^3\text{He}$  diffusion MRI and histology in pulmonary emphysema. *Magn ResonMed* 2006;56:1293-300.
415. Jacob RE, Minard KR, Laicher G, Timchalk C. 3D  $^3\text{He}$  diffusion MRI as a local in vivo morphometric tool to evaluate emphysematous rat lungs. *J ApplPhysiol* 2008;105:1291-300.
416. Emami K, Stephen M, Kadlecsek S, Cadman RV, Ishii M, Rizi RR. Quantitative assessment of lung using hyperpolarized magnetic resonance imaging. *ProcAmThoracSoc* 2009;6:431-8.
417. van Beek EJ, Wild JM. Hyperpolarized 3-helium magnetic resonance imaging to probe lung function. *ProcAmThoracSoc* 2005;2:528-32, 10.
418. Saam B, Happer W, Middleton H. Nuclear relaxation of  $^3\text{He}$  in the presence of  $\text{O}_2$ . *PhysRevA* 1995;52:862-5.
419. Fischer MC, Spector ZZ, Ishii M, et al. Single-acquisition sequence for the measurement of oxygen partial pressure by hyperpolarized gas MRI. *Magn ResonMed* 2004;52:766-73.
420. Deninger AJ, Eberle B, Bermuth J, et al. Assessment of a single-acquisition imaging sequence for oxygen-sensitive  $(^3\text{He})$ -MRI. *Magn ResonMed* 2002;47:105-14.
421. Yu J, Ishii M, Law M, et al. Optimization of scan parameters in pulmonary partial pressure oxygen measurement by hyperpolarized  $^3\text{He}$  MRI. *Magn ResonMed* 2008;59:124-31.
422. Patz S, Hersman FW, Muradian I, et al. Hyperpolarized  $(^{129}\text{Xe})$  MRI: a viable functional lung imaging modality? *EurJ Radiol* 2007;64:335-44.
423. Gast KK, Schreiber WG, Herweling A, et al. Two-dimensional and three-dimensional oxygen mapping by  $^3\text{He}$ -MRI validation in a lung phantom. *EurRadiol* 2005;15:1915-22.

424. Yu J, Law M, Kadlecsek S, et al. Simultaneous measurement of pulmonary partial pressure of oxygen and apparent diffusion coefficient by hyperpolarized <sup>3</sup>He MRI. *Magn ResonMed* 2009;61:1015-21.
425. Altes TA, Powers PL, Knight-Scott J, et al. Hyperpolarized <sup>3</sup>He MR lung ventilation imaging in asthmatics: preliminary findings. *J Magn ResonImaging* 2001;13:378-84.
426. Deninger AJ, Mansson S, Petersson JS, et al. Quantitative measurement of regional lung ventilation using <sup>3</sup>He MRI. *Magn ResonMed* 2002;48:223-32.
427. Emami K, Kadlecsek SJ, Woodburn JM, et al. Improved technique for measurement of regional fractional ventilation by hyperpolarized <sup>3</sup>He MRI. *Magn ResonMed* 2010;63:137-50.
428. Swift AJ, Woodhouse N, Fichele S, et al. Rapid lung volumetry using ultrafast dynamic magnetic resonance imaging during forced vital capacity maneuver: correlation with spirometry. *Invest Radiol* 2007;42:37-41.
429. Holmes JH, Korosec FR, Du J, et al. Imaging of lung ventilation and respiratory dynamics in a single ventilation cycle using hyperpolarized He-3 MRI. *J Magn ResonImaging* 2007;26:630-6.
430. Holmes JH, O'Halloran RL, Brodsky EK, Jung Y, Block WF, Fain SB. 3D hyperpolarized He-3 MRI of ventilation using a multi-echo projection acquisition. *Magn ResonMed* 2008;59:1062-71.
431. Ajraoui S, Lee KJ, Deppe MH, Parnell SR, Parra-Robles J, Wild JM. Compressed sensing in hyperpolarized <sup>3</sup>He lung MRI. *Magn ResonMed* 2010;63:1059-69.
432. Holmes JH, O'Halloran RL, Brodsky EK, et al. Three-dimensional imaging of ventilation dynamics in asthmatics using multiecho projection acquisition with constrained reconstruction. *Magn ResonMed* 2009;62:1543-56.
433. Fain SB, Gonzalez-Fernandez G, Peterson ET, et al. Evaluation of structure-function relationships in asthma using multidetector CT and hyperpolarized He-3 MRI. *Academic Radiology* 2008;15:753-62.
434. de Lange EE, Altes TA, Patrie JT, et al. Evaluation of asthma with hyperpolarized helium-3 MRI: correlation with clinical severity and spirometry. *Chest* 2006;130:1055-62.
435. de Lange EE, Altes TA, Patrie JT, et al. The variability of regional airflow obstruction within the lungs of patients with asthma: assessment with hyperpolarized helium-3 magnetic resonance imaging. *Journal of Allergy and Clinical Immunology* 2007;119:1072-8.

436. Wild JM, Woodhouse N, Teh K. Single-scan acquisition of registered hyperpolarized (3)He ventilation and ADC images using a hybrid 2D gradient-echo sequence. *Magn ResonMed* 2007;57:1185-9.
437. Rizi RR, Baumgardner JE, Ishii M, et al. Determination of regional VA/Q by hyperpolarized 3He MRI. *Magn ResonMed* 2004;52:65-72.
438. Levin DL, Chen Q, Zhang M, Edelman RR, Hatabu H. Evaluation of regional pulmonary perfusion using ultrafast magnetic resonance imaging. *Magn ResonMed* 2001;46:166-71.
439. Hatabu H, Tadamura E, Levin DL, et al. Quantitative assessment of pulmonary perfusion with dynamic contrast-enhanced MRI. *Magn ResonMed* 1999;42:1033-8.
440. Ishii M, Emami K, Kadlecsek S, et al. Hyperpolarized 13C MRI of the pulmonary vasculature and parenchyma. *Magn ResonMed* 2007;57:459-63.
441. Tsai LL, Mair RW, Rosen MS, Patz S, Walsworth RL. An open-access, very-low-field MRI system for posture-dependent 3He human lung imaging. *J Magn Reson* 2008;193:274-85.
442. Fujimoto JG, Brezinski ME, Tearney GJ, et al. Optical biopsy and imaging using optical coherence tomography. *Nature Medicine* 1995;1:970-2.
443. Tearney GJ, Brezinski ME, Bouma BE, et al. In vivo endoscopic optical biopsy with optical coherence tomography. *Science* 1997;276:2037-9.
444. Huang D, Swanson EA, Lin CP, et al. Optical coherence tomography. *Science* 1991;254:1178-81.
445. Williamson JP, McLaughlin RA, Noffsinger WJ, et al. Elastic properties of the central airways in obstructive lung diseases measured using anatomical optical coherence tomography. *Am J Respir Crit Care Med* 2011;183:612-9.
446. Armstrong J, Leigh M, Walton I, et al. In vivo size and shape measurement of the human upper airway using endoscopic longrange optical coherence tomography. *OptExpress* 2003;11:1817-26.
447. Armstrong JJ, Leigh MS, Sampson DD, Walsh JH, Hillman DR, Eastwood PR. Quantitative upper airway imaging with anatomic optical coherence tomography. *AmJ RespirCrit Care Med* 2006;173:226-33.
448. Leigh MS, Armstrong JJ, Paduch A, et al. Anatomical optical coherence tomography for long-term, portable, quantitative endoscopy. *IEEE TransBiomedEng* 2008;55:1438-46.



449. McLaughlin RA, Williamson JP, Phillips MJ, et al. Applying anatomical optical coherence tomography to quantitative 3D imaging of the lower airway. *OptExpress* 2008;16:17521-9.
450. Noble PB, West AR, McLaughlin RA, et al. Airway narrowing assessed by anatomical optical coherence tomography in vitro: dynamic airway wall morphology and function. *J ApplPhysiol* 2010;108:401-11.
451. Thiberville L, Moreno-Swirc S, Vercauteren T, Peltier E, Cave C, Bourg HG. In vivo imaging of the bronchial wall microstructure using fibered confocal fluorescence microscopy. *AmJ RespirCrit Care Med* 2007;175:22-31.
452. Thiberville L, Salaun M, Lachkar S, et al. Human in vivo fluorescence microimaging of the alveolar ducts and sacs during bronchoscopy. *EurRespirJ* 2009;33:974-85.
453. Hsiung PL, Hardy J, Friedland S, et al. Detection of colonic dysplasia in vivo using a targeted heptapeptide and confocal microendoscopy. *Nature Medicine* 2008;14:454-8.
454. Korideck H, Peterson JD. Noninvasive quantitative tomography of the therapeutic response to dexamethasone in ovalbumin-induced murine asthma. *J PharmacolExpTher* 2009;329:882-9.
455. Ntziachristos V. Optical imaging of molecular signatures in pulmonary inflammation. *ProcAmThoracSoc* 2009;6:416-8.
456. Cortez-Retamozo V, Swirski FK, Waterman P, et al. Real-time assessment of inflammation and treatment response in a mouse model of allergic airway inflammation. *J Clin Invest* 2008;118:4058-66.
457. Ntziachristos V, Tung CH, Bremer C, Weissleder R. Fluorescence molecular tomography resolves protease activity in vivo. *Nature Medicine* 2002;8:757-60.
458. Kharitonov S, Alving K, Barnes PJ. Exhaled and nasal nitric oxide measurements: recommendations. The European Respiratory Society Task Force. *Eur Respir J* 1997;10:1683-93.
459. Juniper EF, Cockcroft DW, Hargreave FE. Histamine and methacholine inhalation tests: a laboratory tidal breathing protocol: Astra Draco AB; 1994.
460. Martin RJ, Wanger JS, Irvin CG, Bucher Bartelson B, Cherniack RM. Methacholine challenge testing: safety of low starting FEV1. Asthma Clinical Research Network (ACRN). *Chest* 1997;112:53-6.

461. Juniper EF, O'Byrne PM, Guyatt GH, Ferrie PJ, King DR. Development and validation of a questionnaire to measure asthma control. *European Respiratory Journal* 1999;14:902-7.
462. Juniper EF, Svensson K, Mork AC, Stahl E. Measurement properties and interpretation of three shortened versions of the asthma control questionnaire. *RespirMed* 2005;99:553-8.
463. Gift AG. Visual analogue scales: measurement of subjective phenomena. *Nurs Res* 1989;38:286-8.
464. Juniper EF, Guyatt GH, Epstein RS, Ferrie PJ, Jaeschke R, Hiller TK. Evaluation of impairment of health related quality of life in asthma: development of a questionnaire for use in clinical trials. *Thorax* 1992;47:76-83.
465. Juniper EF, Buist AS, Cox FM, Ferrie PJ, King DR. Validation of a standardized version of the Asthma Quality of Life Questionnaire. *Chest* 1999;115:1265-70.
466. Nakano Y, Muro S, Sakai H, et al. Computed tomographic measurements of airway dimensions and emphysema in smokers - Correlation with lung function. *American Journal of Respiratory and Critical Care Medicine* 2000;162:1102-8.
467. Nakano Y, Muller NL, King GG, et al. Quantitative assessment of airway remodeling using high-resolution CT. *Chest* 2002;122:271S-5S.
468. Hansell DM, Bankier AA, MacMahon H, McLoud TC, Muller NL, Remy J. Fleischner Society: Glossary of terms for thoracic imaging. *Radiology* 2008;246:697-722.
469. Nakano Y, Wong JC, de Jong PA, et al. The prediction of small airway dimensions using computed tomography. *American Journal of Respiratory and Critical Care Medicine* 2005;171:142-6.
470. de Jong PA. Changes in Airway Dimensions on Computed Tomography Scans of Children with Cystic Fibrosis. *American Journal of Respiratory and Critical Care Medicine* 2005;172:218-24.
471. Amirav I, Kramer SS, Grunstein MM, Hoffman EA. Assessment of Methacholine-Induced Airway Constriction by Ultrafast High-Resolution Computed-Tomography. *Journal of Applied Physiology* 1993;75:2239-50.
472. Piegl L. On Nurbs - A Survey. *Ieee Computer Graphics and Applications* 1991;11:55-71.
473. Hu SY, Hoffman EA, Reinhardt JM. Automatic lung segmentation for accurate quantitation of volumetric X-ray CT images. *Ieee Transactions on Medical Imaging* 2001;20:490-8.

474. Palagyi K, Tschirren J, Sonka M. Quantitative analysis of intrathoracic airway trees: methods and validation. *InfProcess MedImaging* 2003;18:222-33.
475. Tschirren J, Hoffman EA, McLennan G, Sonka M. Intrathoracic airway trees: Segmentation and airway morphology analysis from low-dose CT scans. *Ieee Transactions on Medical Imaging* 2005;24:1529-39.
476. Tschirren J, Hoffman EA, McLennan G, Sonka M. Segmentation and quantitative analysis of intrathoracic airway trees from computed tomography images. *ProcAmThoracSoc* 2005;2:484-.
477. Matsuoka S, Kurihara Y, Yagihashi K, Hoshino M, Watanabe N, Nakajima Y. Quantitative assessment of air trapping in chronic obstructive pulmonary disease using inspiratory and expiratory volumetric MDCT. *AJR Am J Roentgenol* 2008;190:762-9.
478. Gevenois PA, de Maertelaer V, De Vuyst P, Zanen J, Yernault JC. Comparison of computed density and macroscopic morphometry in pulmonary emphysema. *Am J Respir Crit Care Med* 1995;152:653-7.
479. Gevenois PA, De Vuyst P, de Maertelaer V, et al. Comparison of computed density and microscopic morphometry in pulmonary emphysema. *Am J Respir Crit Care Med* 1996;154:187-92.
480. Abramoff MD, Magalhaes, P.J., Ram, S.J. Image Processing with ImageJ. *Biophotonics International* 2004;11:36-42.
481. FracLac for ImageJ, version 2.5., 1999-2007. (Accessed 18/11/2011, at <http://rsb.info.nih.gov/ij/plugins/fracLac/FLHelp/Introduction.htm>.)
482. Coxson HO, Whittall KP, Nakano Y, et al. Selection of patients for lung volume reduction surgery using a power law analysis of the computed tomographic scan. *Thorax* 2003;58:510-4.
483. Christner JA, Kofler JM, McCollough CH. Estimating effective dose for CT using dose-length product compared with using organ doses: consequences of adopting International Commission on Radiological Protection publication 103 or dual-energy scanning. *AJR Am J Roentgenol* 2010;194:881-9.
484. Huda W, Ogden KM, Khorasani MR. Converting dose-length product to effective dose at CT. *Radiology* 2008;248:995-1003.
485. Bongartz G, Golding SJ, Jurik AG, et al. European Guidelines on quality criteria for computed tomography. Brussels, Belgium: European Commission; 2000.

486. Gerber TC, Kuzo RS, Morin RL. Techniques and parameters for estimating radiation exposure and dose in cardiac computed tomography. *Int J Cardiovasc Imaging* 2005;21:165-76.
487. Bousquet J, Clark TJ, Hurd S, et al. GINA guidelines on asthma and beyond. *Allergy* 2007;62:102-12.
488. Niimi A, Matsumoto H, Takemura M, Ueda T, Nakano Y, Mishima M. Clinical assessment of airway remodeling in asthma: utility of computed tomography. *Clinical Reviews in Allergy and Immunology* 2004;27:45-58.
489. Landis JR, Koch GG. The measurement of observer agreement for categorical data. *Biometrics* 1977;33:159-74.
490. Kundel HL, Polansky M. Measurement of observer agreement. *Radiology* 2003;228:303-8.
491. Moss M, Wellman DA, Cotsonis GA. An appraisal of multivariable logistic models in the pulmonary and critical care literature. *Chest* 2003;123:923-8.
492. Peng CYJ, Lee KL, Ingersoll GM. An introduction to logistic regression analysis and reporting. *Journal of Educational Research* 2002;96:3-14.
493. Greenberger PA. Allergic bronchopulmonary aspergillosis. *Journal of Allergy and Clinical Immunology* 2002;110:685-92.
494. Patel IS, Vlahos I, Wilkinson TMA, et al. Bronchiectasis, exacerbation indices, and inflammation in chronic obstructive pulmonary disease. *American Journal of Respiratory and Critical Care Medicine* 2004;170:400-7.
495. O'Brien C, Guest PJ, Hill SL, Stockley RA. Physiological and radiological characterisation of patients diagnosed with chronic obstructive pulmonary disease in primary care. *Thorax* 2000;55:635-42.
496. Gompertz S, Bayley DL, Hill SL, Stockley RA. Relationship between airway inflammation and the frequency of exacerbations in patients with smoking related COPD. *Thorax* 2001;56:36-41.
497. Pasteur MC, Bilton D, Hill AT. British Thoracic Society guideline for non-CF bronchiectasis. *Thorax* 2010;65 Suppl 1:i1-58.
498. Naidich DP, McCauley DI, Khouri NF, Stitik FP, Siegelman SS. Computed tomography of bronchiectasis. *J Comput Assist Tomogr* 1982;6:437-44.
499. Kang EY, Miller RR, Muller NL. Bronchiectasis: comparison of preoperative thin-section CT and pathologic findings in resected specimens. *Radiology* 1995;195:649-54.

500. Camiciottoli G, Cavigli E, Grassi L, et al. Prevalence and correlates of pulmonary emphysema in smokers and former smokers. A densitometric study of participants in the ITALUNG trial. *EurRadiol* 2008.
501. Satoh K, Kobayashi T, Misao T, et al. CT assessment of subtypes of pulmonary emphysema in smokers. *Chest* 2001;120:725-9.
502. Lynch DA, Newell J, Hale V, et al. Correlation of CT findings with clinical evaluations in 261 patients with symptomatic bronchiectasis. *American Journal of Roentgenology* 1999;173:53-8.
503. Wongyoucheong JJ, Leahy BC, Taylor PM, Church SE. Airways Obstruction and Bronchiectasis - Correlation with Duration of Symptoms and Extent of Bronchiectasis on Computed-Tomography. *Clinical Radiology* 1992;45:256-9.
504. Parr DG, Sevenoaks M, Deng C, Stoel BC, Stockley RA. Detection of emphysema progression in alpha 1-antitrypsin deficiency using CT densitometry; methodological advances. *RespirRes* 2008;9:21.
505. Robinson TE. Dornase Alfa Reduces Air Trapping in Children With Mild Cystic Fibrosis Lung Disease: A Quantitative Analysis. *Chest* 2005;128:2327-35.
506. Goris ML, Zhu HJ, Blankenberg F, Chan F, Robinson TE. An automated approach to quantitative air trapping measurements in mild cystic fibrosis. *Chest* 2003;123:1655-63.
507. Stolk J, Putter H, Bakker EM, et al. Progression parameters for emphysema: A clinical investigation. *Respiratory Medicine* 2007;101:1924-30.
508. Brown RH, Herold CJ, Hirshman CA, Zerhouni EA, Mitzner W. In vivo measurements of airway reactivity using high-resolution computed tomography. *Am Rev Respir Dis* 1991;144:208-12.
509. Herold CJ, Brown RH, Mitzner W, Links JM, Hirshman CA, Zerhouni EA. Assessment of pulmonary airway reactivity with high-resolution CT. *Radiology* 1991;181:369-74.
510. Coxson HO, Rogers RM. Quantitative computed tomography of chronic obstructive pulmonary disease. *Acad Radiol* 2005;12:1457-63.
511. Gould GA, MacNee W, McLean A, et al. CT measurements of lung density in life can quantitate distal airspace enlargement--an essential defining feature of human emphysema. *Am Rev Respir Dis* 1988;137:380-92.
512. Adams H, Bernard MS, McConnochie K. An appraisal of CT pulmonary density mapping in normal subjects. *Clin Radiol* 1991;43:238-42.

513. Stoel BC, Bakker ME, Stolk J, et al. Comparison of the sensitivities of 5 different computed tomography scanners for the assessment of the progression of pulmonary emphysema: a phantom study. *Invest Radiol* 2004;39:1-7.
514. Shaker SB, Dirksen A, Laursen LC, Skovgaard LT, Holstein-Rathlou NH. Volume adjustment of lung density by computed tomography scans in patients with emphysema. *Acta Radiol* 2004;45:417-23.
515. Boedeker KL, McNitt-Gray MF, Rogers SR, et al. Emphysema: effect of reconstruction algorithm on CT imaging measures. *Radiology* 2004;232:295-301.
516. Yuan R, Mayo JR, Hogg JC, et al. The effects of radiation dose and CT manufacturer on measurements of lung densitometry. *Chest* 2007;132:617-23.
517. Conradi SH, Lutey BA, Atkinson JJ, Wang W, Senior RM, Gierada DS. Measuring small airways in transverse CT images correction for partial volume averaging and airway tilt. *Acad Radiol* 2010;17:1525-34.
518. Dame Carroll JR, Chandra A, Jones AS, Berend N, Magnussen JS, King GG. Airway dimensions measured from micro-computed tomography and high-resolution computed tomography. *Eur Respir J* 2006;28:712-20.
519. Berger P, Laurent F, Begueret H, et al. Structure and function of small airways in smokers: relationship between air trapping at CT and airway inflammation. *Radiology* 2003;228:85-94.
520. Dirksen A. Monitoring the progress of emphysema by repeat computed tomography scans with focus on noise reduction. *ProcAmThoracSoc* 2008;5:925-8.
521. Dirksen A, Friis M, Olesen KP, Skovgaard LT, Sorensen K. Progress of emphysema in severe alpha 1-antitrypsin deficiency as assessed by annual CT. *Acta Radiol* 1997;38:826-32.
522. Horsfield K, Cumming G. Morphology of the bronchial tree in man. *J Appl Physiol* 1968;24:373-83.
523. The Phantom Laboratory, <http://www.phantomlab.us/>. 2012. (Accessed 06/01/2012, at
524. Fain SB, Peterson ET, Sorkness RL, Wenzel S, Castro M, Busse WW. Severe Asthma Research Program – Phenotyping and Quantification of Severe Asthma. *Imaging Decisions MRI* 2009;13:24-7.
525. Emphysema versus Airway disease, EU FP7 funded project. 2012. (Accessed 12/01/2012, at <http://www.eva-copd.eu/eva/english/index.html>.)

526. Parr DG, Stoel BC, Stolk J, Nightingale PG, Stockley RA. Influence of calibration on densitometric studies of emphysema progression using computed tomography. *Am J Respir Crit Care Med* 2004;170:883-90.
527. Parr DG, Dirksen A, Piitulainen E, Deng C, Wencker M, Stockley RA. Exploring the optimum approach to the use of CT densitometry in a randomised placebo-controlled study of augmentation therapy in alpha 1-antitrypsin deficiency. *Respir Res* 2009;10:75.
528. Stoel BC, Stolk J. Optimization and standardization of lung densitometry in the assessment of pulmonary emphysema. *Invest Radiol* 2004;39:681-8.
529. Berger P, Perot V, Desbarats P, Tunon-de-Lara JM, Marthan R, Laurent F. Airway wall thickness in cigarette smokers: quantitative thin-section CT assessment. *Radiology* 2005;235:1055-64.
530. Reinhardt JM, Raab SA, D'Souza ND, Hoffman EA. Intrathoracic airway measurement: ex-vivo validation. In: Hoffman EA, editor.; 1997; Newport Beach, CA, USA: SPIE; 1997. p. 69-80.
531. Hoffman EA, Simon BA, McLennan G. State of the Art. A structural and functional assessment of the lung via multidetector-row computed tomography: phenotyping chronic obstructive pulmonary disease. *Proc Am Thorac Soc* 2006;3:519-32.
532. Stoel BC, Vrooman HA, Stolk J, Reiber JH. Sources of error in lung densitometry with CT. *Invest Radiol* 1999;34:303-9.
533. Kemerink GJ, Lamers RJ, Thelissen GR, van Engelshoven JM. Scanner conformity in CT densitometry of the lungs. *Radiology* 1995;197:749-52.
534. Shaker SB, Dirksen A, Laursen LC, et al. Short-term reproducibility of computed tomography-based lung density measurements in alpha-1 antitrypsin deficiency and smokers with emphysema. *Acta Radiol* 2004;45:424-30.
535. Groell R, Rienmueller R, Schaffler GJ, Portugaller HR, Graif E, Willfurth P. CT number variations due to different image acquisition and reconstruction parameters: a thorax phantom study. *Comput Med Imaging Graph* 2000;24:53-8.
536. Schlesinger RB, McFadden LA. Comparative morphometry of the upper bronchial tree in six mammalian species. *Anat Rec* 1981;199:99-108.
537. Gupta S, Siddiqui S, Haldar P, et al. Qualitative Analysis of High-Resolution CT Scans in Severe Asthma. *Chest* 2009;136:1521-8.
538. Matsuoka S, Kurihara Y, Yagihashi K, Hoshino M, Nakajima Y. Airway dimensions at inspiratory and expiratory multisection CT in chronic obstructive pulmonary disease: correlation with airflow limitation. *Radiology* 2008;248:1042-9.

539. Molimard M, Buhl R, Niven R, et al. Omalizumab reduces oral corticosteroid use in patients with severe allergic asthma: real-life data. *Respir Med* 2010;104:1381-5.
540. Niven R, Chung KF, Panahloo Z, Blogg M, Ayre G. Effectiveness of omalizumab in patients with inadequately controlled severe persistent allergic asthma: an open-label study. *Respir Med* 2008;102:1371-8.
541. Little SA, Chalmers GW, Macleod KJ, McSharry C, Thomson NC. Non-invasive markers of airway inflammation as predictors of oral steroid responsiveness in asthma. *Thorax* 2000;55:232-4.
542. Fahy JV. Eosinophilic and neutrophilic inflammation in asthma: insights from clinical studies. *Proc Am Thorac Soc* 2009;6:256-9.
543. Louis R, Lau LCK, Bron AO, Roldaan AC, Radermecker M, Djukanovic R. The relationship between airways inflammation and asthma severity. *American Journal of Respiratory and Critical Care Medicine* 2000;161:9-16.
544. Matsumoto H, Niimi A, Minakuchi M, Izumi T. Serum eosinophil cationic protein levels measured during exacerbation of asthma: characteristics of patients with low titres. *Clinical and Experimental Allergy* 2001;31:637-43.
545. Bai TR, Cooper J, Koelmeyer T, Pare PD, Weir TD. The effect of age and duration of disease on airway structure in fatal asthma. *Am J Respir Crit Care Med* 2000;162:663-9.
546. Deykin A, Lazarus SC, Fahy JV, et al. Sputum eosinophil counts predict asthma control after discontinuation of inhaled corticosteroids. *J Allergy Clin Immunol* 2005;115:720-7.
547. Jatakanon A, Lim S, Barnes PJ. Changes in sputum eosinophils predict loss of asthma control. *Am J Respir Crit Care Med* 2000;161:64-72.
548. Leckie MJ, ten Brinke A, Khan J, et al. Effects of an interleukin-5 blocking monoclonal antibody on eosinophils, airway hyper-responsiveness, and the late asthmatic response. *Lancet* 2000;356:2144-8.
549. Flood-Page P, Swenson C, Faiferman I, et al. A study to evaluate safety and efficacy of mepolizumab in patients with moderate persistent asthma. *Am J Respir Crit Care Med* 2007;176:1062-71.
550. O'Byrne PM. The demise of anti IL-5 for asthma, or not. *Am J Respir Crit Care Med* 2007;176:1059-60.
551. Juniper EF, Guyatt GH, Ferrie PJ, Griffith LE. Measuring quality of life in asthma. *Am Rev Respir Dis* 1993;147:832-8.



552. Altman DG, Bland JM. Treatment allocation by minimisation. *BMJ* 2005;330:843.
553. BTS. British guideline on the management of asthma - A national clinical guideline. *Thorax* 2008;63:iv1-121.
554. Keene ON, Calverley PM, Jones PW, Vestbo J, Anderson JA. Statistical analysis of exacerbation rates in COPD: TRISTAN and ISOLDE revisited. *Eur Respir J* 2008;32:17-24.
555. Siva R, Green RH, Brightling CE, et al. Eosinophilic airway inflammation and exacerbations of COPD: a randomised controlled trial. *European Respiratory Journal* 2007;29:906-13.
556. Brightling CE, Ward R, Wardlaw AJ, Pavord ID. Airway inflammation, airway responsiveness and cough before and after inhaled budesonide in patients with eosinophilic bronchitis. *European Respiratory Journal* 2000;15:682-6.
557. Brightling CE, Monteiro W, Ward R, et al. Sputum eosinophilia and short-term response to prednisolone in chronic obstructive pulmonary disease: a randomised controlled trial. *Lancet* 2000;356:1480-5.
558. Wardlaw AJ, Silverman M, Siva R, Pavord ID, Green R. Multi-dimensional phenotyping: towards a new taxonomy for airway disease. *Clin Exp Allergy* 2005;35:1254-62.
559. Barnes PJ. Immunology of asthma and chronic obstructive pulmonary disease. *Nat Rev Immunol* 2008;8:183-92.
560. Gupta S, Siddiqui S, Haldar P, et al. Quantitative analysis of high-resolution computed tomography scans in severe asthma subphenotypes. *Thorax* 2010;65:775-81.
561. Wenzel SE. Asthma: defining of the persistent adult phenotypes. *The Lancet* 2006;368:804-13.
562. Haldar P, Brightling CE, Hargadon B, et al. Mepolizumab and Exacerbations of Refractory Eosinophilic Asthma. *New England Journal of Medicine* 2009;360:973-84.
563. Juniper EF, Buist AS, Cox F, Ferrie PJ, King D. Development and validation of the standardised asthma quality of life questionnaire (AQLQ(S)). *Journal of Allergy and Clinical Immunology* 1998;101:S177-S.
564. Kaiser H. An index of factorial simplicity. *Psychometrika* 1974;39:31-6.
565. Kaiser H. A second generation little jiffy. *Psychometrika* 1970;35:401-15.

566. Bartlett MS. A note on the multiplying factors for various chi square approximations. *J of the Royal Statistical Society* 1954;16, Ser. B:296-8.
567. Kaiser HF. The application of electronic computers to factor analysis. *Educational and Psychological Measurement* 1960;20:141-51.
568. Ball GH, Hall DJ. A clustering technique for summarizing multivariate data. *Behav Sci* 1967;12:153-5.
569. Brown N, Salome CM, Berend N, Thorpe CW, King GG. Airway distensibility in adults with asthma and healthy adults, measured by forced oscillation technique. *American Journal of Respiratory and Critical Care Medicine* 2007;176:129-37.
570. Ward C, Johns DP, Bish R, et al. Reduced airway distensibility, fixed airflow limitation and airway wall remodelling in asthma. *Thorax* 2001;56:30-.
571. Moreno RH, Hogg JC, Pare PD. Mechanics of airway narrowing. *Am Rev Respir Dis* 1986;133:1171-80.
572. Wiggs BR, Moreno R, Hogg JC, Hilliam C, Pare PD. A model of the mechanics of airway narrowing. *J Appl Physiol* 1990;69:849-60.
573. Kemerink GJ, Lamers RJ, Thelissen GR, van Engelshoven JM. CT densitometry of the lungs: scanner performance. *J Comput Assist Tomogr* 1996;20:24-33.
574. Wong-You-Cheong JJ, Leahy BC, Taylor PM, Church SE. Airways obstruction and bronchiectasis: correlation with duration of symptoms and extent of bronchiectasis on computed tomography. *Clin Radiol* 1992;45:256-9.
575. Hansell DM, Wells AU, Rubens MB, Cole PJ. Bronchiectasis: functional significance of areas of decreased attenuation at expiratory CT. *Radiology* 1994;193:369-74.
576. King PT. The pathophysiology of bronchiectasis. *Int J Chron Obstruct Pulmon Dis* 2009;4:411-9.
577. Patel R, Patel V, Esan A, Lapidus C, Sung A. The prevalence of tracheobronchomalacia in patients with asthma or chronic obstructive pulmonary disease. *Chest* 2009;136:27S-h-.
578. Sverzellati N, Rastelli A, Chetta A, et al. Airway malacia in chronic obstructive pulmonary disease: prevalence, morphology and relationship with emphysema, bronchiectasis and bronchial wall thickening. *Eur Radiol* 2009;19:1669-78.

579. Bousquet J, Lacoste JY, Chanez P, Vic P, Godard P, Michel FB. Bronchial elastic fibers in normal subjects and asthmatic patients. *Am J Respir Crit Care Med* 1996;153:1648-54.
580. Macklem PT. A theoretical analysis of the effect of airway smooth muscle load on airway narrowing. *Am J Respir Crit Care Med* 1996;153:83-9.
581. Lambert RK, Pare PD. Lung parenchymal shear modulus, airway wall remodeling, and bronchial hyperresponsiveness. *J Appl Physiol* 1997;83:140-7.
582. Wenzel S. Severe asthma: from characteristics to phenotypes to endotypes. *Clin Exp Allergy* 2012.
583. Hoshino M, Ohtawa J. Effects of Adding Omalizumab, an Anti-Immunoglobulin E Antibody, on Airway Wall Thickening in Asthma. *Respiration* 2012.
584. Mauroy B, Filoche M, Weibel ER, Sapoval B. An optimal bronchial tree may be dangerous. *Nature* 2004;427:633-6.
585. Ley S, Zaporozhan J, Morbach A, et al. Functional evaluation of emphysema using diffusion-weighted 3Helium-magnetic resonance imaging, high-resolution computed tomography, and lung function tests. *Invest Radiol* 2004;39:427-34.
586. Fain SB, Altes TA, O'Halloran R, et al. Comparison of diffusion weighted helium-3 MRI in patients with asthma versus those with COPD. In: *Proc Intl Soc Mag Reson Med*; 2006; Seattle; 2006. p. 1665.
587. de Jong PA, Mayo JR, Golmohammadi K, et al. Estimation of cancer mortality associated with repetitive computed tomography scanning. *AmJRespirCrit Care Med* 2006;173:199-203.
588. Mayo JR. Radiation dose issues in longitudinal studies involving computed tomography. *Proc Am Thorac Soc* 2008;5:934-9.
589. Gierada DS, Yusen RD, Pilgram TK, et al. Repeatability of quantitative CT indexes of emphysema in patients evaluated for lung volume reduction surgery. *Radiology* 2001;220:448-54.
590. Brown RH, Mitzner W. Effect of lung inflation and airway muscle tone on airway diameter in vivo. *Journal of Applied Physiology* 1996;80:1581-8.
591. Brown RH, Herold C, Zerhouni EA, Mitzner W. Spontaneous airways constrict during breath holding studied by high-resolution computed tomography. *Chest* 1994;106:920-4.

592. Mayo JR, Webb WR, Gould R, et al. High-resolution CT of the lungs: an optimal approach. *Radiology* 1987;163:507-10.
593. Kulkarni NS, Hollins F, Sutcliffe A, et al. Eosinophil protein in airway macrophages: a novel biomarker of eosinophilic inflammation in patients with asthma. *J Allergy Clin Immunol* 2010;126:61-9 e3.
594. Cox G. New interventions in asthma including bronchial thermoplasty. *Current Opinion in Pulmonary Medicine* 2008;14:77-81.
595. Shrimpton PC, Hillier MC, Lewis MA, Dunn M. National survey of doses from CT in the UK: 2003. *British Journal of Radiology* 2006;79:968-80.
596. Robinson DS, Campbell DA, Durham SR, et al. Systematic assessment of difficult-to-treat asthma. *Eur Respir J* 2003;22:478-83.
597. Heaney LG, Conway E, Kelly C, et al. Predictors of therapy resistant asthma: outcome of a systematic evaluation protocol. *Thorax* 2003;58:561-6.
598. Lipworth BJ. Long-acting beta2-adrenoceptor agonists: a smart choice for asthma? *Trends Pharmacol Sci* 2007;28:257-62.
599. Morgan B. Opportunities and pitfalls of cancer imaging in clinical trials. *Nat Rev Clin Oncol* 2011;8:517-27.
600. Schuster DP. The Opportunities and Challenges of Developing Imaging Biomarkers to Study Lung Function and Disease. *American Journal of Respiratory and Critical Care Medicine* 2007;176:224-30.
601. Lin CL, Tawhai MH, McLennan G, Hoffman EA. Computational Fluid Dynamics Multiscale Simulation of Gas Flow in Subject-Specific Models of the Human Lung. *IEEE Engineering in Medicine and Biology Magazine* 2009;28:25-33.
602. De Backer JW, Vos WG, Gorle CD, et al. Flow analyses in the lower airways: patient-specific model and boundary conditions. *MedEng Phys* 2008;30:872-9.
603. Tgavalekos NT, Tawhai M, Harris RS, et al. Identifying airways responsible for heterogeneous ventilation and mechanical dysfunction in asthma: an image functional modeling approach. *J ApplPhysiol* 2005;99:2388-97.
604. Plotkowiak M, Burrowes K, Wolber J, et al. Relationship between structural changes and hyperpolarized gas magnetic resonance imaging in chronic obstructive pulmonary disease using computational simulations with realistic alveolar geometry. *PhilosTransactA MathPhysEng Sci* 2009;367:2347-69.

605. Choi J, Tawhai MH, Hoffman EA, Lin CL. On intra- and intersubject variabilities of airflow in the human lungs. *PhysFluids* (1994) 2009;21:101901.
606. Freitas RK, Schroder W. Numerical investigation of the three-dimensional flow in a human lung model. *J Biomech* 2008;41:2446-57.
607. Yin Y, Choi J, Hoffman EA, Tawhai MH, Lin CL. Simulation of pulmonary air flow with a subject-specific boundary condition. *J Biomech* 2010.
608. Darquenne C, Harrington L, Prisk GK. Alveolar duct expansion greatly enhances aerosol deposition: a three-dimensional computational fluid dynamics study. *PhilosTransactA MathPhysEng Sci* 2009;367:2333-46.
609. Ma B, Lutchen KR. CFD simulation of aerosol deposition in an anatomically based human large-medium airway model. *AnnBiomedEng* 2009;37:271-85.